

4d

PNL-2674 Vol I

UC-12

**A User's Manual for the
BNW-II Optimization Code for
Dry/Wet-Cooled Power Plants**

May 1978

Prepared for the U.S. Department of Energy
under Contract No. EY-76-C-06-1830

Pacific Northwest Laboratory
Operated for the U.S. Department of Energy
by

 **Battelle**
Memorial Institute

PNL-2674 Vol I

NOTICE

This report was prepared as an account of work sponsored by the United States Government. Neither the United States nor the Department of Energy, nor any of their employees, nor any of their contractors, subcontractors, or their employees, makes any warranty, express or implied, or assumes any legal liability or responsibility for the accuracy, completeness or usefulness of any information, apparatus, product or process disclosed, or represents that its use would not infringe privately owned rights.

The views, opinions and conclusions contained in this report are those of the contractor and do not necessarily represent those of the United States Government or the United States Department of Energy.

PACIFIC NORTHWEST LABORATORY
operated by
BATTELLE
for the
UNITED STATES DEPARTMENT OF ENERGY
Under Contract EY-76-C-06-1830

Printed in the United States of America
Available from
National Technical Information Service
United States Department of Commerce
5285 Port Royal Road
Springfield, Virginia 22151

Price: Printed Copy \$ ____*; Microfiche \$3.00

*Pages	NTIS Selling Price
001-025	\$4.00
026-050	\$4.50
051-075	\$5.25
076-100	\$6.00
101-125	\$6.50
126-150	\$7.25
151-175	\$8.00
176-200	\$9.00
201-225	\$9.25
226-250	\$9.50
251-275	\$10.75
276-300	\$11.00

3 3679 00049 3017

PNL-2674 Vol I
UC-12

A USER'S MANUAL FOR THE
BNW-II OPTIMIZATION CODE
FOR DRY/WET-COOLED POWER PLANTS

VOLUME I

Daniel J. Braun
Judith A. Bamberger
David J. Braun
Duane W. Faletti
Lawrence E. Wiles

May 1978

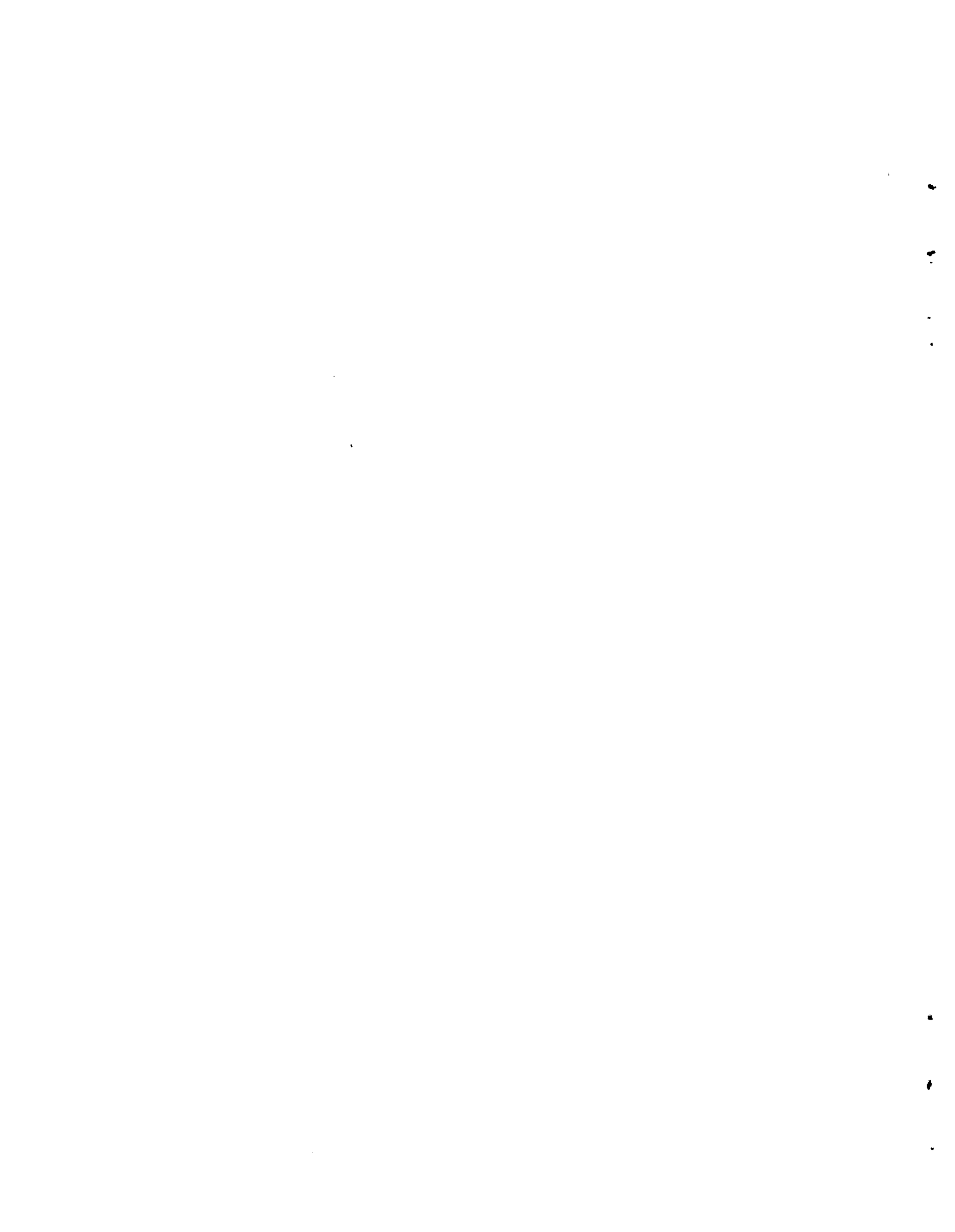
Prepared for the U.S. Department of Energy
under Contract No. EY-76-C-06-1830

Pacific Northwest Laboratory
Richland, Washington 99352



PREFACE

This document has been issued in two volumes to facilitate handling. Volume I is a narrative description of the code's algorithms, as well as logic, input and output information. Volume II is an appendix of Volume I, providing a listing of the BNW-II dry/wet ammonia heat rejection optimization code.



SUMMARY

This User's Manual describes how to operate BNW-II, a computer code developed by the Pacific Northwest Laboratory (PNL) as a part of its activities under the Department of Energy (DOE) Dry Cooling Enhancement Program.

The computer program offers a comprehensive method of evaluating the cost savings potential of dry/wet-cooled heat rejection systems. Going beyond simple "figure-of-merit" cooling tower optimization, this method includes such items as the cost of annual replacement capacity, and the optimum split between plant scale-up and replacement capacity, as well as the purchase and operating costs of all major heat rejection components. Hence the BNW-II code is a useful tool for determining potential cost savings of new dry/wet surfaces, new piping, or other components as part of an optimized system for a dry/wet-cooled power plant.



FOREWORD

The Dry Cooling Enhancement Program at the Pacific Northwest Laboratory (PNL) was initiated with a program scope that included the following near-term and ultimate emphases.

Near-Term Objectives:

- Develop economic and performance models for cost optimization of total heat rejection systems using dry and dry/wet cooling.
- Analyze and disseminate operating experience on existing dry-cooled plant performance.
- Demonstrate certain features of existing technology equipment to provide confidence for specification by utilities.

Ultimate Objective:

- Promote water conservation through industry use of dry cooling by developing and demonstrating the reliability of lower-cost systems. The development of advanced dry/wet systems is also considered to be within this scope.

The following documents have been issued, reporting the results of the work toward these objectives.

Cost optimization of dry-cooled heat rejection systems:

A REVIEW AND ASSESSMENT OF ENGINEERING ECONOMIC STUDIES OF DRY COOLED ELECTRICAL GENERATING PLANTS. B. C. Fryer, BNWL-1976, March 1976.

HEAT TRANSFER AND PRESSURE DROP CHARACTERISTICS OF DRY TOWER EXTENDED SURFACES. PART I: HEAT TRANSFER AND PRESSURE DROP DATA. PFR Engineering Systems, Inc., PFR 7-100, March 1976.

HEAT TRANSFER AND PRESSURE DROP CHARACTERISTICS OF DRY TOWER EXTENDED SURFACES. PART II: DATA ANALYSIS AND CORRELATION. PFR Engineering Systems, Inc., PFR 7-102, June 1976.

Analysis of performance of existing dry-cooled plants:

DRY COOLING TOWER PROGRAM: RESULTS OF INDUSTRIAL CONTACTS THROUGH AUGUST 1974. BNWL-1878, November 1, 1974.

A SURVEY OF MATERIALS AND CORROSION PERFORMANCE IN DRY COOLING APPLICATIONS. A. B. Johnson, Jr., D. R. Pratt and G. E. Zima, BNWL-1958, March 1976.

EUROPEAN DRY COOLING TOWER OPERATING EXPERIENCE. J. G. DeSteele and K. Simhan, BNWL-1995, March 1976.

MATHEMATICAL AND EXPERIMENTAL INVESTIGATIONS ON DISPERSION AND RECIRCULATION OF PLUMES FROM DRY COOLING TOWERS AT WYODAK POWER PLANT IN WYOMING. Y. Onishi and D. S. Trent, BNWL-1982, February 1976.

ALUMINUM ALLOY PERFORMANCE UNDER DRY COOLING TOWER CONDITIONS. A. B. Johnson, Jr., S. Begaj, M. W. Martini, and R. P. May, PNL-2392, December 1977.

Advanced dry (dry/wet) cooled systems:

PRELIMINARY EVALUATION OF WET/DRY COOLING CONCEPTS FOR POWER PLANTS. W. V. Loscutoff, BNWL-1969.

COMPATIBILITY OF AMMONIA WITH CANDIDATE DRY COOLING SYSTEM MATERIALS. D. R. Pratt, BNWL-1992, April 1976.

SCALE FORMATION IN DELUGED DRY COOLING SYSTEMS. D. R. Pratt, BNWL-2060, March 1976.

AMMONIA AS AN INTERMEDIATE HEAT EXCHANGE FLUID FOR DRY COOLED TOWERS. R. T. Allemann, B. M. Johnson, and G. C. Smith, BNWL-SA-5997, September 1976.

A group of reports (including this report) has recently been issued. This group serves the dual purpose of developing cost optimization models for dry cooling systems based on available technology and comparing the results of analyzing the costs of these systems with the projected cost of several advanced dry and dry/wet systems. Included in this group are:

AN ENGINEERING AND COST COMPARISON OF THREE DIFFERENT ALL-DRY COOLING SYSTEMS. B. C. Fryer, D. W. Faletti, Daniel J. Braun, David J. Braun and L. E. Wiles, BNWL-2121, September 1976.

A STUDY OF THE COMPARATIVE COSTS OF FIVE WET/DRY COOLING TOWER CONCEPTS. F. R. Zaloudek, R. T. Allemann, D. W. Faletti, B. M. Johnson, H. L. Parry, G. C. Smith, R. D. Tokarz, and R. A. Walter, BNWL-2122, September 1976.

DRY COOLING OF POWER GENERATING STATIONS: A SUMMARY OF THE ECONOMIC EVALUATION OF SEVERAL ADVANCED CONCEPTS VIA A DESIGN OPTIMIZATION STUDY AND A CONCEPTUAL DESIGN AND COST ESTIMATE. B. M. Johnson, R. T. Allemann, D. W. Faletti, B. C. Fryer and F. R. Zaloudek, BNWL-2120, September 1976.

COSTS AND COST ALGORITHMS FOR DRY COOLING TOWER SYSTEMS. P. A. Ard, C. H. Henager, D. R. Pratt and L. E. Wiles, BNWL-2123, September 1976.

A USER'S MANUAL FOR THE BNW-I OPTIMIZATION CODE FOR DRY-COOLED POWER PLANTS. David J. Braun, Daniel J. Braun, Warren V. De Mier, D. W. Faletti and L. E. Wiles, BNWL-2180, January 1977.

COMPARATIVE COST STUDY OF FOUR WET/DRY COOLING CONCEPTS THAT USE AMMONIA AS THE INTERMEDIATE HEAT EXCHANGE FLUID R. D. Tokarz, Daniel J. Braun, B. M. Johnson, R. T. Allemann, David J. Braun, H. L. Parry, G. C. Smith and F. R. Zaloudek, PNL-2661, May 1978.

A DESCRIPTION AND COST ANALYSIS OF A DELUGE DRY/WET COOLING SYSTEM. L. E. Wiles, J. A. Bamberger, Daniel J. Braun, David J. Braun, D. W. Faletti and C. E. Willingham, PNL-2498, June 1978.

A USER'S MANUAL FOR THE BNW-II OPTIMIZATION CODE FOR DRY/WET-COOLED POWER PLANTS. Daniel J. Braun, Judith A. Bamberger, David J. Braun, Duane W. Faletti and Larry E. Wiles, PNL-2674, May 1978.

Two reports have been issued which consider the future need for any cooling and the potential benefit/cost ratio of a large-scale demonstration.

AN OVERVIEW OF ECONOMIC, LEGAL, AND WATER AVAILABILITY FACTORS AFFECTING THE DEMAND FOR DRY AND WET/DRY COOLING OF THERMAL POWER PLANTS. P. L. Hendrickson, BNWL-2268, June 1977.

ESTIMATION OF BENEFITS FROM DEMONSTRATING ADVANCED DRY COOLING TECHNOLOGY: A FRAMEWORK AND PARTIAL ANALYSIS. J. W. Currie and T. J. Foley, BNWL-2182, April 1977.



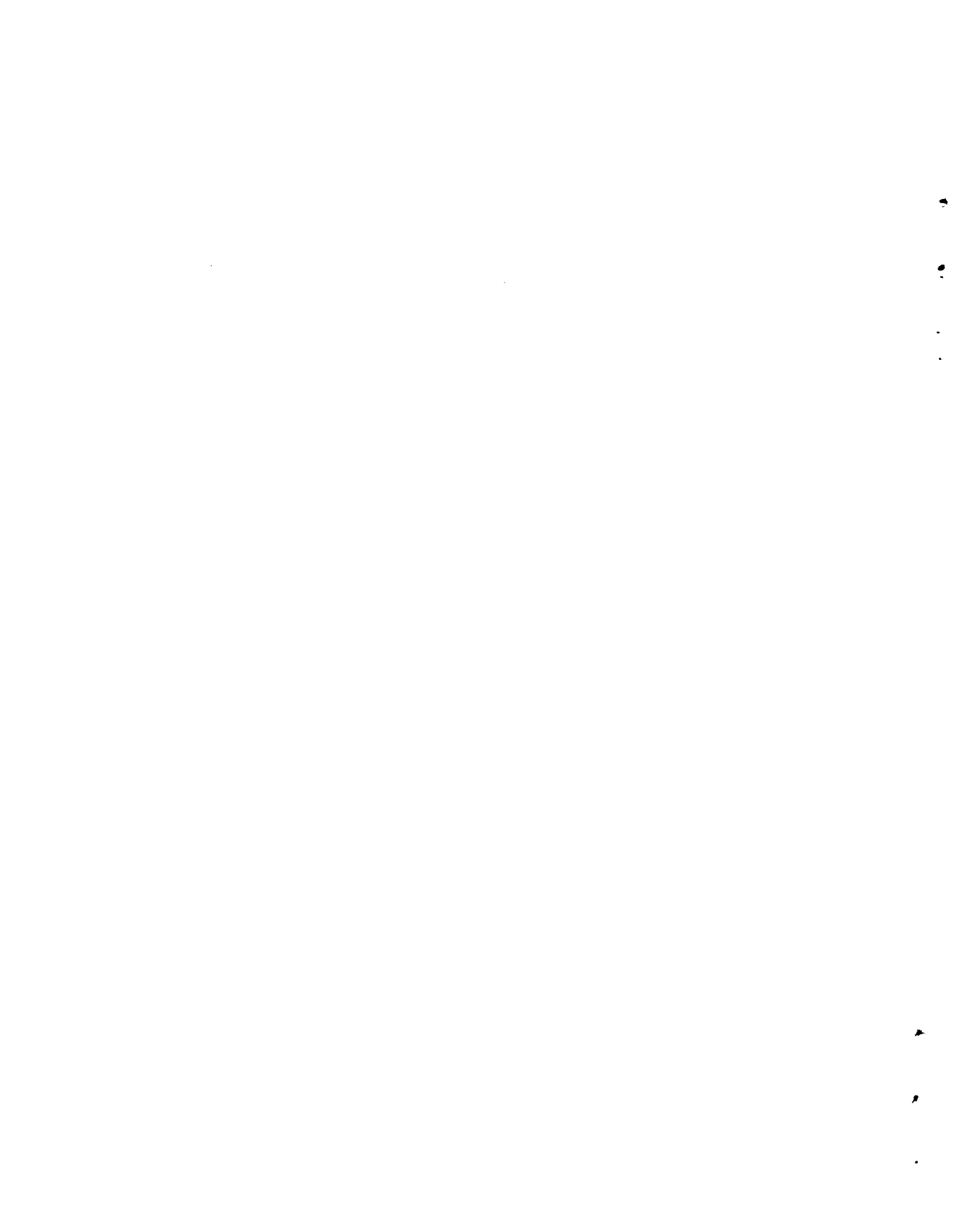
CONTENTS

PREFACE	iii
SUMMARY	v
FOREWORD	vii
FIGURES	xiii
1.0 INTRODUCTION	1.1
2.0 COOLING SYSTEM PHYSICAL DESCRIPTION	2.1
2.1 OVERVIEW	2.1
2.2 COOLING SYSTEM FEATURES	2.4
2.2.1 Condenser/Reboiler	2.4
2.2.2 Piping System	2.4
2.2.3 Cooling Towers	2.5
3.0 COOLING SYSTEM OPTIMIZATION RATIONALE	3.1
3.1 UTILITY MODEL	3.1
3.2 OPERATING STRATEGY	3.1
3.3 STEAM SUPPLY AND PLANT SCALING	3.3
3.4 COSTING METHOD	3.5
3.5 CALCULATIONAL ORDER	3.7
3.6 OPTIMIZATION	3.8
4.0 CALCULATION PROCEDURE	4.1
4.1 INTERMEDIATE AMMONIA DRY/WET COOLING SYSTEM (CALC)	4.3
4.2 CONDENSER/REBOILER DESIGN AND COSTING	4.7
4.2.1 Condenser/Reboiler Design (SPDES)	4.7
4.2.2 Condenser/Reboiler Costing (SURCON)	4.8
4.3 HEAT EXCHANGER DESIGN AND COSTING (COSTEX)	4.9
4.4 FAN SYSTEM SELECTION (FAN)	4.10
4.5 PIPING SYSTEM DESIGN AND COSTING	4.11
4.5.1 NH ₃ Piping System Design and Costing (PIPCLS and PIPCLR)	4.11
4.5.2 DeLuge Piping System Design and Costing (DELUGEP)	4.14

4.6	PLANT SCALING DUE TO ALL-DRY OPERATIONAL MODE	4.15
4.6.1	Steam System Scaling (SSCALE)	4.15
4.6.2	Plant Scaling (SCALP)	4.16
4.7	DELUGE ENHANCEMENT (CONSUMP)	4.18
4.8	INCREMENTAL COST OF THE DRY/WET COOLING SYSTEM FOR THE POWER PLANT OPERATING OVER THE YEARLY TEMPERATURE PROFILE (NOVART)	4.21
5.0	COMPUTER PROGRAM	5.1
5.1	GENERAL INFORMATION	5.1
5.2	INPUT	5.2
5.3	DRY/WET MODEL OUTPUT	5.2
	REFERENCES	Ref.1
	ACKNOWLEDGMENTS	
	APPENDIX A - AIR-SIDE PERFORMANCE CORRELATIONS FOR HÖTERV SURFACE	A.1
	APPENDIX B - FIN EFFICIENCY OF PLATE FIN HEAT EXCHANGERS	B.1
	APPENDIX C - COMPUTATION OF DELUGE PERFORMANCE	C.1
	APPENDIX D - METEOROLOGY METHODOLOGY	D.1
	APPENDIX E - COMPARISON OF AIR VELOCITY THROUGH DELUGE AND DRY SECTIONS FOR HÖTERV SURFACES	E.1
	APPENDIX F - HEAT TRANSFER AND PRESSURE DROP CORRELATIONS	F.1
	APPENDIX G - COST ALGORITHMS FOR THE HÖTERV PLATE FIN HEAT EXCHANGER BUNDLE	G.1
	APPENDIX H - OPTIMIZATION TECHNIQUE	H.1
	APPENDIX I - BNW-II COMPUTER CODE LISTING	I.1

FIGURES

1	Dry/Wet Cooling System with Ammonia as Intermediate Coolant	2.2
2	Temperature Relationships for Steam, Ammonia, and Air (dry/bulb) for the Cooling System with Ammonia as the Intermediate Coolant	2.3
3	Main Circulation Vapor Supply and Liquid Return Piping	2.5
4	Ammonia Distribution Piping in an 8-Sided Tower	2.6
5	Ammonia Distribution Piping in a 16-Sided Tower	2.7
6	Ammonia Distribution and Collection to the Heat Exchanger Bundles for an 8-Sided Tower	2.8
7	Ammonia Distribution and Collection to the Heat Exchanger Bundles for a 16-Sided Tower	2.9
8	Heat Exchanger Plate Fin and Tube Arrangement	2.10
9	Tower Side Cross Section	2.11
10	Operating Regimes for a Power Plant with a Deluged Cooling System	3.2
11	Heat Rate Versus Back Pressure - Fossil Turbines	3.4
12	Typical Annual Performance of a Dry-Cooled Plant	3.4
13	Dry/Wet Cooling System Computer Optimization	3.10
14	BNW-II Program Flow Diagram	4.2
15	Subroutine CALC Flow Diagram	4.4
16	Operating Regimes for a Power Plant with a Deluged Cooling System	4.19
17	Sample Input for Dry/Wet Model	5.4
18	Dry/Wet Model Sample Output	5.21



A USER'S MANUAL FOR THE BNW-II OPTIMIZATION
CODE FOR DRY/WET-COOLED POWER PLANTS

1.0 INTRODUCTION

This report describes BNW-II, a computer code developed by the Pacific Northwest Laboratory (PNL) as part of its Dry Cooling Enhancement Program sponsored by the U.S. Department of Energy (DOE).

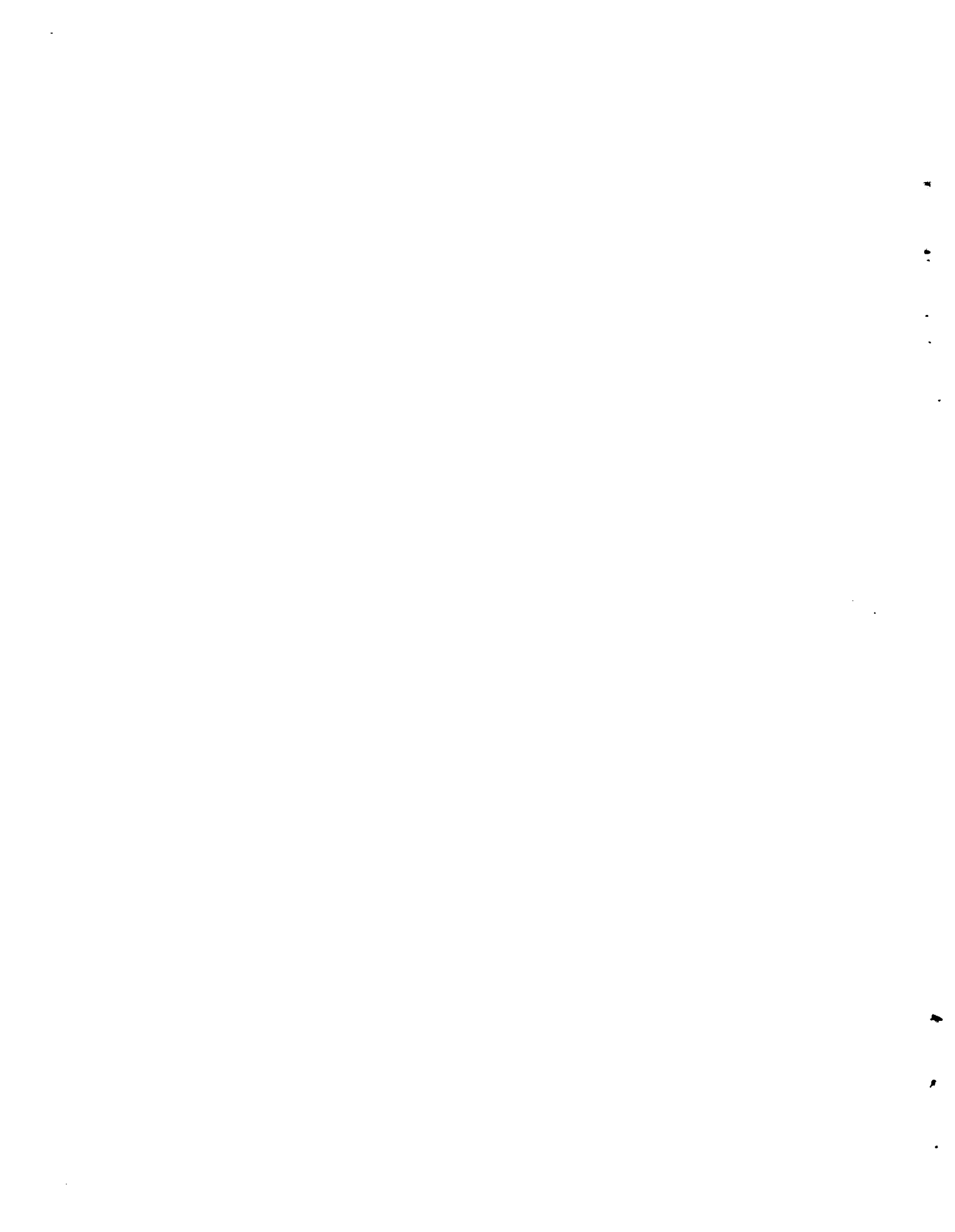
The manual is primarily intended to show how the BNW-II code is used. Hence, details are provided on preparing the required input and interpreting the output.

Although the BNW-II code described here was developed to model a specific cooling system concept, it can be made applicable to a wide range of dry/wet concepts by appropriately modifying the cost and performance algorithms for the heat rejection system.

BNW-II was previously used to compare costs of an all-dry cooling system with those of a dry/wet cooling system.^(1,2) Data obtained with this optimization code revealed a significant difference in costs of the two cooling systems examined.

Along with the BNW-II user's instructions, this document also covers

- the physical description of the dry/wet cooling system modeled by the code;
- the rationale used to optimize the cooling system;
- the main calculation procedures used in the BNW-II program; and
- the basis for the performance and cost models.



2.0 COOLING SYSTEM PHYSICAL DESCRIPTION

The BNW-II computer code was written to model a power plant dry/wet cooling system with these three features:

- an intermediate ammonia cooling loop
- plate finned heat exchanger surfaces (wet augmentation achieved by deluging the surfaces with water)
- induced draft air flow.

2.1 OVERVIEW

The power plant cooling system is defined herein to include all plant components connected by, or directly associated with, the primary coolant medium of the heat rejection system. In general, this comprises the plant components beyond the low pressure turbine exhaust flange.

The cooling system modeled by BNW-II is shown schematically in Figure 1. The primary coolant medium is ammonia, which indirectly transfers the low availability energy from the low pressure exhaust steam to the atmosphere. The principal features of the cooling system are the condenser/reboiler, the ammonia distribution piping, and the cooling towers.

The temperature relationship between the steam, ammonia, and air for the heat rejection cycle is shown in Figure 2.

The heat rejection process begins as low pressure steam enters the condenser/reboiler. Heat is transferred from the steam in the shell to the ammonia in the tubes while both fluids experience a phase change. That is, the steam condenses at constant temperature and the liquid ammonia vaporizes at constant temperature after being heated from a slightly subcooled state. The condensed steam is returned to the feedwater circuit. At the condenser/reboiler outlet the ammonia vapor is separated from the ammonia liquid, which is collected for recirculation to the condenser/reboiler. The nearly saturated ammonia vapor is distributed to the cooling towers. Pressure losses in the distribution

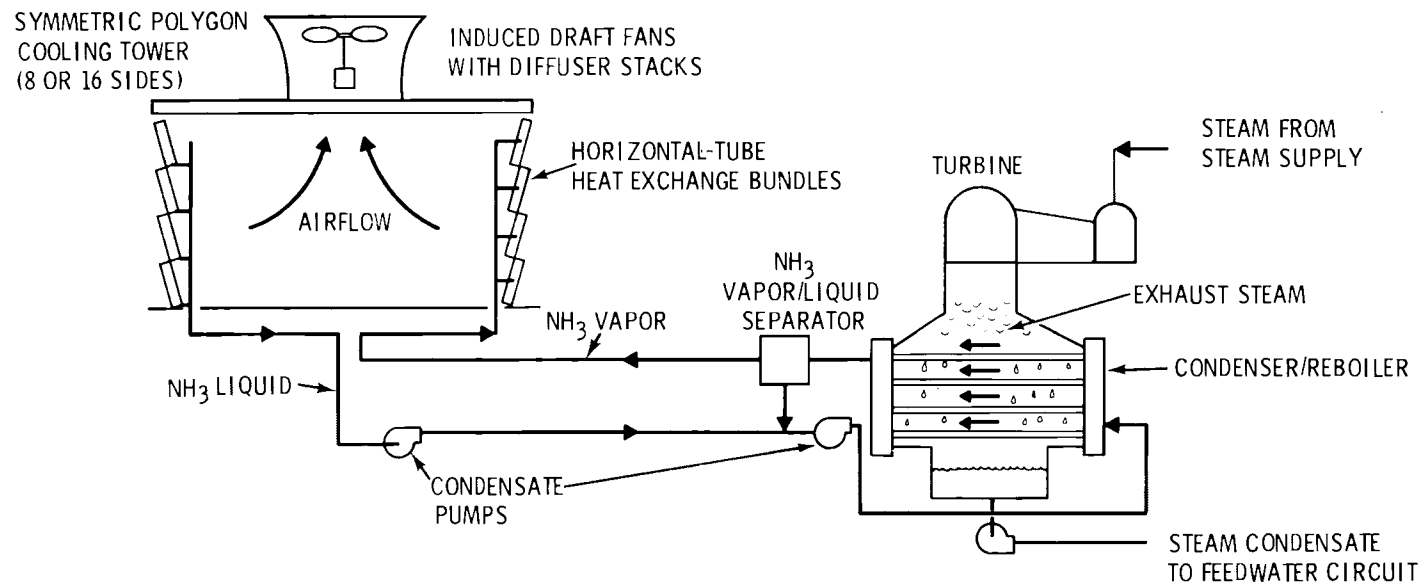


FIGURE 1. Dry/Wet Cooling System with Ammonia as Intermediate Coolant

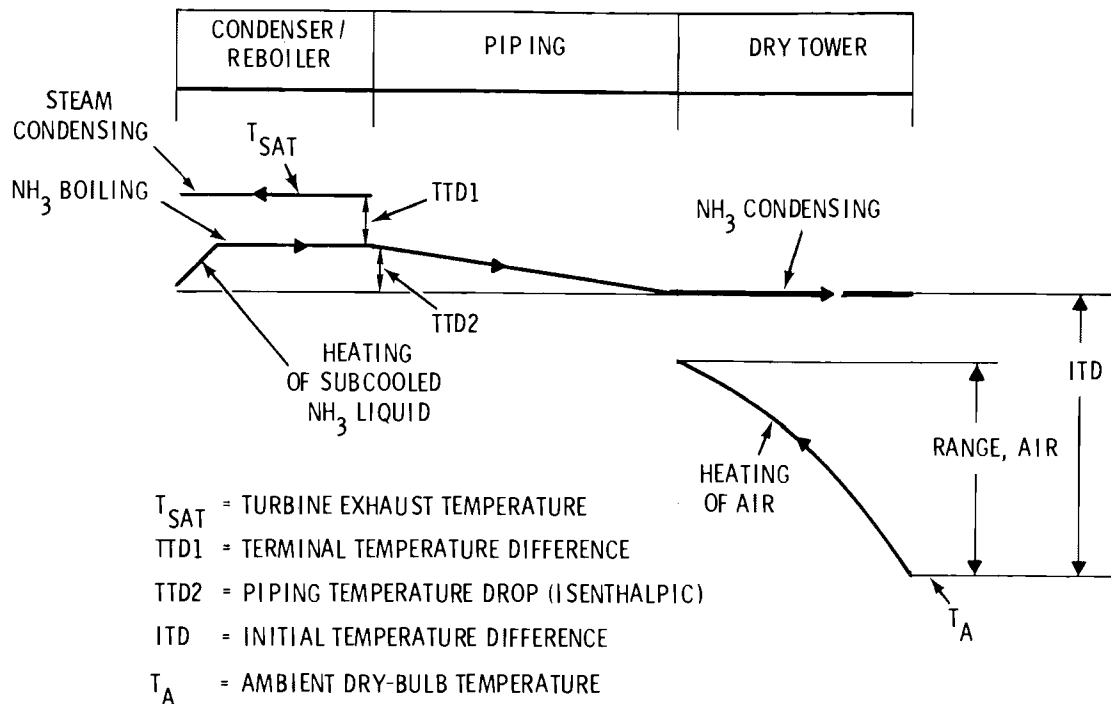


FIGURE 2. Temperature Relationships for Steam, Ammonia, and Air (dry-bulb) for the Cooling System with Ammonia as the Intermediate Coolant

piping cause the temperature of the saturated vapor to decrease slightly. The vapor is passed through horizontal tubes in the plate finned heat exchanger bundles where it condenses at constant temperature. The ammonia liquid is returned to the condenser/reboiler.

Condensation of the ammonia vapor occurs as heat is transferred to air passed over the finned surface of the heat exchanger. The air flow is induced by a system of fans located on the cooling tower roof.

To enhance the cooling capacity of the finned surface when the air dry-bulb temperature is high, water is distributed to the top of the cooling tower. The water forms a film over the plate fins and is allowed to flow to the base of the tower where it is collected and recirculated. This form of enhanced cooling is called "deluge" cooling. The water is referred to as the deluge water or delugeate.

2.2 COOLING SYSTEM FEATURES

The condenser/reboiler, ammonia distribution piping, and the cooling towers are described in the following subsections.

2.2.1 Condenser/Reboiler

The condenser/reboiler is similar in appearance to the conventional single-pass shell and tube surface condenser. The most significant modification employed in this study has been the use of enhanced heat transfer surfaces on both the ammonia side and steam side of the horizontal tubes. The aluminum tubing requires stainless steel impingement shields to protect against steam erosion. The conventional condenser water boxes are replaced with tube headers. The headers, tubes and tube sheets are specified to accommodate ammonia pressures up to 400 psi.

Design specifications of the condenser/reboiler include

- nominal tube OD of 1 inch
- tube length of 50 feet
- condensate drain-off at every 10 feet of tube depth
- two shells
- ammonia exit quality of 0.8.

2.2.2 Piping System

The ammonia distribution piping system is divided into the supply piping, which transports the ammonia vapor from the condenser/reboiler to the heat exchanger bundles, and the return piping, which transports the ammonia liquid from the heat exchanger bundles to the condenser/reboiler. Both the supply and return piping have been further divided into the main circulation piping and the tower distribution piping. The tower distribution piping is described in Section 2.2.3 on cooling towers.

The main circulation supply and return piping are shown in Figure 3. The supply and return piping are modeled as having nearly identical "plan views". The pipe diameters are different, however, because of dramatically different densities and design velocities of the ammonia vapor and liquid. In addition

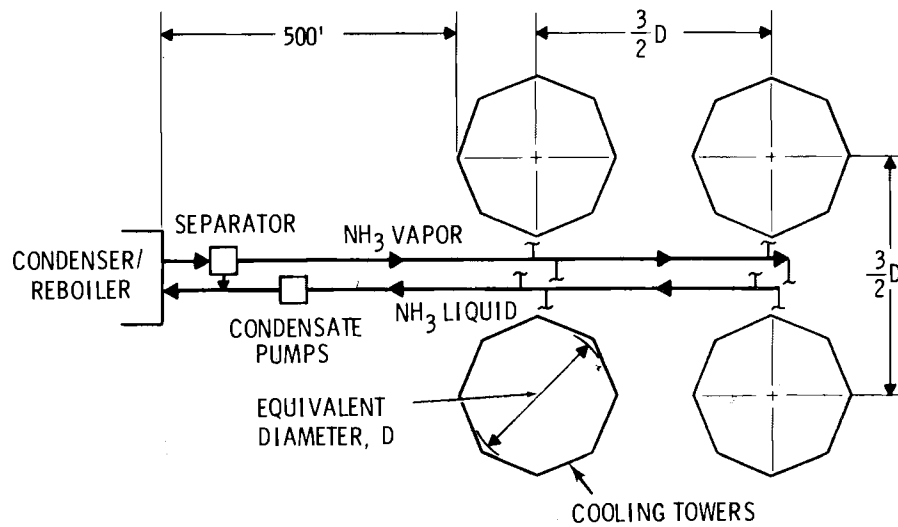


FIGURE 3. Main Circulation Vapor Supply and Liquid Return Piping

to the pipe, the design includes specification of valves, tees, elbows, reducers, and flanges, as required. All pipe, valves, and fittings are designed for 350 psi. All pipe components are assumed to be available in sizes from 6- to 144-inch diameters in 6-inch increments. Pipe sizing is based on the mass flow rate and design velocity. The distance from the condenser/reboiler outlet to the first tower is usually 500 feet. Otherwise, pipe lengths are based on the tower spacing, which is $3/2$ of the equivalent tower diameter. Further details of the circulation piping design are available in References 1 and 2.

2.2.3 Cooling Towers

The cooling towers are modeled as symmetric polygons having either 8 or 16 sides. As shown in Figure 3 the towers are spaced on a square grid; the distance between adjacent towers is $3/2$ of the equivalent tower diameter. The diameter is based on the roof area of each tower. It should not be implied from Figure 3 that only four towers are allowed. Designs may have any number of towers. Towers are evenly spaced in the direction of the main circulation piping. All towers are opposed by a tower on the opposite side of the main circulation piping unless the total number of towers is odd, in which case one of the corner positions on the grid would be vacant.

The principal components within the cooling towers are the ammonia and deluge piping, the heat exchanger bundles, and the fan system.

2.2.3.1 Ammonia Piping

The ammonia distribution piping in the towers is shown in Figure 4 for an 8-sided tower and in Figure 5 for a 16-sided tower. The design also includes specification of valves, tees, elbows, reducers and flanges, as required. All pipe, valves, and fittings are designed for 350 psi. All pipe components are assumed to be available in sizes from 6- to 144-inch diameters in 6-inch increments. Pipe sizing is based on mass flow rate and design velocity. The supply and return systems follow nearly identical routes. However, pipe diameters are different due to the dramatically different densities and design velocities of ammonia liquid and vapor. The ammonia vapor from the main circulation piping is distributed to the four tower quadrants through the tower distribution header. Isolation valves are provided for each

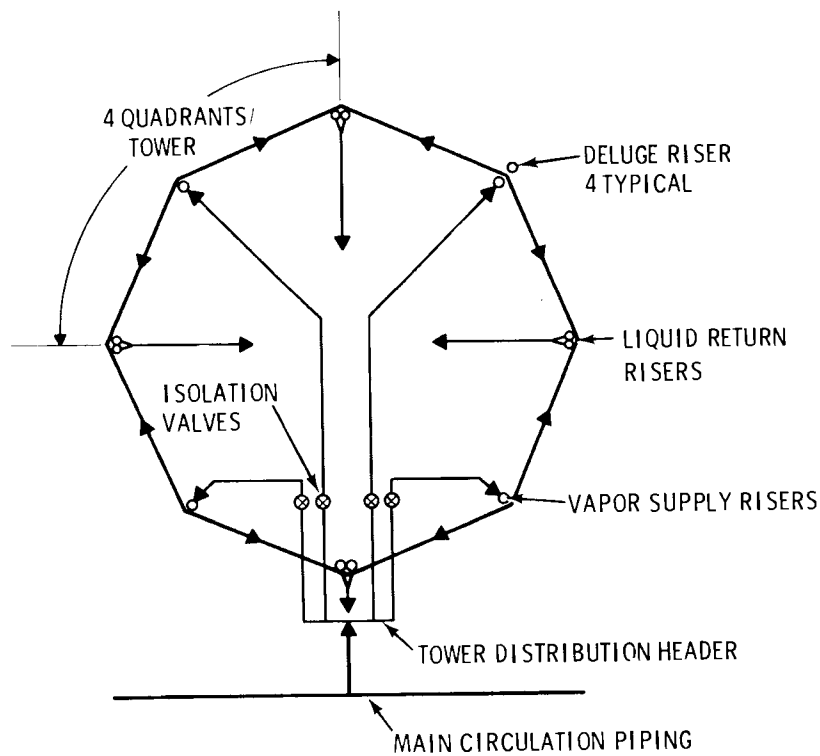


FIGURE 4. Ammonia Distribution Piping in an 8-Sided Tower

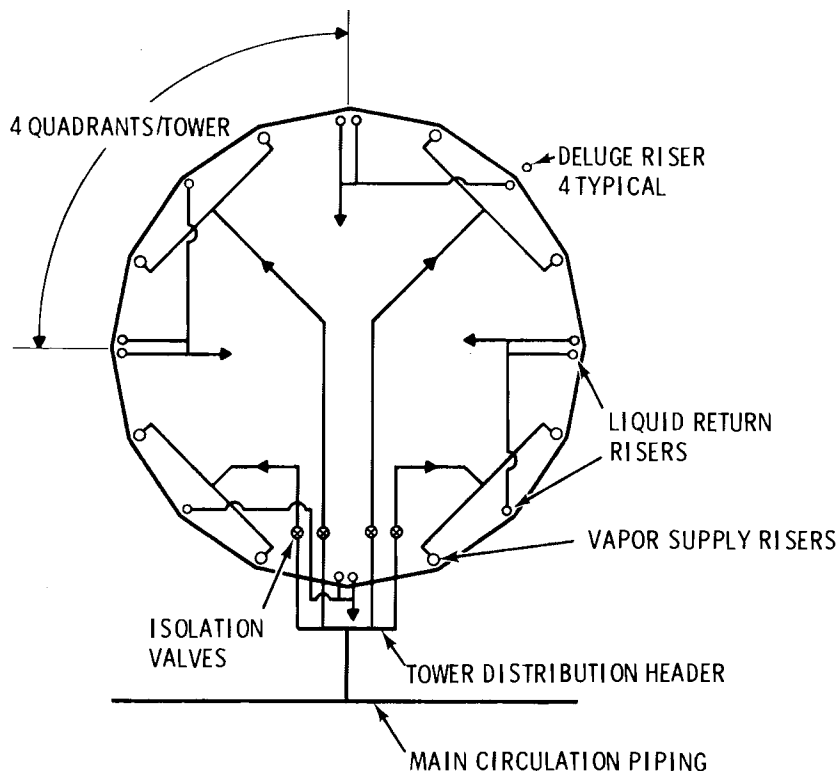


FIGURE 5. Ammonia Distribution Piping in a 16-Sided Tower

quadrant for safety and operational control. The vapor is distributed to the headers of the horizontal tube heat exchanger bundles by a riser. The ammonia is distributed to headers on either side of the riser as shown in Figures 6 and 7 for the 8-sided and 16-sided towers, respectively.

The features of the tower piping for the vertical tube circular tower all-dry ammonia cooling system^(3,4) formed the starting point for this design. The references will provide further details, as many similarities exist.

2.2.3.2 Heat Exchanger Bundles

The plate fin heat exchanger bundles comprise a staggered arrangement of circular, parallel tubes tied together by continuous plate fins. These fins are perpendicular to the tubes in two directions; i.e., both the face and the leading edge of the plate fin are perpendicular to the axis of each

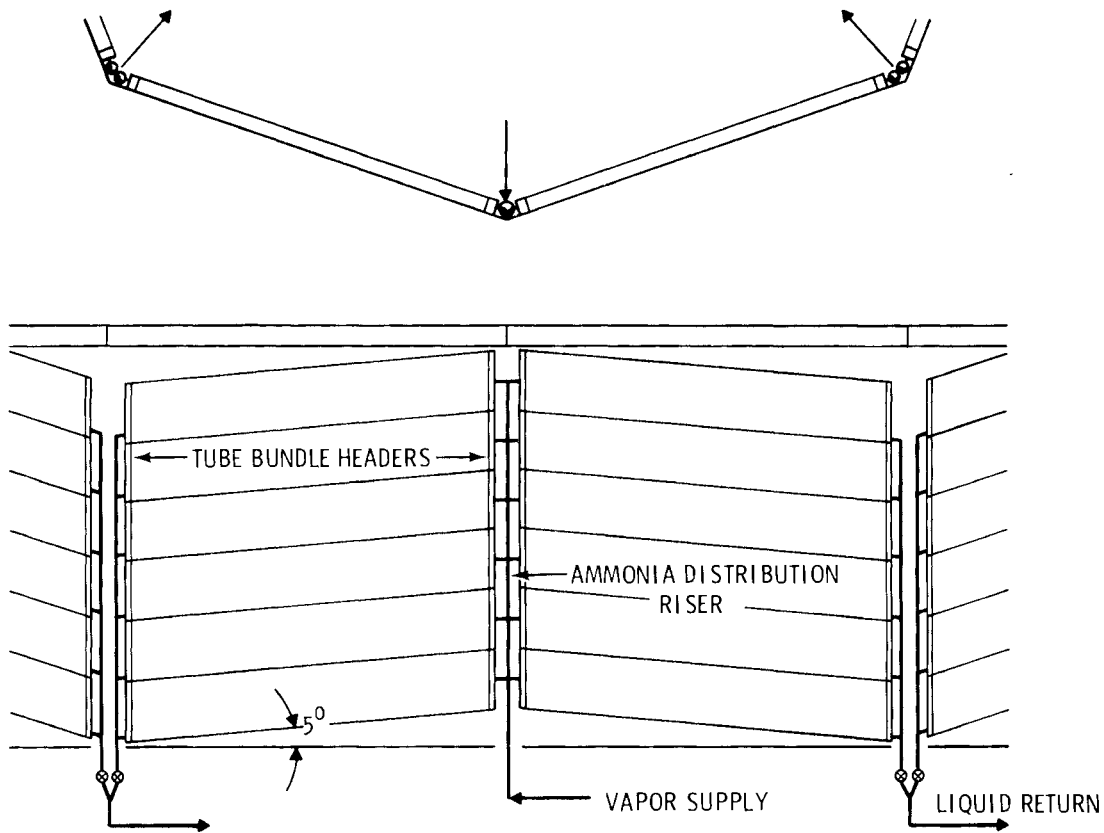


FIGURE 6. Ammonia Distribution and Collection to the Heat Exchanger Bundles for an 8-Sided Tower

tube. This surface is shown in Figure 8. Headers on either end of the tube and plate fin assembly distribute and collect the ammonia coolant in the tubes.

The bundle width, i.e., the width of the bundle face, is 12 feet to allow for shipping. The total bundle length is not limited because any number of bundle segments can be bolted end-to-end. The bundles are arranged on the sides of the towers as shown in Figures 6, 7 and 8. The bundles are tilted 5 degrees from horizontal (Figures 6 and 7) to assist in collecting the ammonia liquid. The bundle face is tilted 15 degrees from vertical (Figure 9) so that the effects of gravity and air friction will balance to prevent the leading edge of the plate fins from drying out during deluge operation.

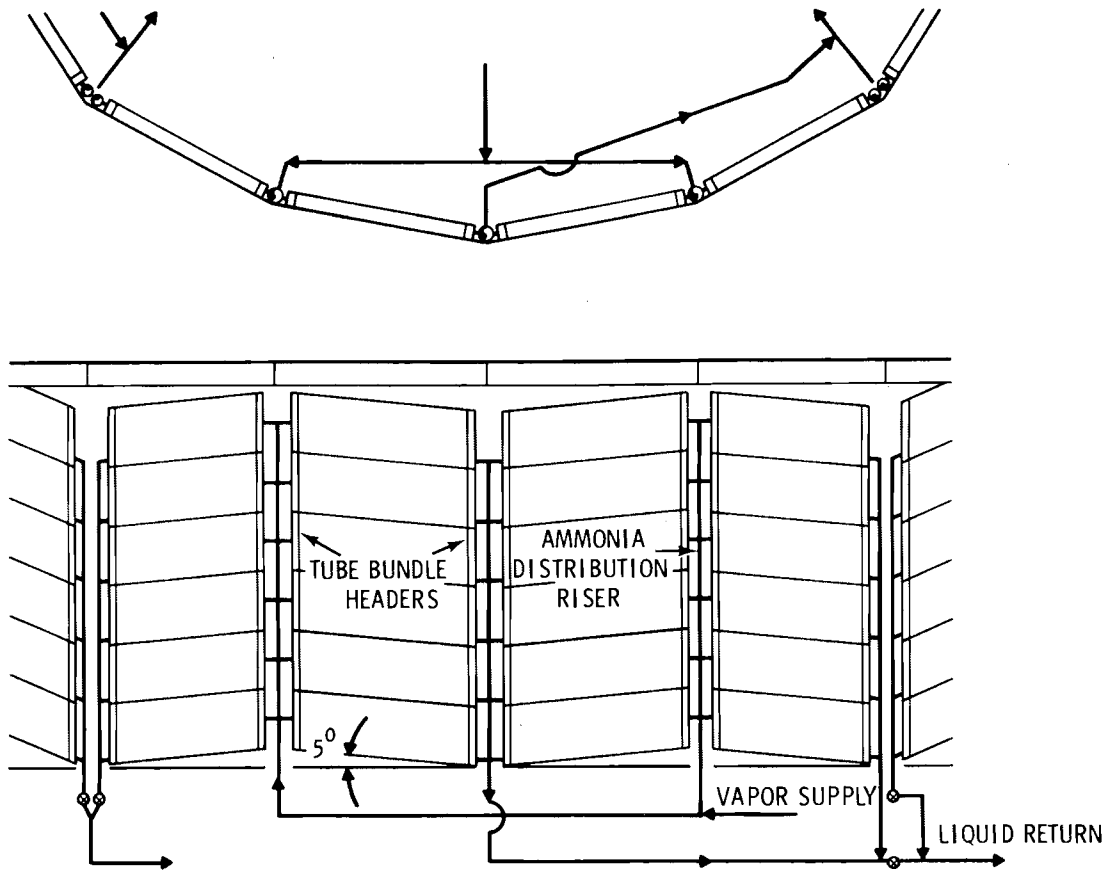


FIGURE 7. Ammonia Distribution and Collection to the Heat Exchanger Bundles for a 16-Sided Tower

2.2.3.3 Deluge Piping

The deluge water is pumped to the top of the tower via a riser at the center of each tower quadrant. The plan view of the deluge distribution piping layout is similar to that of the ammonia piping (Figures 4 and 5) except for the pipe used to distribute the deluge water onto the heat exchangers (Figure 9). The bulk of the deluge water is distributed to the deluge distribution plate at the top of the tower by a pipe extending from the riser to the ends of the quadrant. At the top of each subsequent tube bundle, deluge water is supplied by a smaller pipe, which also extends from the riser to the end of the quadrant. This secondary deluge water is provided to make up the water that has evaporated from the adjacent upper bundle.

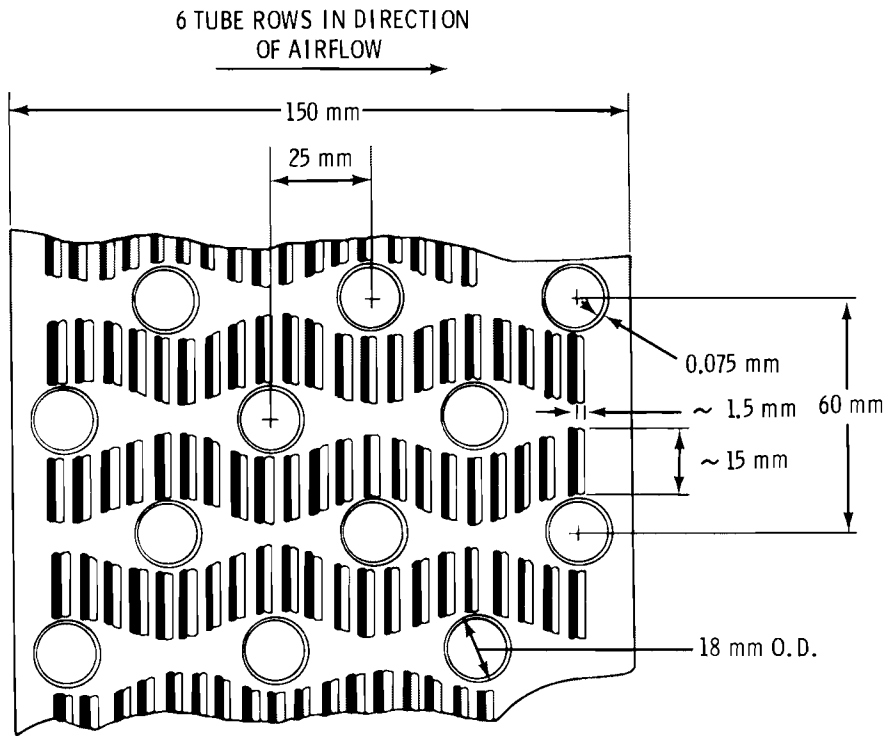


FIGURE 8. Heat Exchanger Plate Fin and Tube Arrangement

The deluge distribution plates catch the nonevaporated deluge water and redistribute it along with the make-up water to the bundle below. At the base of each tower a gravity drain returns the deluge water to a sump. Water is treated and the appropriate amount of make-up water is provided.

2.2.3.4 Fan System

Air flow through the heat exchanger is induced by single-speed, single-pitch fans resting on the roof of the cooling tower. Fans are assumed to be available with blade diameters of 24, 26, 28, 30, 40 or 60 feet.

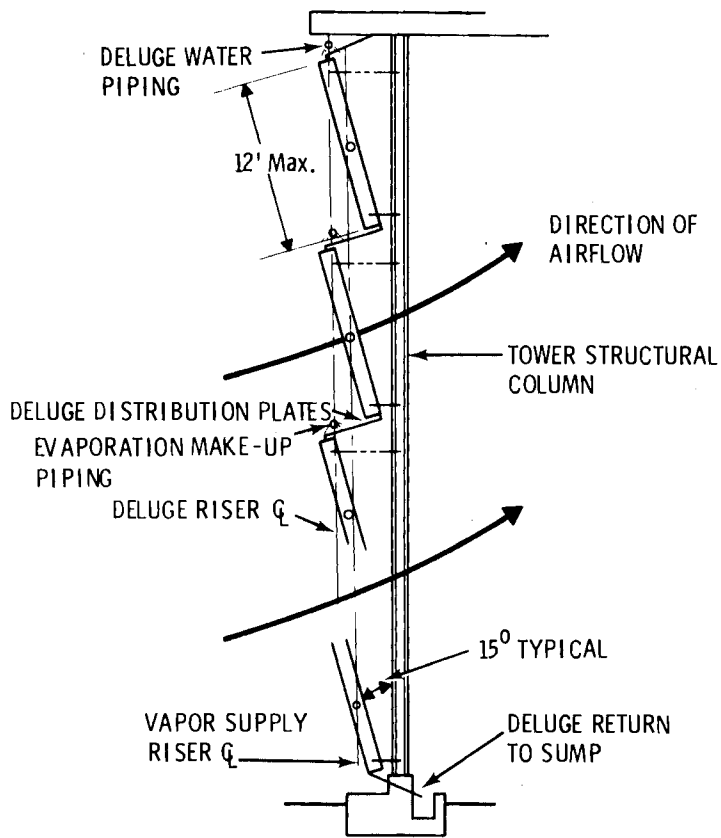
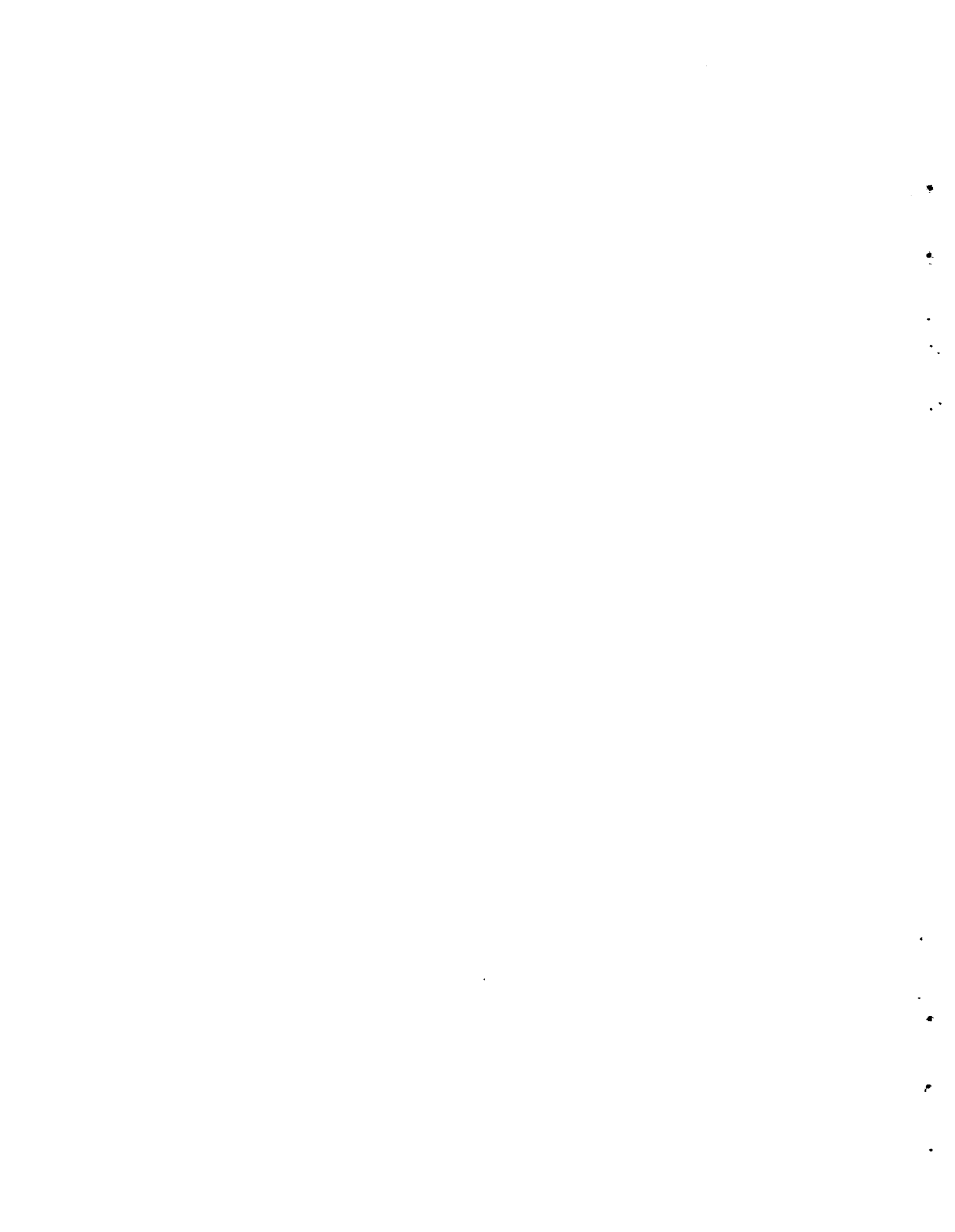


FIGURE 9. Tower Side Cross Section



3.0 COOLING SYSTEM OPTIMIZATION RATIONALE

The cooling system is designed to minimize the power production costs of an idealized power plant using a dry/wet cooling system. The "cost" of the cooling system is defined as an incremental increase in power production costs compared to the cost of producing power with a power plant having a zero-cost cooling system and a conventional turbine operating at 3.5 in. Hg. (See Section 3.5 for details on how the cost of the cooling system is calculated.)

3.1 UTILITY MODEL

The idealized power plant consists of one dry/wet-cooled, base-loaded power plant with a gas turbine complement^(a) to provide power at higher ambient temperatures. (The reference plant requires no gas turbine complement because its turbine back pressure is constant at 3.5 in. Hg.) This idealized utility operates in an on-off mode. It supplies full power at a constant level (fixed demand) when in the "on" mode and no power during the "off" mode. The fraction of time that the idealized utility is in the "on" mode is equal to the capacity factor. Power for the cooling system fans and pumps is provided by the dry/wet plant.

The power plant can produce more than the utility system's power requirements below the design temperature (the ambient temperature at which the power plant, when operating all dry, has a net power output equal to the utility system's demand). Because no market exists for this excess power, the power plant is not given credit for this excess generation capacity. However, the power plant is given credit for reduced base plant fuel consumption resulting from the lower turbine back pressures.

3.2 OPERATING STRATEGY

The strategy selected by PNL for operating the plant was to hold the turbine back pressure constant to the extent possible once deluging is used. This was accomplished by increasing the fraction of the heat exchanger surface

(a) Other sources of replacement energy such as hydro or cycling plants can be simulated by appropriate changes in the capital and fuel costs used as inputs to the computer program.

deluged as the ambient temperature increases. Constant back pressure operation during deluge was selected because it minimized the size (hence cost) of the gas turbine contingent without incurring any obvious cost penalties.

Three operating zones are shown in Figure 10.

Constant back pressure operation during deluge, the most common mode of operation occurs in Zone 2. Constant back pressure operation during deluge is not always feasible because of the back pressure limitations of steam turbines. It also is not feasible during times when the ambient temperature exceeds that at which 100% deluging is required. Operation in Zone 3 results in an increase in turbine back pressure once the ambient temperature exceeds that at which the heat exchangers are 100% deluged. Constant back pressure operation is not possible in Zone 1 because of limitations in either the number of times per year or in the number of hours per year which the turbine can reach or exceed certain back pressure limits. For a given turbine specification and a given meteorology, these limitations can be represented as a series of steps as shown by the maximum turbine back pressure curve which forms the upper bound of Zone 1 in Figure 10.

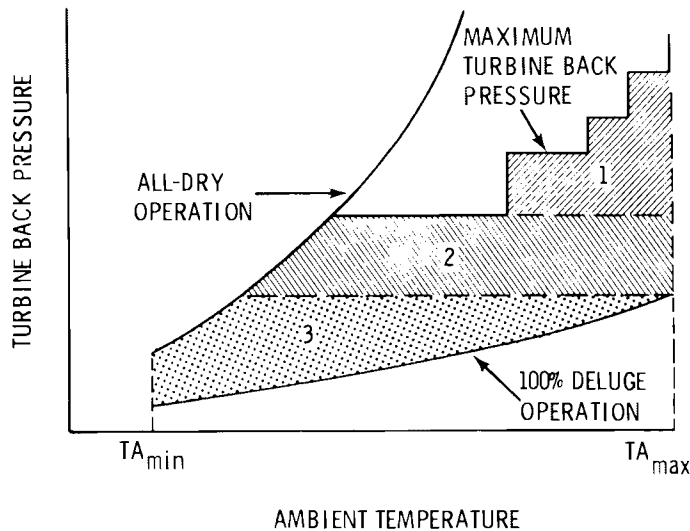


FIGURE 10. Operating Regimes for a Power Plant with a Deluged Cooling System

3.3 STEAM SUPPLY AND PLANT SCALING

As mentioned previously, the incremental cost is computed against that of a plant with a conventional turbine operating at 3.5 in. Hg with a zero cost cooling system. The choice of 3.5 in. Hg was made because it is the turbine back pressure at which the power output of conventional turbines is often rated. That is, a 1000-MWe turbine will produce 1000 MWe at 3.5 in. Hg. Higher back pressures result in less power; lower back pressures result in more power. Because BNW-II considers other than conventional turbines with 3.5 in. Hg rated back pressure, steam supply scaling is used. Because BNW-II designs plants operating at other than the rated back pressure of the turbine under consideration, plant scaling for heat rate is carried out. Further, because the utility model upon which BNW-II is based requires the plant to produce power for its own cooling system auxiliaries (fans and pumps), plant scaling for auxiliary power is carried out. These three scaling processes are described in more detail below. As background, Figure 11 gives the comparative heat ratio of three candidate turbines and Figure 12 shows the relationship between the reference plant power output and the gross and net power output of the dry/wet-cooled plant.

Steam supply scaling is best illustrated by an example. Assume that the turbine under consideration is a high back pressure turbine with a rated back pressure (the back pressure at which it delivers rated power) of 6 in. Hg. This turbine was selected because it can operate at back pressures up to 15 in. Hg instead of the 5 in. Hg maximum typical of the conventional turbine. This higher back pressure capability introduced a penalty of a 5% larger heat rate than that of a conventional turbine. This turbine will therefore require a 5% larger steam supply. Therefore, the steam supply is scaled up by 5% and the increase in plant cost is computed by assuming that the steam supply system makes up 1/3 the cost of the nominal power plant construction cost.

Scaling for heat rate is also best illustrated by example. Suppose that, at the design temperature, the heat rejection system is capable of maintaining the turbine back pressure at 4.0 in. Hg. At 4.0 in. Hg, the high back pressure turbine puts out 2% more power than at 6 in. Hg. Remember that at the design

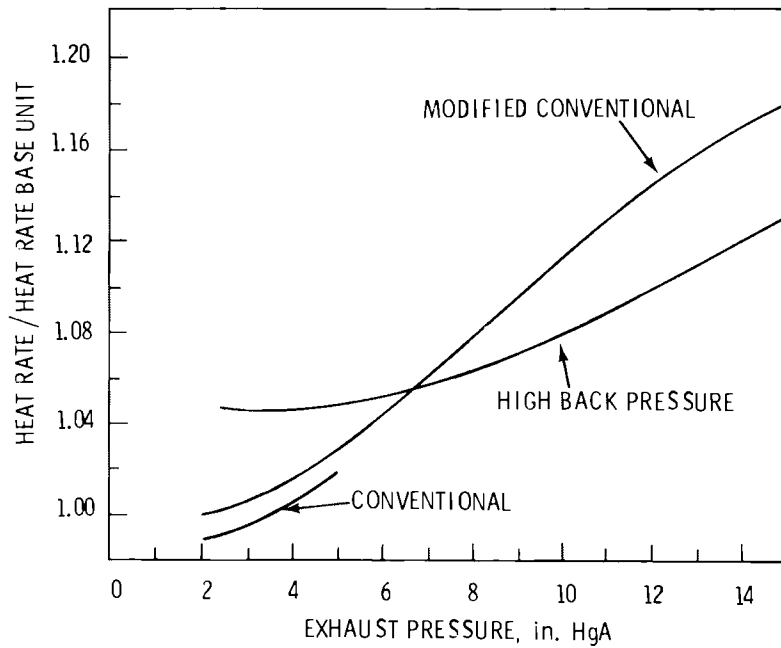


FIGURE 11. Heat Rate Versus Back Pressure - Fossil Turbines

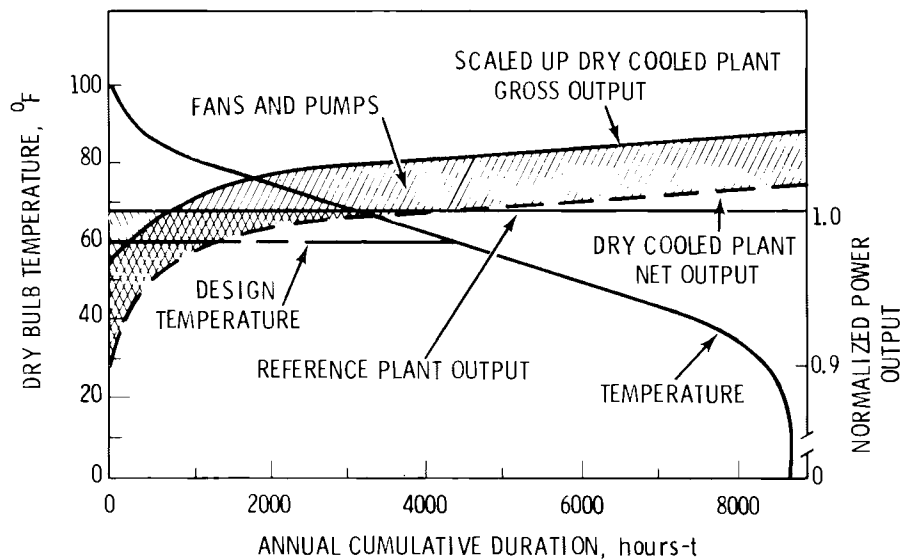


FIGURE 12. Typical Annual Performance of a Dry-Cooled Plant

temperature the output of the power plant is equal to the fixed demand of the utility system. Therefore, a power plant which is 2% too large is designed. Hence, the size and cost of the plant is reduced by 2%. No change is made in heat rejection system size because it was sized for a turbine operating at 4.0 in. Hg.

Continuing on, suppose a 1000-MWe plant requires 30 MWe for fan power and 10 MWe for pump power for the cooling system. Thus, the plant's net power output is only 960 MWe instead of the 1000 MWe required to meet demand. Plant scaling for auxiliary power refers to scaling up the plant so that its net power is equal to the fixed demand; in this example, the required increase in plant size is $40/(1000-40) \times 1000 = 41.67$ MWe, not 40 MWe, because of the increased power demands of the larger cooling system.

A trade-off exists between plant scaling and the size of the gas turbine contingent. The BNW-II optimization code takes this trade-off into account.

3.4 COSTING METHOD

The incremental cost of dry/wet cooling includes the following capital items:

- a. cooling system equipment and installation costs (including indirect costs such as profit, overhead and engineering)
- b. increased steam supply system cost
- c. change in plant cost due to difference between the turbine rated back pressure and the turbine design back pressure
- d. increased base plant costs for supplying power to auxiliaries
- e. gas turbine capital costs.

The incremental costs of dry/wet cooling include the following fuel costs:

- a. increased base plant fuel required for producing power for the pumps and fans

- b. difference in the amount of base plant fuel required for the dry/wet-cooled plant versus that of the reference plant operating at 3.5 in. Hg back pressure
- c. gas turbine fuel.

Operation and maintenance costs are calculated as a percentage of the cooling system capital cost. No operation and maintenance costs are applied to the gas turbines.

Items and related costs not included within the BNW-II code are:

- a. cover gas system
- b. cooling system instrumentation costs
- c. cooling loop water treatment costs.

The incremental cost, C, is expressed in mills/kWh by

$$C = \frac{FCR (\text{capital costs}) + \text{Fuel Costs} + OM}{CF \times 24 \times 365 \times 1000 \times P}$$

where

FCR = the fixed charge rate

OM = the operation and maintenance cost

CF = the capacity factor (fraction of the year that the plant operates)

P = the output, kW,

and the capital, fuel, and operation and maintenance costs (OM) are as given above.

All costs are in January 1976 dollars. Interest during construction and inflation prior to or during construction is not considered. Effects of the cooling system's construction schedules and their impact on the balance of plant construction schedule are also not considered. The uncertainty involved in defining these items appears to outweigh any additional understanding obtained by including them in a comparative analysis.

3.5 CALCULATIONAL ORDER

The calculational order of the BNW-II code proceeds as follows:

- The set of values for the five internally independent variables which, along with the input, completely specify the design and performance of the dry cooling system are selected.
- The dry-cooled cooling system is designed to provide the utility's power requirements at the design temperature with no provision for auxiliary power.
- Steam supply and plant scaling are conducted to provide a power plant capable of meeting the utility's power requirements at the design temperature and the power for the heat rejection system's auxiliaries.
- The performance and fuel consumption of the plant under dry/wet operation throughout the year is determined. The design is thrown out if the plant cannot operate within Zones 1 through 3 within the constraint of using all of the available water.
- The size of the gas turbine contingent and the annual cost of gas turbine fuel consumption is computed.
- The incremental cost is calculated.
- The above process is repeated under the control of an optimization algorithm to obtain the design giving the minimum incremental cost (a 1% change in incremental cost is the cut-off criterion).

The design temperature must be less than the temperature at which deluging commences if meaningful results are to be obtained. The reason for this is that the utility model upon which the design and sizing of the plant and upon which the incremental cost is computed is a fixed demand system. No credit is given for excess production of power; only a relatively small credit is given for fuel savings resulting from lower turbine back pressure. Because the design temperature is by definition, the temperature at which the plant can meet the fixed demand with dry cooling only, the plant will put out

more power than the fixed demand over the entire year^(a) if it is deluged below the design temperature. In effect, the plant is oversized and an artificially high incremental cost results.

3.6 OPTIMIZATION

Optimization of the dry/wet cooling system involves selecting the values for the set of independent parameters that fix the cooling system's design after which all other dependent parameters (including incremental power production cost) can then be calculated; and the repetition of the process until the least incremental power production cost is obtained.

The computer optimization involves parameters of four types:

1. internally optimized independent parameters;
2. internally optimized dependent parameters;
3. externally optimized independent parameters; and
4. external fixed parameters.

The major parameters and options in each of the above groups are listed in Table 1. General input and output of the program is indicated in Figure 13.

The external fixed parameters are those imposed on the analysis. They are generally fixed at a given site for a particular plant. However, the investigator may vary these "fixed" parameters when comparing the cost of dry cooling for nuclear plants with coal plants, or evaluating cost differences at different sites. The effect of changes in fuel costs, capacity factors, etc., can also be investigated by varying these parameters.

The externally optimized independent parameters are those optimized by changing one or more parameters at a time and observing the resultant changes in costs and cooling system design. These include simple factors such as the effect of fin spacing, as well as more complex elements such as using different types of turbines.

(a) True for operation in Zones 2 and 3 of Figure 10, true for all but the highest ambient temperatures in Zone 1.

TABLE 1. Computer Analysis - Major Cooling System Parameters and Options

	Internally Optimized Independent	Internally Optimized Dependent	Externally Optimized Independent	External Fixed
I. Heat Exchanger	<ol style="list-style-type: none"> 1. Tube Length* 2. Number Tubes In-Depth* 3. Face Velocity* 	<ol style="list-style-type: none"> 1. Frontal Area 2. Width/Length Ratio 3. Total Tubes (Bundle Number or Overall Size) 	<ol style="list-style-type: none"> 1. Unit Geometry (Tube OD, Tube Pitch, Fin Height, Staggered vs In-Line, etc.) 2. Tube and Fin Material 3. Fin Type 4. Spacer Material and Type 5. Header Type 	
II. Fan System		<ol style="list-style-type: none"> 1. Number 2. Blade Diameter* 3. Blade Angle* 4. Number of Blades* 5. Fan Power 	<ol style="list-style-type: none"> 1. Velocity Recovery vs No Velocity Recovery 	
III. Tower		<ol style="list-style-type: none"> 1. Number* (Polygonal) 2. Diameter (Polygonal) 		
IV. Piping and Pump		<ol style="list-style-type: none"> 1. Pump Power 2. Pipe Lengths 3. Pipe Diameter 	<ol style="list-style-type: none"> 1. Design Velocity 2. Pipe Wall Thickness 3. Piping Temperature Drop 	
V. Condenser/Reboiler (NH ₃)	<ol style="list-style-type: none"> 1. Terminal Temperature Difference (NH₃)* 	<ol style="list-style-type: none"> 1. Tube Number 	<ol style="list-style-type: none"> 1. Tube Length 2. Tube Material 3. Tube Diameter 4. Tube Type 5. Exit Quality 	
VI. Turbine	<ol style="list-style-type: none"> 1. Design Turbine Exhaust Temperature* 		<ol style="list-style-type: none"> 1. Turbine Type 	
VII. Common to Two or More Components		<ol style="list-style-type: none"> 1. Range of Air 2. Tower Initial Temperature Difference (ITD) 	<ol style="list-style-type: none"> 1. Ratio of Tower Roof Area to Fan Swept Area 2. Design Ambient Temperature 3. Water Consumption 	
VIII. Base Plant				<ol style="list-style-type: none"> 1. Fuel Cost 2. Plant Cost 3. Heat Rate 4. Capacity Factor 5. Fixed Charge Rate 6. Size
IX. Capacity Leveling				<ol style="list-style-type: none"> 1. Energy Penalty Charges 2. Capacity Penalty Charges
X. Site				<ol style="list-style-type: none"> 1. Meteorology

* Optional treatment as externally fixed parameter.

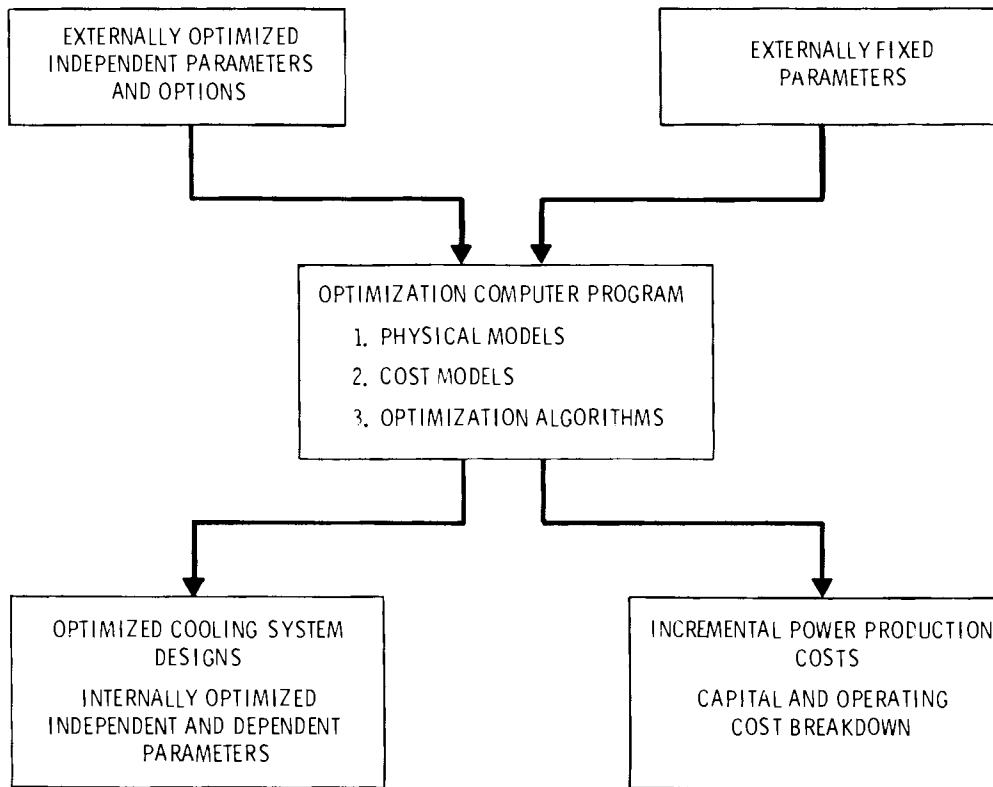


FIGURE 13. Dry/Wet Cooling System Computer Optimization

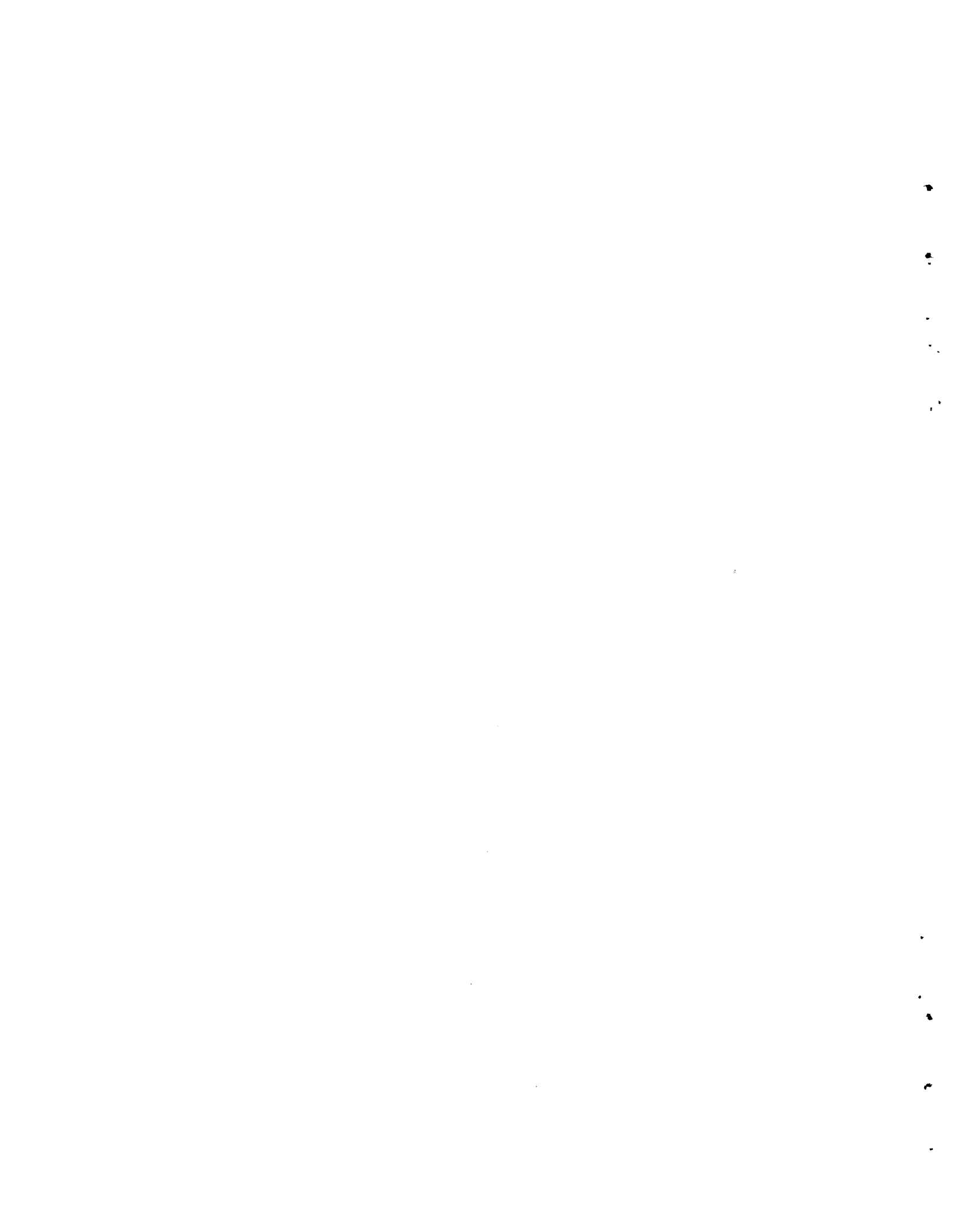
For a given set of external parameters, there are five internally optimized independent parameters. Once these five independent parameters are specified, all other system design and operating dependent parameters can be calculated. The cost of electricity attributed to the cooling system is then evaluated based on capital expenditures, operating expenses, and costs associated with the power plant/utility system interface. In brief, the optimization is performed by selecting sets of variables and comparing the subsequent costs. The variable set associated with the least cost system is considered to be the optimum.

The BNW-II computer program contains an optimization technique to determine which combination of internal dependent parameters results in the minimum incremental power production costs associated with dry/wet cooling. This optimization technique developed by Andeen and Glicksman of MIT⁽⁵⁾ is described in Appendix H.

The BNW-II computer code performs the optimization process in two steps.

In the first step an extensive grid is established with each grid point being a set of values for the five internal independent variables. The values of the variables in each set are determined by the input starting point on the basis of a programmed incremental step size for each variable. For each set of five variables in the matrix, a cooling system is designed and costed. The set of variables associated with the lowest incremental cost is used as the starting point for the second step.

In the second step a single variable is adjusted to find the optimal value, i.e., the value associated with the lowest cost, while the four remaining variables are fixed. The optimization is a hill-climbing technique with programmed reduced step sizes. If the incremental cost increases, the value of the variable being adjusted is then readjusted in the opposite direction. All five variables are singly optimized in this fashion to determine an optimal set. The process is repeated at least four times. If the result of the fifth optimization is within 1% of the fourth, then the optimization is complete. Otherwise, successive optimizations are developed until the improvement in cost is less than 1%.



4.0 CALCULATION PROCEDURE

A dry/wet cooling tower heat rejection system is optimized by varying five independent variables (shown in Table 1) to obtain the minimum incremental cost. The five independent variables are varied according to the optimization routine developed by MIT,⁽⁵⁾ discussed in Section 3 and Appendix H. Once these variables have been determined, effects of design and incremental cost of the dry/wet cooling system on the cost of generating electrical power can then be determined.

The dry/wet cooling tower code is, therefore, composed mainly of two parts:

- optimizing (choosing the five independent variables in a logical manner)
- designing and determining cost of the dry/wet cooling system on the electrical generating cost.

The different parts of the code interact as shown in Figure 14. The five parameters selected by the optimization part of the code are:

1. steam exit temperature of the turbine - T1
2. velocity of the air entering the heat exchanger - FVAIR
3. temperature difference between the saturated steam and the saturated ammonia in the condenser/reboiler - TTD
4. length of the tubes in the heat exchanger - ELENH
5. number of tubes in depth in the heat exchanger - ZD.

These variables are then supplied to the design and costing part of the code.

A description of the calculation procedure used to design and cost the intermediate ammonia dry/wet cooling system follows. The description is divided into several major categories detailing specific calculations dealing with a particular aspect of the design or costing of the dry/wet cooling

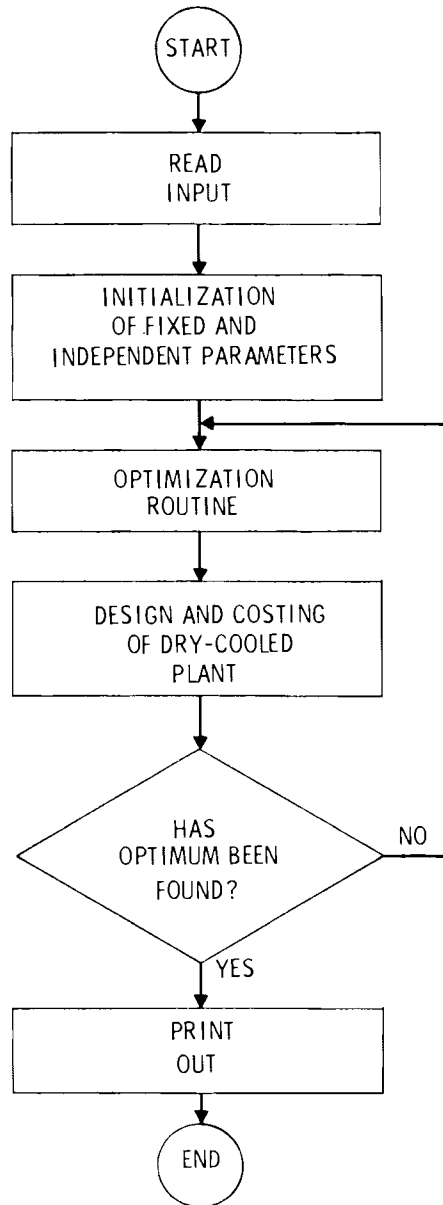


FIGURE 14. BNW-II Program Flow Diagram

system. The subroutine in which a major portion of the computations is carried out is given in parentheses in the heading describing the major categories.

Each subroutine has an extensive number of comment statements as shown in the printout of the program in Appendix I. Therefore, the subroutines will only be outlined here and not described in detail.

4.1 INTERMEDIATE AMMONIA DRY/WET COOLING SYSTEM (CALC)

Subroutine CALC is part of the code in which the five independent variables are used to design and cost the cooling system. Not all of the calculations are performed in this subroutine, but most of the other subroutines of the code are called from it. Where another subroutine does the major portion of calculations in the following calculation procedure, it will be given in parentheses and described later in the text. Figure 15 outlines the calculation procedure given below.

1. The heat rejected by the plant is determined by using the saturation temperature of the steam leaving the turbine to find the turbine back pressure, which is then used to find the efficiency of the plant. The efficiency is then used along with the plant size to determine the heat rejected by the plant.
2. The thermal and thermodynamic properties of the ambient air and NH_3 are determined by using the saturation temperature of the steam, the temperature difference in the condenser/reboiler, and the ambient air temperature.
3. Using the thermal properties of the NH_3 and the amount of heat rejected by the plant, the mass flow rate of NH_3 is calculated.
4. The design of the condenser/reboiler is performed by using the heat rejected by the plant, the saturated steam temperature, and the temperature difference between the steam and the NH_3 in the condenser/reboiler (SPDES, see Section 4.2).
5. The tower system design, consisting of the sizing of the heat exchanger, tower, fan, and supply NH_3 piping is determined by a triple iteration loop. This calculation procedure consists of the following steps:

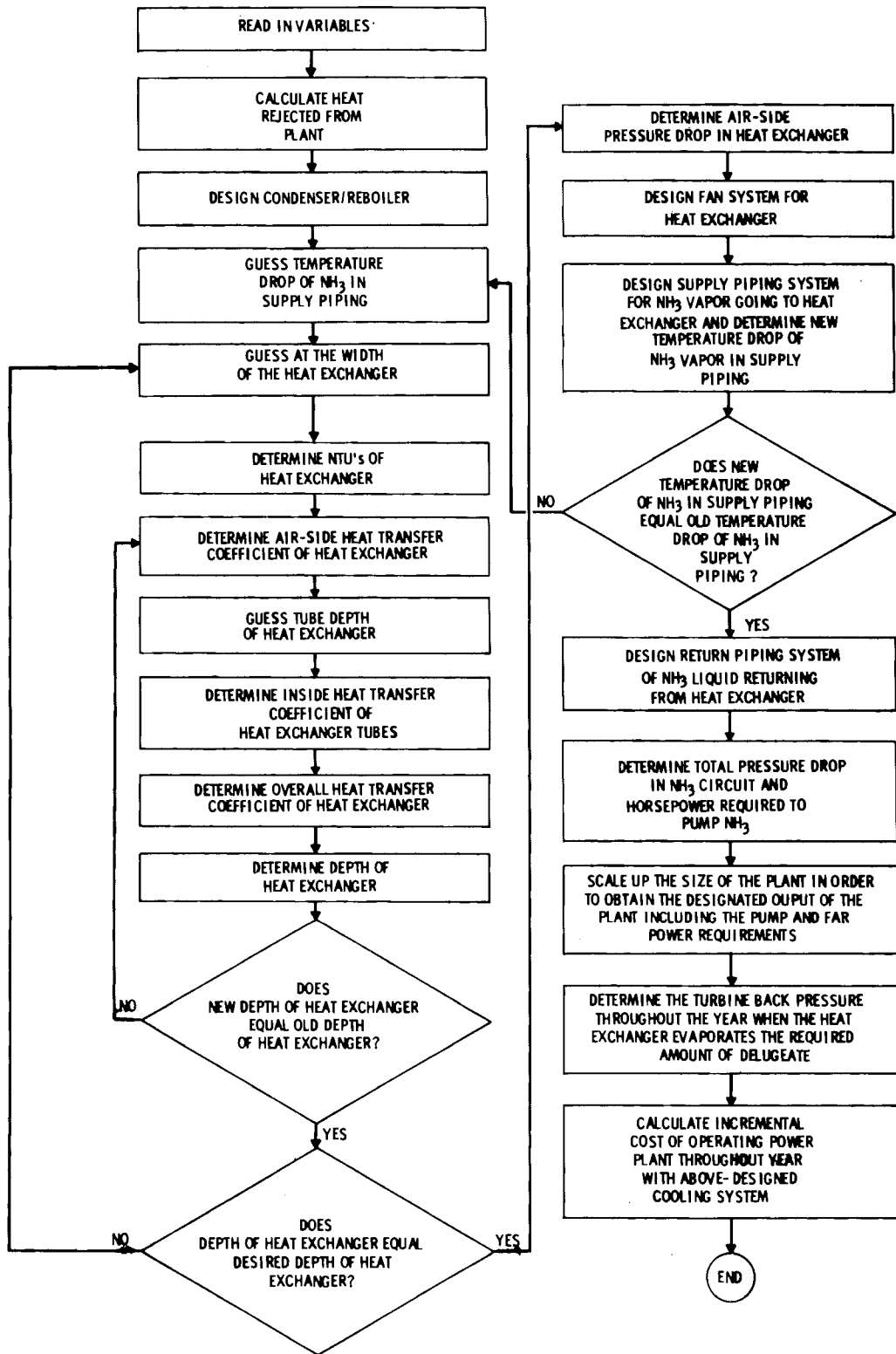


FIGURE 15. Subroutine CALC Flow Diagram

- (1) The size of the heat exchanger is determined by a double iteration loop after an estimation of the temperature drop of the NH_3 in the piping from the condenser/reboiler to the towers has been made. The steps required are:
- (i) The number of transfer units (NTU) in the heat exchanger is determined by using estimates of the temperature drop in the NH_3 from the condenser/reboiler to the towers and the width of the heat exchanger.
 - (ii) The air-side heat transfer coefficient of the heat exchanger is calculated by using the estimate of the width of the heat exchanger, the length of the tubes in the heat exchanger, the velocity of the air entering the heat exchanger, and the heat exchanger's unit geometry.
 - (iii) The fin and surface efficiency of the heat exchanger is calculated as a function of the air-side heat transfer coefficient.
 - (iv) The inside heat transfer coefficient is determined by an iteration loop that finds the depth of the heat exchanger. The following steps are contained in the loop:
 - (a) An estimate of the heat exchanger depth is used to determine the liquid Reynolds number in the tubes, which is then used to find the inside heat transfer coefficient.
 - (b) The overall heat transfer coefficient is determined from the air-side and inside heat transfer coefficients and the fin effectiveness of the outside surface.
 - (c) Using the number of transfer units (NTU), the air mass flow rate, and the overall heat transfer coefficient, the depth of the heat exchanger is determined. If the depth does not agree with the estimated tube depth in (i), a new depth is estimated and steps (a) through (c) are performed again.

- (v) If the heat exchanger depth just calculated does not equal the desired tube depth (ZD), a new heat exchanger width is estimated and steps (i) through (v) are performed again.
 - (2) Knowing the tube depth of the heat exchanger and the air-side Reynolds number, the pressure drop across the heat exchanger is calculated.
 - (3) The heat exchanger cost is determined from its size (COSTEX, see Section 4.3).
 - (4) Using the pressure drop and the frontal area of the heat exchanger, the fan diameter, number of blades, and blade angle are determined. Once the type of fan is chosen, the number of fans and the number and height of the towers are calculated (FAN, see Section 4.4).
 - (5) Using the number, diameter, and height of the towers, the supply piping is designed and the temperature drop of the NH_3 vapor is determined (PIPCLS, see Section 4.5).
 - (6) If the temperature drop in Step (5) differs significantly from the temperature drop used in Step (1), the temperature drop of Step (5) is used in Step (1) and the procedure is repeated.
6. After the tower system is known, the return piping is designed and the pressure drop of the NH_3 liquid returning from the towers is calculated (PIPCLR, see Section 4.5).
 7. The pressure drop of the two-phase flow of NH_3 in the heat exchanger tubes is calculated.
 8. The pressure drop throughout the entire NH_3 loop is calculated along with the horsepower required for the pump power.
 9. The plant is scaled up to obtain the designated plant output, including the pump and fan power at the design ambient temperature. Costs of the cooling system are also scale up (SCALP, see Section 4.6).

10. Using the amount of water allocated for deluging the heat exchanger, the turbine back pressure for each ambient temperature in the meteorological profile is determined (CONSUMP, see Section 4.7). The deluge piping is then designed and costed (DELUGEP, see Section 4.5).
11. The incremental cost of operating the power plant with the dry/wet cooling system over the entire year is calculated (NOVART, see Section 4.8).

4.2 CONDENSER/REBOILER DESIGN AND COSTING

Two subroutines, SPDES and SURCON, design and cost the condenser/reboiler.

4.2.1 Condenser/Reboiler Design (SPDES)

Subroutine SPDES determines the size of the condenser/reboiler on the basis of:

- the designated temperature difference between the saturated steam and NH_3
- the amount of heat to be transferred
- the temperature of the steam
- the length of the tubes
- exit quality of the ammonia leaving the condenser/reboiler tubes.

The condenser/reboiler is designed by a double iteration loop using correlations for the steam- and NH_3 -side heat transfer coefficients to determine the temperature drops across both fluid boundaries and the average bulk velocity of the ammonia inside the condenser tubes. Once these values are found, the size of the condenser/reboiler is determined along with the system performance parameters.

The condenser/reboiler design is determined in the following sequence:

1. The average velocity of NH_3 through the condenser/reboiler tubes is determined by a double iteration loop. The procedure consists of the following steps:
 - (1) The forced convection heat transfer coefficient is calculated by guessing the velocity of ammonia in the tubes.

- (2) The temperature drop across the fluid layers and the condenser tube wall is determined by an iteration loop. The procedure is:
 - (i) Calculate the heat flux through the outside tube wall by estimating the temperature drop on the inside fluid boundary and the forced convection coefficient.
 - (ii) Calculate the temperature drops across the steam condensate and the tube wall using the heat flux through the wall.
 - (iii) Determine the total temperature drop caused by estimating ammonia-side temperature drop and then determine a new estimate for the ammonia-side temperature drop and repeat Steps (i) through (iii) until the total temperature drop converges to the desired value.
- (3) Using the heat flux previously determined, a new ammonia velocity is calculated. This new velocity is used in Steps (1) through (3) until the velocity does not vary from its previous value by a certain percentage.

2. Using the heat flux from Step 3 and the amount of heat transferred through the condenser/reboiler per unit time, the outside heat transfer area and the overall, outside, and inside heat transfer coefficients are determined.

3. Using the velocity in the tubes, the pressure drop incurred by the ammonia flowing through the tubes of the condenser/reboiler is calculated.

4.2.2 Condenser/Reboiler Costing (SURCON)

Subroutine SURCON costs the components (shell, tubes, accessories) of the condenser/reboiler. The cost of field erection of the condenser/reboiler is also added into the total cost of the system. The modified code is set up to handle regular condenser tubing and enhanced tubing (enhanced heat transfer).

The calculations performed by subroutine SURCON proceed according to the following sequence:

1. Select tubing cost arrays to be used in costing.
2. Calculate total length of tubing required in the condenser/reboiler.
3. Determine the cost discount rate based on the total amount of tubing.
4. Determine the penalty for the length of tubing chosen.
5. Calculate the total cost of the tubing material.
6. Calculate the shell cost of the condenser/reboiler.
7. Calculate the field erection costs of the condenser/reboiler.
8. Determine the total cost of the condenser/reboiler.

4.3 HEAT EXCHANGER DESIGN AND COSTING (COSTEX)

The heat exchanger bundle costing is based on the algorithms and cost models given in Appendix G. The cost of the heat exchanger bundle is broken down into several subcomponents:

- header
- tubing
- tubing sealant
- spacers
- bundle frame
- bundle assembly.

The total weight of the heat exchanger bundles consists of the weight of the heat exchanger materials and the water contained inside the tubing and the headers. The cost and weight of the heat exchanger bundles are calculated in the following order:

1. liner tubing costs
2. fin weight
3. cost of bonding the fins to the tubing
4. protective coating costs
5. tubing and fin costs
6. tubing spacer costs
7. end preparation costs
8. cooling surface total cost

9. header and nozzle costs, based on values calculated for
 - a. number of bundles in entire cooling tower system
 - b. number of tubes per bundle
 - c. header depth and width
 - d. header costs
10. bundle assembly and frame costs
11. weight of heat exchanger bundles, consisting of
 - a. material weight of heat exchanger bundle
 - b. weight of NH_3 in heat exchanger bundle
12. heat exchanger total cost.

4.4 FAN SYSTEM SELECTION (FAN)

The fan system chosen is that which has the minimum annual capital and energy costs. The type of fan selected is specified in terms of:

- blade diameter
- hub diameter
- number of blades per fan
- blade angle.

Each fan system consists of fans having the same diameter, the same number of blades, and operating at the same blade angle. The cost of each fan system investigated is determined. Each fan system is designed on the basis of:

- the pressure drop across the heat exchanger
- the total air mass flow rate induced through the heat exchanger, and
- the frontal dimensions of the heat exchanger.

The number and height of the polygonal towers are determined from the total fan swept area, the ratio of tower roof area to fan swept area, and the frontal area of the heat exchanger. Knowing the total cost of the fan system and the circular tower structures, the annual cost of these two components can be determined. On this basis, the optimum fan system is determined.

The fan selection is performed as follows:

1. Determine the volumetric flow rate of the fan system using the mass flow rate of air through the heat exchanger, inlet temperature, and plant site elevation.
2. Choose fan to be analyzed (fan diameter, number of blades, blade angle).
3. Determine number of fans required, the volumetric flow rate through each fan and the total pressure drop across each fan.
4. Determine horsepower required by each fan.
5. Determine number and diameter of towers.
6. Determine fan motor and electrical costs.
7. Calculate capital, stack, and shipping and assembly costs to determine fan system total capital cost.
8. Calculate fan system annual cost (the sum of the annual capital and energy costs).
9. Calculate annual costs for the foundation and structure needed for fans.
10. Total annual cost of the fan and fan system structure and foundation is calculated, then stored or dropped, depending on its value relative to the lowest cost of the previous fans. If the value is lower, the parameters of the fan system are saved.
11. Return to Step 2 and repeat the above process until all desired fan combinations have been investigated.

4.5 PIPING SYSTEM DESIGN AND COSTING

Three subroutines calculate the ammonia and deluge piping system designs and costs.

4.5.1 NH₃ Piping System Design and Costing (PIPCLS and PIPCLR)

Subroutines PIPCLS and PIPCLR perform two basic functions. First, they calculate the cost of all the piping and the pumps between the condenser and

the heat exchanger bundles. Second, they determine the pressure drop in the piping system so that the total system pumping power requirements can be determined.

The ammonia distribution piping system is composed of the supply piping (determined by subroutine PIPCLS), which transports the ammonia vapor from the condenser/reboiler to the heat exchanger bundles, and the return piping (determined by subroutine PIPCLR), which transports the ammonia liquid from the heat exchanger bundles to the condenser/reboiler. The supply and return piping can be further subdivided into the main circulation, tower distribution, and quadrant piping.

The supply and return piping are modeled as having nearly identical plan views. The pipe diameters are different, however, because of the significant difference in densities and design velocities of the ammonia vapor and liquid. All components of the ammonia piping system are designed to withstand 350 psi. They are assumed to be available in 6-inch increments with 6- to 144-inch diameters.

Each piping system is determined by PIPCLS and PIPCLR on the basis of:

- total mass flow rate of NH_3 (vapor, liquid)
- NH_3 design velocity (vapor, liquid)
- number, diameter, height and number of sides of circular towers
- length of the heat exchanger tubes, and
- the width of the heat exchanger tube bundles.

The calculation procedure followed by both subroutines is shown in the following steps.

1. Perform the preliminary calculations required.
 - (1) Determine the properties of the liquid or vapor NH_3 entering the supply or return piping systems.
 - (2) Determine the number of sides of the polygonal tower in each quadrant and the number of tube bundles per quadrant.
 - (3) Determine the NH_3 mass flow rate per tower, per quadrant and per tube bundle.

The calculation procedure is as follows.

2. Design the main circulation, tower distribution, and quadrant piping using the following series of calculations:
 - (1) Determine the diameter of the header section based on the NH_3 mass flow rate and design velocity.
 - (2) Select the diameter from the available pipe sizes. Pipe diameter selection also specifies the cost of pipe, tees, elbows, flanges and valves.
 - (3) Determine whether a reducer is required. This is accomplished by comparing the diameter of the section with the diameter of the last section. If the diameters differ by more than a previously specified amount, then a reducer is necessary. Reducer prices apply whether the reduction is for 6, 12 or 18 in. The prices are based on a standard reducer length of 2 ft and an included angle of $22\frac{1}{2}^\circ$.
 - (4) Determine the length of the header section.
 - (5) Determine the equivalent length of pipe and flow velocity in the header section.
 - (6) Determine the pressure drop in the header section.
 - (7) Subtract the flow of one branch line to a heat exchanger bundle to determine the flow in the next header section.
 - (8) If no flow remains, go to Step 9; the last header section has been designed. If flow remains, return to Step 2.
 - (9) Determine the branch diameter based on the ammonia mass flow rate and the design velocity.
 - (10) Calculate the cost of the tees connecting the main piping to the branch piping. The tee cost is assumed to be 0.67 times the cost of a tee with the main circulation diameter and 0.33 times the cost of a tee with the branch diameter.

(11) Sum the cost of each header section including the piping, tees, reducers, and elbows to determine the total cost of the header.

(12) Determine the pressure drops throughout the header sections.

3. Sum the pressure drops for the supply or return cooling system.

4. Sum the costs for the supply or return piping.

4.5.2 Deluge Piping System Design and Costing (DELUGEPE)

The deluge piping cost algorithm calculates the cost of the deluge piping based on the water mass flow rate. The deluge piping system is composed of two main parts--the makeup water piping system and the tower piping system. The makeup water piping parallels the ammonia supply and return main circulation piping. The tower piping system is composed of piping to the center of each quadrant in the towers, a riser to the top and piping along the top of each quadrant.

The deluge piping is designed on the basis of:

- mass flow rate of the delugeate
- mass flow rate of the makeup water
- deluge design velocity
- number of deluged towers
- tower diameter
- tower height
- density of the deluge water
- distance from the deluge water supply to the boundary of the towers.

The deluge cost algorithm is an approximation of the cost of the deluge piping system based upon the mass flow rates of the makeup water and the delugeate. The deluge piping system can be divided into two components:

- makeup water piping system
- tower piping system.

The major cost components associated with this system are costs of the pipe and valves and the pumping requirements.

Analysis of various main distribution and tower piping systems showed that piping, pumping and valve requirements comprised 90.0 and 51.5% of the cost of the main distribution and tower piping systems, respectively. Therefore, the total cost of the deluge piping has the form.

$$\text{DELUGE PIPING COSTS} = \frac{\text{MAIN DISTRIBUTION COSTS}}{0.900} + \frac{(\text{NUMBER OF DELUGED TOWERS})(\text{TOWER SYSTEM COSTS})}{0.515}$$

The expressions for the main distribution and the tower piping systems considered of the pump, piping, and valve costs for each system. These costs were based upon the diameters of the main circulation and distribution piping, respectively.

4.6 PLANT SCALING DUE TO ALL-DRY OPERATIONAL MODE

Two subroutines, SSCALE and SCALP, modify the size of the power plant to account for the effects of heat exchanger operation with no water augmentation.

4.6.1 Steam System Scaling (SSCALE)

The power plants steam supply system is scaled up so that the plants specified power output will be produced at the rated back pressure of the steam turbine during all-dry operation of the cooling system. This accounts for the increased heat rate of the steam turbine being used over that of the reference plant's conventional turbine rated at 3.5 in. Hg back pressure. This computation is carried out once for each power plant cooling system optimization.

The incremental cost due to scaling up the steam supply system is calculated in the following order:

1. heat rate factor of the dry-cooled plant turbine at rated back pressure
2. plant cost as a result of the scale-up of the steam supply of the power plant

3. incremental costs of steam supply system of the power plant due to a change in size of the steam supply system to meet increased steam requirements of the turbine.

4.6.2 Plant Scaling (SCALP)

The plant and cooling towers are scaled up or down linearly so that the specified power output of the plant will be produced when:

- the turbine back pressure at all-dry design conditions does not correspond to the rated back pressure of the all-dry cooled plant turbine, and
- part of the total power output of the all-dry cooled plant is used to supply the power requirements of the fan and pumping systems.

Two factors are calculated for use in scaling the plant and the cooling towers. The purpose of each scaling factor is given separately below:

1. HRFA21--scale plant to account for difference in heat rate factor of the turbine at rated back pressure and design back pressure.
2. YFPP1--scale plant and dry cooling system to provide power for the dry cooling system fans and pumps at the turbine design back pressure.

The scaling factors are determined in the following sequence of calculations:

1. Scaling factor to account for change in heat rate factor from the rated back pressure of the turbine to the design back pressure.
2. Power output of the turbine generator at the rated back pressure which gives the required power output at the design back pressure.
3. Plant cost at design conditions, including the steam supply and plant back pressure scaling.
4. Incremental cost of scaling up plant due to increased heat rate factor.
5. Scaling factor for the plant and dry cooling tower to meet pump and fan power requirements.

6. Gross power output of the turbine generator when operated at the rated back pressure, which meets the power requirements of the fans and pumps and the power output of the plant at the design back pressure.
7. Gross power output of the turbine generator when operated at the design back pressure.
8. Plant cost, excluding the cooling tower cost.
9. Incremental cost of plant due to all-dry cooling if the plant operates at design conditions only.

Having calculated the scaling factor (YFPP1), the plant and cooling towers are scaled up to meet the increased heat rejection in the all-dry mode. This is accomplished in the following sequence of calculations.

1. Linearly scale up four independent parameters:
 - a. mass flow rate of NH_3
 - b. mass flow rate of air
 - c. heat exchanger frontal area
 - d. width of the heat exchanger
2. Design and cost the condenser for increased NH_3 flow rate and heat load.
3. Scale the heat exchanger width and number of tubes in width.
4. Scale the fan and pumping system.
5. Scale the heat exchanger weight.
6. Calculate the incremental cost of fuel for the steam supply system due to all-dry cooling.
7. Scale the land and piping costs.
8. Scale the cost of the tower structure, foundation and plenum.
9. Calculate the hail and louver screen costs.
10. Sum the total capital cost of the cooling towers.

11. Calculate the total incremental cost of operating the power plant with the cooling system operating in the all-dry mode at design conditions (unused in optimization procedure):
 - a. yearly capital cost of the cooling towers^(a)
 - b. yearly maintenance cost of the cooling towers^(a)
 - c. incremental cost of plant due to cooling tower heat rejection
 - d. yearly capital cost of the piping and pumping system^(a)
 - e. yearly capital cost of the surface condenser^(a)
 - f. incremental cost of fuel for the power plant operating with an all-dry cooling tower heat rejection system.

4.7 DELUGE ENHANCEMENT (CONSUMP)

The deluge enhancement calculation is dominated by the requirement that the cooling system, defined by the dry mode calculations, consume all of the available water. Second the turbine model used in the design will have a prescribed turbine back pressure limit curve that is a function of ambient temperature. The first step in the calculations is, therefore, to bracket the problem to assure that all of the available water can be consumed while maintaining the turbine exhaust pressure at or below its limit for all ambient temperatures.

To determine if the dry mode design will satisfy the water and back pressure requirements, three calculation zones were established. These are shown in Figure 16. The following sequential steps are taken to define the deluge enhancement.

1. The entire heat exchanger surface is deluged throughout the year. The total water consumption is evaluated. If the water consumed is less than the water available, then the design is disregarded. The turbine back pressures for each ambient temperature are stored. If any of these back pressures are greater than the limit back pressure at the same ambient temperature, then the design requirements for the turbine can not be satisfied.

(a) Yearly cost for capital is equal to the fixed charge rate times the capital cost.

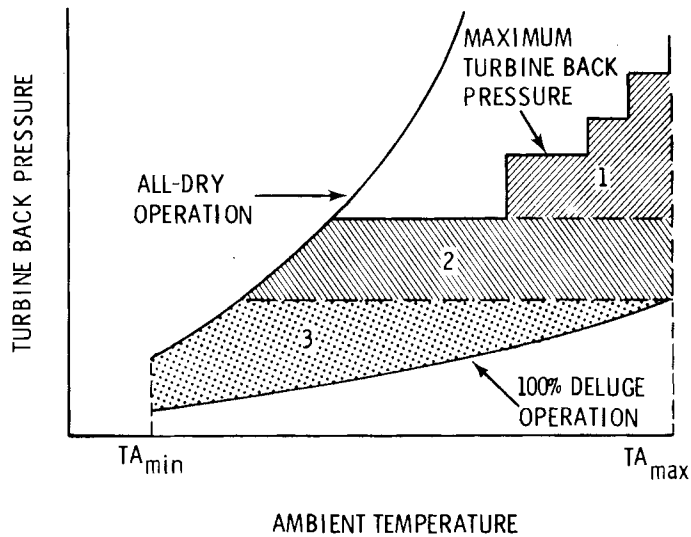


FIGURE 16. Operating Regimes for a Power Plant with a Deluged Cooling System

2. The lowest ambient temperature is determined for which the dry mode exhaust pressure is greater than the turbine back pressure limit at that ambient temperature. For this temperature and each higher temperature, the deluge water consumption necessary to bring the back pressure down to the back pressure limit is evaluated. The subsequent total deluge consumption needed to keep the back pressure down to the back pressure limit is determined. If the water consumed is greater than the water available, then the design is disregarded.
3. If the design passes the tests in Steps 1 and 2, then a solution is known to exist. The next step is to determine which calculation zone should be investigated. This is done by bracketing Zone 2 in a fashion similar to Steps 1 and 2.
 - (a) The back pressure on the hottest day, TA_{max} , for 100% deluge defines the bottom of Zone 2. The lowest ambient temperature is determined for which the dry mode exhaust pressure is greater than the back pressure, defining the bottom of Zone 2. The amount of deluge water

required to maintain this exhaust pressure for ambient temperatures at and above the defined value is determined. If the water consumed is more than the water available, then the solution lies in either Zone 1 or 2. (If the water consumed is less the water available, then the solution lies in Zone 3.)

(b) The lowest exhaust pressure specified by the exhaust pressure limit curve defines the top of Zone 2. The lowest ambient temperature is determined for which the dry mode exhaust pressure is greater than the back pressure defining the top of Zone 2. The water consumption required to maintain the exhaust pressure for ambient temperatures at and above the defined value is determined. If the water consumed is less, than the water available, then the solution lies below Zone 1. (If the water consumed is greater then the water available, then the solution lies in Zone 1.)

(c) If the design satisfied both 3a and 3b, then the solution is in Zone 2.

4. If in Zone 2 an iterative procedure is used to determine the operating back pressure curve for which all of the water available is consumed. This exhaust pressure is assumed to be a constant value for each ambient temperature for which deluge enhancement is used. The dry/wet split,^(a) i.e., the percentage of the heat exchanger surface which is dry and that which is wet, is determined for each ambient temperature.
5. If the water available designates that the back pressure operating curve is in Zone 3 the back pressure is assumed to be a constant value for each ambient temperature for which deluge enhancement is used. However, when

(a) Whenever the heat exchanger is partially deluged it is necessary to compute, by an iterative process, the fraction of the heat exchanger that is deluged. The computation for the fraction is carried out many times throughout CONSUMP to determine the operating back pressure of the turbine over the entire ambient temperature range. The subroutine performing this calculation is TRPMAX and is documented in Appendix I so that each step of the subroutine can be understood.

the ambient temperature is reached for which the back pressure with 100% deluge is greater than the constant back pressure, the back pressure corresponding to 100% deluge is used. The dry/wet split is evaluated at each ambient temperature.

6. If the amount of water available designates that the back pressure operating curve is in Zone 1, then the operating back pressure curve follows the turbine back pressure limit curve up to one of the steps in the curve. Then somewhere inside the step the curve remains at a constant value up to the maximum ambient temperature. The generating back pressure curve is found by determining through which step the curve will pass. This is done by passing the curve through the upper and lower bounds of each step and determining how much water is needed for the curve to go through both boundaries. If the amount of water available is less than the lower curve's water consumption and more than the upper curve's water consumption, then the step is where the curve must pass. If those two conditions are not met then the operating back pressure curve must pass through some other step in the turbine back pressure limit curve. Once the step through which the operating curve must pass is found, an iterative procedure is used to determine the location through which it passes. The dry/wet split of the heat exchanger is evaluated for each ambient temperature in each operating back pressure curve.

When the deluge enhancement calculations are concluded, the operating back pressure is known for each ambient temperature.

4.8 INCREMENTAL COST OF THE DRY/WET COOLING SYSTEM FOR THE POWER PLANT OPERATING OVER THE YEARLY TEMPERATURE PROFILE (NOVART)

The incremental cost of operating a dry/wet-cooled plant over the entire year is determined by using the plant operating conditions, which are a function of a yearly ambient temperature profile for the plant site and the amount of water available for evaporative cooling.

The subroutine proceeds in the sequence shown below.

1. Determine the thermal efficiency for the plant at both the design and rated back pressure of the low-pressure turbine.
2. Select the turbine back pressure at which the plant is operating from the turbine back pressure array specifying the back pressure of the turbine over the ambient temperature range when the heat exchange system is deluged (CONSUMP, see Section 4.7).
3. The back pressure is then used to determine the thermal efficiency of the steam turbine and the amount of heat rejected from the plant.
4. The total power output of the steam turbine, the power output of the plant to the electrical power transmission network, the cost for auxiliary power, the increased fuel cost of the plant, and the capital cost of the auxiliary power are determined for the turbine back pressure chosen.
5. Calculate the incremental cost of operating the power plant with the dry cooling system at the back pressure chosen. The cost is then multiplied by the percent of the year that the back pressure exists to obtain a portion of the yearly incremental power production cost.
6. Repeating Steps 2 through 5 for a back pressure array that approximates the yearly back pressure profile of the plant site, a set of incremental power production costs is obtained.
7. Sum the set of incremental power production costs from Step 5 to obtain the incremental power production costs of operating the plant over the entire year.

5.0 COMPUTER PROGRAM

This section describes the BNW-II computer program developed for the dry/wet cooling tower cost optimizations.

5.1 GENERAL INFORMATION

The dry/wet cooling tower cost optimization code is coded in FORTRAN-IV EXTENDED and ASCII FORTRAN. It was compiled and executed on a CDC-7600 computer under the SCOPE 2.1 system (FORTRAN-IV EXTENDED) and on a UNIVAC 1100/44 (ASCII FORTRAN). Central memory requirements (actual words) are approximately 130,000 for the CDC-7600 and 70,000 for the UNIVAC 1100/44. Execution time ranges from 30 to 300 seconds on the CDC-7600, depending mostly upon whether the full optimization procedure is used (pattern and gradient search techniques) or only a portion of it is used (gradient search technique only). Execution time is also affected by the proximity of the starting point to the final conditions, as well as the number and severity of the constraints imposed (e.g., heat exchanger geometry, turbine outlet temperature, number of fans to be considered).

Execution time can be affected quite strongly by the number of fans considered, as specified by the input parameters LFB and LFE (see card type S1 in Input Description). If the code is restricted to fans of only one diameter, execution time can be decreased by as much as 40 seconds or more, compared to when all the fan diameters are considered.

Particular care should be used to avoid overconstraining the model. Experience has shown that the optimization scheme may fail to converge or may converge to a false minimum if the constraints are too numerous or too severe. Input variables which impose constraints and thus could interfere with optimization are:

- turbine outlet temperature constraints (TLIM, TFIX);
- air velocity through heat exchanger (FIXV);
- minimum air-side pressure drop (XDEPA);

- heat exchanger depth and length limits (DEEPL, FIXL);
- temperature difference in the condenser/reboiler (FIXTTD);
- maximum number of towers (TOWMAX); and
- the minimum number of towers per group (TOWMIN).

The subroutine in which these variables are active, and the mechanisms through which they function to impose constraints, are summarized in Table 2.

The complex interaction of variables in the system being optimized makes it extremely difficult to predict which constraints are likely to cause problems in any one case. In general, an unconstrained case should be run before any attempt is made to apply constraints.

The BNW-II program has been run through a wide range of runs and has shown no spurious results. Any problem areas found in the runs have been eliminated by corrective actions and therefore the program should be mostly error-free. However, problems can be encountered by extending the variables of the program outside their range of applicability. This can be done by setting the initial starting point of the program at unreasonable values or setting other input variables at unreasonable values.

As an aid to visualizing the interrelationships among the subprograms of the code, a subroutine linkage chart is shown in Appendix I. It indicates which subroutines may call or be called by other subroutines.

5.2 INPUT

All input to the program is by punched cards. A sample input listing is printed out in Figure 17. In the following input description, the card type symbols correspond to the symbols in the input summary of the output of the dry/wet model at the beginning of Figure 18 (pages 5.20 and 5.21).

TABLE 2. Subroutines Containing Constraint-
Imposing Variables

<u>Subroutine</u>	<u>Variable</u>	<u>Mechanism</u>
CALC	DEEPL	Set trial depth of heat exchanger equal to DEEPL
	FIXL	Set trial length of heat exchanger equal to FIXL
SERCH	TFIX	Value of turbine temperature is set equal to TFIX
	FIXTTD	Value of temperature difference in condenser/reboiler is set equal to FIXTTD
	FIXV	Value of air velocity in heat exchanger is set equal to FIXV
	XDEPA	If air-side pressure drop is less than XDEPA, call subroutine CHNGE for two-variable search.
SHOT	TFIX	Same as in subroutine SERCH
	FIXTTD	Same as in subroutine SERCH
	FIXV	Same as in subroutine SERCH
	XDEPA	If pressure drop is less than XDEPA, reduce frontal area of heat exchanger.
CHNGE	TFIX	Same as in subroutine SERCH
	FIXTTD	Same as in subroutine SERCH
	FIXV	Same as in subroutine SERCH
	XDEPA	Make two-point search by changing a variable different from that being changed by SERCH
XTEND	TFIX	Same as in subroutine SERCH
	FIXTTD	Same as in subroutine SERCH
	FIXV	Same as in subroutine SERCH
	XDEPA	Do not consider this point as a new starting point; pick another one.
FAN	TOWMAX,TOWMIN	If total number of towers exceeds TOWMAX or if the number of towers per group is less than TOWMIN, trial point is rejected.
NOVART	TLIM	If back pressure of turbine on the hottest day is above TLIM, trial point is rejected.

```

*****      2500 ACRE FEET OF WATER AVAILABLE      *****
55.0      55.0      100.0      8.00      5.00      80.0      6.00
101. 96.  92. 90.  87. 82.  77. 72.  .0002.0049.0059.0099.0379.0459.0561.0673
67. 62.  57. 52.  47. 42.  37. 33.  .0783.0811.0744.0742.0784.0812.0810.2233
71. 67.  66. 65.  63. 61.  59. 56.  8.0 8.0  7.0 6.0  5.5 5.5  5.5 5.5
53. 49.  45. 42.  39. 36.  34. 33.  5.5 5.5  5.5 5.5  5.5 5.5  5.5 5.5
1000.      .40952      .758      .18      .01      1.      5509.      40.
66.9      24.      571.      0.      190.14      121000.      30.
1.8043      1.6836      1.614      1.210      1.331      1.210      1.464
3.5      .99121      -0.0073095      .0028095      -1.0964E-15
.85
1.0      0.      180.      3.00
0.90
1.74      1.0      0.00      1.82      2.22      2.5      .55      4.6
1.0      12.0      1.      3.2      5.
15.      0.      0.      500.
150.      0.      0.      10.      5.
2500.0      0.00      0.77      90.00      1000000.0  1000000.0  1.00
2.36220      0.98425      1.53745      0.1003937  1.72056      0.012990  0.000
0.72835      0.66929      22.00      ALUMINUM      118.00
PLATE      ALUMINUM      118.00
0.      0.      0.00      0.00      0.00
FORM REMOVABLE      ALUMINUM      1.500      20.0      8
1.00      1.50      1.00      20.0      9.00      0.53      8.00
.05      .5      0.125
2.      1.      1.      12.      118.      5.      LINDE AL12
1.      50.      .8
1
55      88
HOTERV      SKIP SHOT DELBAW

```

FIGURE 17. Sample Input for Dry/Wet Model

5.4

```

C
C
C          I N P U T   D E S C R I P T I O N
C          FOR BNWII DRY/WET COOLING TOWER AMMONIA
*-----*
C          M A Y   1 9 7 8
C          *-----*
C
C*** *** ***
C
C          IN THE DESCRIPTIONS BELOW THE SYMBOL (DF) MEANS
C          DECIMAL FRACTION
C
C          T
C          Y
C CARD      NAME OF P
C TYPE COLUMNS  FORMAT  VARIABLE E      DESCRIPTION AND (UNITS)
C-----
C
C  A1      1-80  (8A10  DESCR(I) R  COMMENTS OR CASE DESCRIPTION TO BE
C          PRINTED AT TOP OF FIRST OUTPUT PAGE.
C          ANY NUMBER OF TYPE A1 CARDS MAY BE
C          USED BUT A BLANK A1 CARD IS NOT
C          ALLOWED.
C
C.....
C
C  A2      1-80  BLANK IN ALL COLUMNS. ONE TYPE A2 CARD ONLY
C
C.....
C.....
C
C  B1      1-10  (E10.0, TSTAR   R  LOWEST DESIGN TEMPERATURE TO USE
C          (DEGREES F)
C
C          11-20  E10.0, TEND    R  HIGHEST DESIGN TEMPERATURE TO USE
C          (DEGREES F)
C
C          21-30  E10.0, VAS(1)  R  INITIAL VALUE FOR TURBINE OUTLET
C          TEMPERATURE (DEGREES F)
C
C          31-40  E10.0, VAS(2)  R  INITIAL VALUE FOR VELOCITY OF AIR
C          ENTERING THE HEAT EXCHANGER (FT/SEC)
C
C          41-50  E10.0, VAS(3)  R  INITIAL VALUE FOR ITD1, TERMINAL
C          TEMPERATURE DIFFERENCE (DEGREES F)
C
C          51-60  E10.0, VAS(4)  R  INITIAL VALUE FOR LENGTH OF HEAT
C          EXCHANGER TUBES (FT)
C
C          61-70  E10.0, VAS(5)  R  INITIAL VALUE FOR THE NUMBER OF
C          HEAT EXCHANGER TUBES IN DEPTH
C
C.....
C.....
C
C  B2      1-10  (E10.0, TFIX    R  FIXED TUBINE OUTLET TEMPERATURE (F)
C          ENTRY IS IGNORED IF BLANK OR ZERO
C
C          11-20  E10.0, FIXV    R  FIXED FACE VELOCITY OF THE AIR
C          ENTERING THE HEAT EXCHANGER (FT/SEC)
C          ENTRY IS IGNORED IF BLANK OR ZERO
C

```

```

C
C      21-30   E10.0,  FIXTTD   R  FIXED TERMINAL TEMPERATURE
C                                     DIFFERENCE OF THE SURFACE CONDENSER
C                                     (F) ENTRY IS IGNORED IF BLANK OR
C                                     ZERO
C
C      31-40   E10.0,  FIXL     R  FIXED LENGTH OF HEAT EXCHANGER (FT)
C                                     IGNORED IF SET EQUAL TO ZERO
C                                     ENTRY IS IGNORED IF BLANK OR ZERO
C
C                                     IF THE ABSOLUTE VALUE OF FIXL=0.
C                                     THEN THE PROGRAM WILL CALCULATE
C                                     THE LENGTH.
C
C      41-50   E10.0)  DEEPL    R  FIXED NUMBER OF TUBES IN DEPTH
C                                     ENTRY IS IGNORED IF BLANK OR ZERO
C
C.....
C.....
C
C  C1      1-40   (8F5.0,  TA(I)   R  TEMPERATURES REPRESENTATIVE OF
C                                     TPER(I) FRACTION OF YEAR (DEGREES F)
C
C      41-80   8F5.0)  TPER(I)  R  FRACTION OF YEAR OVER WHICH TEMPERA-
C                                     TURE TA(I) IS TYPICAL. (DF)
C                                     C A U T I O N - HIGHEST TA
C                                     MUST BE FIRST
C
C.....
C
C  C2      1-40   (8F5.0,  TA(I)   R  CONTINUATION OF TA(I) FOR I= 9 TO 16
C
C      41-80   8F5.0)  TPER(I)  R  CONTINUATION OF TPER(I)
C
C      NOTE - A TYPE C2 CARD IS REQUIRED EVEN IF BLANK.
C
C.....
C.....
C
C  C1A     1-40   (8F5.0,  TAWB(I) R  WET BULB AIR TEMPERATURE REPRESENTA-
C                                     TIVE OF TPER(I) FRACTION OF YEAR
C                                     (DEGREES F)
C
C      41-80   8F5.0)  BPLIM(I) R  BACK PRESSURE LIMIT ON THE STEAM
C                                     TURBINE REPRESENTATIVE OF TPER(I)
C                                     FRACTION OF YEAR (IN. HG.)
C
C.....
C.....
C
C  C2A     1-40   (8F5.0,  TAWB(I) R  CONTINUATION OF TAWB(I) FOR I = 9
C                                     TO 16
C
C      41-80   8F5.0)  BPLIM(I) R  CONTINUATION OF BPLIM(I) FOR I = 9
C                                     TO 16
C
C      NOTE - A TYPE C2A CARD IS REQUIRED EVEN IF BLANK
C
C.....
C.....

```

C					
C	D1	4-10	(E10.0,	PSIZE	R BASE PLANT SIZE (MEGAWATTS)
C		11-20	E10.0,	TEFF	R BASE THERMAL EFFICIENCY (DF)
C		21-30	E10.0,	CAPF	R CAPACITY FACTOR (DF)
C		31-40	E10.0,	FCR	R FIXED CHARGE RATE (DF)
C		41-50	E10.0,	PER	R RATIO MAINTENANCE COST TO CAPITAL COST (DF)
C		51-60	E10.0,	CCM	R CONSTRUCTION COST MULTIPLIER (DF)
C		61-70	E10.0,	ELEV	R SITE ELEVATION ABOVE SEA LEVEL (FT)
C		71-80	E10.0)	ROOFL	R ROOF LOAD (LB/SQ FT)
C					
C				
C				
C					
C	E1	1-10	(E10.0,	FCOS	R FUEL COST (CENTS/MMBTU)
C		11-20	E10.0,	PWCOS	R REPLACEMENT POWER COST (MILLS/KWH)
C		21-30	E10.0,	PLANC	R POWER PLANT CONSTRUCTION COST (\$/KW)
C		31-40	E10.0,	COSTL	R COST OF LAND (\$/SQ FT)
C		41-50	E10.0,	CSSPKW	R COST OF STEAM SUPPLY (\$/KW)
C		51-60	E10.0,	CAPCHG	R CAPACITY CHARGE (\$/MEGAWATT)
C		61-70	E10.0,	HPCST	R COST OF ELECTRIC MOTORS (\$/HP)
C		71-80	E10.0)	CTURB	R ADDITIONAL TURBINE COST BECAUSE OF NUCLEAR POWER PLANT (\$/KW)
C					
C				
C					
C	E2	1-10	(E10.0,	POHBAF	R INDIRECT COST FACTORS FOR - BUNDLE ASSEMBLE AND FRAME
C		11-20	E10.0,	POHFAN	R FANS
C		21-30	E10.0	POHLEC	R ELECTRICAL
C		31-40	E10.0	POHCIR	R CIRCULATION PIPING
C		41-50	E10.0	POHCND	R CONDENSER
C		51-60	E10.0,	POHSTC	R STRUCTURE
C		61-70	E10.0)	POHSCL	R SCREENS AND LOUVERS
C					
C				
C					
C	F1	1-10	(F10.0,	RBP	R TURBINE RATING BACK PRESSURE (INCHES OF MERCURY)
C		11-70	4F15.8)	TPO(I)	R COEFFICIENTS FOR THIRD ORDER POLY-

NOMIAL FOR HEAT RATE AS A FUNCTION
OF TURBINE BACK PRESSURE.

C
C
C
C.....
C.....
C
C G1 1-10 E10.0 EFFP R EFFICIENCY OF PUMPS (DF)
C
C.....
C.....
C
C H1 1-10 (E10.0, VELREC R CONTROL VARIABLE.
C =1 FOR VELOCITY RECOVERY
C =0 FOR NO VELOCITY RECOVERY
C
C 11-20 E10.0, XDEPA R MINIMUM AIR SIDE PRESSURE DROP THRU
C HEAT EXCHANGER (LB FORCE/SQ FT)
C
C 21-30 E10.0, TLIM R MAXIMUM STEAM TEMPERATURE FOR THE
C TURBINE (DEGREES F).
C ASSUMED 180 IF FIELD IS BLANK OR 0.
C
C 31-40 E10.0, TOWMIN R THE MINIMUM ALLOWABLE NUMBER OF
C TOWERS PER GROUP.
C ASSUMED 1 IF NOT SPECIFIED
C
C 41-50 E10.0, TOWMAX R THE MAXIMUM ALLOWABLE NUMBER OF
C TOWERS PER GROUP ASSUMED 9999 IF
C NOT SPECIFIED
C
C 51-60 E10.0) PFACT R PACKING FACTOR, RATIO OF CIRCULAR
C TOWER ROOF AREA TO FAN SWEEP AREA
C (DF)
C
C.....
C
C H2 1-10 E10.0 GBEFF R FAN GEARBOX EFFICIENCY
C
C.....
C.....
C
C I1 1-10 (E10.0, CPM R PLENUM COST (\$/LB)
C
C 11-20 E10.0, WPL R WEIGHT OF PLENUM MATERIAL (LB/SQ FT)
C
C 21-30 E10.0, CLUVR R COST OF LOUVERS (\$/SQ FT)
C
C 31-40 E10.0, CHAILS R COST OF HAIL SCREENS (\$/SQ FT)
C
C 41-50 E10.0, UCS R UNIT COST OF STACK \$/LB
C
C 51-60 E10.0, UWS R UNIT WT OF STACK LB/CU FT
C
C 61-70 E10.0, CVM R FAN RING MATERIAL UNIT COST \$/LB
C
C 71-80 E10.0) WFV R UNIT WT OF STRAIGHT CYLINDER LB/SQ FT
C
C.....
C.....
C
C J1 1-10 (F10.0, HXNP R NUMBER OF PASSES THRU HEAT EXCHANGER

C					
C		11-20	F10.0,	WB	R HEADER LENGTH (FEET)
C		21-30	F10.0,	NTUB	R NUMBER OF TUBES THRU PLATE FINS
C		31-40	F10.0,	SS	R SUPPORT SPACING (FT)
C		41-50	F10.0)	ANGLE	R HEAT EXCHANGER ANGLE (DEGREES)
C					
C				
C	J2	1-10	(F10.0,	DESVEL	R DESIGN VELOCITY (LIQUID) FOR PIPING (FT/SEC)
C		11-20	F10.0,	REDUCE	R MINIMUM STEP CHANGE IN PIPE DIAMETER FOR LIQUID PHASE TOWER PIPING (INCHES) MAY BE 6, 12, OR 18
C		21-30	F10.0,	QREDUCE	R MINIMUM STEP CHANGE IN PIPE DIAMETER FOR LIQUID PHASE QUADRANT HEADERING (INCHES) MAY BE 6, 12, OR 18
C		31-40	F10.0)	DIST	R DISTANCE FROM TOWER TO CONDENSER ROOM (FT)
C					
C				
C	J3	1-10	(F10.0,	DESVELV	R DESIGN VELOCITY (VAPOR) FOR PIPING. (FT/SEC)
C		11-20	F10.0,	REDUCEV	R MINIMUM STEP CHANGE IN PIPE DIAMETER FOR VAPOR PHASE TOWER PIPING (INCHES) MAY BE 6, 12, OR 18
C		21-30	F10.0,	QREDUCV	R MINIMUM STEP CHANGE IN PIPE DIAMETER FOR VAPOR PHASE QUADRANT HEADERING (INCHES) MAY BE 6, 12, OR 18
C		31-40	F10.0,	DESVELD	R DESIGN VELOCITY OF WATER THROUGH THE DELUGE PIPING (FT/SEC)
C		41-50	F10.0)	FACTORD	R RATIO OF WATER FLOWING THROUGH THE DELUGE WATER SYSTEM TO THE AMOUNT OF MAKE UP WATER
C					
C				
C	J4	1-10	(F10.0,	WATCONA	R ALLOWED WATER CONSUMPTION (ACRE- FEET)
C		11-20	F10.0,	WATCOST	R COST OF THE DELUGE WATER (\$/1000 GAL)
C		21-30	F10.0,	FACTOR	R RATIO OF THE WET AIR VELOCITY OVER THE DRY AIR VELOCITY OF THE HEAT EXCHANGER (DIMENSIONLESS)
C					

```

C      31-40   F10.0, HCD      R METAL TO DELUGEATE HEAT TRANSFER
C                                         COEFFICIENT (BTU/HR-SQ FT-DEG F)
C
C      41-50   F10.0, BETAF    R AIR SIDE FOULING COEFFICIENT
C                                         (BTU/HR-SQ FT DEG F)
C
C      51-60   F10.0, BETAI    R TUBESIDE FOULING COEFFICIENT
C                                         (BTU/HR-SQ FT-DEG F)
C
C      61-70   F10.0) RHOUT    R RELATIVE HUMIDITY OF THE AIR
C                                         LEAVING THE HEAT EXCHANGER
C
C.....
C.....
C
C  K1   1-10   (E10.0, XW      R TUBE TRANSVERSE PITCH (NORMAL TO AIR
C                                         FLOW) (INCHES)
C
C      11-20   E10.0, XD      R TUBE PITCH IN DIRECTION OF AIR FLOW
C                                         (INCHES)
C
C      21-30   E10.0, XDG     R TUBE DIAGONAL PITCH (INCHES)
C
C      31-40   E10.0, SF      R FIN SPACING (INCHES)
C
C      41-50   E10.0, DFIN    R FIN DIAMETER (INCH(ES)
C
C      51-60   E10.0) THFIN   R FIN THICKNESS (INCHES)
C
C.....
C.....
C
C  L1   1-10   (F10.0, ODL    R HX LINER OUTSIDE DIAMETER (INCHES)
C
C      11-20   F10.0, DI     R HX LINER INSIDE DIAMETER (INCHES)
C
C      21-30   F10.0, GAGLIN  R GAGE OF HX LINER TUBE (MAY BE
C                                         22. 20. 19. 18. 17. 16. 15.
C                                         14.5 14. 13. 12. 11. 10. )
C
C      31-50   2A10, TUBMAT,  R LINER MATERIAL. MUST BEGIN IN COL 3
C      XTUBMA  R
C
C                                         MAY BE -
C                                         ADMIRALTY
C                                         COPPER
C                                         CU-10 NI
C                                         CU-30 NI
C                                         ALUMINUM
C                                         STEEL WELDED
C                                         STEEL SEAMLESS
C                                         WELDED SST
C
C      51-60   F10.0) CONL   R THERMAL CONDUCTIVITY OF LINER MATER-
C                                         IAL (BTU/(HR SQFT DEG F/ FT) )
C
C.....
C.....
C
C  M1   1-20   (2A10   FINTYP  R TYPE OF FIN. MUST START IN COLUMN 1.
C      XFINTY

```



```

C.....
C
C Q1  1-10 (E10.0, CRJ  R COST OF ROLLED JOINT, TUBE TO HEADER
C          ($/TUBE)
C
C      11-20  E10.0, CWJ  R COST OF WELDED JOINT, TUBE TO HEADER
C          ($/TUBE)
C
C      21-30  E10.0, CHH  R TUBE AND PLUG HOLE PREPARATION COST
C          ($/HOLE)
C
C      31-40  E10.0, CN   R NOZZEL AND ATTACHING COST ($/HOLE)
C
C      41-50  E10.0, CMW  R COST OF HEADER MACHINING AND WELDING
C          ($/FT)
C
C      51-60  E10.0, CST  R STRUCTURAL STEEL COST ($/LB)
C
C      61-70  E10.0) CBJ  R COST OF BOLTED HEADER JOINT ($/FT)
C
C.....
C.....
C
C Q2  1-10  F10.0, CSH  R BUNDLE STIFFNER HOLE PREPARATION
C          COST ($/HOLE)
C
C      11-20  F10.0, CSHP R TUBE HOLE PREPARATION COST FOR
C          SECTION JOINT ($/HOLE)
C
C      21-30  F10.0, TSP  R PLATE THICKNESS FOR BUNDLE STIFFNERS
C          (IN)
C
C.....
C.....
C
C R1  1-10  (E10.0, XNS  R NUMBER OF CONDENSER SHELLS
C
C      11-20  E10.0, VELN R NOMINAL DESIGN VELOCITY THRU CONDEN-
C          SER TUBES (FT/SEC)
C
C      21-30  E10.0, ODC  R CONDENSER TUBE O.D. (INCHES)
C
C      31-40  E10.0, GA   R CONDENSER TUBE WALL GAGE. MAY BE
C          12. 14. 16. 18. 20. 22. 24.
C
C      41-50  E10.0, TKCT R THERMAL CONDUCTIVITY OF CONDENSER
C          TUBING
C          (BTU/(HR SQFT DEG F/FT))
C
C      51-60  E10.0, TTD2QE R TERMINAL TEMPERATURE DIFFERENCE
C          ESTIMATE
C          (DEGREES F)
C
C      61-80  2A10) CONMAT, R          CONDENSER TUBING MATER-
C          CONMA2  R          IAL. MUST START IN
C          COLUMN 61. MAY BE -
C
C
C          ADMIRALTY
C          CU-10 NI
C          304 S/S WELDED
C.....

```

```

C
C R2 1-10 (E10.0, XNP R NUMBER OF PASSES THRU CONDENSER
C
C 11-2 E10.0, TLA R CONDENSER TUBING LENGTH (FEET)
C
C 21-3 E10.0) XQUALY R AMMONIA VAPOR QUALITY OUT OF
C CONDENSER.
C
C.....
C
C R3 1-5 (15) LINOR R CONTROL VARIABLE
C =1 FOR LINDE TUBING
C =0 FOR BARE TUBES
C
C.....
C.....
C
C S1 1-5 (15, LFB I LFB AND LFE SPECIFY FIRST AND LAST
C 6-10 15, LFE I POSITION TO BE CONSIDERED IN THE
C TABLE OF FANS. DEFAULT VALUES ARE
C LFB=1 AND LFE=153
C
C
C DIAMETER IFAN LFAN
C
C 24. 1 27
C 26. 28 54
C 28. 55 88
C 30. 89 111
C 40. 112 135
C 60. 136 153
C
C 11-15 15) MXEXT I THE MAXIMUM ALLOWABLE NUMBER OF
C CALLS TO SUBROUTINE XTEND FOR ANY
C ONE DESIGN TEMPERATURE.
C
C DEFAULT VALUE IS 10
C
C.....
C.....
C
C T1 1-10 A10 FFHX R CONTROL VARIABLE FOR SPECIFYING
C METHOD TO USE IN COMPUTING FRICTION
C FACTOR. MUST START IN COLUMN 1 .
C MAY BE -
C
C HOTERV
C
C 11-20 A10 FSHOT R CONTROL VARIABLE FOR SPECIFYING
C TYPE OF SEARCH ROUTINE TO BE USED
C IN SEARCH FOR OPTIMUM MAY BE -
C
C SKIP SHOT
C CONSTANT
C
C 21-30 A10 FDELUG R CONTROL VARIABLE FOR SELECTING TYPE
C OF METHOD TO CALCULATE EVAPORATIVE
C HEAT TRANSFER MAY BE -
C
C DELUG
C DELBAW
C

```

5.3 DRY/WET MODEL OUTPUT

Complete output from a typical run of the dry/wet model is shown in Figure 18. The circled numbers on the figure correspond to the numbers in parentheses in this section. The output report is divided into the following sections:

(100) through (300) Input Summary

(400) through (500) Plant scaling for increased steam, and for fans and pumps

(600) through (700) Heat Exchanger

(800) Piping

(900) Condenser

(1000) Fans

(1100) through (1200) Plant performance as a function of ambient temperature

(1300) Cost summary

(1400) Operating Summary

(100) Output printed by subroutine SETUP.

This line begins a card-by-card summary of input data. Any cards preceding the first blank card are printed as title or description cards. After the first blank card the values are printed as they are read, and the variable name is printed immediately below the value. The line tags A1, B1, etc. correspond to the Card Type designations used in the Input Description (see Section 5.2). Variable names printed here are defined in the Input Description section. Every input variable read by the program appears in this summary.

(200) through (230) Output printed by subroutine INPSUM.

Some of the more frequently changed input parameters are summarized here with more descriptive labels than are given in the preceding summary.

(205) The options summarized here are those selected by the variables TFIX, FIXV, FIXTTD, FIXL, DEEPL, on Card Type B2; VELREC and TLIM on Card Type H1; and FFHX on Card Type T1.

(210) The starting point in the search for an optimum is specified by T1, FVAIR, TTD, ELENH, and ZD. These correspond to the values of VAS(1), VAS(2), VAS(3), VAS(4), and VAS(5) on Card Type B1.

(220) Input data pertaining to the turbine are summarized here.

(230) Unit costs and costing factors from Card Types D1 and E1 are reported here.

(300) Output printed by Main Program.

TD is the design temperature ($^{\circ}$ F) used in calculations for this case. The design temperature of the plant is the air temperature at which the power plant and cooling towers are designed to give a net power of PSIZE.

(400) Output printed by subroutine OUT2.

This report is printed upon return from subroutine SSCALE, after the steam supply system is scaled to allow for increased heat rate at the rating back pressure. The term HRFAC1 is the heat rate factor at the rating back pressure, RBP.

(500) Output printed by subroutine OUT4.

Values reported here are intermediate results after the plant is scaled for increased steam, but before it is scaled for fan and pump power requirements. HRFAC2 is the heat rate factor at the indicated design back pressure. PLANC2 is the plant cost; PSIZ12 is the plant size needed at rating back pressure to provide the specified plant power output (PSIZE on Card Type D1) at design back pressure. $PSIZ12 = PSIZE * (HRFAC2/HRFAC1)$. SPBP is the cost differential incurred in scaling the plant to allow for the difference between design conditions and base plant conditions (conventional turbine at rated back pressure).

(550) Output printed by subroutine OUT4.

The information reported here is for the plant after scaling to provide for additional power to drive fans and pumps. The scaling factor, S.F., is the ratio PSIZE/(PSIZE power required by fans and pumps). PSIZ13 corresponds to PSIZ12 above, but now the fan and pump power requirements are included. PSIZ13 = (PSIZ12) x (S.F.). The power PTOTAL is the size of the scaled plant. PTOTAL = (PSIZE) x (S.F.). PLANC3 is the plant cost per kilowatt, excluding fan and pump capital costs, at design conditions. SPC is the plant cost excluding fans and pumps. SPCD is the differential cost of the plant due to the use of a dry cooling tower as a heat rejection system. It is the difference in cost between the plant using a conventional turbine at rated back pressure and the plant using a nonconventional turbine at plant design conditions.

(600) Output printed by subroutine RPTHXD.

This report summarizes the input data pertaining to heat exchanger design, materials, and unit costs. Values are entered on Card Type K1, L1, M1, P1, and Q1.

(700) through (760) Output printed by subroutine RPTHXC.

The heat exchanger design, operating conditions, performance characteristics and costs are reported here.

(710) Fluid flow and heat transfer characteristics are summarized. The term TTD1 is terminal temperature difference, and corresponds to VAS(3) on Card Type B1.

(720) Heat Exchanger geometry terms reported here are defined as

$$AFTR = \frac{\text{Fin Area}}{\text{Total Area for Heat Transfer}}$$
$$ALPHA = \frac{\text{Heat Transfer Area (ft}^2\text{)}}{\text{Unit Volume of Heat Exchanger (ft}^3\text{)}}$$

$$\text{SIGMA} = \frac{\text{Free Flow Area}}{\text{Frontal Area}}$$

$$\frac{\text{FITCO}}{\text{ATOT}} = \frac{\text{Finned Tube Cost (\$)}}{\text{Heat Transfer Area (ft}^2\text{)}}$$

(730) Weights of major dry/wet cooling tower components are reported.

(740) Fluid flow rates and heat exchanger geometry previously printed are repeated here for convenience.

(750) An itemized list of costs associated with fabricating, shipping and installing the heat exchanger.

(760) Parameters pertaining to the heat exchanger when it is deluged are listed here as a function of the ambient air temperatures at which the heat exchanger is deluged. Abbreviations used in column headings are:

TAIN - Temperature of the ambient air entering the deluged heat exchanger.

RIIN - Enthalpy of air entering heat exchanger.

SIGIN - Tube to air mass transfer coefficient at point where air enters the heat exchanger.

SIGMA - Mass transfer coefficient between the delugeate and the air.

UDPS - Overall mass transfer coefficient between the tube-side fluid and the delugeate-air interface.

DTDR - Quantity for transforming the tubeside to delugeate heat transfer coefficient to the tubeside to delugeate coefficient.

HI - Tubeside heat transfer coefficient.

CSS - Heat capacity of saturated air at the delugeate-air interface.

TS - Temperature of the delugeate-air interface.

RIS - Enthalpy of saturated air at the temperature of the delugeate-air interface.

RII - Enthalpy of the saturated air at the tubeside temperature.
AHIN - Absolute humidity of the air entering the heat exchanger.
TOUT - Temperature of the ambient air exiting the deluged heat exchanger.
RILVG - Enthalpy of the air leaving the heat exchanger.
SIGLVG - Tubeside to air mass transfer coefficient evaluated for conditions at the trailing edge of the heat exchanger.
QSEC - Heat transfer rate.
RMEVAP - Water evaporation rate.
AHLVG - Absolute humidity of the air leaving the heat exchanger.

(800) Output printed by subroutine RPTSUP.

Supply piping costs are itemized separately for circulation piping, quadrant piping, and distribution piping. Pump and piping costs are reported in thousands of dollars ($\$ *10^{**3}$).

(850) Output printed by subroutine RPTRET. A cost report for the return piping system is provided here.

(900) Output printed by subroutine RPRT2.

Condenser design and costing are reported in this section.

(1000) Output printed by subroutine RPTFAN.

Fan geometry, costs, and design conditions are reported here. Design condition values reported in the column labeled ADJUSTED are for air reduced to standard conditions. The space labeled DRIVE SYSTEM is reserved for future use. In its present form, the model assumes a spiral bevel drive system only.

(1100) Output printed by subroutine VARIT.

System performance and costs are reported for one year of operation at times and temperatures specified on Card Types C1 and C2. Abbreviations used in column headings are:

HX - heat exchanger
ITD - initial temperature difference
LMTD - log mean temperature difference
CAP - capacity
TEMP - temperature
PCT - percent
TTDP - terminal temperature difference (condenser).

(1200) Output printed by main program.

FINAL INCREMENTAL COST is the total of the entries in PORTION OF INCREMENTAL POWER COST column. Units are mills/kWh. Capacity charge of gas turbine is computed by the expression

$$\text{CAPACITY CHARGE} = (\text{CAPCHG})(\text{PSIZE}-\text{PGEN}),$$

where

PGEN is the power generated at highest ambient temperature;
(PSIZE-PGEN) is the replacement capacity (kW);
CAPCHG is the cost of replacement capacity (\$/kW);
PSIZE and CAPCHG are input values on Card Types D1 and E1.

(1300) Output printed by subroutine SUMCOS.

Major cost components are summarized here. Costs reported under the heading CAPITAL COST SUMMARY (1340) are in dollars; those reported under UNIT ENERGY COST SUMMARY are in mills/kWh. The ENERGY PENALTY (1350) is the summation of the products of two columns in the performance cost table (1100), that is, (COST TO REPLACE LOST CAP) x (PCT TIME AT AMBIENT TEMP). Similarly, the ADDITIONAL BASE PLANT FUEL (1360)

is the summation of the products (CHANGE IN FUEL COST) x (PCT TIME AT AMBIENT TEMPERATURE). OPERATION AND MAINTENANCE unit cost (1370) is based on the cooling system capital cost and the input variable PER (Card Type D1), which is simply the ratio of maintenance cost to capital cost. The calculation is made in subroutine SCALP. The final TOTAL (1380) is the same as the FINAL INCREMENTAL COST reported in the preceding table (1200).

(1400) Output printed by subroutine SUMMARY.

Gives an overview of the dry/wet cooling system in terms of size, operating parameters, and incremental cost.

100 AN-11 DRY/WET COOLING TOWER COST MODEL -- AMMONIA CIRCULAR TOWER VERSION THIS RUN MADE 05/24/74 15.43.34															
***** 25% ACRE FEET OF WATER AVAILABLE *****															
(A1)	85,000,000	55,000,000	100,000,000	8,000,000	5,000,000	80,000,000	4,000,000								
(B1)	TSTAR	TEND	VAS(1)	VAS(2)	VAS(3)	VAS(4)	VAS(5)								
(B2)	FIXA	FIXV	FIXTD	FIXL	DEEPL										
(C1)	TA(1)	TA(2)	TA(3)	TA(4)	TA(5)	TA(6)	TA(7)	TA(8)	TPER(1)	TPER(2)	TPER(3)	TPER(4)	TPER(5)	TPER(6)	
(C2)	TA(9)	TA(10)	TA(11)	TA(12)	TA(13)	TA(14)	TA(15)	TA(16)	TPER(9)	TPER(10)	TPER(11)	TPER(12)	TPER(13)	TPER(14)	
(C1A)	TWR(1)	TWR(2)	TWR(3)	TWR(4)	TWR(5)	TWR(6)	TWR(7)	TWR(8)	RPLM(1)	RPLM(2)	RPLM(3)	RPLM(4)	RPLM(5)	RPLM(6)	
(C2A)	TWR(9)	TWR(10)	TWR(11)	TWR(12)	TWR(13)	TWR(14)	TWR(15)	TWR(16)	RPLM(9)	RPLM(10)	RPLM(11)	RPLM(12)	RPLM(13)	RPLM(14)	
(D1)	PER	CCM	ELEV	MODEL											
(E1)	FCIS	PACOS	PLANC	CJSTL	CSPKW	CAPCW	HPCST	CTURB							
(E2)	PUMHAF	PUMFA	PUMLEF	PUMCIR	PUMCND	PUMSTC	PUMRCL								
(F1)	TRP(1)	TRP(2)	TRP(3)	TRP(4)											
(G1)	EFFP														
(H1)	VELNEC	KUPPA	TLIM	TUMIN	TOMAX	PFACT									
(H2)	GAFF														
(I1)	CPM	HPL	CLJVK	CHALLS	UCS	UMS	CVM	HV							
(J1)	HXP	H	NTM	SS	ANGLE										
(J2)	DESVEL	REDUCE	REDUCE	DIST											
(J3)	DESVELV	REDUCV	REDUCV	DESVELD	FACTURD										
(J4)	HATCUNA	HATCOST	FACTRM	HCD	BETAF	BETAZ	RHOUT								
(K1)	K	KD	KDG	BF	DFIN	TWIN									

FIGURE 18. Dry/Wet Model Sample Output

(L1) .72635 .06929 22.00000 ALUMINUM 118.00000
 PDL DT GAGLTH TUBHA CONL

(M1) PLATE ALUMINUM 118.00000
 FINMAY CONV

(N1) 0% COATE 0% ZINCC 0% CASTC 0% FUREPC

(P1) FURN REMOVABLE ALUMINUM 1.5% 20% SEGL 5% SIDES
 HEDTYP HENKAT TH

(Q1) 1.0000000 1.5000000 1.3000000 20.000000 9.0000000 5.3000000 4.0000000
 CHJ CHJ CHM CM CHM CHJ

(Q2) .500000001 .5000000 .1250000
 CHM CHMP TSP

(R1) 2.0000000 1.0000000 1.0000000 12.000000 118.00000 5.0000000 LINEE AI IS
 XNS YELN DDC GA TROY TROWE CONKAT

(R2) 1.0000000 50.000000 .4000000
 XNP TLA EQUALY

(R3) 1
 LINR

(S1) 55 AB -U
 LFR LFF XHEXT

(T1) ROTERY SNIP SHOT DELBAH
 PEMA PSHOT PDEUG

(200) INPUT SUMMARY AND CASE DESCRIPTION

(205)

OPTIONS SELECTED FOR THIS RUN

UPPER LIMIT ON TURBINE TEMP 1800 F
 FRICTION FACTOR AND HT TRAC COEFF BY HOTEV
 EXIT TEMPERATURE OF TURBINE UNCONSTRAINED
 FRONTAL AIR VELOCITY UNCONSTRAINED
 TERMINAL TEMPERATURE DIFFERENCE UNCONSTRAINED
 EXCHANGER LENGTH UNCONSTRAINED
 EXCHANGER DEPTH UNCONSTRAINED
 RUN WITH VELOCITY RECOVERY

(210)

STARTING CONDITIONS

TURBINE OUTLET TEMPERATURE, T1 100.000 F
 FRONTAL AIR VELOCITY, VAIR 8.00 FT/SEC
 TERMINAL TEMPERATURE DIFFERENCE TTA1 5.000 F
 LENGTH OF HEAT EXCHANGER TUBES FT/IN 40.0 FEET
 NUMBER OF H.T. TUBES IN DEPTH 20

(220)

HEAT RATE FACTOR AS FUNCTION OF BACKPRESSURE (INCHES OF MERCURY)
 TURBINE RATING BACKPRESSURE 3.50 INCHES OF MERCURY
 SITE ELEVATION 5500 FEET ABOVE SEA LEVEL

COEFFICIENTS FOR POLYNOMIAL CURVE FIT
 A0 9.01210E-01 A1 -7.30950E-03 A2 2.40950E-07 A3 -1.00640E-15 A4

(230) UNIT COSTS AND COSTING FACTORS

FUEL 06.900 CENTS/WHRTM	POWER PLANT CONSTRUCTION 571.000 \$/KW	FIXED CHARGE RATE .180
LAND 0.000 \$/SQ FT	REPLACEMENT POWER 24.000 MILLS/KWH	CAPACITY FACTOR .750
WATER 30.000 \$ / HP	STEAM SUPPLY 190.000 \$/KW TURBINE OUTPUT	BASE THERMAL EFFICIENCY .400
	CAPACITY CHARGE 121000.000 \$/KW	CONSTRUCTION COST MULTIPLIER 1.000
		MAINT COSTS / CAPITAL COSTS .010

FIGURE 18. (contd)

5.23

(300) TO USED IN THE FOLLOWING CALCULATIONS IS # 55,000

IN BR LIMIT TMAX,THIN,RIMAX,RIMIN# 1.99953E+02 2.00000E+00 1.84130E+03 1.93274E+00

(400) STEAM SUPPLY SCALING TO COMPENSATE FOR INCREASED HEAT RATE AT RATING BACKPRESSURE. RRPE 1.50 IN. HG WRFAC1# 1.000043
 STEAM SUPPLY COST DIFFERENTIAL \$ 8400. TURBINE COST DIFFERENTIAL 0. \$/KW
 PLANT COST INCLUDING STEAM SUPPLY AND TURBINE \$ 571008200. PLANT UNIT COST INCLUDING STEAM SUPPLY AND TURBINE 571. \$

(500) CONDITIONS AFTER SCALING PLANT AND STEAM SUPPLY (REQUIRE SCALING FOR FANS AND PUMPS) WRFAC2# .9999216 W#
 PSIZ12# 999.8807 \$/KW
 PLANT2# 570.3691 \$
 SPRPE# 10002.789 IN. HG
 BACK PRESSURE# 1.407473 DEG F
 SAT TEMPERATURE# 119.600000

AMMONIA FLOW RATE 10672457.5 LB MASS / HR
 HEAT REJECTED 2.001217A2E+10 BTU/HR
 AIR FLOW RATE 55034042.1 LB MASS / HR
 PUMP POWER 590.744923 KILOWATTS
 FAN POWER 9678.36544 KILOWATTS
 HX SURFACE AREA 18264465.4 SQ FT
 FRONTAL AREA 306183.481 SQ FT
 WIDTH/LENGTH RATIO 34.1540669
 WIDTH 17359 TUBES
 HEIGHT 3417.22635 FEET
 CONDENSER HT TRF AREA 411054.465 SQ FT TOTAL
 NO. CONDENSER TUBES 11402.0000
 CONDENSER TUBE LENGTH 50.000000 FT.
 AMMONIA VELOCITY .999655233 FT/SEC

(550) SCALING FOR FAN AND PUMP POWER DELIVERMENTS

SCALING FACTOR 1.01037546 W#
 PSIZE 1000.00000 W#
 PRIZ13 1009.24479 W#
 PTOTAL 1010.37546 W#
 PLAND3 474.287053 \$/KW
 SFC 474247053 \$
 KRPD 4287052.65 \$

AMMONIA FLOW RATE 10795171.1 LB MASS / HR
 HEAT REJECTED 2.006314537E+10 BTU/HR
 AIR FLOW RATE 55609468.1 LB MASS / HR
 PUMP POWER 596.474221 KILOWATTS
 FAN POWER 9778.78466 KILOWATTS
 HX SURFACE AREA 18057011.7 SQ FT
 FRONTAL AREA 300369.334 SQ FT
 WIDTH/LENGTH RATIO 34.5340010
 WIDTH 17530 TUBES
 HEIGHT 3452.09233 FEET
 CONDENSER HT TRF AREA 415319.365 SQ FT TOTAL
 NO. CONDENSER TUBES 11727.1164
 CONDENSER TUBE LENGTH 50.000000 FT.
 AMMONIA VELOCITY .995655233 FT/SEC

FIGURE 18. (contd)

600 NON-DELTA HEAT EXCHANGER DESCRIPTION

SUPPORT SPACING	3.200	FEET	ROOT DIAMETER	.7543	INCH
TUBE PITCH NORMAL TO AIR FLOW	2.362	INCH	FIN THICKNESS	.0130	INCH
TUBE PITCH IN DIRECTION OF AIR FLOW	.984	INCH	FIN DIAMETER	1.720	INCH
TUBE DIAGONAL PITCH	1.537	INCH	FIN SPACING	.1000	INCH
LINER GAP	22.0		FIN TYPE	PLATE	
TUBES THRU EACH FIN	1	TUBES	AREA OF PLATE FIN	1.9	SQ IN.
LINER MATERIAL	ALUMINUM		FIN MATERIAL	ALUMINUM	
LINER THERMAL CONDUCTIVITY	118,000		FIN THERMAL COND.	118.0	BTU/HR SQ FT DEG F/FT
LINER TUBING OUTSIDE DIAMETER	.7284	INCH	HEADER TYPE	FURN REMOVABLE	
LINER TUBING INSIDE DIAMETER	.6724	INCH	HEADER LENGTH	12,000	FEET

--- UNIT COSTS ---

FIN BURNING	\$ 0.	/SQ FT	HEADER MATERIAL (ALUMINUM)	\$	0.000/LB
PROTECTIVE COATING	\$ 0.	/SQ FT	ROLLED JOINT, TUBE TO HEADER	\$	1.000/TUBE
ZINC FOR SPACERS	\$ 0.	/LB	ROLLED JOINT, TUBE TO HEADER	\$	1.000/TUBE
SPACER CASTING	\$ 0.	/EA	TUBE AND PLUG HOLE PREPARATION	\$	1.000/HOLE
END PREPARATION	\$ 0.	/TUBE	NOZZLE AND ATTACHING	\$	25.000/HOLE
			ROLLED HEADER JOINT	\$	1.000/FT
			HEADER MACHINING AND WELDING	\$	0.000/FT
			STRUCTURAL STEEL	\$.830/LB
LINER TUBING	\$ 1.0771	/FT			
PROTECTIVE COATING	\$ 0.	/FT			
PLATING	\$ 0.1168	/FT			
FINISHED TUBE	\$ 1.0799	/FT			
TUBE SPACERS	\$ 0.	/FT			

700 HEAT EXCHANGER

12x6 FANS 1.0 PASS

710

REYNOLDS NUMBER	4.93447E+02	1.20376E+04
VELOCITY (FT/SEC)	1.37359E+01	2.14535E+01
PRESSURE DROP FILM FORCE/50 IN	9.24629E+03	1.34833E+04
HEAT TRFR COEFF (BTU/HR SQ FT DEG F)	9.47372E+00	1.71071E+03
FRICTION FACTOR	9.35943E+01	7.09006E+03
INLET TEMPERATURE (F)	5.50000E+01	1.11003E+02
EXIT TEMPERATURE (F)	9.21154E+01	1.11003E+02
RANGE (F)	3.71154E+01	
ITOT	4.48000E+00	
INT	1.00000E+00	
OVERALL H (BTU/HR SQ FT DEG F)	7.47316E+00	
EFFECTIVENESS	.6627	
FIN EFFICIENCY	.8903	

720 AFM .9444339
ALPHA 141.41403
SIGMA .00208401

FTTC/ATJT .23143703

730

WT OF AMMONIA	77610	LB
WT OF TUBES	2412372	LB
WT OF FRAME	1645007	LB
WT OF HEADER	1120676	LB
PIPE LOAD	12370413	LB

80.00 LB/50 FT

740

AMMONIA FLOW RATE	10743171	LB/HR
AIR FLOW RATE	55609660	LB/HR
TUBES IN DEPTH	1.00	TUBES (3 FT DEEP)
TUBES ACROSS FRONT	17439	TUBES (3452.7 FT WIDE)
LENGTH OF TUBES	90.	FEET

SUPFACE AREA	14457911	SQ FT
FRONTAL AREA	319300	SQ FEET

750

COOLING SURFACE	\$	762630.
HEADER AND NOZZLE	\$	121562.
BUNDLE ASSEMBLY AND FRAME	\$	374757.
PLENUM	\$	24196.
DOVERS	\$	0.
MAIL SCREENS	\$	42420.
STRUCTURE	\$	507600.
FOUNDATION	\$	40777.

BUNDLE STIFFENER COST	\$	300916.
SECTION JOINT COST	\$	172071.
BUNDLE FRAME COST	\$	249039.
CHAIN PLATE COST	\$	52015.
BUNDLE ASSEMBLY COST	\$	1250230.

FIGURE 18. (contd)

(760) DELUGED HEAT EXCHANGER DATA

MU	9.0000E+01	RETA	1.0000E+06	PETAT	1.0000E+06
AM	6.9943E+01	AF	1.1043E+01	AIT	7.0408E+01
AW	7.3340E+01	TM	4.6667E-03	PKW	1.1809E+02
ATM	8.1030E+01	RMA	4.6782E+02		

LEADING EDGE OF HEAT EXCHANGER

TAIN	RIN	SIGIN	SIGMA	UDPS	DTOP	MI	FR	TS	RIS
5.7000E+01	1.9401E+01	8.3304E+00	1.4472E+01	1.8931E+01	3.8883E+01	1.9015E+03	2.6076E+01	9.4197E+01	7.5023E+01
6.2000E+01	2.2254E+01	8.2954E+00	1.4472E+01	1.8707E+01	3.8677E+01	1.8708E+03	2.6100E+01	9.4402E+01	7.5313E+01
6.7000E+01	2.4927E+01	8.2222E+00	1.4472E+01	1.8368E+01	3.8482E+01	1.8193E+03	2.6131E+01	9.4887E+01	7.6623E+01
7.2000E+01	2.7094E+01	8.1607E+00	1.4472E+01	1.8113E+01	3.8326E+01	1.7743E+03	2.6153E+01	9.5296E+01	7.7259E+01
7.7000E+01	2.9416E+01	8.1119E+00	1.4472E+01	1.7845E+01	3.8158E+01	1.7333E+03	2.6177E+01	9.5830E+01	7.7953E+01
8.2000E+01	3.1057E+01	8.0717E+00	1.4472E+01	1.7649E+01	3.8039E+01	1.7032E+03	2.6199E+01	9.5867E+01	7.8449E+01
8.7000E+01	3.2778E+01	8.0226E+00	1.4472E+01	1.7419E+01	3.7914E+01	1.6668E+03	2.6212E+01	9.6115E+01	7.8972E+01
9.2000E+01	3.4584E+01	7.9732E+00	1.4472E+01	1.7186E+01	3.7780E+01	1.6315E+03	2.6231E+01	9.6376E+01	7.9526E+01
9.7000E+01	3.5521E+01	7.9471E+00	1.4472E+01	1.7067E+01	3.7716E+01	1.6131E+03	2.6241E+01	9.6411E+01	7.9914E+01
9.8000E+01	3.6482E+01	7.9198E+00	1.4472E+01	1.6941E+01	3.7647E+01	1.5943E+03	2.6252E+01	9.6649E+01	8.0111E+01
1.0100E+02	4.0573E+01	7.7949E+00	1.4472E+01	1.6799E+01	3.7352E+01	1.5136E+03	2.6294E+01	9.7290E+01	8.1398E+01

TI	RIT	AHTN
1.11107E+02	1.1841E+02	5.4670E-03
1.11107E+02	1.1841E+02	6.5726E-03
1.11107E+02	1.1841E+02	7.8499E-03
1.11107E+02	1.1841E+02	8.7128E-03
1.11107E+02	1.1841E+02	9.6891E-03
1.11107E+02	1.1841E+02	1.0060E-02
1.11107E+02	1.1841E+02	1.0500E-02
1.11107E+02	1.1841E+02	1.1045E-02
1.11107E+02	1.1841E+02	1.1838E-02
1.11107E+02	1.1841E+02	1.1820E-02
1.11107E+02	1.1841E+02	1.4334E-02

TRAILING EDGE OF HEAT EXCHANGER

TOUT	RIVG	SIGLVG	SIGMA	UDPS	DTOP	MI	FR	TS	RIS
6.8780E+01	3.8240E+01	8.1809E+00	1.4472E+01	1.8090E+01	3.7160E+01	1.9015E+03	2.6326E+01	9.7255E+01	8.2236E+01
7.0605E+01	4.0150E+01	8.1235E+00	1.4472E+01	1.7902E+01	3.7012E+01	1.8908E+03	2.6340E+01	9.7024E+01	8.2499E+01
7.2492E+01	4.2209E+01	8.0647E+00	1.4472E+01	1.7819E+01	3.6872E+01	1.8193E+03	2.6371E+01	9.8207E+01	8.3532E+01
7.3936E+01	4.3475E+01	8.0129E+00	1.4472E+01	1.7737E+01	3.6762E+01	1.7743E+03	2.6388E+01	9.8431E+01	8.4035E+01
7.5075E+01	4.5673E+01	7.9615E+00	1.4472E+01	1.7133E+01	3.6636E+01	1.7333E+03	2.6408E+01	9.8888E+01	8.4413E+01
7.6513E+01	4.6940E+01	7.9234E+00	1.4472E+01	1.6958E+01	3.6548E+01	1.7032E+03	2.6427E+01	9.8864E+01	8.5019E+01
7.7504E+01	4.8269E+01	7.8788E+00	1.4472E+01	1.6751E+01	3.6461E+01	1.6668E+03	2.6437E+01	9.9041E+01	8.5425E+01
7.8648E+01	4.9667E+01	7.8317E+00	1.4472E+01	1.6543E+01	3.6367E+01	1.6315E+03	2.6452E+01	9.9233E+01	8.5868E+01
7.9197E+01	5.0392E+01	7.8071E+00	1.4472E+01	1.6434E+01	3.6318E+01	1.6131E+03	2.6468E+01	9.9335E+01	8.6199E+01
7.9751E+01	5.1135E+01	7.7815E+00	1.4472E+01	1.6321E+01	3.6267E+01	1.5943E+03	2.6480E+01	9.9438E+01	8.6334E+01
4.2028E+01	5.4366E+01	7.6678E+00	1.4472E+01	1.5828E+01	3.6054E+01	1.5136E+03	2.6480E+01	9.9872E+01	8.7357E+01

TSER	RMFVAP	AHLVG
6.6701E+03	6.4814E+00	1.0321E+02
8.3762E+03	6.5687E+00	2.0613E+02
5.0850E+03	6.8209E+00	2.2022E+02
7.8506E+03	6.7602E+00	2.3176E+02
7.6057E+03	6.8974E+00	2.4433E+02
7.4364E+03	7.1426E+00	2.5328E+02
7.2473E+03	7.3763E+00	2.5267E+02
7.0558E+03	7.4002E+00	2.7263E+02
6.9507E+03	7.4091E+00	2.7783E+02
6.9552E+03	7.7175E+00	2.8317E+02
6.4246E+03	7.6159E+00	3.0812E+02

FIGURE 18. (contd)

 (800) SUPPLY PIPING

CIRCULATION PIPING

HEADER	DIAMETER (INCHES)	LENGTH (FEET)	COST IN 1000 DOLLARS FOR				
			PIPE	TEES	REDUCERS	EXPANSION JOINTS (1)	FLANGES (3)
1	60.0	617.1	1172.2	77.2	63.3	62.8	76.6
2	60.0	0.0	0.0	61.9	44.2		
3	50.0	351.2	450.0	49.2	37.3		
4	48.0	0.0	0.0	30.4	20.4		
5	42.0	351.2	306.0	31.6	16.0		
6	30.0	0.0	0.0	11.5	0.0		

TOTAL COST OF CIRCULATION SUPPLY PIPING 42521.61000

HORIZONTAL QUADRANT SUPPLY PIPING

HEADER	DIAMETER (INCHES)	LENGTH (FEET)	COST IN 1000 DOLLARS FOR		
			PIPE	TEES	REDUCERS
1	18.0	0.0	0.0	1.4	0.0

VERTICAL QUADRANT SUPPLY PIPING

HEADER	DIAMETER (INCHES)	LENGTH (FEET)	COST IN 1000 DOLLARS FOR		
			PIPE	TEES	REDUCERS
1	18.0	0.0	0.0	1.5	0.0
2	18.0	4.1	.6	1.5	.8
3	12.0	8.0	.7	.9	0.0
4	12.0	8.0	.7	.9	0.0
5	12.0	8.0	.7	.9	0.0
6	12.0	8.0	.7	.9	0.0
7	12.0	8.0	.7	.9	.3
8	0.0	9.6	.3	0.0	0.0

NUMBER OF BUNDLES PER QUADRANT 16

FITTINGS COST PER BUNDLE \$ 411.01000

COST OF SUPPLY HEADERS PER QUADRANT \$ 23.701000

TOTAL COST OF QUADRANT SUPPLY HEADERS \$ 569.01000

TOWER SUPPLY PIPING

NUMBER OF TOWERS 6
 NUMBER OF TOWERS WITH DRUDGE PIPING 3
 TOWER DIAMETER 234. FEET
 TOWER HEIGHT 71.0 FEET
 BUNDLE WIDTH 12.0 FEET
 DIAMETER OF PIPE FROM CIRCULATION HEADER TO TOWER DISTRIBUTION HEADER 30. INCHES
 DIAMETER OF TOWER DISTRIBUTION PIPE 16. INCHES

COST OF DISTRIBUTION PIPING PER TOWER \$ 327.01000

TOTAL COST OF TOWER DISTRIBUTION PIPING \$ 1959.01000

VAPOR DESIGN VELOCITY 150. FPS
 MASS FLOW RATE 1,007,000 LBM/HR
 CONDENSER OUTLET TEMPERATURE 114.02 DEG. F
 HEAT EXCHANGER INLET TEMPERATURE 111.00 DEG. F
 SUPPLY PIPING PRESSURE DROP 2177.7 PSF
 SUPPLY PIPING DYNAMIC HEAD 2607.5 FEET

TOTAL SUPPLY PIPING SYSTEM COST \$ 5050.01000

FIGURE 18. (contd)

 (850) RETURN PIPING

CIRCULATION PIPING

HEADER	DIAMETER (INCHES)	LENGTH (FEET)	COST IN 10**3 DOLLARS FOR				
			PIPE	TEES	REDUCERS	EXPANSION JOINT(1)	FLANGES (3)
1	36.0	617.1	447.2	21.7	11.4	16.1	16.0
2	30.0	0.0	0.0	12.8	0.0		
3	30.0	351.2	173.8	12.8	6.8		
4	24.0	0.0	0.0	3.9	0.0		
5	24.0	351.2	93.1	3.9	2.2		
6	18.0	0.0	0.0	1.6	0.0		

TOTAL COST OF CIRCULATION RETURN PIPING \$ 823. *10**3

HORIZONTAL QUADRANT RETURN PIPING

HEADER	DIAMETER (INCHES)	LENGTH (FEET)	COST IN 10**3 DOLLARS FOR		
			PIPE	TEES	REDUCERS
1	12.0	0.0	0.0	.8	.4
2	6.0	170.2	7.4	.3	0.0

EXTERIOR VERTICAL QUADRANT RETURN PIPING

HEADER	DIAMETER (INCHES)	LENGTH (FEET)	COST IN 10**3 DOLLARS FOR		
			PIPE	TEES	REDUCERS
1	6.0	0.0	0.0	.4	0.0
2	6.0	0.8	.4	.4	0.0
3	6.0	0.8	.4	.4	0.0
4	6.0	0.8	.4	.4	0.0
5	6.0	0.8	.4	.4	0.0
6	6.0	0.8	.4	.4	0.0
7	6.0	0.8	.4	.4	0.0
8	6.0	0.8	.4	.3	0.0

NUMBER OF BUNDLES PER QUADRANT 16

FITTINGS COST PER BUNDLE \$.785 *10**3

COST OF RETURN HEADERS PER QUADRANT \$ 33.6 *10**3

TOTAL COST OF QUADRANT RETURN HEADERS \$ 405. *10**3

FIGURE 18. (contd)

TOWER RETURN PIPING

TOWER DIAMETER 234. FEET
DIAMETER OF PIPE FROM CIRCULATION
HEADER TO TOWER DISTRIBUTION HEADER 16. INCHES
DIAMETER OF TOWER DISTRIBUTION PIPE 12. INCHES
COST OF DISTRIBUTION PIPING PER TOWER \$ 170. *10**3

TOTAL COST OF TOWER DISTRIBUTION PIPING \$1017. *10**3

LIQUID DESIGN VELOCITY 15. FPS
MASS FLOW RATE 1,107,007 LBM/HR
RETURN PIPING PRESSURE DROP 645.0 PSF
RETURN PIPING DYNAMIC HEAD 16.9 FEET

TOTAL RETURN PIPING SYSTEM COST \$ 2646. *10**3

P U M P S

PUMP COST \$ 291. *10**3
PUMP FITTINGS \$ 304. *10**3
PUMP ELECTRICAL \$ 144. *10**3

PUMP STATION \$ 874. *10**3

SEPARATOR COST \$ 1207. *10**3

DELUGE PIPING COST \$ 1008. *10**3

FIGURE 18. (contd)

(900) -----
 CONDENSER

--- DESIGN CONDITIONS ---

STEAM TEMPERATURE 119.6 F
 AMMONIA TEMPERATURE 114.0 F
 INLET AMMONIA VELOCITY 1.00 FT/SEC
 OUTLET AMMONIA VELOCITY 33.10 FT/SEC
 PRESSURE DROP THRU CONDENSER 304.6 LR/30 FT

--- CONDENSER DESCRIPTION ---

NUMBER OF SHELLS 2
 HEAT TRANSFER AREA PER SHELL 20553E+06 SQ FT
 NUMBER OF PASSES PER SHELL 1
 TUBE LENGTH 50 FEET
 NUMBER OF TUBES PER SHELL 15701

--- DESIGN OPERATING CONDITIONS ---

OVERALL HEAT TRANSFER COEFFICIENT 2553.46 BTU/HR SQ FT DEG F
 STEAM HEAT TRANSFER COEFFICIENT 4409.33 BTU/HR SQ FT DEG F
 AMMONIA HEAT TRANSFER COEFFICIENT 16367.36 BTU/HR SQ FT DEG F
 WALL HEAT TRANSFER COEFFICIENT 11516.85 BTU/HR SQ FT DEG F
 FORCED CONVECTION COEFFICIENT 498.93 BTU/HR SQ FT DEG F

--- CONDENSER COSTS ---

TUBING MATERIAL \$ 3756630.05 (LINDE AL12)
 SHELLS \$ 1792424.44
 FIELD ERECTION \$ 1436172.71
 TOTAL COST OF CONDENSER \$ 6985227.20

(1000) -----
 FANS

FANS EQUIPPED WITH VELOCITY RECOVERY DIFFUSERS

--- DRIVE SYSTEM ---

BLADE AND HUB COST/FAN \$ 6966.
 MOTOR COST/FAN \$ 4647.
 SPEED REDUCER DRIVE COST/FAN \$ 13051.
 STACK COST/FAN \$ 16107.
 ELECTRICAL COST/FAN \$ 22622.

*** ANNUAL OPERATIONAL COSTS \$ 2777510.

--- FAN GEOMETRY ---

HUB DIAMETER 6.31 FEET
 BLADE DIAMETER 24.00 FEET
 BLADE ANGLE 10.00 DEGREES
 NUMBER OF BLADES/FAN 6.00
 NUMBER OF FANS 127.

--- DESIGN CONDITIONS ---

	(ACTUAL)	(ADJUSTED)
VOLUMETRIC FLOW RATE/FAN	1257406.00	CU FT/MIN
TOTAL VOLUMETRIC FLOW RATE	15956655.00	CU FT/MIN
TOTAL AIR PRESSURE DROP OF M.V.	.01443	PSI .01857
PRESSURE DROP ACROSS M.V. BUNDLE	.00925	PSI .01190
NON-RECOVERABLE VELOCITY HEAD	.00518	PSI .00667
NONPOWERED/FAN	104.	HP 133.
FAN POWER REQUIREMENTS	12470.	HP

THE NUMBER OF TIMES NO FAN HAS FOUND
 THE NUMBER OF TIMES LUMP ESCAPE HAS REQUIRED :

7

FIGURE 18. (contd)

1100		AMBIENT	TURBINE	BACK	HEAT	RANGE		HX	HX	POWER	CHANGE IN	COST TO	POWER COST	PCT TIME	PORTION OF
TEMP	OUTLET	PRESSURE	RATE	FACTOR	TTOP	LMTD	ITD	GENERATED	FUEL COST	REPLACE	AT AMBIENT	AT AMBIENT	PERCENT	INCREMENTAL	
DEG F	DEG F	IN. HG	BTU/HR		DEG F	DEG F	DEG F	MEGAWATTS	MILLS/KWH	MILLS/KWH	MILLS/KWH	PERCENT	MILLS/KWH		
101.0	119.7	3.42	.0001	6.799	4.001	6.05	10.07	999.843	.05179	.37642E-02	1.8728	.020	.31457E-03		
96.0	119.7	3.42	.0001	10.139	4.001	9.07	15.07	999.843	.05179	.37642E-02	1.8728	.400	.77070E-02		
92.0	119.7	3.42	.0001	12.800	4.001	11.51	19.07	999.843	.05179	.37642E-02	1.8728	.800	.92798E-02		
90.0	119.7	3.42	.0001	14.126	4.001	12.72	21.07	999.843	.05179	.37642E-02	1.8728	.900	.15571E-01		
87.0	119.7	3.42	.0001	16.116	4.001	14.55	24.07	999.843	.05179	.37642E-02	1.8728	1.700	.59611E-01		
82.0	119.7	3.42	.0001	19.476	4.001	17.57	29.07	999.843	.05179	.37642E-02	1.8728	4.000	.72194E-01		
77.0	119.7	3.42	.0001	22.737	4.001	20.66	34.07	999.843	.05179	.37642E-02	1.8728	5.410	.88237E-01		
72.0	119.7	3.42	.0001	25.979	4.001	23.76	39.07	999.843	.05179	.37642E-02	1.8728	6.730	.10585		
67.0	119.7	3.42	.0001	29.297	4.001	26.80	44.07	999.843	.05179	.37642E-02	1.8728	7.830	.12315		
62.0	119.7	3.42	.0001	32.516	4.001	29.92	49.07	999.843	.05179	.37642E-02	1.8728	8.110	.12756		
57.0	119.7	3.42	.0001	35.809	4.001	32.99	54.07	999.843	.05179	.37642E-02	1.8728	7.840	.11702		
52.0	119.7	3.42	.0001	37.043	4.071	34.10	55.91	1002.843	.03600	0.	1.8533	7.420	.11525		
47.0	112.1	2.77	.0025	36.900	4.050	34.00	55.75	1006.550	.01549	0.	1.8328	7.840	.12017		
42.0	107.5	2.43	.0000	36.983	4.051	33.93	55.65	1009.097	.00157	0.	1.8189	8.120	.12333		
37.0	103.0	2.13	.0000	36.841	4.045	33.91	55.60	1010.770	-.00758	0.	1.8097	8.100	.12229		
33.0	94.5	1.02	.0075	36.816	4.042	33.89	55.57	1011.652	-.01237	0.	1.8049	22.330	.33605		

PERCENT OF PERCENT OF		WATER EVAPORATED	
HE DELUGED	HEAT REJECT	ACRE FEET	
BY NET HA			
40.1320	89.7670	3.4010	
38.3124	83.1504	73.1510	
35.2085	77.0770	78.5832	
33.4217	74.0591	121.0682	
30.4157	69.7842	430.8083	
25.0930	61.1851	431.4633	
21.5010	51.9961	422.7913	
18.8082	41.7764	347.5136	
11.0029	30.4678	312.4180	
8.0670	18.5221	158.4506	
1.0000	5.4565	48.7793	
0.0000	0.0000	0.0000	
0.0000	0.0000	0.0000	
0.0000	0.0000	0.0000	
0.0000	0.0000	0.0000	
0.0000	0.0000	0.0000	

1200 FINAL INCREMENTAL COST 1.9436
CAPACITY CHARGE \$ 18977.8525

FIGURE 18. (contd)

CAPITAL COST SUMMARY

1300 UNIT ENERGY COST SUMMARY

COOLING SYSTEM CAPITAL		46052463.
TOWER	30108569.	
HEAT EXCHANGER	1542567.	
PLENUM	24196A.	
LOUVERS	0.	
MILL SCREENS	824294.	
FAN SYSTEM	7005051.	
STRUCTURE	5076942.	
FOUNDATION	447776.	
PIPING	10685703.	
CONDENSER	7058112.	
CAPACITY PENALTY		18978.
PLANT SCALING		5287053.
STEAM SUPPLY	8276.	
BASE PLANT	5278777.	
HEAT RATE	4639093.	
FANS AND PUMPS	5917870.	
WATER		0.
LAND		0.
TOTAL CAPITAL COST	\$	53358494.

COOLING SYSTEM CAPITAL		1.30261
TOWER	.816187	
HEAT EXCHANGER	.419703	
PLENUM	.764362E-02	
LOUVERS	0.	
MILL SCREENS	.223448E-01	
FAN SYSTEM	.216731	
STRUCTURE	.137026	
FOUNDATION	.121384E-01	
PIPING	.205092	
CONDENSER	.191332	
CAPACITY PENALTY		.514454E-03
PLANT SCALING		.143322
STEAM SUPPLY	.224336E-03	
BASE PLANT	.143098	
HEAT RATE	-.173246E-01	
FANS AND PUMPS	.160422	
WATER		0.
TOTAL CAPITAL COST		1.44845

1340	TOTAL CAPITAL COST	1.44845
1350	ENERGY PENALTY	.173246E-02
1360	ADDITIONAL BASE PLANT FUEL	.245992E-01
1370	OPERATION AND MAINTENANCE	.708489E-01
1380	TOTAL	1.54359

FIGURE 18. (contd)

1400

***** 2500 ACWF FEET OF WATER AVAILABLE *****

AIR FLOW PARAMETERS		
AIR FLOW RATE	10000 LHM/HR	550.
AIR VELOCITY	FT/SEC	13.7
DELTA P, MAX.	PSI	.0092
DELTA P, DISCHARGE	PSI	.0052
FAN POWER	HP	9.8
FANS	NUMBER	120
AMMUNIA PARAMETERS		
NHS FLOW RATE	10000 LHM/HR	10.7
DELTA P, NHS	PSI	1.348
PUMP POWER	HP	.507
HEAT EXCHANGER DESIGN		
TOWERS	NUMBER	6
APPROX. TOWER DIAMETER	FT	234.
TOWER HEIGHT	FT	71.9
FRONTAL AREA	10000 SQFT	.309
HEAT TRANSFER AREA	10000 SQFT	16.5
TUBE LENGTH	FT	80.0
TUBE ROWS IN DEPTH	NUMBER	4
CONDENSER DESIGN		
HEAT TRANSFER AREA	10000 SQFT	.415
TTD	DEG F	4.68
PERFORMANCE PARAMETERS		
DESIGN TBP	IN HG	3.41
MAXIMUM TBP	IN HG	3.42
PUMP AT MAXIMUM TBP	HP	999.8
MAX. PERCENT DFLUGE		44.1
MAX. EVAPORATION RATE	WPM	10540.
COST SUMMARY		
COOLING SYSTEM	MILLS/KWH	1.30
CAPACITY	MILLS/KWH	.00
STEAM SUPPLY SCALING	MILLS/KWH	.00
HEAT RATE SCALING	MILLS/KWH	.02
FAN AND PUMP SCALING	MILLS/KWH	.16
ENERGY	MILLS/KWH	.00
HAZE FUEL	MILLS/KWH	.02
O AND M	MILLS/KWH	.07
WATER	MILLS/KWH	0.00
INCR. COST OF COOLING	MILLS/KWH	1.50

FIGURE 18. (contd)

ACKNOWLEDGMENTS

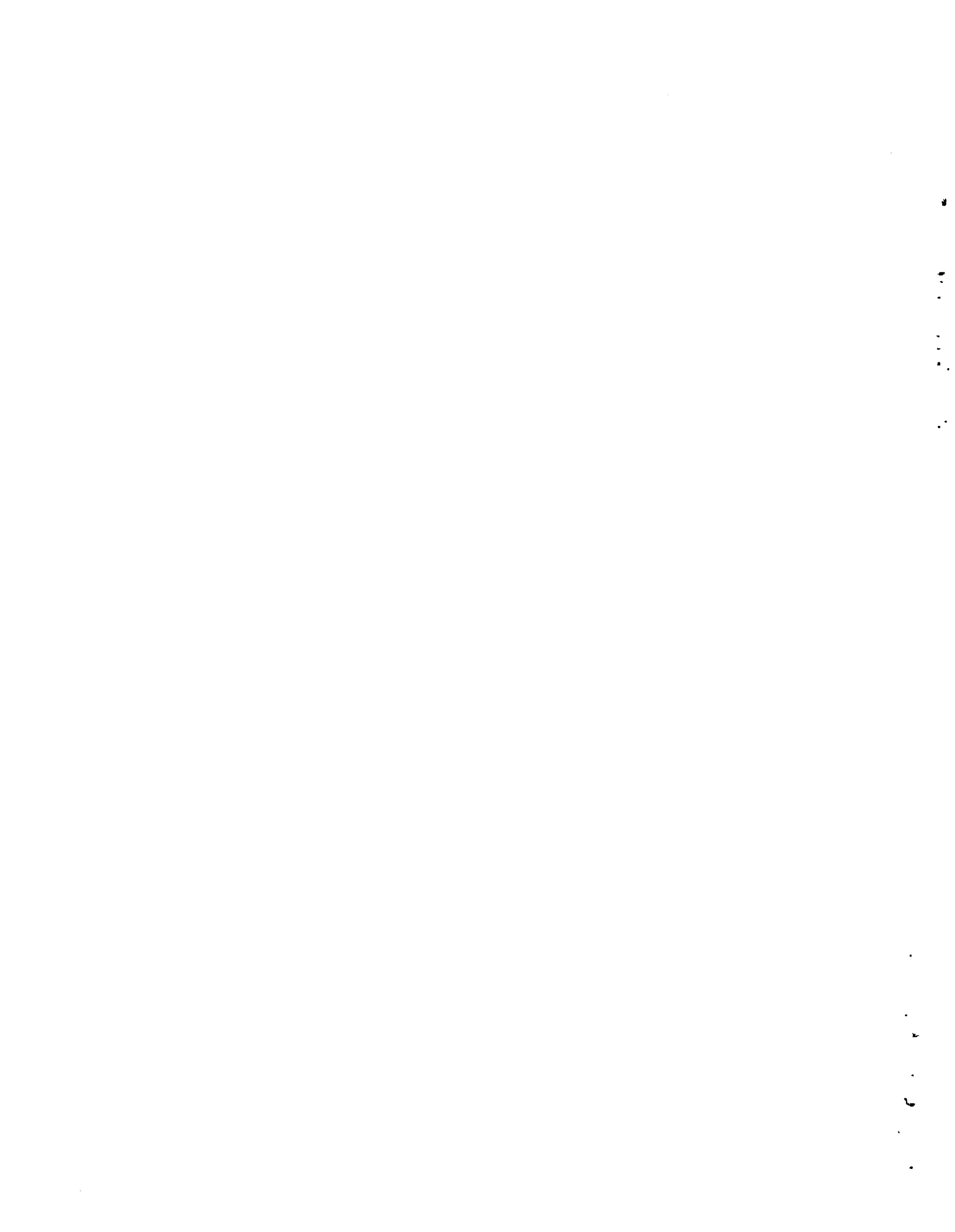
This report contains an account of the work sponsored by the Division of Advanced Systems and Materials Production of the U.S. Department of Energy (DOE) under the Dry Cooling Enhancement Program at the Pacific Northwest Laboratory (PNL). This work was completed under the direction of I. Helms, Project Officer; W. F. Savage, Manager of Advanced Concepts Evaluation Branch, DOE Division of Advanced Systems and Materials Production; B. M. Johnson, Manager of the Dry Cooling Enhancement Program, PNL; and R. T. Allemann, Project Engineer, PNL.

The authors wish to acknowledge Dennis Kreid, PNL, for technical contributions. Thanks also go to PNL word processor Ruth Keefe for typing, and to editor/writers Marsha Dunstan and Andrea Currie for editing and coordinating final production of this report.



REFERENCES

1. L. E. Wiles, J. A. Bamberer, Daniel J. Braun, David J. Braun, D. W. Faletti, C. E. Willingham, A Description and Cost Analysis of a Deluge Dry/Wet Cooling System. PNL-2498, Battelle, Pacific Northwest Laboratories, Richland, WA, January 1978.
2. B. C. Fryer, Daniel J. Braun, David J. Braun, D. W. Faletti, and L. E. Wiles, An Engineering and Cost Comparison of Three Different All-Dry Cooling Systems. BNWL-2121, Battelle, Pacific Northwest Laboratories, Richland, WA, September 1976.
3. P. A. Ard, C. H. Henager, D. R. Pratt, and L. E. Wiles, Costs and Cost Algorithms for Dry Cooling Tower Systems, BNWL-2123, Battelle, Pacific Northwest Laboratories, Richland, WA, September 1976.
4. David J. Braun, Daniel J. Braun, W. V. DeMier, D. W. Faletti, and L. E. Wiles, A User's Manual for the BNW-I Optimization Code for Dry-Cooled Power Plants. BNWL-2180, Battelle, Pacific Northwest Laboratories, Richland, WA, September 1976.
5. B. R. Andeen and L. R. Glicksman, Dry Cooling Towers for Power Plants. DSR 73047-1, Massachusetts Institute of Technology, Cambridge, MA, February 1972.



APPENDIX A

AIR-SIDE PERFORMANCE CORRELATIONS
FOR HÖTERV SURFACE

APPENDIX A
AIR-SIDE PERFORMANCE CORRELATIONS FOR HÖTERV SURFACE

The PNL method of predicting the performance of the deluged HÖTERV heat exchanger bundle is based on the air-side heat transfer coefficient, h_s , whereas the B&W approach to determining the heat transfer performance is based on a delugeate water mass transfer coefficient, σ_s (Appendix C).

There are two different options by which the heat transfer performance of the HÖTERV heat exchanger bundle can be predicted. The correlations that are the basis for each option are given below. The pressure drop through the heat exchanger bundle is calculated using a correlation for the friction factor, f . Correlations for h_s , σ_s , and friction factor used in the BNW-II code are given below.

HEAT TRANSFER COEFFICIENT

The PNL method for predicting the performance of the HÖTERV heat exchanger bundle is based on using the all-dry mode heat transfer coefficient correlation in conjunction with the enthalpy driving force in predicting the amount of water evaporated.

The heat transfer coefficient correlation was developed from a correlation provided by Babcock and Wilcox.^(a) The correlation is

$$h_o = 0.12518 (Re_{air_{min}})^{0.515} Pr^{1/3} (k_a/D_H) \quad (A.1)$$

where

h_o = overall air-side heat transfer coefficient
 $Re_{air_{min}}$ = Reynolds number at the minimum flow area of the heat exchanger

(a) This information was provided by W. W. Sowa, New Products, Power Generation Group, Babcock and Wilcox, Barberton, OH, in a private communication to PNL on February 4, 1977.

Pr = Prandtl number of the air

k_a = thermal conductivity of the air

D_H = hydraulic diameter of the heat exchanger.

Since this is in terms of an overall heat transfer coefficient, the effect of fin efficiency of the surface is built into the correlation. The local heat transfer coefficient is given by the following:

$$h_s = h_o (A_b + A_f) / (A_b + \eta_f A_f) \quad (A.2)$$

where

h_s = local heat transfer coefficient

h_o = overall heat transfer coefficient

A_b = air-side tube area excluding the fin

A_f = air-side fin area

η_f = fin effectiveness.

With the fin effectiveness, η_f , a function of the local heat transfer coefficient, h_s , the solution for the local heat transfer coefficient in terms of the overall heat transfer coefficient is an iterative process. For various Reynolds numbers the overall heat transfer coefficient is calculated using Equation A.1. Using Equation A.2 the local heat transfer coefficient is determined by a simple iterative process for each Reynolds number. A curve fit is then made for the local heat transfer coefficient as a function of Reynolds number resulting in the following:

$$h_c = 0.18534 (Re_{air_{min}})^{0.577} Pr^{1/3} (k_a / D_H) \quad (A.3)$$

The range of Reynolds numbers over which the correlation is applicable is 500 to 1500.

MASS TRANSFER COEFFICIENT

The Hungarian method of predicting the amount of water being evaporated from the surface of the heat exchanger is based on a mass transfer correlation. The correlation was provided by Babcock and Wilcox.^(a) The correlation is provided here in the form in which it was used.

$$\sigma_s = 0.0250 (Re_{air_{min}})^{0.615} \quad (A.4)$$

where

σ_s = mass transfer coefficient
 $Re_{air_{min}}$ = Reynolds number at the minimum flow area of the heat exchanger

The range of Reynolds numbers over which this correlation is applicable is 500 to 1500.

PRESSURE DROP

The pressure drop through the heat exchanger bundles was calculated using a friction factor correlation derived from information provided by Babcock and Wilcox.^(a) The pressure drop equation is of the following form:

$$\Delta p = (\rho V^2 / g_c) N_D f \quad (A.5)$$

where

Δp = pressure drop
 ρ = average density of air in the heat exchanger
 V = maximum velocity of air in the heat exchanger
 g_c = gravitational constant
 N_D = number of tubes in depth
 f = friction factor

(a) This information was provided by W. W. Sowa, New Products, Power Generation Group, Babcock and Wilcox, Barberton, OH, in a private communication to PNL on February 4, 1977.

The friction factor is given by the following correlation:

$$f = 4.781 (Re_{air_{min}})^{-0.24} \quad (A.6)$$

where

$Re_{air_{min}}$ = Reynolds number of the airflow at the minimum cross-sectional flow area of the heat exchanger.

The range of Reynolds numbers over which the correlation is applicable is 500 to 1500.

APPENDIX B

FIN EFFICIENCY OF PLATE
FIN HEAT EXCHANGERS

APPENDIX B
FIN EFFICIENCY OF PLATE FIN HEAT EXCHANGERS

The temperature difference between a fin and the bulk fluid decreases with distance from the base of the fin because of heat transfer resistance of the fin material. As a result the heat transfer does not increase in direct proportion to the fin area and a correction, the fin efficiency, η_f , must be applied. Thus the heat transfer rate, Q , is given by Equation B.1

$$Q = h_s (A_b + \eta_f A_f) (T_b - T_\infty) \quad (\text{B.1})$$

where

- h_s = the air-side transfer coefficient, Btu/hr-ft²-°F
- A_b = tube area between the fins which is exposed to the air, ft²
- A_f = area of the fins, ft²
- η_f = fin efficiency, dimensionless
- T_b = temperature at the fin base, °F
- T_∞ = temperature of the bulk air, °F

For example, a fin will have a fin efficiency of 0.5 if the mean temperature difference between the fin and the bulk air (averaged over the entire fin area) is 1/2 of the temperature difference between the fin root and the bulk air. In effect, a fin with a fin efficiency of 0.5 behaves (in regard to heat transfer) as if it had only half the area of a fin having an infinite thermal conductivity.

The accuracy of the PNL method (see Appendix A) for computing the performance of deluged heat exchangers depends upon a sufficiently accurate method for determining the fin efficiency of the plate fin surface studied in this report. The purpose of this appendix is to describe the method used to compute the fin efficiency (both in dry operation and in deluged operation) of the plate fin heat exchanger surface studied. We begin by describing how the plate fin heat exchanger was treated for the purpose of computing the fin efficiency as an annular fin heat exchanger.

TRANSFORMATION OF THE PLATE FIN INTO AN ANNULAR FIN EQUIVALENT

The heat exchanger configuration studied was one developed by the HÖTERV Institute. As shown in Figure B.1 it is a plate fin configuration with 18.5-mm OD tubes located in a staggered isosceles triangular arrangement with a 60-mm transverse (to the direction of flow) pitch and a 50-mm longitudinal pitch. The plate fins are 0.33-mm thick and are located at a center to center spacing of 2.88 mm, giving an interfin gap of 2.5 mm.

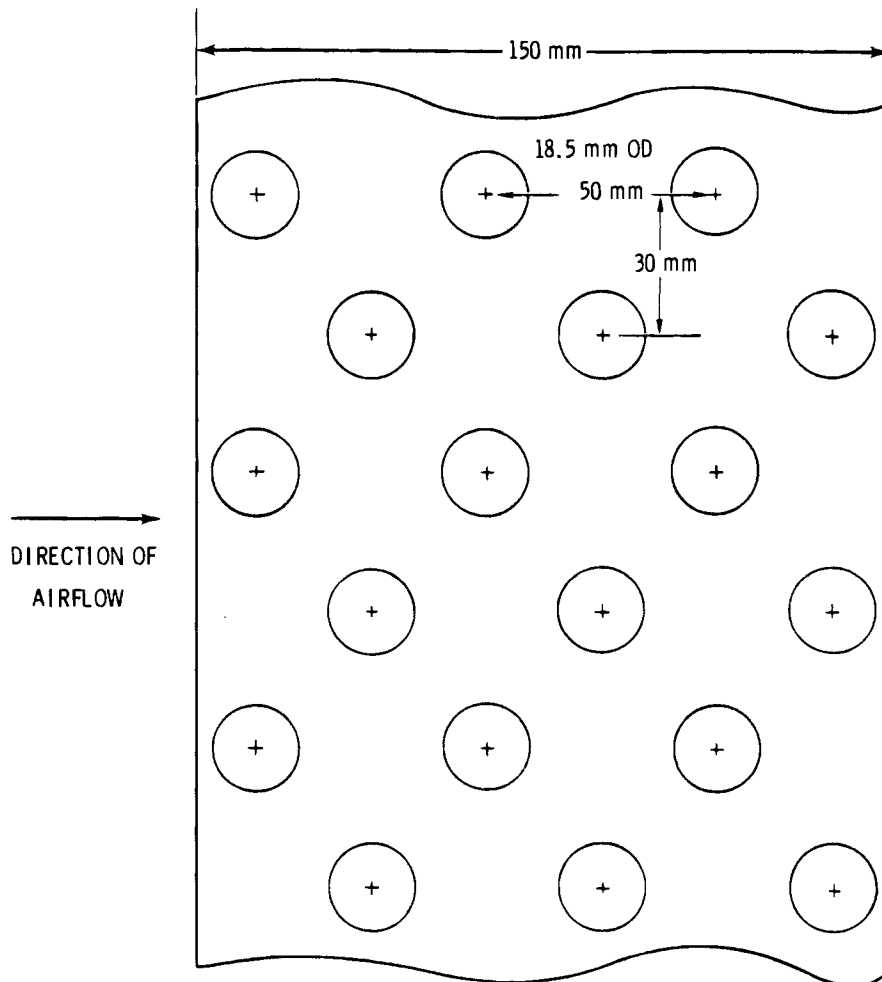


FIGURE B.1. Unit Geometry of Plate Fin Studied

The approximation was used that the plate fin heat exchanger's fin effectiveness could be computed with sufficient accuracy by assuming that the plate fin was replaced by annular fins with the same cross section per tube. A 43.7-mm fin OD results (Figure B.2). Fin thickness and spacing were left unchanged. The shaded areas of Figure B.2 show where the equivalent annular fins overlap and the regions which they "miss." Though the annular fin approximation introduces some error, it is probably a reasonable approximation which should be adequate for the present purpose.

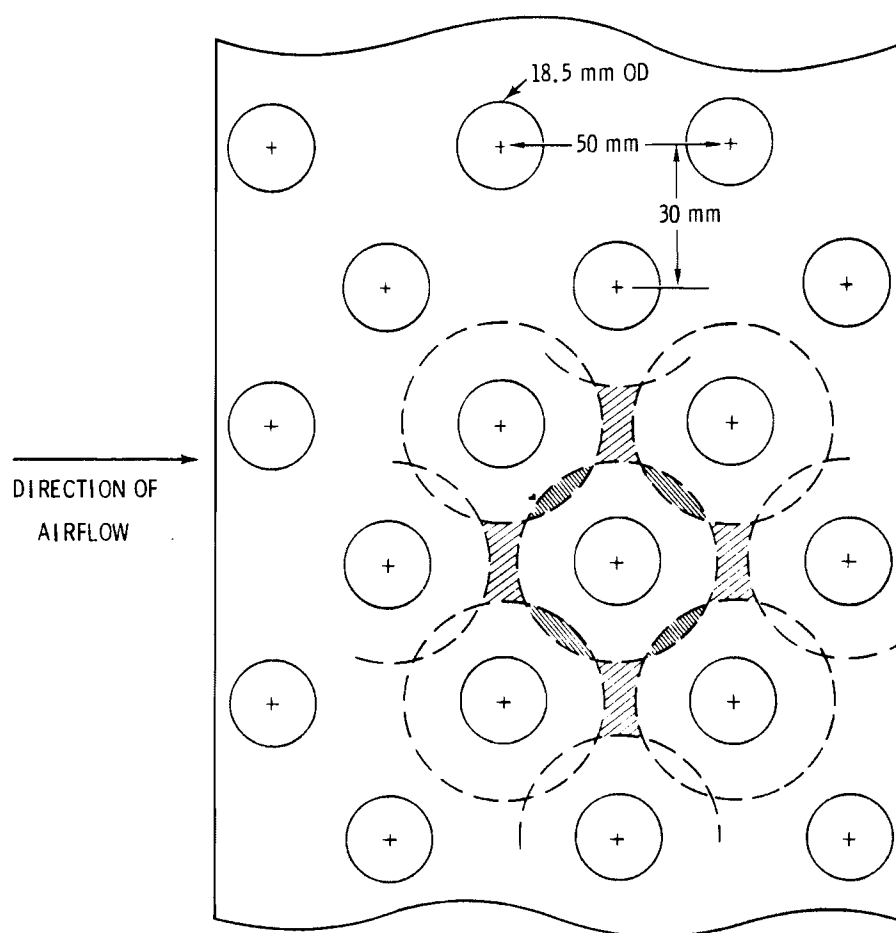


FIGURE B.2. Annular Fin Equivalent of Plate Fin
(The shaded areas show where the annular fins overlap and where they "miss.")

The heat transfer data provided PNL by Babcock and Wilcox gave values of the lumped air-side heat transfer coefficient, h' , which includes the effect of fin efficiency such that Equation B.2 applies.

$$Q = h' (A_b + A_f) (T_b - T_\infty) \quad (B.2)$$

The relationship between h' and h_s can be derived by equating Equations B.1 and B.2 giving Equation B.3.

$$h_s = h' (A_b + A_f) / (A_b + \eta_f A_f) \quad (B.3)$$

The heat transfer of dry surfaces can be computed from h' ; however, values of h_s are required for deluge computations. Thus both the dry and the wet performance of the heat exchangers were computed from correlations for h_s derived from the experimental values of h' (See Appendix A). These values of h_s were obtained by iterative solutions involving Equation B.3 and the equation for fin effectiveness (Equation B.4).

COMPUTATION OF FIN EFFICIENCY

DRY OPERATION

Gardner^(B.1) derived Equation B.4 for the fin efficiency of annular fins of constant thickness with the following assumptions:

1. The heat flow and temperature distribution throughout the fin are independent of time, i.e., the heat flow is steady.
2. The fin material is homogeneous and isotropic.
3. There are no heat sources in the fin itself.
4. The heat flow to or from the fin surface at any point is directly proportional to the temperature difference between the surface at that point and the surrounding fluid.
5. The thermal conductivity of the fin is constant.

6. The heat-transfer coefficient is the same over all the fin surface.
7. The temperature of the surrounding fluid is uniform.
8. The temperature of the base of the fin is uniform.
9. The fin thickness is so small compared to its height that temperature gradients normal to the surface may be neglected.
10. The heat transferred through the outermost edge of the fin is negligible compared to that passing through the sides.

$$\eta_f = \frac{2}{U_b \left[1 - \left(\frac{U_e}{U_b} \right)^2 \right]} \frac{I_1(U_b) - \beta_1 K_1(U_b)}{I_0(U_b) + \beta_1 K_0(U_b)} \quad (\text{B.4})$$

where

$$\beta_1 = \frac{I_1(U_e)}{K_1(U_e)} \quad (\text{B.5})$$

$$U_b = \frac{(r_e - r_b) [h_s / (k y_b)]^{1/2}}{\left(\frac{r_e}{r_b} - 1 \right)} \quad (\text{B.6})$$

$$U_e = U_b \left(\frac{r_e}{r_b} \right) \quad (\text{B.7})$$

I_n and K_n are Bessel functions of order n of the first and second kind, respectively. Other terms are:

h_s = air-side heat transfer coefficient

k = thermal conductivity of the fin material

r_e = fin outside radius

r_b = fin root radius

y_b = 1/2 of the fin thickness.

Thus, the fin efficiency is a function of the fin geometry, the thermal conductivity of the fin material and the local heat transfer coefficient.

DELUGE OPERATION

The fin efficiency relationship for deluge operation will now be derived. This relationship is identical to Equation B.4 except that the quantity h_s is replaced by the quantity

$$U^*_{r\infty} / \left(C_a \frac{dT}{di} \right)$$

where

$U^*_{r\infty}$ = the overall heat transfer coefficient (enthalpic driving force) between the fin root and the bulk air, $\text{Btu}/\text{ft}^2\text{-hr-}^\circ\text{F}$

C_a = the heat capacity of humid air, $\text{Btu}/^\circ\text{F-lb}$ of dry air

dT/di = the derivative of temperature with respect to the enthalpy of dry air, $^\circ\text{F-lb}$ of dry air/Btu.

These terms are defined in Appendix C.

Equation B.4 is the solution for the equation

$$\frac{d^2\theta}{dr^2} + \left(\frac{1}{a_r} \frac{da_r}{dr} \right) \frac{d\theta}{dr} - \left(\frac{h_s}{ka_r} \frac{dA}{dr} \right) \theta = 0 \quad (\text{B.8})$$

with the boundary conditions

$$\theta = \theta_b \text{ when } r = r_b$$

$$\frac{d\theta}{dr} = 0 \text{ when } r = r_e$$

where

$$\theta = T_r - T_\infty$$

T_r = fin temperature at distance r from the centerline

T_∞ = temperature of the bulk air

a_r = the cross sectional area of the fin at distance r from the centerline.

The method of solution to arrive at Equation B.4 from Equation B.8 is the same for both the dry and the deluge applications. The reader is

referred to References B.1 and B.2 for the details. We shall derive the equation analogous to Equation B.8 for deluge operation and show that it has the same form and boundary conditions.

The driving force used in the BNW method for computing deluge performance is $\Delta i/C_a$ where Δi is the enthalpy difference, Btu/lb of dry air. Thus the heat transfer between the fin root and the air immediately adjoining it is given by

$$Q = U^*_{r\infty} A \frac{\Delta i}{C_a} \quad (\text{B.9})$$

where

$U^*_{r\infty}$ = the overall heat transfer coefficient between the fin root and the air, Btu/ft²-hr-°F, and

A = the heat transfer area under consideration.

Since our driving force is $\Delta i/C_a$, the quantity analogous to θ , is θ' , where

$$\theta' = \frac{i' - i_\infty}{C_a} \quad (\text{B.10})$$

and i' is the enthalpy of saturated air at the fin temperature at any distance from the centerline.

Consider the case where $(i - i_\infty)$ is positive (i.e., the case where heat is being transferred to the air). Let Q be the amount of heat transferred to the air between the edge of the fin and radius r . Let A be the total surface area between the edge of the fin and radius r , and let a_r be the cross sectional area of the fin at radius r . Then

$$dQ = U^*_{r\infty} \theta' dA \quad (\text{B.11})$$

Differentiating Equation B.11 gives

$$\frac{dQ}{dr} = U^*_{r\infty} \theta' \frac{dA}{dr} \quad (\text{B.12})$$

The conduction equation gives

$$Q = -k a_r \frac{d\theta}{dr} = -k a_r \frac{d\theta}{d\theta'} \frac{d\theta'}{dr} \quad (\text{B.13})$$

Differentiating Equation B.13 gives

$$\frac{dQ}{dr} = -k a_r \frac{d\theta}{d\theta'} \frac{d^2\theta'}{dr^2} - k \frac{da_r}{dr} \frac{d\theta}{d\theta'} \frac{d\theta'}{dr} \quad (\text{B.14})$$

Equating Equations B.12 and B.14 gives

$$\frac{d^2\theta'}{dr^2} + \left(\frac{1}{a_r} \frac{da_r}{dr} \right) \frac{d\theta'}{dr} + \left(\frac{U^* r_\infty}{k a_r \frac{d\theta}{d\theta'}} \frac{dA}{dr} \right) \theta' = 0 \quad (\text{B.15})$$

From the definition of θ and θ'

$$\frac{d\theta}{d\theta'} = \lim_{\Delta \rightarrow 0} \frac{(T + \Delta T - T_\infty) - (T - T_\infty)}{\frac{(i' + \Delta i' - i_\infty) - (i' - i_\infty)}{C_a}} = C_a \frac{dT}{di'} \quad (\text{B.16})$$

Inserting Equation B.16 into Equation B.15 gives

$$\frac{d^2\theta'}{dr^2} + \left(\frac{1}{a_r} \frac{da_r}{dr} \right) \frac{d\theta'}{dr} + \left(\frac{U^* r_\infty}{k a_r C_a \frac{dT}{di'}} \frac{dA}{dr} \right) \theta' = 0 \quad (\text{B.17})$$

The boundary conditions for Equation B.17 are

$$\theta' = \theta'_b \text{ when } r = r_b \quad (\text{B.18})$$

and

$$\frac{d\theta'}{dr} = 0 \text{ when } r = r_e \quad (\text{B.19})$$

These boundary conditions arise from the same assumptions used to derive Equation B.8. Equation B.17 and its boundary conditions are identical to Equation B.8 except that θ' replaces θ and that the coefficient of the third term differs. Equating these coefficients gives us the relationship

$$h_s = \frac{U^*_{r_\infty}}{C_a \frac{dT}{di'}} \quad (B.20)$$

Thus Equation B.4 can be used to compute the fin effectiveness for deluged systems if the right side of Equation B.17 is substituted for h_s . The discussion here has been limited to annular fins of constant thickness. A study of References B.1 and B.2 shows that the substitution suggested by Equation B.20 is also applicable to other extended surfaces such as spines and straight fins, as well as annular fins of nonconstant thickness. By analogy it is quite possible that Equation B.18 is applicable to most extended surfaces.

The quantity $U^*_{r_\infty}/(C_a \frac{dT}{di'})$ must be constant if Equation 4 is to be exact. $U^*_{r_\infty}$ is as likely to be constant as h_s . The value of $\frac{dT}{di'}$ will vary somewhat if there is a large temperature drop across the fin. However, the percentage variation in heat transfer coefficient within the fins is probably just as large as any variation in $\frac{dT}{di'}$ when one considers the nature of the flow.

C_a is approximately 0.24. $\frac{dT}{di'}$ is seldom much greater than unity and is often less than unity. For the same face velocity, $U^*_{r_\infty}$ is generally within 10% of h_s . Therefore, the quantity $U^*_{r_\infty}/(C_a \frac{dT}{di'})$ is generally four times that of h_s and as a result the fin efficiency during deluge is often near 0.7 compared to the 0.9⁺ found in dry operation.

APPROXIMATE SOLUTION FOR FIN EFFICIENCY

In order to reduce computation time, a curve fit of the results predicted by Equation B.4 was used to compute the fin efficiency in the BNW-II computer code. The resulting equation was

$$\eta_f = \frac{1}{1 + Ch_s} + 0.06313766 (1 - e^{-0.00745032h_s})$$

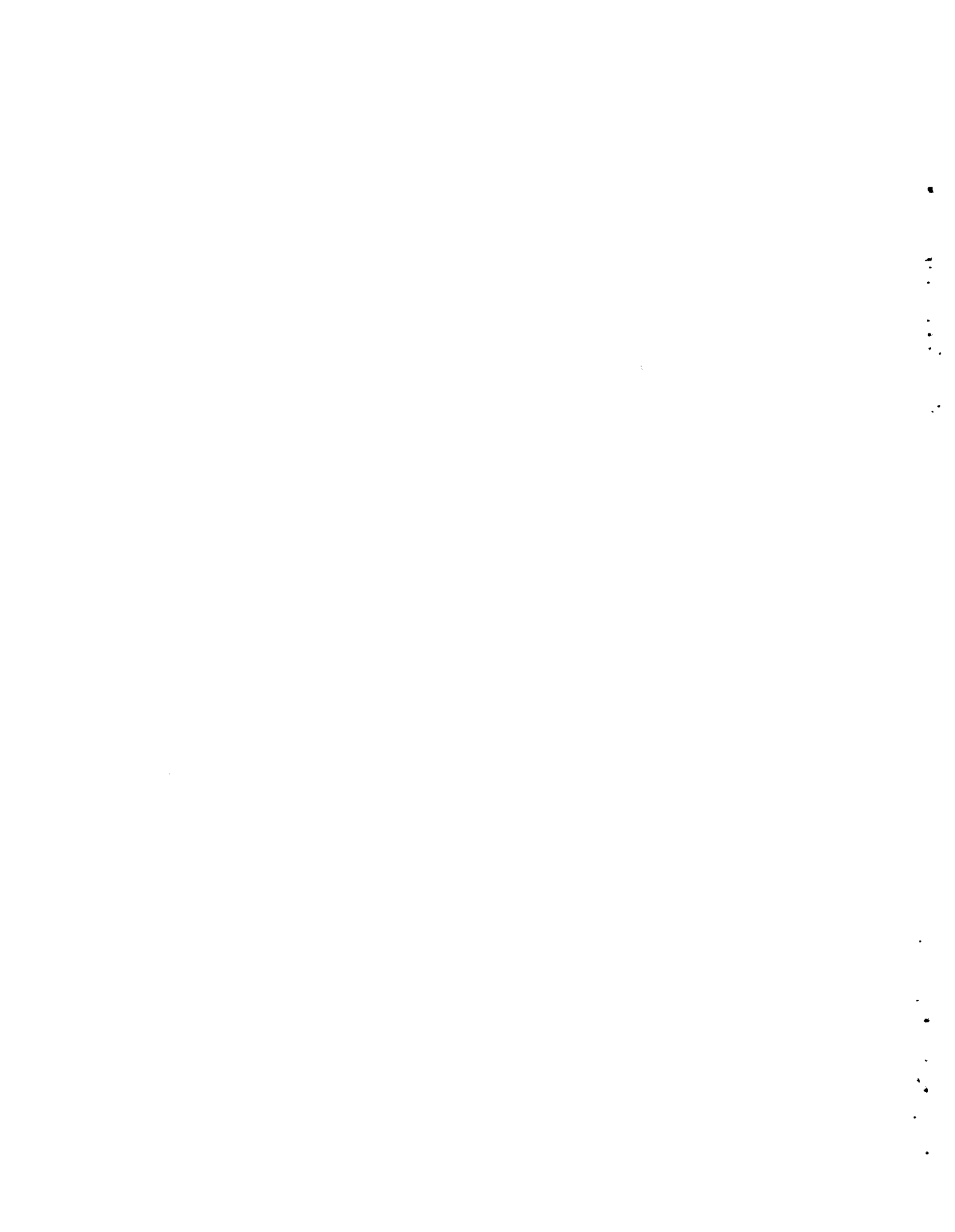
where

$$C = (r_e - r_b)^2 \frac{(r_e/r_b)^{1/2}}{3k y_b}$$

and the units of h_s are $\text{Btu/ft}^2\text{-hr-}^\circ\text{F}$.

REFERENCES

- B.1. K. A. Gardner, Trans. ASME, 67, 621-632, 1945.
- B.2. D. G. Kern, Process Heat Transfer. First Edition, McGraw-Hill Book Co., New York, NY, 1950.



APPENDIX C

COMPUTATION OF DELUGE PERFORMANCE

APPENDIX C
COMPUTATION OF DELUGE PERFORMANCE

Deluging, as used in this study, refers to a method of augmenting a heat exchanger's performance by distributing water (delugeate) onto the exchanger in such a way that the normally dry exterior surfaces are covered with a thin layer of water. This layer of water is thin compared to the interfin spacing thus permitting air to flow between the fins though at a somewhat larger resistance to airflow due to the somewhat smaller air passages as well as possible bridging of the liquid film.

This type of water augmentation of dry heat transfer surfaces is under intensive development by the HÖTERV Institutue, Budapest Hungary. Babcock and Wilcox (B&W) is the U.S. licensee for this technology.

The mechanism for transport of heat between the surface of the delugeate and the air is the same in a deluged heat exchanger as that in an evaporative tower--combined mass and heat transfer. However, in an evaporative tower the primary fluid (water) is in direct contact with the air. Thus the resistance to heat transfer from the bulk of the primary fluid to the air-water surface is relatively small in contrast to the situation found in a deluged heat exchanger where the heat must pass from the primary fluid (in this study, NH_3) through several resistances to heat transfer before reaching the delugeate-air interface. Evaporative towers are designed by use of the enthalpy driving force. (C.1, p.356) The design methods given here for deluged towers also use the enthalpy driving force; the heat transfer terms arising from the heat transfer resistance between the tube side fluid and the surface of the delugeate are transformed from use of the temperature driving force to use of the enthalpy driving force.

Two computational methods were used in this study. The first method was that recommended by B&W which was used in conjunction with experimental data obtained by the HÖTERV group. Since it was the most accurate it was used in all but a few cases.

The second method was developed by PNL.^(C.2) The PNL method, though less accurate, predicts the performance of a deluged heat exchanger given only its dry heat transfer data. Because of its potential utility for evaluating the performance of candidate surfaces for which experimental deluged data is not available, a description of the PNL method is also presented.

Both the B&W and the PNL methods take into account all resistances to heat transfer between the tube-side fluid and the bulk air. The B&W method makes use of the enthalpy driving force used routinely in evaporative tower design. Thus all heat transfer resistance terms which are expressed in terms of a temperature driving force are converted to an enthalpy driving force. An analogous approach is used by the PNL method.

The remainder of this appendix is divided into four sections:

- basics and definitions,
- B&W method for determining the overall heat transfer coefficient,
- PNL method for determining the overall heat transfer coefficient,
- computation of overall heat transfer and water evaporation rate of a deluged heat exchanger, and
- nomenclature.

BASICS AND DEFINITIONS

The purpose of this section is to introduce the reader to the quantities which are used in the sections which follow.

The absolute humidity, the ratio of the weight of water to the weight of air in moist air, is given by

$$H = \frac{18.02 p}{(28.97)(29.92 P_a - p)} \quad (C.1)$$

where

p = the partial pressure of water, in. Hg

P_a = atmospheric pressure, in. Hg.

The heat capacity of moist air, expressed as Btu/lb of dry air-°F (also known as the humid heat capacity), is given by

$$C_a = 0.24 + 0.45 H \quad (C.2)$$

The contribution of the water vapor to the humid heat capacity is given by the second term of Equation 2.

The enthalpy of moist air, i , expressed as Btu/lb of dry air is given by

$$i = C_a T + 1094 H \quad (C.3)$$

where

T = dry-bulb temperature, °F.

The reference condition is 0°F for both the air and the steam. The constant 1094 is the extrapolated heat of vaporization of water at 0°F. (C.1, p.358)

Before proceeding further, it is worthwhile to digress and present some background information on how H , i and T are interrelated and to describe several methods of computing these quantities which are used in BNW-II code.

First, the value of i for a moist air mixture can be determined from a knowledge of its dry-bulb temperature, relative humidity and the atmospheric pressure. This follows since H can be determined from Equation C.1, C_a from Equation C.2 and finally i from Equation C.3. However, an alternate, extremely useful way of determining i is from a knowledge of the moist air mixture's dry-bulb temperature, wet-bulb temperature and the atmospheric pressure. This is possible because the enthalpy of air at the wet-bulb temperature is very nearly the same as the enthalpy of the moist air mixture at the dry-bulb temperature (This can be best visualized by examining a psychrometric chart and observing the near parallelism of the constant enthalpy and constant wet-bulb lines.).

The procedure is as follows. Since the air is saturated at the wet-bulb temperature the partial pressure of air at the wet-bulb is equal to the vapor pressure of air at the (known) wet-bulb temperature. The absolute

humidity at the wet-bulb conditions is then calculated from Equation C.1 from which C_a is calculated from Equation C.2 and finally the enthalpy, i , from Equation C.3.

From a knowledge of i , the absolute humidity at the actual air condition can be obtained from Equations C.2 and C.3 by inserting the dry-bulb temperature. This permits the computation of C_a at the actual conditions from Equation C.2 and finally a computation of the partial pressure and relative humidity from Equation C.1.

Another operation which is conducted frequently in computing the performance of a deluge heat exchanger is the determination of the temperature of a moist air mixture given its enthalpy and relative humidity, and given the atmospheric pressure. This involves using Equations C.1, C.2 and C.3 in an iterative computation. With this background we can now proceed to discuss the use of the enthalpy driving force.

For an evaporative tower the heat transfer is computed by use of an enthalpy driving force as shown in Equation C.4:

$$Q = \sigma_S A_S (i'_W - i_\infty) \quad (C.4)$$

where

- Q = the heat transfer rate, Btu/hr,
- σ_S = the mass transfer coefficient (enthalpic driving force), lb of dry air/ft²-hr, (a)
- A_S = the surface area,
- i'_W = the enthalpy of saturated air at the cooling water temperature, Btu/lb of dry air, and
- i_∞ = the enthalpy of the bulk air, Btu/lb of dry air.

(a) σ_S is the mass transfer coefficient when absolute humidity is used as the driving force, e.g.,

$$\dot{m}_W = \sigma_S A (H'_S - H_\infty)$$

where

- \dot{m}_W = the evaporation rate of water, lb_W/ft²-hr
- H'_S = the absolute humidity of saturated air at the air-water interface, lb_W/lb_a
- H_∞ = the absolute humidity of the bulk air, lb_W/lb_a.

Reference C.1 gives a good description of the development of the use of this driving force. The use of an enthalpy driving force is most nearly correct if the convective Lewis number, given by Equation C.5:

$$Le = \frac{h_s}{\sigma_s C_s} \quad (C.5)$$

is equal to one, (C.2) which is a reasonable approximation for water.

The B&W approach uses an equation of the form of Equation C.4 for the computation of the heat transfer rate. Values of σ_s from correlations based on experimentally determined values of σ_s were used in the computations.

The PNL approach was developed to permit the prediction of the performance of deluged heat exchangers when dry heat transfer data (but not deluged data) were available. With the assumption that the Lewis number is unity, $\sigma_s = h_s/C_s$, which allows us to arrive at Equation C.6 from Equation C.4,

$$Q = \left(\frac{h_s}{C_s} \right) A (i'_w - i_\infty) = h_s A \frac{(i'_w - i_\infty)}{C_a} \quad (C.6)$$

Either the enthalpy difference, or the enthalpy difference divided by the humid heat capacity, can be used as the driving force. The latter was selected since we found it convenient to work with heat transfer coefficients; rather than the ratio of the heat transfer coefficient and the humid heat capacity.

Note that no approximations are introduced by use of Equation C.6 that are not used by Equation C.4, if the Lewis number is unity. The approximation used by the PNL approach is to assume that the value of h obtained from dry heat transfer correlations is equal to h_s , the local value of convective heat transfer at the deluge-air interface. Corrections for the case when the Lewis number is not equal to unity could be used; however, this was not deemed necessary in this study.

Before one can solve for the overall heat transfer coefficient between tube-side fluid and the bulk air in terms of an enthalpy driving force, all resistances to heat transfer, such as the heat transfer coefficient between tube-side fluid and the tube wall, must be also transformed to an enthalpy driving force. In the next section we shall show how this is done for the B&W approach.

B&W METHOD FOR DETERMINING THE OVERALL HEAT TRANSFER COEFFICIENT

As mentioned in the previous section, the B&W method makes use of the enthalpy difference between tube side fluid and the bulk air as a driving force. Thus the heat transfer rate is given by

$$Q = \Sigma_{p\infty} A_t (i'_p - i_\infty) \quad (C.7)$$

where

- Q = the heat transfer rate, Btu/hr
- $\Sigma_{p\infty}$ = the overall tube side to bulk air mass transfer coefficient, lb of dry air/ft²-hr
- A_t = the total transfer area on the air side, ft², and
- i'_p = the enthalpy of saturated air at the temperature of the tube-side fluid, Btu/lb of dry air.

The total air-side heat transfer area, A_t , is given by

$$A_t = A_b + A_f \quad (C.8)$$

where A_b is the area of the tubes between the fins which is exposed to air and A_f is the area of the fin.

There are five resistances to heat transfer in series between the tube-side fluid and the bulk air. These are:

- the resistance between the tube-side fluid and the inside of the tube wall (heat transfer coefficient h_p),
- fouling on the inside of the wall (equivalent heat transfer coefficient β_{fp}),
- conduction through the wall (k_w/t_w),
- the resistance between the fins and the delugeate (heat transfer coefficient h_d),
- the resistance between the surface of the delugeate and the bulk air (mass transfer coefficient, σ_s).

The first four of these resistances use temperature as the driving force, the fifth uses enthalpy. In order to arrive at an overall coefficient using enthalpy, the first four coefficients must be lumped together and then converted over to an enthalpic driving force. This is done by first computing the overall heat transfer coefficient between the tube-side fluid and the bulk of the delugeate, U_{ps} , by use of Equation C.9:

$$U_{ps} = \left[(A_b + A_f) \left(\frac{1}{h_p A_p} + \frac{1}{\beta_{fp} A_p} + \frac{t_w}{k_w A_w} + \frac{1}{h_d (A_b + A_f)} \right) \right]^{-1} \quad (C.9)$$

where A_p and A_w are the tube side and average tube wall areas, respectively.

We shall now derive the equation for obtaining the value of the tube side to delugeate overall heat transfer coefficient in enthalpic terms given the tube side to delugeate coefficient U_{ps} and temperature driving force terms. Letting Σ_{ps} be the heat transfer coefficient with enthalpic driving force and equating the heat transfer via temperature driving force to heat transfer via enthalpic driving force, we arrive at Equation C.10:

$$\Sigma_{ps} (i'_p - i'_s)(A_b + A_f) = U_{ps} (T_p - T_s)(A_b + A_f) \quad (C.10)$$

where

$$T_s = \text{bulk temperature of the delugeate}^{(a)}$$

$$i'_s = \text{enthalpy of saturated air at } T_s.$$

Dividing out the area terms and rearranging, we arrive at

$$\Sigma_{ps} = U_{ps} \frac{(T_p - T_s)}{(i'_p - i'_s)} \quad (C.11)$$

which is used to give the overall pipe to bulk delugeate heat transfer coefficient in enthalpic terms. We have now reduced the heat transfer problem

(a) The heat transfer resistance between the bulk of the delugeate and the delugeate-air interface is assumed to be negligible.

to that of having two resistances in series, that between the tube-side fluid and the delugeate and that between the delugeate and the bulk air, both of which are enthalpic driving force equivalents. Therefore, the tube side to bulk air overall coefficient is given by

$$\Sigma_{p\infty} = \left[\frac{1}{\Sigma_{ps}} + \frac{1}{\sigma_s} \right]^{-1} \quad (C.12)$$

from which the heat transfer rate can be computed by Equation C.13:

$$Q = \Sigma_{p\infty} (A_b + A_f) (i'_p - i_\infty) \quad (C.13)$$

The heat transfer rate can be computed via Equations C.8 through C.13 from a knowledge of the tube-side and bulk air temperatures, the five heat transfer coefficients involved and a knowledge of the tube side, average tube wall, and outside surface areas. However, use of Equation C.11 requires either a knowledge of T_s and i'_s or, as recommended by B&W, an approximation for the quantity $(T_p - T_s)/(i'_p - i'_s)$ obtained from the enthalpy-temperature curve over the region of interest. While use of the approximation is satisfactory for hand calculations, it was decided to evaluate T_s and i'_s in the BNW-II code. The resulting computation is of the iterative type; the convergence criteria is a sufficiently small change in $\Sigma_{p\infty}$ (generally 0.1%).

PNL METHOD FOR COMPUTING THE TUBE SIDE TO BULK AIR ENTHALPY-BASED HEAT TRANSFER COEFFICIENT

Equation C.14 gives the heat transfer rate for the PNL method:

$$Q = U^*_{p\infty} (A_b + \eta_f A_f) (i'_p - i_\infty) / C_a \quad (C.14)$$

Note as mentioned above that the driving force, instead of being the quantity $(i'_p - i_\infty)$ is now the quantity $(i'_p - i_\infty) / C_a$. The transformed overall pipe to air heat transfer coefficient is denoted by $U^*_{p\infty}$. In addition to the difference in driving force, provisions are made for use of the fin efficiency, η_f .

The matter of the inclusion of the fin efficiency bears further comment. The fin efficiency is defined as the ratio of heat actually transferred from a fin to that transferred from a hypothetical fin with a uniform surface temperature the same as that at the fin root. As described in Appendix B, equations exist for predicting the fin efficiency for a number of fin geometries; we have adapted one of these to the prediction of the fin efficiency of plate fins for both dry and deluged operations. The fin efficiency is typically near 90% during dry operation and 70% during deluge operation. Thus, corrections for fin effectiveness are large during deluge operation and must be included.

The B&W approach does not involve the use of fin efficiency because it is based upon experimentally obtained data. It was convenient to lump the effects of fin effectiveness into the value of σ_s . The relationship given between the local value of the mass transfer coefficient, $\sigma_{s(\text{local})}$ and $\sigma_{s(\text{lumped})}$ is given by

$$\sigma_{s(\text{lumped})} = \sigma_{s(\text{local})} \frac{A_b + \eta_f A_f}{A_b + A_f} \quad (\text{C.15})$$

where η_f is the (unknown) value of fin effectiveness during deluge operation. A similar situation exists in dry heat transfer where the lumped heat transfer coefficient, $h_{s(\text{lumped})}$ and the local heat transfer coefficient, $h_{s(\text{local})}$ are related by

$$h_{s(\text{lumped})} = h_{s(\text{local})} \frac{A_b + \eta_f A_f}{A_b + A_f} \quad (\text{C.16})$$

The quantity h_s used in the PNL approach is the local value of the convective heat transfer coefficient; the quantity σ_s used in the B&W method is the lumped mass transfer coefficient.

The resistances to heat transfer (with their equivalent heat transfer coefficients) between the tube-side fluid and the bulk air include the following:

- tube-side fluid to wall, h_p ,
- tube-side fouling coefficient, β_{fp} ,
- conduction through wall, k_w/t_w ,
- conduction along the fin(a),
- fin to delugeate, h_d , and
- delugeate to air coefficient, h_s .

All of the above heat transfer coefficients are in terms of temperature driving force. We shall now show how these are transformed into overall coefficients in terms of the enthalpy-heat capacity driving force given in Equation C.14.

The transformed coefficient between tube-side fluid and the base of the fins is computed by use of Equation C.17 and C.18 below:

$$U_{pr} = \left[(A_b + \eta_f A_f) \left(\frac{1}{h_p A_p} + \frac{1}{\beta_{fp} A_p} + \frac{t_w}{A_w k_w} \right) \right]^{-1} \quad (C.17)$$

$$U^*_{pr} = U_{pr} C_a \left(\frac{T_p - T_r}{i'_p - i'_r} \right) \quad (C.18)$$

where T_r and i'_r are the temperature and enthalpy of saturated air at the fin root, respectively.

The heat transfer path between the fin root and the bulk delugeate contains two resistances, the fouling on the air-side surface and the air-side surface to bulk delugeate resistance.

Equation C.19 gives the transformed overall coefficient between the fin root and the delugeate, U^*_{rs} .

$$U^*_{rs} = \left[\frac{1}{h_d} + \frac{1}{\beta_{ff}} \right]^{-1} C_a \left[\frac{T_r - T_s}{i'_r - i'_s} \right] \quad (C.19)$$

(a) Taken into account by η_f , the fin efficiency.

where β_{ff} is the air-side fouling coefficient, T_s is the temperature of the delugeate and i'_s is the enthalpy of saturated air at temperature T_s .

Similar reasoning gives Equation 20 for $U^*_{r\infty}$, the transformed overall coefficient between the fin root and the bulk air:

$$U^*_{r\infty} = \left[\frac{1}{U^*_{rs}} + \frac{1}{h_s} \right]^{-1} \quad (C.20)$$

The quantity h_s is the air-side heat transfer coefficient based on temperature driving force. Thus, if the effects of the geometric changes caused by the presence of delugeate can be neglected or compensated for, values of h_s from dry operation can be used to predict the deluge performance.

In the above manner all of the convective terms except that of the delugeate to air are transformed to enthalpic driving forces by the use of a ratio of a temperature difference to an enthalpy difference at the same temperature as seen in terms used in Equations C.18 and C.19. Examination of the derivation of Equation C.6 from Equation C.5 shows that no such transformation is required for the delugeate to air heat transfer coefficient.

The overall tube side to air transformed heat transfer coefficient is given by Equation C.21,

$$U^*_{p\infty} = \left[\frac{1}{U^*_{pr}} + \frac{1}{U^*_{r\infty}} \right]^{-1} \quad (C.21)$$

The computation of fin efficiency is described in Appendix B. The fin efficiency of a deluged system is computed identically to that of a dry system except the quantity $U^*_{r\infty}/(C_a \frac{dT}{di})$ is used in place of h_s . The derivative of temperature with respect to enthalpy, dT/di is evaluated at the average fin temperature \bar{T}_f .

In order to solve Equations C.17 through C.21 for $U^*_{p\infty}$, given values of A_p , A_w , A_b , A_f , h_p , k_w , β_{fp} , β_{ff} , h_d , h_s , T_p , T_a , i'_p and i'_a , values of T_r , T_s , and \bar{T}_f must be evaluated. This was done by an iterative process; the convergence criteria was a change in $U^*_{p\infty}$ of less than 0.1%. Derivations of

relationships for computing values of enthalpy of saturated air at the fin root (i'_r), at the deluge-air surface (i'_s) and at the average condition on the fin surface (\bar{i}'_f) are given by Equations C.22 through C.24.

$$Q = U^*_{r\infty} (i'_r - i_\infty) (A_b + \eta_f A_f) / C_a = U^*_{p\infty} (i'_p - i_\infty) (A_b + \eta_f A_f) / C_a \quad (C.22a)$$

Therefore,

$$i'_r = i_\infty + \frac{U^*_{p\infty}}{U^*_{r\infty}} (i'_p - i_\infty) \quad (C.22b)$$

$$\begin{aligned} Q &= U^*_{r\infty} (A_b + \eta_f A_f) (i'_r - i_\infty) / C_a \quad (C.23a) \\ &= h_s (A_b + A_f) (i'_s - i_\infty) / C_a \end{aligned}$$

Therefore,

$$i'_s = i_\infty + \frac{U^*_{r\infty}}{h_s} \frac{(A_b + \eta_f A_f)}{(A_b + A_f)} (i'_r - i_\infty) \quad (C.23b)(a)$$

(a) Equation C. 23b gives a value of i'_s which is the average value over the total outside area ($A_b + A_f$). This choice of the value of i'_s with its corresponding T_s used for the calculation of $U^*_{r_s}$ is probably the most reasonable. If the value of i'_s at the fin root is desired, it can be obtained from

$$i'_s = \frac{U^*_{r\infty}}{h_s} (i'_r - i_\infty) + i_\infty.$$

If the average value of i'_s on the fin is desired, it can be obtained from

$$i'_s = \frac{U^*_{r\infty}}{h_s} \eta_f (i'_r - i_\infty) + i_\infty$$

Note that for

$$h_b = \beta_{ff} = \infty$$

the equation for the average value of i'_s on the fin reduces to Equation C. 24b as it should.

By definition

$$\eta_f = \frac{h_s A_f (\bar{i}'_f - i_\infty)/C_a}{h_s A_f (i'_r - i_\infty)/C_a} \quad (\text{C.24a})$$

Therefore,

$$\bar{i}'_f = i_\infty + \eta_f (i'_r - i_\infty) \quad (\text{C.24b})$$

T_r , T_s and \bar{T}_f are computed from the values of i'_r , i'_s and \bar{i}'_f computed from Equations C.21b, C.22b and C.23b, respectively (see "Basics and Definitions," this appendix).

COMPUTATION OF OVERALL HEAT TRANSFER AND WATER EVAPORATION RATE

Both the B&W and the PNL methods use the NTU approach for computing heat exchanger performance. This approach is described in detail for temperature driving force by Kaynes and London,^(C.3) which we shall now give a brief review. The heat exchanger effectiveness for temperature driving force is defined by

$$\phi_T = \frac{T_{\infty 2} - T_{\infty 1}}{T_p - T_{\infty 1}} \quad (\text{C.25})$$

where T_p is the tube-side temperature, and $T_{\infty 1}$ and $T_{\infty 2}$ are the bulb temperatures of the air entering and exiting the heat exchanger, respectively.

The heat transfer rate is given by

$$Q = \dot{m}_a C_{pa} (T_{\infty 2} - T_{\infty 1}) = \dot{m}_a C_{pa} \phi_T (T_p - T_{\infty 1}) \quad (\text{C.26})$$

For the NH_3 condenser the relationship for ϕ_T is

$$\phi_T = 1 - e^{-N_T} \quad (\text{C.27})$$

where N_T , the number of NTUs based on the temperature driving force is given by

$$N_T = \frac{A U}{\dot{m}_a C_{pa}} \quad (C.28)$$

where

U = the overall heat transfer coefficient, $\text{Btu}/\text{ft}^2\text{-}^\circ\text{F}$

A = heat transfer area, ft^2

\dot{m}_a = flow rate of air, lb/hr

C_{pa} = heat capacity of air.

Relationships for a deluged heat exchanger for both the B&W and the PNL method are

$$\phi = \frac{i_{\infty 2} - i_{\infty 1}}{i'_p - i_{\infty 1}} \quad (C.29)$$

$$Q = \dot{m}_a \phi (i'_p - i_{\infty}) \quad (C.30)$$

and

$$\phi = 1 - e^{-N} \quad (C.31)$$

However, because the B&W approach uses the enthalpy difference as the driving force

$$N = \sum_{p\infty} (A_b + A_f) / \dot{m}_a \quad (C.32a)$$

for the B&W approach. For the PNL approach, which uses enthalpy difference divided by the heat capacity as the driving force, and incorporates fin efficiency into Equation C.14,

$$N = U^*_{p\infty} (A_b + \eta_f A_f) / (C_{pa} \dot{m}_a) \quad (C.32b)$$

The performance of a deluged heat exchanger was computed in a similar manner no matter whether the B&W or the PNL method was used. Changes in the mass (or heat) transfer coefficient between the leading and the trailing edge of the heat exchanger were taken into account in the following manner. A value of $\Sigma_{p\infty 1}$ (or $U_{p\infty 1}$) was computed for the leading edge and the number of enthalpy transfer units N_1 were computed by Equation C.33a for the B&W method

$$N_1 = \Sigma_{p\infty 1} (A_b + A_f) / \dot{m}_a \quad (C.33a)$$

and by Equation C.32b for the PNL method.

$$N_1 = U^*_{p\infty} (A_b + \eta_f A_f) / (C_{a1} \dot{m}_a) \quad (C.33b)$$

where \dot{m}_a is the flow rate of the air through the heat exchanger and the subscript 1 refers to the leading edge. In a similar manner, N_2 , the number of enthalpy transfer units based upon conditions at the trailing edge was computed from Equations C.34a and C.34b for the B&W and for the PNL methods, respectively.

$$N_2 = \Sigma_{p\infty 2} (A_b + A_f) / \dot{m}_a \quad (C.34a)$$

$$N_2 = U^*_{p\infty 2} (A_b + \eta_f A_f) / (C_{a2} \dot{m}_a) \quad (C.34b)$$

The arithmetic mean of the number of enthalpy transfer units, based upon conditions at the leading and trailing edge, are taken (Equation C.35)

$$\bar{N} = (N_1 + N_2) / 2 \quad (C.35)$$

from which the heat exchanger effectiveness was computed from Equation C.31. The total heat transfer, Q , was computed from Equation C.30 and the water evaporation rate, \dot{m}_v , from Equation C.36.

$$\dot{m}_v = \dot{m}_a (H_2 - H_1) \quad (C.36)$$

where

\dot{m}_a is the flow rate of the entering air

H_1 is the absolute humidity of the entering air

H_2 is the absolute humidity of the exiting air.

As mentioned under "Basics and Definitions" H_1 can be computed from a knowledge of the atmospheric pressure, the dry-bulb temperature and either the relative humidity or the wet-bulb temperature of the entering air. The computation of H_2 is a little more complicated. First, the enthalpy of the exiting air is computed from Equation C.37.

$$i_{\infty 2} = i_{\infty 1} + \phi(i'_p - i_{\infty 1}) \quad (C.37)$$

Then from an assumed relative humidity of the exiting air (generally 100%), the temperature and absolute humidity of the exiting air was computed from Equations C.1, C.2 and C.3 (and from the known vapor pressure-temperature relationship for water).

The computation of the performance of a deluged heat exchanger was iterative in nature because the value of N_2 , the number of transfer units at the trailing edge was dependent upon the conditions at the trailing edge. The convergence criterion was a change of less than a specified amount (generally 0.1%) in both Q and \dot{m}_v .

NOMENCLATURE

A = area, ft^2

A_b = area of the tubes between the fins, ft^2

A_f = surface area of the fins, ft^2

A_p = wetted surface area, primary side

A_t = total air-side surface area, ft^2

A_w = average area of the tube wall, ft^2

C_a = specific heat of moist air, Btu/lb of dry air-°F

H = absolute humidity, lb water/lb air
 h = heat transfer coefficient, Btu/ft²-hr-°F
 h_d = heat transfer coefficient, fin/delugeate surface, Btu/ft²-hr-°F
 h_p = heat transfer coefficient, primary fluid/tube surface, Btu/ft²-hr-°F
 h_s = heat transfer coefficient, delugeate/air surface, Btu/ft²-hr-°F
 i = enthalpy of moist air, Btu/lb of dry air
 i_∞ = enthalpy of moist air in the free stream, Btu/lb of dry air
 i'_p = enthalpy of saturated air evaluated at the primary fluid temperature, T_p , Btu/lb of dry air
 i'_r = enthalpy of saturated air evaluated at the temperature of the fin root, T_r , Btu/lb of dry air
 i'_s = enthalpy of saturated air evaluated at the water/air surface temperature, T_s , Btu/lb of dry air
 k_w = thermal conductivity of tube/fin material
 Le = Lewis number
 \dot{m}_a = mass flow rate of air
 \dot{m}_v = evaporation rate
 N = NTU rating of heat exchanger
 \bar{N} = average NTU rating of heat exchanger
 p = partial pressure of water, in. Hg
 P_a = atmospheric pressure, in. Hg
 Q = heat transfer rate, Btu/hr
 T = dry-bulb temperature, air
 \bar{T}_f = average temperature at the fin/water interface, °F
 T_p = temperature of the primary fluid
 T_r = temperature at the fin root

- T_s = temperature at the air/water interface
 T_∞ = temperature of the free stream moist air
 t_w = tube wall thickness, ft
 U_{pr} = overall heat transfer coefficient between the tubeside fluid and the fin root, $\text{Btu/ft}^2\text{-hr-}^\circ\text{F}$
 U^*_{pr} = overall enthalpy-based heat transfer coefficient between the tube-side fluid and the fin root, $\text{Btu/hr-ft}^2\text{-}^\circ\text{F}$
 U_{ps} = overall heat transfer coefficient between the tube-side fluid and the delugeate-air surface, $\text{Btu/ft}^2\text{-hr-}^\circ\text{F}$
 U^*_{ps} = enthalpy-based heat transfer coefficient between the tube-side fluid and the delugeate-air surface, lb of dry air/ $\text{ft}^2\text{-hr}$
 $U^*_{p\infty}$ = overall enthalpy-based heat transfer coefficient between the tube-side fluid and the bulk air, $\text{Btu/hr-ft}^2\text{-}^\circ\text{F}$
 U^*_{rs} = overall enthalpy-based heat transfer coefficient between the fin root and the delugeate-air surface, $\text{Btu/hr-ft}^2\text{-}^\circ\text{F}$
 $U^*_{r\infty}$ = overall enthalpy-based heat transfer coefficient between the fin root and the bulk air, $\text{Btu/hr-ft}^2\text{-}^\circ\text{F}$
 β_{ff} = fouling factor at the fin water surface, $\text{Btu/hr-ft}^2\text{-}^\circ\text{F}$
 β_{fp} = fouling factor on the tube side, $\text{Btu/hr-ft}^2\text{-}^\circ\text{F}$
 σ_s = delugeate-air mass transfer coefficient, lb of dry air/ $\text{ft}^2\text{-hr}$
 ϕ = heat exchanger effectiveness, dimensionless
 η_f = fin efficiency
 Σ_{ps} = overall mass transfer coefficient between the tube-side fluid and the delugeate-air interface, lb of dry air/ $\text{ft}^2\text{-hr}$
 $\Sigma_{p\infty}$ = overall mass transfer coefficient between the tube-side fluid and the bulk air, lb of dry air/ $\text{ft}^2\text{-hr}$

Superscripts

()* = denotes transformed or wet parameter

i' = denotes saturated air enthalpy

Subscripts

p = primary fluid

s = air/water interface

w = tube/fin material property

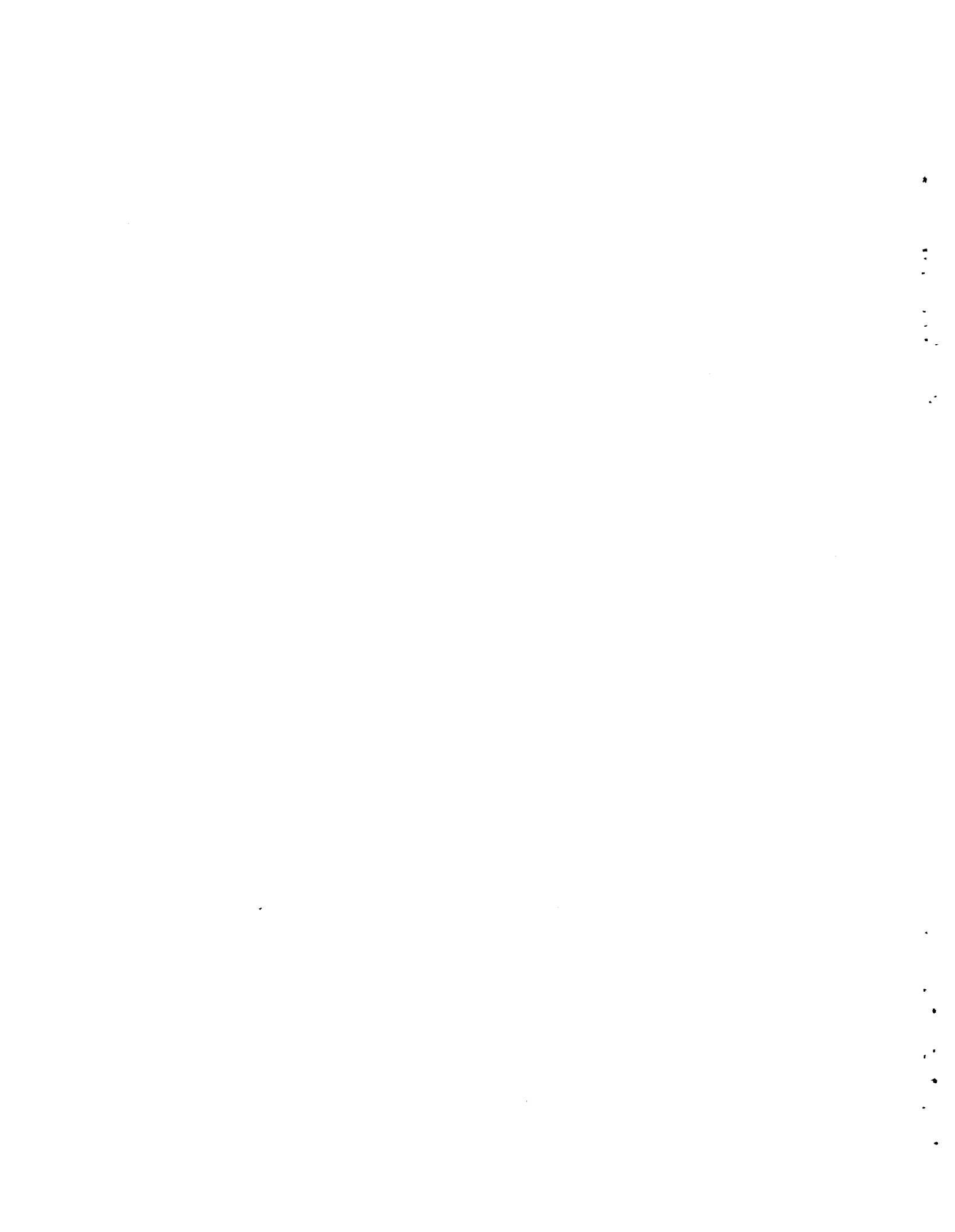
1 = inlet (leading edge)

2 = outlet (trailing edge)

∞ = free stream condition

REFERENCES

- C.1. W. H. McAdams, Heat Transmission, 3rd Ed., McGraw-Hill Book Co., New York, NY, 1954.
- C.2. W. M. Kays, and A. L. London, Compact Heat Exchangers. McGraw-Hill Book Co., New York, NY, 1964.
- C.3. D. K. Kreid, B. M. Johnson and D. W. Faletti, Approximation Analysis of Heat Transfer from the Surface of a Wet Finned Heat Exchanger. PNL-SA-6422, Battelle, Pacific Northwest Laboratories, Richland, WA 99352, February 1977. (Also presented at the Second AIAA/ASME Thermophysics and Heat Transfer Conference, Palo Alto, CA, May 24-26, 1978) (reprint number 78-HT-26).



APPENDIX D

METEOROLOGY METHODOLOGY

APPENDIX D METEOROLOGY METHODOLOGY

The meteorology of a particular site is characterized by a maximum temperature and a cumulative distribution of wet-bulb and dry-bulb temperatures. Eight sites were selected for this analysis: San Juan, NM; Miami, FL; Chicago, IL; San Francisco, CA; Washington DC; Boston, MA; Phoenix, AZ; and Bakersfield, CA. Wet-bulb and dry-bulb cumulative temperature curves for these eight sites are shown in Figures D.1 through D.8. The top curve in Figures D.1 through D.8 represents the dry-bulb temperatures, and the bottom curve represents the wet-bulb temperatures. Figure D.9 is a dry-bulb temperature distribution for all the sites and Figure D.10 presents a cumulative graph of the wet-bulb temperature distributions. All temperature profiles were adjusted so that the cumulative hours below 30°F were included in the cumulative hours at 30°F. This adjustment had no effect on the cooling system designs for these sites.

The BNW-II Dry/Wet Optimization Code requires the following information in order to accurately model the meteorology of a specific site.

- Dry-bulb cumulative temperature distribution
- Wet-bulb cumulative temperature distribution
- Turbine back pressure curve corresponding to the dry- and wet-bulb temperature distributions.

Three types of turbines were considered in this analysis. Each turbine has a distinct maximum turbine back pressure curve. High back pressure turbines can operate continuously at 15.0 in. Hga. Modified conventional turbines have a maximum continuous turbine back pressure of 8.0 in. Hga. Conventional turbines have a maximum continuous back pressure of 5.5 in. Hga; however, under certain circumstances operation above 5.5 in. Hga is allowed. Westinghouse Electric Company has developed guidelines for operation of their turbines above 5.5 in. Hga. An excerpt from their procedure follows.

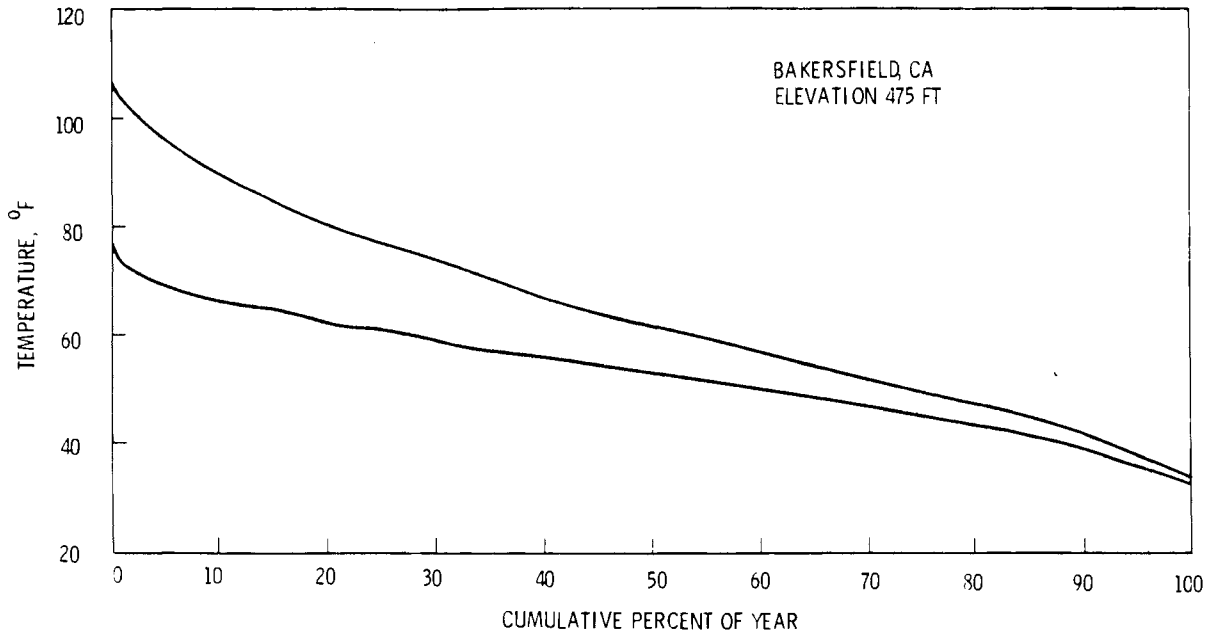


FIGURE D.1. Cumulative Dry-Bulb and Wet-Bulb Temperature Distribution Taken from an Eleven-Year Average for Bakersfield, CA

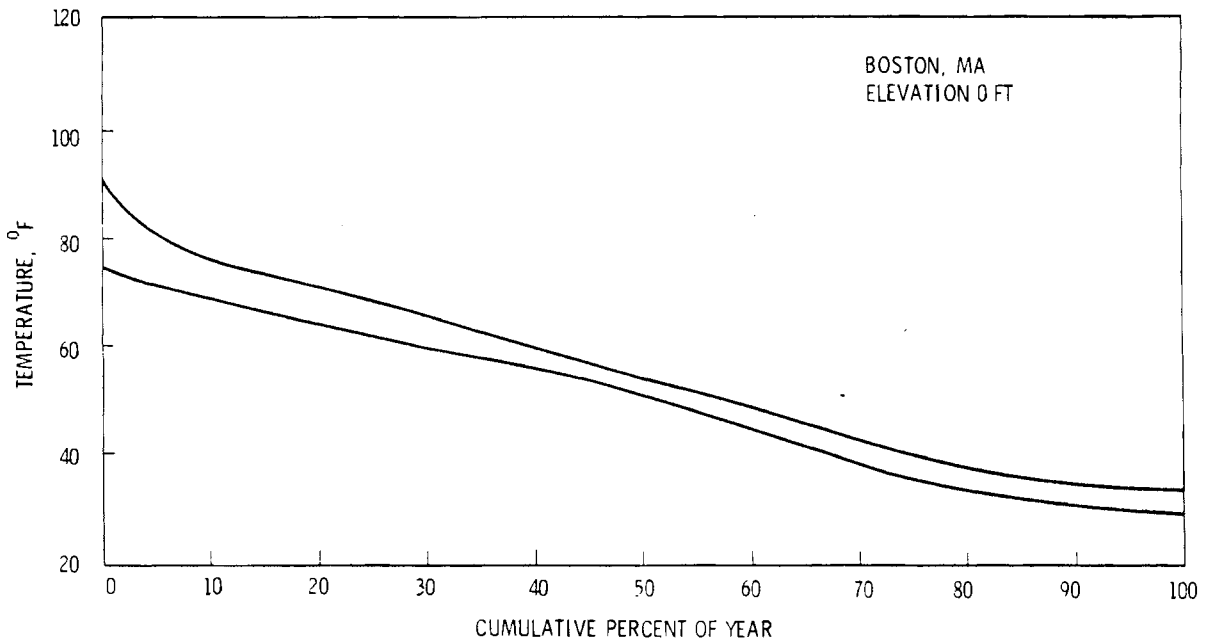


FIGURE D.2. Cumulative Dry-Bulb and Wet-Bulb Temperature Distribution Taken from a Twenty-Year Average for Boston, MA

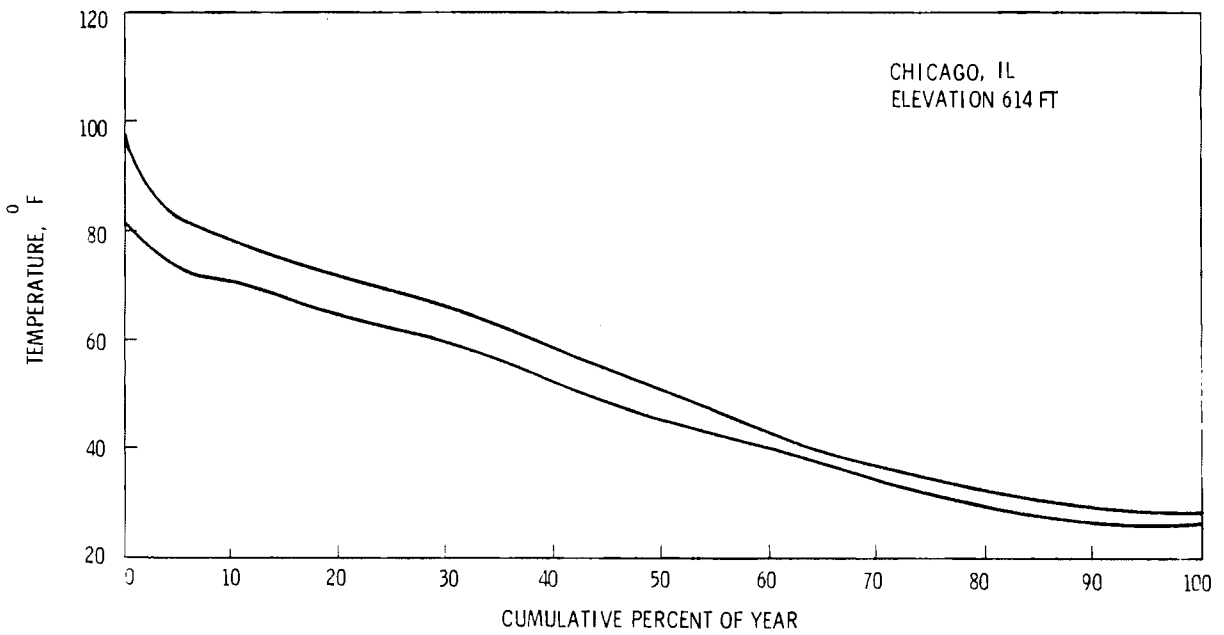


FIGURE D.3. Cumulative Dry-Bulb and Wet-Bulb Temperature Distribution Taken from a Nineteen-Year Average for Chicago, IL

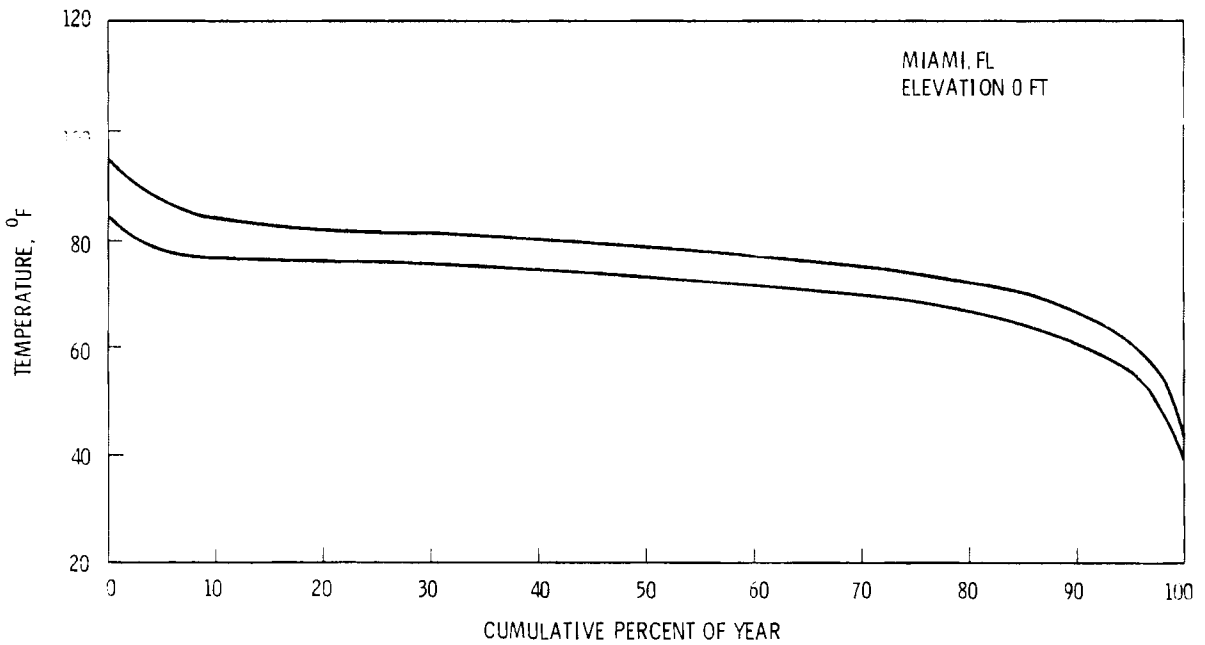


FIGURE D.4. Cumulative Dry-Bulb and Wet-Bulb Temperature Distribution Taken from a Twenty-Year Average for Miami, FL

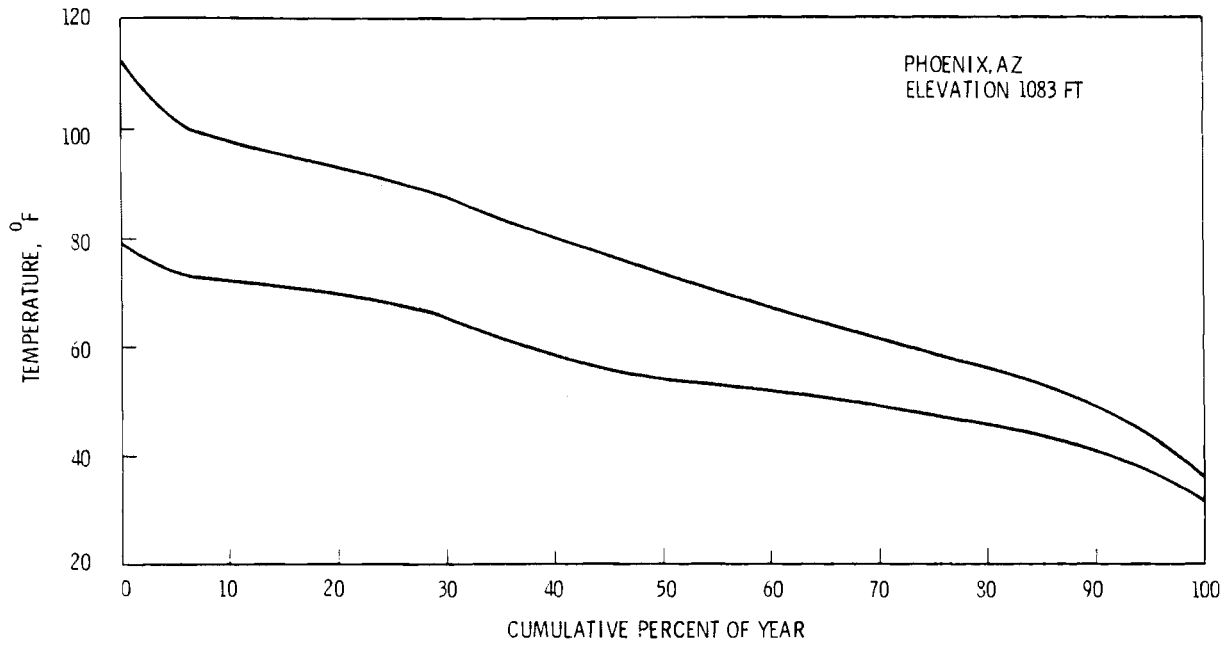


FIGURE D.5. Cumulative Dry-Bulb and Wet-Bulb Temperature Distribution Taken from a Twenty-Six Year Average for Phoenix, AZ

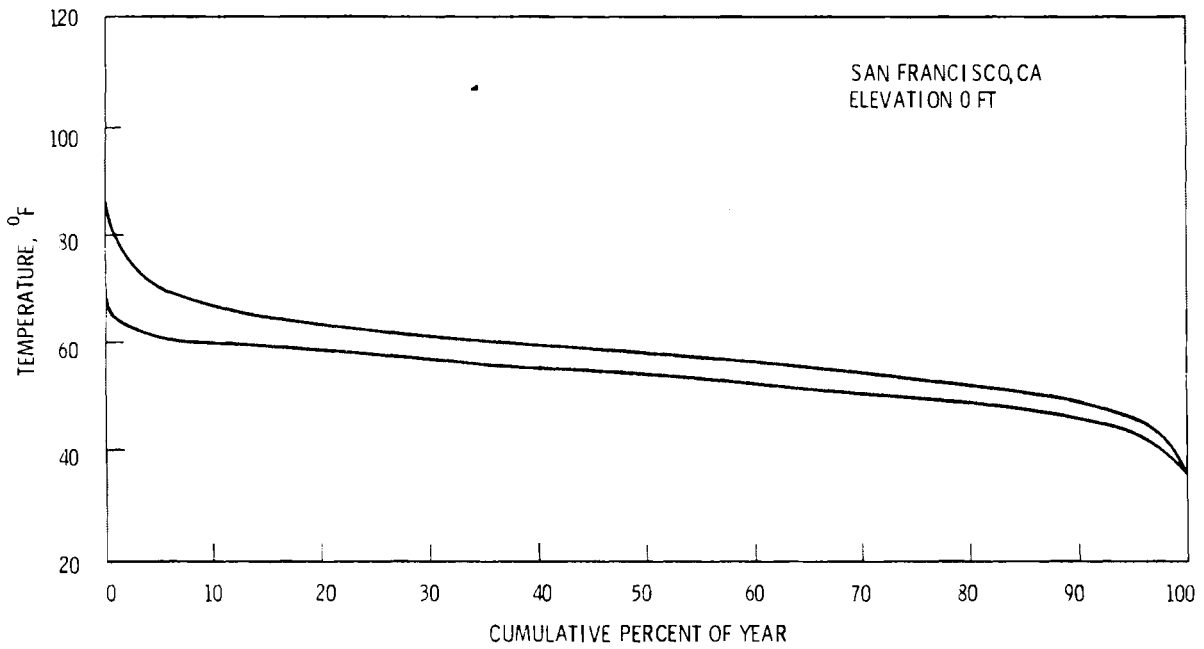


FIGURE D.6. Cumulative Dry-Bulb and Wet-Bulb Temperature Distribution Taken from a Seventeen-Year Average for San Francisco, CA

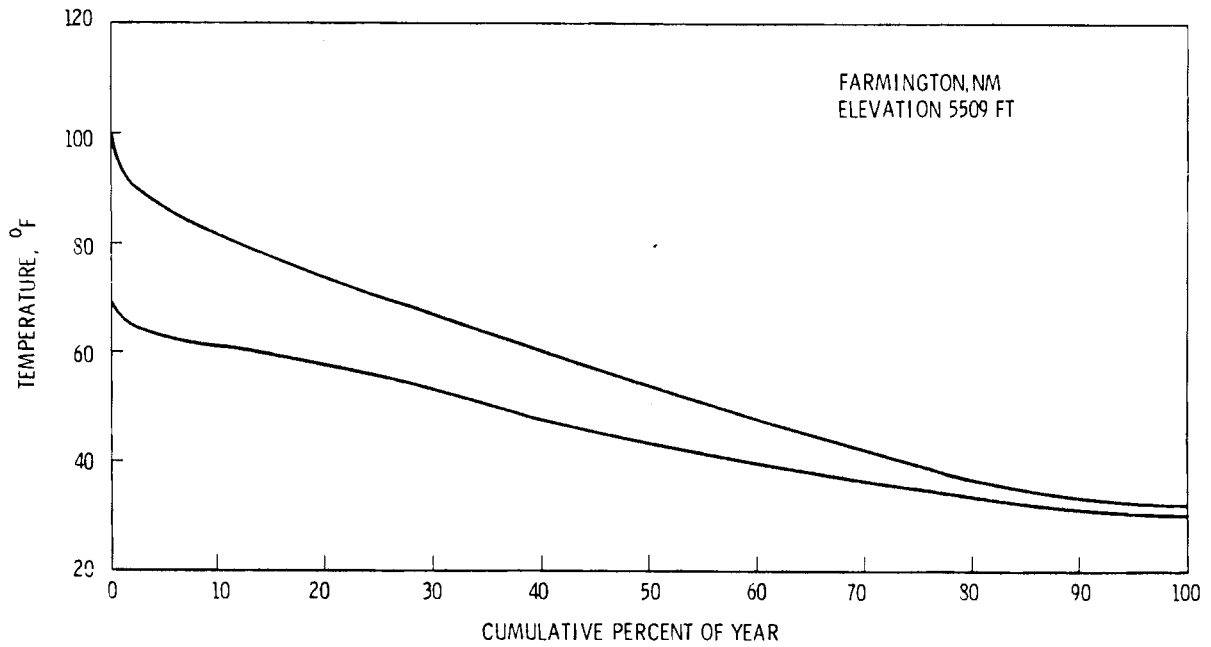


FIGURE D.7. Cumulative Dry-Bulb and Wet-Bulb Temperature Distribution Taken from a Five-Year Average for San Juan, NM

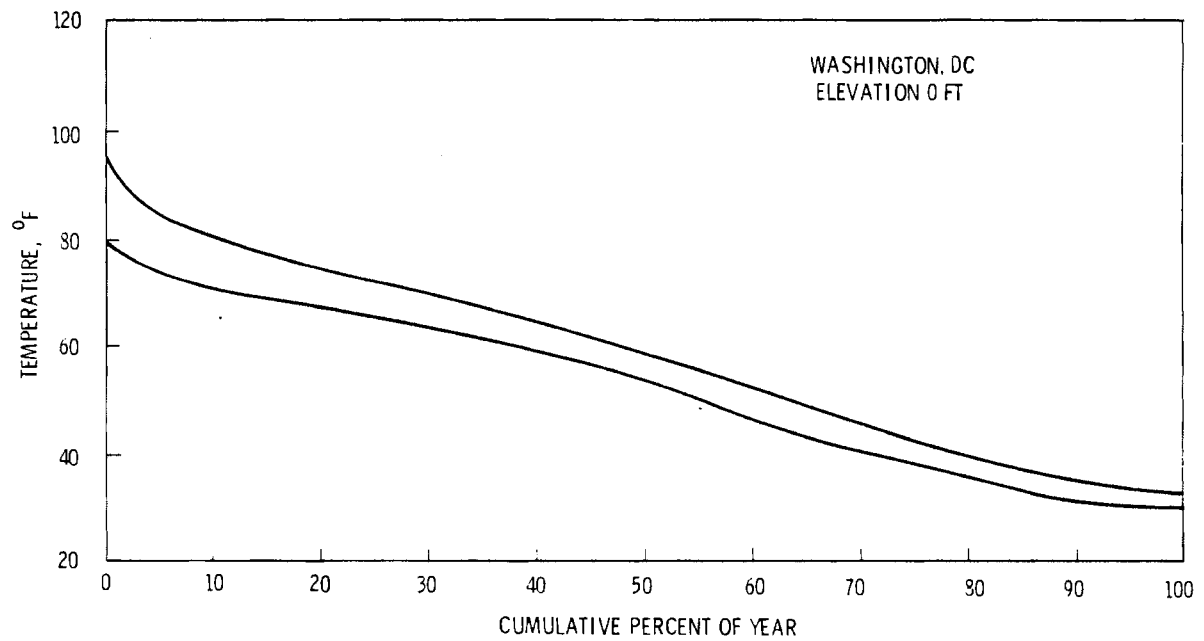


FIGURE D.8. Cumulative Dry-Bulb and Wet-Bulb Temperature Distribution Taken from a Thirty-Three-Year Average for Washington, DC

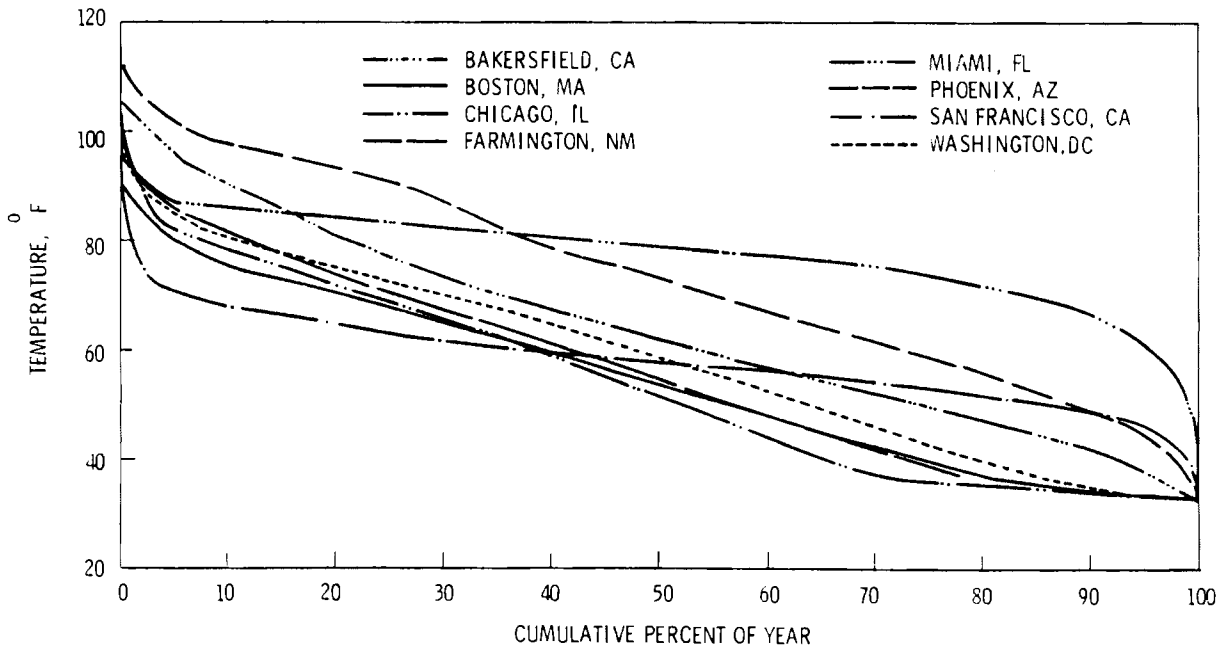


FIGURE D.9. Cumulative Comparison of Dry-Bulb Temperature Profiles for All Eight Meteorological Sites

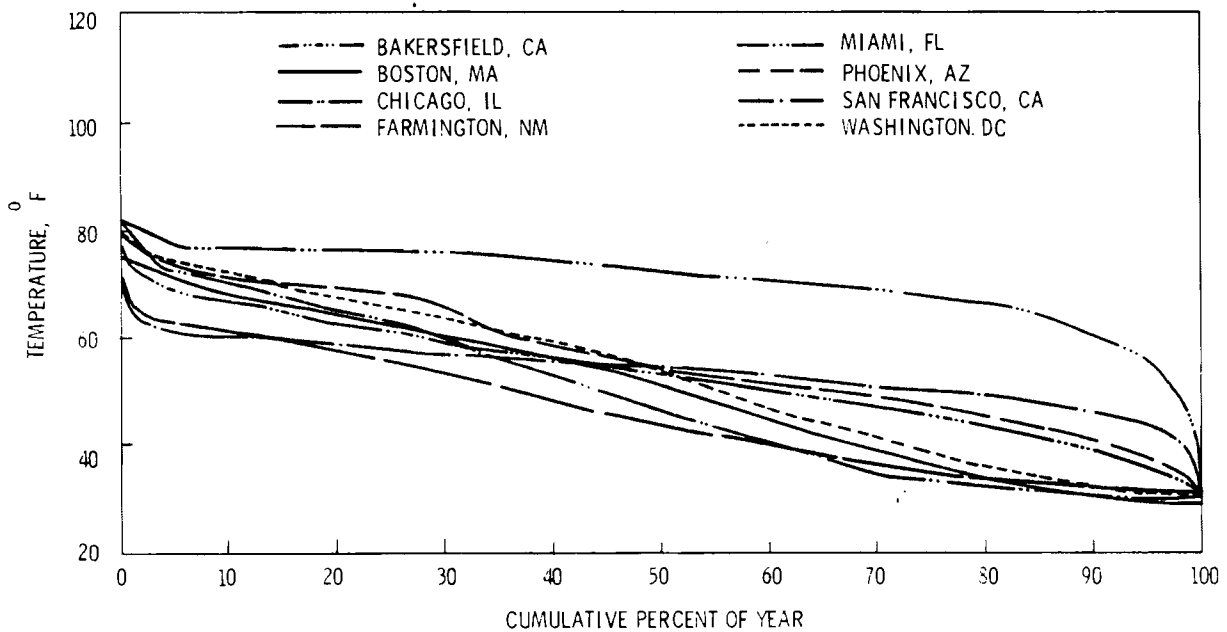


FIGURE D.10. Cumulative Comparison of Wet-Bulb Temperature Profiles for All Eight Meteorological Sites

TURBINE OPERATION AT HIGH CONDENSER PRESSURES

The turbine may be operated continuously over the load range with condenser pressures up to 5.5 In. Hg Abs. For short periods the turbine may be operated with condenser pressures up to 8 In. Hg Abs for a maximum of 72 days or part days in any 12 month period providing such operation is accomplished in accordance with the following guidelines and at loads equal to or greater than those specified in Figure D.11:

- 1) The turbine may be operated for 36 days or part days with condenser pressures between 5.5 In. Hg Abs and 8 In. Hg Abs;
- 2) The turbine may be operated for 19 additional days or part days with condenser pressures between 5.5 In. Hg Abs and 7 in. Hg Abs;
- 3) The turbine may be operated for 17 additional days or part days with condenser pressures between 5.5 In. Hg. Abs and 6 In. Hg Abs;
- 4) Any excursion above 5.5 In. Hg Abs, whether for one hour or a full day, shall be considered as a full day in the summation of days;
- 5) When operating with high condenser pressure, avoid rapid and frequent changes to this pressure.

To use Figure D.11, enter at the selected condenser pressure, proceed horizontally to intersect the curve and then vertically downward to read the minimum allowable load (in percent of maximum calculated load) for operation at the selected condenser pressure. Operation below this minimum load at the selected condenser pressure is not permitted.

An example of a maximum turbine back pressure curve for a conventional turbine is shown in Figure D.12. The "steps" in Region 1 correspond to the Westinghouse turbine back pressure model. The conventional turbine will be used throughout the remainder of the meteorology development. Use of the conventional turbine represents the most complex turbine back pressure model. In this model the back pressure is varied from 5.5 to 8.0 in. Hg as the ambient dry-bulb temperature increases. The maximum turbine back pressure limits for the modified conventional turbine and the high back pressure turbine models are 8.0 and 15.0 in. Hg, respectively, throughout the entire temperature range.

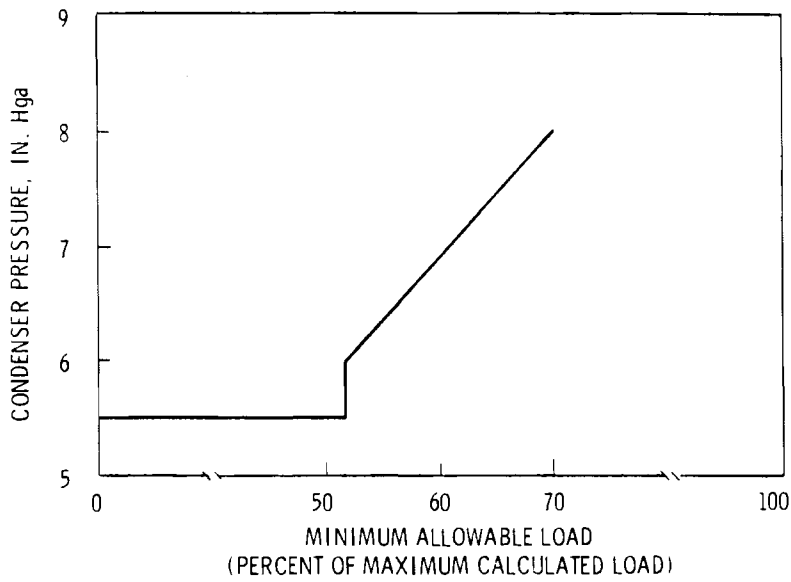


FIGURE D.11. Minimum Allowable Load at Condenser Pressures Above 5.5 in. Hga

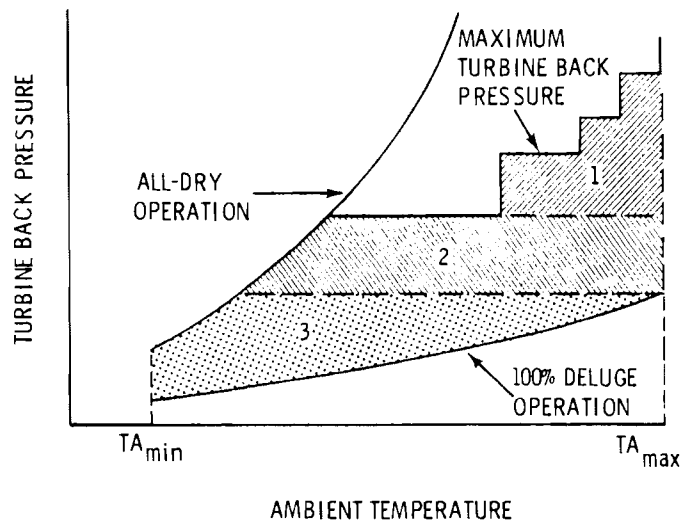


FIGURE D.12. Operating Regimes for a Power Plant with a Deluged Cooling System

The nature of the turbine back pressure model dictated the format of the input data for the BNW-II Dry/Wet Computer Code. The meteorological profile of each site was divided into 8 or 16 intervals. Each interval was represented by four points:

- average dry-bulb temperature
- corresponding average wet-bulb temperature
- residence time in the interval (expressed as fraction of the year)
- maximum allowable turbine back pressure.

Two types of meteorological data were necessary to complete the meteorological profile of each site in a manner compatible with the turbine back pressure data:

- summary of daily maximum ambient temperature, and
- cumulative summary of dry-bulb and wet-bulb temperatures and their frequency distribution.

These summaries were obtained from the National Climatic Center, Asheville, NC. A summary of the type of information received, the site locations and elevations are presented in Table D.1. When data were not available for a specific site, data from a site with similar meteorological conditions in close proximity to the actual site were obtained. For example, the National Climatic Center had no Summary of Meteorological Observations, Surface for the Bakersfield, CA site; therefore, data from Le Moore, CA was substituted (see Table D.1).

The local climatological data provided a daily record of maximum temperatures for the period of January through December 1976. This period was considered the reference interval for all the meteorological sites. This data in conjunction with the turbine back pressure data from Westinghouse Electric Company defined the ambient temperature boundaries for the turbine back pressure intervals above 5.5 in. Hg.

The local climatological data was tabulated to determine the daily maximum temperature profiles of each site for one year. Table D.2 provides a cumulative summary of this data for the reference site, San Juan, NM. Using

TABLE D.1. Meteorological Data for Each Site

<u>Site</u>	<u>Elevation, ft</u>	<u>Local Climatological Data, January - December 1976</u>	<u>Summary of Meteorological Observations, Surface</u>	
Bakersfield, CA	475	Bakersfield, CA	Le Moore, CA	1961-1972
Boston, MA	0	Boston, MA	Boston, MA	1945-1965
Chicago, IL	614	Chicago, IL	Chicago, IL	1946-1965
Miami, FL	0	Miami, FL	Miami, FL	1948-1970
Phoenix, AZ	1083	Phoenix, AZ	Phoenix, AZ	1941-1946 1951-1972
San Francisco, CA	0	San Francisco, CA	San Francisco, CA	1948-1965
San Juan, NM	5509	Farmington, NM	Farmington, NM	1954-1959
Washington, DC	0	Washington, DC	Washington, DC	1943-1967

TABLE D.2. Summary of Daily Maximum Temperatures for San Juan, NM

<u>Temperature,</u> <u>°F</u>	<u>Number of</u> <u>Occurrences</u>	<u>Cumulative</u> <u>Occurrences</u>	<u>Temperature,</u> <u>°F</u>	<u>Number of</u> <u>Occurrences</u>	<u>Cumulative</u> <u>Occurrences</u>
103	1	1	60	3	254
102			59	6	260
101	2	3	58	7	267
100	2	5	57	5	272
99	3	8	56	1	273
98	3	11	55	9	282
97	5	16	54	5	287
96	4	20	53	10	297
95	7	27	52	2	299
94	6	33	51	8	307
93	9	42	50	10	317
92	6	48	49	3	320
91	11	59	48	8	328
90	10	69	47	4	332
89	6	75	46	4	336
88	11	86	45	6	342
87	6	92	44	6	348
86	5	97	43	1	349
85	13	110	42	2	351
84	4	114	41		
83	5	119	40		
82	5	124	39	1	352
81	3	127	38	2	354
80	9	136	37	1	355
79	3	139	36	3	358
78	5	144	35	1	359
77	5	149	34		
76	5	154	33		
75	9	163	32	1	360
74	7	170	31	1	361
73	3	173	30		
72	7	180	29	1	362
71	6	186	28		
70	5	191	27	1	363
69	4	195	26		
68	2	197	25		
67	4	201	24	1	364
66	12	213	23		
65	9	222	22	1	365
64	2	224	21		
63	6	230			
62	5	235			
61	10	245			

this profile and the turbine information from Westinghouse, the 36 highest temperature days were allowed to reach a maximum turbine back pressure of 8.0 in. Hg. For the San Juan site this temperature interval ranged from 94 to 103°F and included 33 temperature occurrences. 94°F was chosen as the lower limit of the interval because the number of occurrences at this point (33) was still within the limit of 36 allowed occurrences. Because this temperature range was so large these data were separated into two temperature intervals. The 19 next highest temperatures (days 37 through 55) were allowed maximum turbine back pressures of 7.0 in. Hg. This interval ranged from 92 to 93°F and included up to the 48th temperature occurrence. Days 56 through 72 were allowed maximum turbine back pressures of 6.0 in. Hg. This corresponded to the temperature interval from 90 to 91°F. For the remainder of the year (days 73 through 365) the back pressure limit was 5.5 in. Hg. For the modified conventional turbine and the high back pressure turbine the maximum turbine back pressures would remain constant at 8.0 and 15.0 in. Hg, respectively throughout the temperature range.

The turbine back pressure range above 5.5 in. Hg was composed of four intervals, one each for 6.0 and 7.0 in. Hg and two for 8.0 in. Hg. The 8.0 in. Hg range was divided into two intervals because the 36 highest temperature days usually spanned 10 to 20 degrees. This data defined the turbine back pressure curve and the first four dry-bulb temperature intervals, 90 through 101°F, listed in Table D.3. The remainder of the temperature range was divided equally into 4 or 12 intervals to make a total of 8 or 16 intervals.

The wet-bulb temperatures and the residence time in each interval was determined from the Summary of Meteorological Observations, Surface. The summary presented cumulative dry-bulb and wet-bulb temperature data. An excerpt from the table description follows.

PART E - PSYCHROMETRIC SUMMARIES

In this section are presented various summaries of dry- and wet-bulb temperatures, dew points, and relative humidity. The order and manner of presentation follows:

TABLE D.3. Meteorological Data for San Juan, NM,
8 and 16 Temperature Intervals

	<u>Tdb, °F</u>	<u>Twb, °F</u>	<u>Tdb Range, °F</u>	<u>Fraction</u>	<u>Maximum Turbine Back Pressure, in. Hga</u>
<u>16 Intervals</u>	101	71	99-103	0.0022	8
	96	67	94-98	0.0049	8
	92	66	92-93	0.0059	7
	90	65	90-91	0.0099	6
	87	63	85-89	0.0379	5.5
	82	61	80-84	0.0459	5.5
	77	59	75-79	0.0501	5.5
	72	56	70-74	0.0673	5.5
	67	53	65-69	0.0783	5.5
	62	49	60-64	0.0811	5.5
	57	45	55-59	0.0744	5.5
	52	42	50-54	0.0742	5.5
	47	39	45-49	0.0784	5.5
	42	36	40-44	0.0812	5.5
	37	34	35-39	0.0810	5.5
	33	31	low-34	0.2233	5.5
<u>8 Intervals</u>	101	71	99-103	0.0022	8
	96	67	94-98	0.0049	8
	92	66	92-93	0.0059	7
	90	65	90-91	0.0099	6
	82	61	75-89	0.1399	5.5
	67	53	60-74	0.2268	5.5
	52	42	45-59	0.2270	5.5
	35	32	low-44	0.3854	5.5

3. Bivariate percentage frequency distribution and computations of dry-bulb versus wet-bulb temperature.

This tabulation is derived from hourly observations and is presented by month and annual, all hours and all years combined. The following information is provided:

- a. The main body of the summary consists of a bivariate percentage frequency distribution of wet-bulb depression in 17 classes spread horizontally; by 2-degree intervals of dry-bulb temperature vertically. Also provided for each dry-bulb temperature interval is the percentage of observations with dry-bulb and wet-bulb temperature combined; and again for dry-bulb, wet-bulb, and dew-point temperatures separately. Total observations for these four items is also provided in two lines at end of each tabulation table, which may require two pages in some cases.

The average sampling period for the psychrometric summaries was 20 years. The psychrometric summary provided the percentage of temperature observations occurring within each temperature interval. It also provided the wet-bulb temperature corresponding to the same cumulative percentage as the average dry-bulb temperature for each interval.

The following rationale was used to determine the residence time in each of the back pressure regions of the maximum turbine back pressure curve for the conventional turbine. These data were taken from the statistical summaries obtained from the National Climatic Center for each site (see Table D.1). The residence time was determined from the actual meteorological data. For example, from Table D.3 the fraction of the year at 8.0 in. Hg is 0.0071. This is equivalent to 2.6 days or 62 hours. This means that during the plant design the turbine back pressure drops from 8.0 in. Hg to 7.0 in. Hg after 62 hours of operation. It drops to 6.0 Hg after 114 hours of operation and drops to 5.5 in. Hg after 200 hours of operation. The amount of time spent in each back pressure region is site specific. This can be noted by comparing the fraction columns in Tables D.3 through D.10.

TABLE D.4. Meteorological Data for Bakersfield, CA,
8 and 16 Temperature Intervals

	<u>Tdb, °F</u>	<u>Twb, °F</u>	<u>Tdb Range, °F</u>	<u>Fraction</u>	<u>Maximum Turbine Back Pressure, in. Hga</u>
<u>16 Intervals</u>	109	77	107-114	0.0012	8
	104	73	100-106	0.0176	8
	98	70	97-99	0.0166	7
	94	68	93-96	0.0261	6
	88	66	85-92	0.0678	5.5
	82	63	80-84	0.0570	5.5
	77	61	75-79	0.0645	5.5
	72	58	70-74	0.0728	5.5
	67	56	65-69	0.0822	5.5
	62	53	60-64	0.0910	5.5
	57	50	55-59	0.1033	5.5
	52	47	50-54	0.1114	5.5
	47	43	45-49	0.1021	5.5
	42	39	40-44	0.0836	5.5
	37	35	35-39	0.0611	5.5
	33	31	low-34	0.0417	5.5
<u>8 Intervals</u>	109	77	107-114	0.0012	8
	104	73	100-106	0.0176	8
	98	70	97-99	0.0166	7
	94	68	93-96	0.0261	6
	85	64	75-92	0.1893	5.5
	67	56	60-74	0.2460	5.5
	52	47	45-59	0.3168	5.5
	35	32	low-44	0.1864	5.5

TABLE D.5. Meteorological Data for Boston, MA,
8 and 14 Temperature Intervals

	<u>Tdb, °F</u>	<u>Twb, °F</u>	<u>Tdb Range, °F</u>	<u>Fraction</u>	<u>Maximum Turbine Back Pressure, in. Hga</u>
<u>14 Intervals</u>	95	78	93-100	0.0023	8
	89	74	86-92	0.0130	8
	84	72	83-85	0.0125	7
	80	70	79-82	0.0251	6
	76	68	75-78	0.0406	5.5
	72	65	70-74	0.0768	5.5
	67	61	65-69	0.0949	5.5
	62	57	60-64	0.0923	5.5
	57	53	55-59	0.0892	5.5
	52	49	50-54	0.0851	5.5
	47	43	45-49	0.0890	5.5
	42	38	40-44	0.0906	5.5
	37	33	35-39	0.0939	5.5
	33	29	1ow-34	0.1947	5.5
<u>8 Intervals</u>	95	78	93-100	0.0023	8
	89	74	86-92	0.0130	8
	84	72	83-85	0.0125	7
	80	70	79-82	0.0251	6
	75	67	71-78	0.0992	5.5
	67	61	60-70	0.2055	5.5
	52	49	45-59	0.2633	5.5
	35	32	1ow-44	0.3791	5.5

TABLE D.6. Meteorological Data for Chicago, IL,
8 and 14 Temperature Intervals

	<u>Tdb, °F</u>	<u>Twb, °F</u>	<u>Tdb Range, °F</u>	<u>Fraction</u>	<u>Maximum Turbine Back Pressure, in. Hga</u>
<u>14 Intervals</u>	98	81	95-102	0.0011	8
	90	77	86-94	0.0208	8
	84	73	84-85	0.0110	7
	82	72	81-83	0.0207	6
	77	69	75-80	0.0640	5.5
	72	65	70-74	0.0734	5.5
	67	61	65-69	0.0842	5.5
	62	56	60-64	0.0759	5.5
	57	51	55-59	0.0714	5.5
	52	47	50-54	0.0664	5.5
	47	43	45-49	0.0672	5.5
	42	39	40-44	0.0662	5.5
	37	34	35-39	0.0846	5.5
	33	31	low-34	0.2931	5.5
<u>8 Intervals</u>	98	81	95-102	0.0011	8
	90	77	86-94	0.0208	8
	84	73	84-85	0.0110	7
	82	72	81-83	0.0207	6
	75	67	70-80	0.1374	5.5
	67	61	60-69	0.1600	5.5
	52	47	45-59	0.2051	5.5
	35	33	low-44	0.4439	5.5

TABLE D.7. Meteorological Data for Miami, FL,
8 and 15 Temperature Intervals

	<u>Tdb, °F</u>	<u>Twb, °F</u>	<u>Tdb Range, °F</u>	<u>Fraction</u>	<u>Maximum Turbine Back Pressure, in. Hga</u>
<u>15 Intervals</u>	96	82	94-98	0.0005	8
	91	80	89-93	0.0230	8
	88	78	88	0.0191	7
	87	71	87	0.0191	6
	82	76	80-86	0.2542	5.5
	77	71	75-79	0.2841	5.5
	72	67	70-74	0.1962	5.5
	67	61	65-69	0.0960	5.5
	62	57	60-64	0.0500	5.5
	57	51	55-59	0.0310	5.5
	52	47	50-54	0.0159	5.5
	47	42	45-49	0.0075	5.5
	42	37	40-44	0.0028	5.5
	37	33	35-39	0.0006	5.5
	33	31	low-34	0.0000	5.5
<u>8 Intervals</u>	96	82	94-98	0.0005	8
	91	80	89-93	0.0230	8
	88	78	88	0.0191	7
	87	77	87	0.0191	6
	82	76	75-86	0.5382	5.5
	67	61	60-74	0.3422	5.5
	52	47	45-59	0.0543	5.5
	35	33	low-44	0.0036	5.5

TABLE D.8. Meteorological Data for Phoenix, AZ,
8 and 16 Temperature Intervals

	<u>Tdb, °F</u>	<u>Twb, °F</u>	<u>Tdb Range, °F</u>	<u>Fraction</u>	<u>Maximum Turbine Back Pressure, in. Hga</u>
<u>16 Intervals</u>	112	79	109-118	0.0054	8
	106	76	105-108	0.0163	8
	103	74	102-104	0.0216	7
	100	73	100-101	0.0178	6
	90	68	85-99	0.2060	5.5
	82	61	80-84	0.0859	5.5
	77	57	75-79	0.0863	5.5
	72	53	70-74	0.0818	5.5
	67	51	65-69	0.0858	5.5
	62	49	60-64	0.0853	5.5
	57	46	55-59	0.0884	5.5
	52	43	50-54	0.0791	5.5
	47	39	45-49	0.0675	5.5
	42	35	40-44	0.0442	5.5
	37	33	35-39	0.0220	5.5
	33	31	low-34	0.0066	5.5
<u>8 Intervals</u>	112	79	109-118	0.0054	8
	106	76	105-108	0.0163	8
	103	74	102-104	0.0216	7
	100	73	100-101	0.0178	6
	88	65	75-99	0.3782	5.5
	67	51	60-74	0.2529	5.5
	52	43	45-59	0.2350	5.5
	35	32	low-44	0.0728	5.5

TABLE D.9. Meteorological Data for San Francisco, CA,
8 and 13 Temperature Intervals

	<u>Tdb, °F</u>	<u>Twb, °F</u>	<u>Tdb Range, °F</u>	<u>Fraction</u>	<u>Maximum Turbine Back Pressure, in. Hga</u>
<u>13 Intervals</u>	93	70	90-104	0.0006	8
	86	67	83-89	0.0030	8
	79	65	76-82	0.0108	8
	74	63	74-75	0.0066	7
	72	62	72-73	0.0101	6
	67	60	65-71	0.0879	5.5
	62	57	60-64	0.1434	5.5
	57	54	56-59	0.2606	5.5
	52	49	50-54	0.2665	5.5
	47	44	45-49	0.1400	5.5
	42	40	40-44	0.0537	5.5
	37	35	35-39	0.0143	5.5
	33	31	low-34	0.0025	5.5
<u>8 Intervals</u>	93	70	90-104	0.0006	8
	86	67	83-89	0.0030	8
	79	65	76-82	0.0108	8
	74	63	74-75	0.0066	7
	72	62	72-73	0.0101	6
	67	60	60-71	0.2313	5.5
	52	49	45-59	0.6671	5.5
	35	33	low-44	0.0705	5.5

TABLE D.10. Meteorological Data for Washington, DC,
8 and 16 Temperature Intervals

	<u>Tdb, °F</u>	<u>Twb, °F</u>	<u>Tdb Range, °F</u>	<u>Fraction</u>	<u>Maximum Turbine Back Pressure, in. Hga</u>
<u>16 Intervals</u>	95	80	93-96	0.0037	8
	91	78	90-92	0.0086	8
	88	76	88-89	0.0090	7
	86	75	86-87	0.0125	6
	84	74	82-85	0.0245	5.5
	80	72	79-81	0.0567	5.5
	76	69	75-78	0.0465	5.5
	72	65	70-74	0.1007	5.5
	67	61	65-69	0.1001	5.5
	62	57	60-64	0.0861	5.5
	57	51	55-59	0.0847	5.5
	52	46	50-54	0.0767	5.5
	47	42	45-49	0.0792	5.5
	42	37	40-44	0.0812	5.5
	37	33	35-39	0.0842	5.5
	33	30	low-34	0.1456	5.5
<u>8 Intervals</u>	95	80	93-96	0.0037	8
	91	78	90-92	0.0086	8
	88	76	88-89	0.0090	7
	86	75	86-87	0.0125	6
	82	73	75-85	0.1277	5.5
	67	61	60-74	0.2869	5.5
	52	46	45-59	0.2406	5.5
	35	31	low-44	0.3110	5.5

According to the turbine specifications for operation at 8.0 in. Hg 36 occurrences are permitted, each with maximum duration of 24 hours. This means the allowed time at 8.0 in. Hg could be as great as 864 hours. In fact, the turbine specifications allow 72 days, 1728 hours, of operation above 5.5 in. Hg. Although the turbine specifications allow this much operation above 5.5 in. Hg, this model was not used in the determination of the step size of the turbine back pressure curve. However, it was used as the upper limit of each back pressure interval where the original site specific meteorology was interpreted.

Analysis of the effect of water availability on the maximum turbine back pressure shows that the maximum turbine back pressure rose above 5.5 in. Hg for only one case presented in this report. This was where no water was available. A graph of the maximum turbine back pressure versus available water is shown in Figure 6.1. In fact, the representation of the meteorology and the turbine back pressure data used in this study is the exact representation of the data required to model an all-dry heat exchanger. The tight tolerances of the back pressure model did not place any severe restrictions on the optimization process of this computer code.

An example of the input meteorological data is shown in Table D.3 for San Juan, NM, the reference site. Data are shown for both 8 and 16 input intervals. Throughout this parametric study 16 meteorological intervals were used because a greater number of data points provided a more accurate model of the temperature profile. In Table D.3 the range of each temperature interval is shown for clarity, in comprehension of the meteorology development these data were not necessary for input to the computer code. The input meteorological data for the remainder of the sites are shown in Tables D.4 through D.10.

APPENDIX E

COMPARISON OF AIR VELOCITY THROUGH DELUGE AND
DRY SECTIONS FOR HÖTERV SURFACES

APPENDIX E
COMPARISON OF AIR VELOCITY THROUGH DELUGE AND
DRY SECTIONS FOR HÖTERV SURFACES

The ratio of air velocity during deluging to the air velocity during all-dry operation can be determined by computing the total pressure losses as each side of a tower is deluged. The pressure drop correlations for a HÖTERV surface, provided by Babcock and Wilcox,^(a) were used as a basis to compute mass flow rates and other related quantities.

The B&W correlations for dry and wet HÖTERV surfaces are given below:

$$\begin{aligned} \text{Dry Surface: } \Delta P &= 2.8895 \times 10^{-6} (G_D)^{1.76} \\ \text{Wet Surface: } \Delta P &= 4.5532 \times 10^{-6} (G_W)^{1.76} \end{aligned}$$

where

ΔP = pressure drop across the heat exchanger (psf)
 G_D, G_W = mass flow rates per unit area (lbm/hr-ft²).

These correlations are for dry air at 20°C ($\rho_a = 0.07522$ lbm/ft³). The HÖTERV equations should be corrected for air density when different conditions are assumed.

Fan performance under varying degrees of tower deluging was examined using Hudson Corporation fan performance curves.^(E-2) The operating point for the fan system was found in the following manner:

1. Assume that the pressure drop through the dry and wet sections will be the same. Guess a value for $\Delta P_{h.x.}$ (pressure drop through the heat exchanger) and solve for the mass flow rates using the HÖTERV equations.

(a) This information was provided by W. W. Sowa, New Products, Power Generation Group, Babcock and Wilcox, Barberton, OH, in a private communication to PNL on March 16, 1977.

2. Calculate the total air mass flow,

$$\dot{m}_{\text{TOTAL}} = G_{\text{DRY}}(A_{\text{DRY}}) + G_{\text{WET}}(A_{\text{WET}})$$

where

A_{DRY} = dry frontal area

A_{WET} = frontal area that is deluged.

3. Determine the volumetric flow rate per fan,

$$Q_{\text{FAN}} = \frac{\dot{m}_{\text{TOTAL}}}{(N_{\text{FANS}})(\rho_{\text{air}})}$$

where

N_{FANS} = number of fans in one tower

ρ_{air} = air density at given elevation and temperature.

4. Using the Q_{FAN} obtained in Step 3, calculate the velocity pressure according to

$$\text{velocity pressure} = VP_{\text{COEFF.}} [0.2 (\text{VEL}_{\text{NR}})^2 + 0.8 (\text{VEL}_{\text{R}})^2]$$

where

$VP_{\text{COEFF.}}$ = velocity pressure coefficient

VEL_{NR} = velocity with no recovery

VEL_{R} = velocity with recovery.

5. Total Pressure = $\Delta P_{\text{h.x.}} + \Delta P_{\text{VEL. PRESS.}}$
6. The total pressure should correspond to the total pressure read from the fan curve (See Figure E.1). Otherwise, guess a new $\Delta P_{\text{h.x.}}$ to either increase or decrease the airflow.

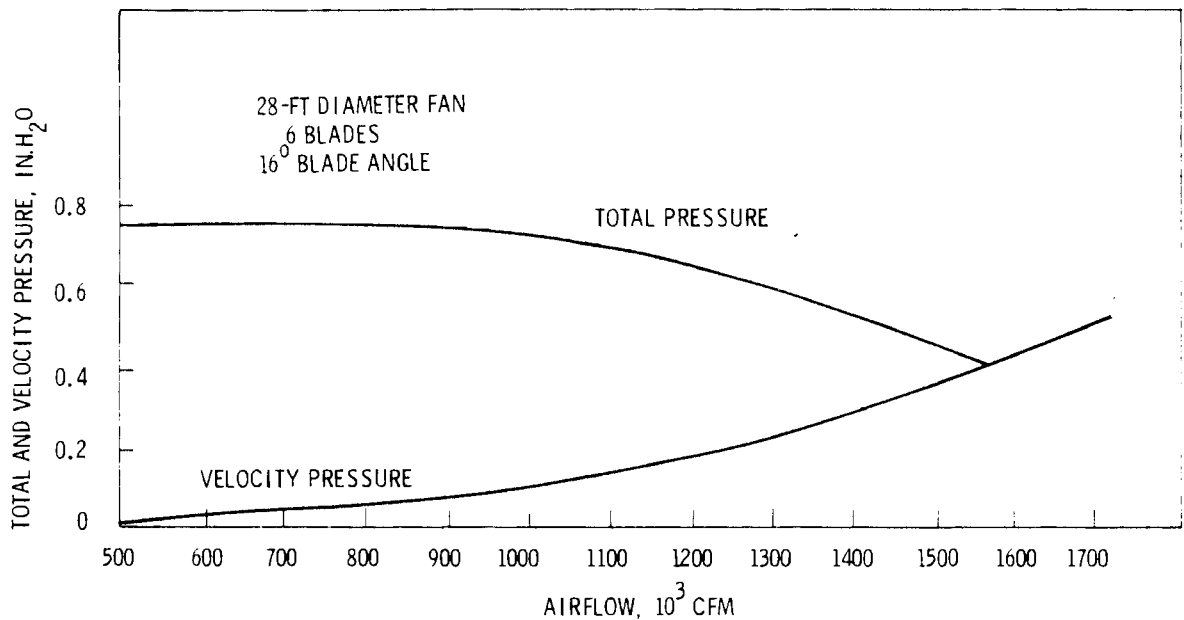


FIGURE E.1. Pressure Versus Airflow for a 27-ft Diameter Fan with 6 Blades and a 16 Degree Blade Pitch Angle

Once the correct pressure drop across the heat exchanger is determined (through successive iterations) the mass flow rates can be used to arrive at the air velocities for the dry/wet sections. The example given below will illustrate the calculational procedures used for a particular fan system.

The reference design case conditions will be used to find the ratio of the air velocity through the deluged section to the air velocity through the dry section.

- a) San Juan meteorological site
- b) Elevation = 5509 ft
- c) Exit air temperature = 83.549°F
- d) Type of fans - 28-ft diameter, 6 blades/fan, and blade angle = 16 degrees
- e) Each tower has 8 sides
- f) Number of fans/tower = 23
- g) Frontal area/4 towers = $0.218930 \times 10^6 \text{ ft}^2$

h) Stack height - 13 ft, diffuser angle is 8 degrees

i) Flow area of fan = 584 ft²

Calculate the specific volume of air leaving the heat exchanger at the elevation specified for the plant. The altitude correction (Bar_{ln}) for the density of air can be found by:

$$\text{Bar}_{ln} = 3.3985 - 3.8183 \times 10^{-5} (5509 \text{ ft}) = 3.1882$$

The barometric pressure of air (Bar) is calculated as shown:

$$\text{Bar} = \exp(\text{Bar}_{ln}) = 24.24 \text{ in. Hg}$$

The specific volume is found according to

$$\text{Sp. Vol.} = (459.67 + 83.549)^\circ\text{R}/\text{C}/24.24$$

where

$$C = \frac{2116.22 \text{ lbf/ft}^2}{(29.92 \text{ in. Hg})(53.34 \frac{\text{ft-lbf}}{\text{lbm-}^\circ\text{R}})}$$
$$= 1.325 \frac{\text{lbm-}^\circ\text{R}}{\text{ft}^3\text{-in. Hg}}$$

$$\text{Specific Volume} = 16.9104 \text{ ft}^3/\text{lbm}$$

$$\rho_{\text{air}} = 0.05913 \text{ lbm/ft}^3$$

Correct HÖTERV equations for example conditions by multiplying the coefficients in the pressure drop equations by the ratio of the densities:

$$\frac{\rho_{\text{air}(20^\circ\text{C})}}{\rho_{\text{example}}} = \frac{0.07522 \text{ lbm/ft}^3}{0.05913 \text{ lbm/ft}^3}$$

The corrected HÖTERV equations for this particular site location and air temperature are:

$$\Delta P = 3.6754 \times 10^{-6} (G_D)^{1.76}$$

$$\Delta P = 5.7917 \times 10^{-6} (G_W)^{1.76}$$

Calculate \dot{m}_{TOTAL} , Q_{FAN} , and velocity pressure. Assume all dry tower;
 $\Delta P_{h.x.} = 0.01382$ psi. Solve for G:

$$0.01382 \frac{\text{lb}_f}{\text{in.}^2} (144) \frac{\text{in.}^2}{\text{ft}^2} = 3.6754 \times 10^{-6} (G_D)^{1.76}$$

$$G_D = 1.810 \times 10^3 \text{ lbm/hr-ft}^2$$

$$\begin{aligned} \dot{m}_{TOTAL} &= 1.810 \times 10^3 \frac{\text{lbm}}{\text{hr-ft}^2} (54732.5 \text{ ft}^2) \\ &= 9.906 \times 10^7 \text{ lbm/hr} \end{aligned}$$

$$\begin{aligned} Q_{FAN} &= 9.906 \times 10^7 \frac{\text{lbm}}{\text{hr}} / (23 \text{ fans}) (0.059134 \frac{\text{lbm}}{\text{ft}^3}) (60 \frac{\text{min}}{\text{hr}}) \\ &= 1.214 \times 10^6 \text{ ft}^3/\text{min} \end{aligned}$$

$$\text{Velocity Pressure} = VP_{COEFF.} [(0.2 (\text{VEL}_{NR})^2 + 0.8 (\text{VEL}_R)^2]$$

$$\begin{aligned} \text{where } VP_{COEFF} &= \frac{\left(0.07495 \frac{\text{lbm}}{\text{ft}^3}\right) \left(29.92 \text{ in. Hg}\right) \left(13.5951 \frac{\text{in. H}_2\text{O}}{\text{in. Hg}}\right)}{2 \left(32.174 \frac{\text{lbm-ft}}{\text{lb}_f\text{-sec}^2}\right) \left(14.694 \frac{\text{lb}_f}{\text{in.}^2}\right) \left(144 \frac{\text{in.}^2}{\text{ft}^2}\right)} \\ &= 2.238 \times 10^{-4} \text{ in. H}_2\text{O} - \frac{\text{sec}^2}{\text{ft}^2} \end{aligned}$$

$$\text{VEL}_{NR} = Q_{FAN} / (60) \frac{\text{sec}}{\text{min}} (\text{flow area of fan})$$

$$\text{VEL}_R = Q_{FAN} / \left\{ (60) \frac{(\text{sec})}{\text{min}} \frac{\pi}{4} \left[(\text{FAN}_{DIAM} (1 + \text{ESF})) \right]^2 \right\}$$

where

$$\begin{aligned} \text{ESF} &= \text{exit stack factor} \\ &= 2(\tan 8^\circ) \frac{(\text{stack height})}{(\text{Fan diameter})} \frac{\text{ft}}{\text{ft}} \end{aligned}$$

$$\begin{aligned} \text{Velocity Pressure} &= 2.238 \times 10^{-4} \left[0.2 \left((1.214 \times 10^6 / (60)(584)) \right)^2 \right. \\ &\quad \left. + 0.8 \left((1.214 \times 10^6) (2.117 \times 10^{-5}) \right)^2 \right] = 0.171 \text{ in. H}_2\text{O} \end{aligned}$$

Calculate the total pressure:

$$\text{Total pressure} = \Delta P_{\text{h.x.}} + \Delta P_{\text{VEL. pressure}}$$

Correct $\Delta P_{\text{h.x.}}$ to air conditions:

$$(0.01382) (1.27) = 0.01755 \text{ psi}$$

$$\begin{aligned} \text{Total pressure} &= 0.01755 \text{ psi} + 0.0062 \\ &= 0.02375 \text{ psi} \end{aligned}$$

The total pressure (0.656 in. H₂O) corresponds to the total pressure read from the fan performance curve. If one side of the 8-sided towers is deluged, the calculation goes as follows:

$$A_{\text{DRY SECTION}} = 47891 \text{ ft}^2$$

$$A_{\text{WET SECTION}} = 6841 \text{ ft}^2$$

$$\Delta P_{\text{h.x.}} = 0.0142 \text{ psi}$$

$$0.0142 \text{ psi} (144) \frac{\text{in.}^2}{\text{ft}^2} = 3.6754 \times 10^{-6} (G_D)^{1.76}$$

$$G_D = 1.838 \times 10^3 \text{ lbm/hr-ft}^2$$

$$0.0142 \text{ psi (144)} \frac{\text{in.}^2}{\text{ft}^2} = 5.7917 \times 10^{-6} (G_W)^{1.76}$$

$$G_W = 1.419 \times 10^3 \text{ lbm/hr-ft}^2$$

$$\begin{aligned} \dot{m}_{\text{TOTAL}} &= 1.419 \times 10^3 (6841) + 1.838 \times 10^3 (47891) \\ &= 9.773 \times 10^7 \text{ lbm/hr} \end{aligned}$$

$$\begin{aligned} Q_{\text{FAN}} &= 9.773 \times 10^7 / (23)(60)(0.059134) \\ &= 1.197 \times 10^6 \text{ ft}^3/\text{min} \end{aligned}$$

$$\begin{aligned} \text{Velocity pressure} &= 2.238 \times 10^{-4} \left[0.2 \left(\frac{1.197 \times 10^6}{60(584)} \right)^2 \right. \\ &\quad \left. + 0.8 \left(\frac{1.197 \times 10^6}{60(584)} (2.117 \times 10^{-5}) \right)^2 \right] \\ &= 0.167 \text{ in. H}_2\text{O} \end{aligned}$$

$$\text{Total pressure} = \Delta P_{\text{h.x.}} + \Delta P_{\text{VEL. pressure}}$$

$$\text{Correct } \Delta P_{\text{h.x.}} \text{ to air conditions: } 0.0142(1.27) = 0.0180$$

$$\begin{aligned} \text{Total pressure} &= 0.0180 \text{ psi} + 0.0060 \text{ psi} \\ &= 0.0240 \text{ psi} \end{aligned}$$

The procedure for determining the pressure losses for the rest of the deluging amounts are done in the same manner. The results of these calculations are shown in Table E.1.

The air velocity through the deluged and dry sections can be determined as follows:

$$\text{VEL} = \frac{G(\text{lbm/hr-ft}^2)}{\rho_{\text{air}} \frac{\text{lbm}}{\text{ft}^3} (3600) \frac{\text{sec}}{\text{hr}}}$$

TABLE E.1. Air Characteristics for a Deluged Cooling Tower

	G_D lbm/hr-ft ²	G_W lbm/hr-ft ²	Q_{FAN} ft ³ /min	Velocity Pressure psi	$\Delta P_{h.x.}$ psi	Total Pressure psi
All-Dry Sections	1.810×10^3	0	1.214×10^6	0.0062	0.01755	0.02375
7 Sides Dry 1 Side Deluged	1.838×10^3	1.419×10^3	1.197×10^6	0.0060	0.0180	0.0240
6 Sides Dry 2 Sides Deluged	1.860×10^3	1.436×10^3	1.176×10^6	0.0058	0.0184	0.0242
5 Sides Dry 3 Sides Deluged	1.896×10^3	1.464×10^3	1.163×10^6	0.0056	0.0190	0.0246
4 Sides Dry 4 Sides Deluged	1.924×10^3	1.486×10^3	1.142×10^6	0.0054	0.0195	0.0249
3 Sides Dry 5 Sides Deluged	1.936×10^3	1.498×10^3	1.115×10^6	0.0052	0.0198	0.0251
2 Sides Dry 6 Sides Deluged	1.964×10^3	1.520×10^3	1.094×10^6	0.0050	0.0203	0.0253
1 Side Dry 7 Sides Deluged	1.999×10^3	1.547×10^3	1.076×10^6	0.0048	0.0209	0.0257
8 Sides Deluged	0	1.563×10^3	1.049×10^6	0.0046	0.0213	0.0259

$$\text{Example: } \text{VEL}_D = 1.83 \times 10^3 / (0.059134)(3600)$$

$$= 8.64 \text{ ft/sec}$$

$$\text{VEL}_W = 1.419 \times 10^3 / (0.059134)(3600)$$

$$= 6.66 \text{ ft/sec}$$

$$\text{VEL}_{WET} / \text{VEL}_{DRY} = 6.66 / 8.64 = 0.77$$

This ratio holds to within 1% for the wet/dry velocities for each amount of deluging (1-8 sides deluged). Table 2 presents the air velocities for each section.

TABLE E.2. Comparison of Air Velocities Through Wet and Dry Surfaces

	<u>VEL_{DRY} SECTION</u> ft/sec	<u>VEL_{WET} SECTION</u> ft/sec
0 Sides Deluged	8.50	0
1 Side Deluged	8.64	6.66
2 Sides Deluged	8.73	6.74
3 Sides Deluged	8.91	6.87
4 Sides Deluged	9.04	6.98
5 Sides Deluged	9.10	7.03
6 Sides Deluged	9.22	7.14
7 Sides Deluged	9.39	7.26
8 Sides Deluged	0	7.34

REFERENCES

- E.1. Hudson Fan Performance Catalogue. Hudson Products Corporation, Houston, Texas, 1974.

APPENDIX F

HEAT TRANSFER AND PRESSURE DROP
CORRELATIONS

APPENDIX F
HEAT TRANSFER AND PRESSURE
DROP CORRELATIONS

HEAT TRANSFER COEFFICIENT AND FRICTION FACTOR
CORRELATIONS FOR THE AMMONIA COOLING LOOP

CONDENSER/REBOILER

The condenser/reboiler is similar in design to that of a conventional water shell and tube condenser. The differences are:

- ammonia instead of water passes through the tubes, and
- header wall thickness is increased to provide sufficient strength to withstand the pressure of the ammonia.

Condenser designs were considered with the smooth tubing used in commercial condensers built and used today and with enhanced tubing. The enhanced tubes have better heat transfer coefficients obtained by use of sintered metal on the inside surface and by use of a proprietary outside surface developed by LINDE Division of Union Carbide.

The nomenclature for correlations given in this section is found on page F.11.

Heat Transfer Correlations

Smooth Tubing

The design of the condenser/reboiler with smooth tubing is accomplished by determining the number and length of tubes in the condenser. This is done by finding the average overall coefficient for a specific temperature difference, heat load, and tube length. To find the overall coefficient the average inside and outside heat transfer coefficients of the horizontal tubes must be determined. The outside coefficient must take into account steam velocity, condensate film thickness, and condensate film buildup and removal due to

splashing down from one tube to the next in a bank of tubes. The following correlation, used to handle these effects, was derived by Nusselt⁽¹⁾ and modified by Kern.

$$h_s = 0.728 \left(\frac{g \rho_L (\rho_L - \rho_v) k_L^3 h_{fg}}{D_o \mu_L \Delta T_s} \right)^{1/4} \left(\frac{1}{N} \right)^{1/6} \quad (F.1)$$

The original equation by Nusselt was derived with the number of tubes in depth (N) in the tube bank taken to the 1/4 power. Kern later modified the equation by changing it to the 1/6 power so that conditions in the condenser could be better predicted.

The steam-side coefficient obtained from Equation F.1 by the optimization code typically ranges from 1000 to 1500 Btu/hr-°F-ft² for the smooth tubing.

The inside heat transfer coefficient of the smooth tubing is composed of the sum of nucleate boiling and forced convection heat transfer:

$$h_i = h_{fc} + h_B \quad (F.2)$$

The forced convection coefficient in Equation F.2 is found by the correlation developed by Dittus-Boelter:⁽²⁾

$$h_{fc} = 0.023 Re_L^{0.8} Pr_L^{0.4} k_L / D_i \quad (F.3)$$

The range of values obtained from this correlation by the optimization code is from 200 to 500 Btu/hr-°F-ft² with liquid inlet velocities into the tubes varying from 0.5 ft/sec to 1.5 ft/sec. The boiling coefficient is obtained from the correlation developed by Rohsenow:⁽³⁾

$$h_B = \left(Cp_L / h_{fg} (0.015) Pr_L^{1.7} \right)^3 \frac{\mu_L h_{fg} \Delta T_a^2}{\sqrt{\frac{\sigma}{\rho_L - \rho_v}}} \quad (F.4)$$

The boiling coefficient ranges from 800 to 1200 Btu/hr-°F-ft² in the optimization code.

Enhanced Tubing

Design of the condenser/reboiler with enhanced tubing is done by the same method as for smooth tubing. Different heat transfer correlations are used to obtain the inside and outside coefficients of the horizontal tubes. The correlations used for the enhanced surfaces are derived from experimental data obtained from Union Carbide Corporation, LINDE Division. The correlations are derived from two data points of heat flux versus temperature difference.

The steam-side correlation is derived from experimental data⁽⁴⁾ for steam condensing at one atmosphere on the outside of a single horizontal tube. The correlation is used for pressures below one atmosphere with the assumption that the effect of pressure does not have a large influence on the condensation coefficient. The influence of condensate film buildup due to the film of one tube falling on another tube in a tube bank is taken care of by adding to the experimental correlation the relationship for the tube bank depth (N) from Equation F.1. The following correlation is used to describe the condensation process.

$$h_s = 16700 \Delta T_s^{-0.572} \left(\frac{1}{N}\right)^{1/6} \quad (\text{F.5})$$

The steam-side coefficients obtained by the code from Equation F.5 range in values from 3000 to 6000 Btu/hr-°F-ft².

The heat transfer correlation for the ammonia-side of the enhanced tubing includes, as before, the effect of two processes; nucleate boiling and forced convection heat transfer. It is assumed that the forced convection correlation does not change from Equation F.4. The boiling correlation does change with the change in the tubing. The boiling correlation used was developed from experimental data⁽⁴⁾ for a piece of the enhanced surface heated in a pool of ammonia so that boiling occurred at different temperatures of the surface. The correlation takes the form:

$$h_B = 18000 \Delta T_a^{1.72} \quad (\text{F.6})$$

The boiling coefficients obtained from Equation F.6 by the optimization code range in values from 14,000 to 20,000 Btu/hr-°F-ft².

Pressure Drop Correlations

Smooth Tubing

The correlation used to determine the pressure drop in the smooth tubes of the condenser/reboiler was developed by Lockhart and Martinelli⁽⁵⁾ for two-phase flow:

$$\Delta P = \phi_L^2 f_L \frac{L}{D_i} \frac{G_L^2}{L} \quad (F.7)$$

The Martinelli function (ϕ_L) is provided by a curve fit of the Lockhart-Martinelli parameter (X):

$$X = f_L G_L^2 \rho_V / f_V G_V^2 \rho_L \quad (F.8)$$

The Fanning friction factor (f) is provided by four separate correlations covering three different regimes of flow. The regimes are differentiated by four ranges of Reynolds numbers.

- Laminar Regime ($0 < Re \leq 1600$) (F.9)

$$f = 16/Re$$

- Transition Regime ($1600 < Re \leq 3950$) (F.10)

$$f = 0.01$$

- Turbulent Regime ($3950 < Re \leq 52,000$) (F.11)

$$f = 0.0791/Re^{0.25}$$

- Turbulent Regime ($52,000 \leq Re$) (F.12)

$$f = 0.046/Re^{0.20}$$

The flow regime usually found by the code is the turbulent flow regime. The pressure drops are within one-half to two pounds per square inch.

Enhanced Tubing

The method used to determine the pressure drop through the enhanced tubes of the condenser/reboiler is the same as for the smooth tubes.

COOLING TOWER

Cooling Tower Arrangements

The arrangement of the towers for the HÖTERV surface is specified by the fact that the plates of the surface must be vertical or close to vertical so that deluge water may flow down the fins. This precludes vertical tubes in either circular or rectangular towers. Horizontal or near horizontal tubes can be placed in polygonal or rectangular towers. Polygonal towers were chosen as tower arrangements because of lower possible piping costs.

Condensation

The three cocurrent flow conditions possible in a condensation process are shown in Figures F.1 through F.3. The stratified flow condition in Figure F.1 results when low vapor velocities occur in the tubes which are either sloped or horizontal. Figure F.2 shows annular flow which occurs when high vapor velocities are prevalent in horizontal tubes and low and high vapor velocities in vertical tubes. Figure F.3 shows annular flow with mist in the vapor core which occurs at very high vapor velocities in both horizontal and vertical tubes. The last situation does not occur in an air-cooled condensation process because of the high heat transfer rate needed to obtain high vapor velocities.

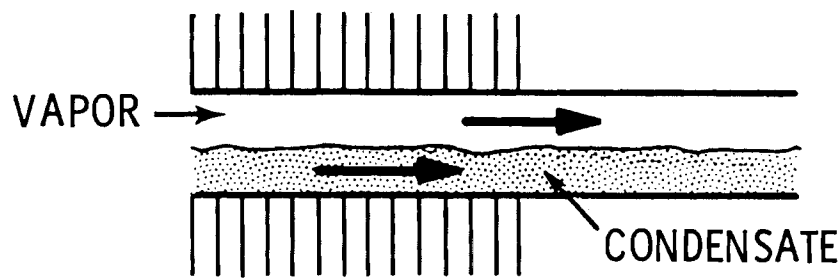


FIGURE F.1. Stratified Flow

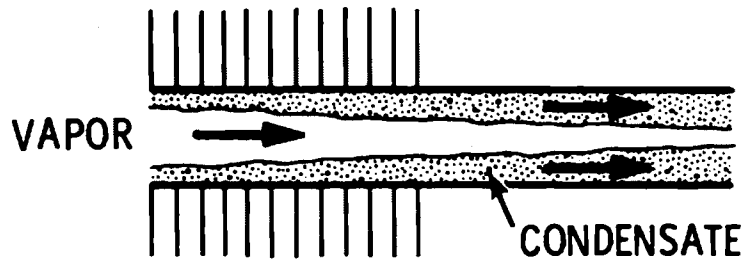


FIGURE F.2. Annular Flow

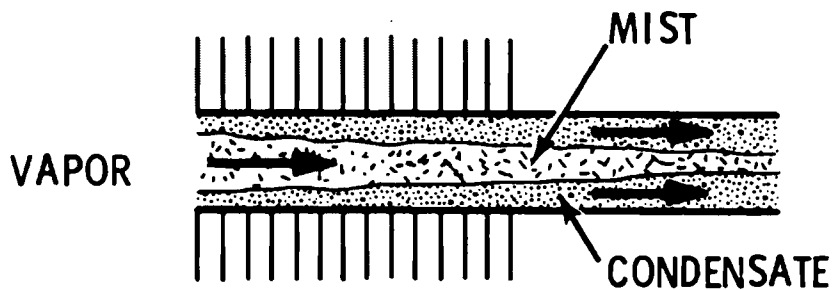


FIGURE F.3. Annular Flow with Mist

Heat Transfer and Pressure Drop Correlations - Tower Heat Exchanger

Air-Side

The air-side heat transfer and pressure drop correlations are the same as those described in Appendix A.

Ammonia-Side

Because the condensation of ammonia takes place in almost horizontal tubes of the heat exchanger, three flow regimes must be modeled to find the correct heat transfer coefficient. All the regimes depend on the thickness of the average condensate layer and the velocity of the vapor entering the tube. This depends on whether gravity or vapor shear is the predominating force.

When the average condensate thickness is small and the velocity of the vapor is low (gravity force predominates over the vapor shear force) the resulting laminar film condensation can be predicted with the classical analysis of Nusselt or the stratified flow analysis by Chato⁽⁶⁾ as embodied in the following equations.

$$h_i = 1.47 K_L \left(g \sin \theta \rho_L (\rho_L - \rho_V) / \mu_L^2 \right)^{1/3} / (\text{Re}_L (1 - X_0))^{1/3} \quad (\text{F.13})$$

$$h_i = 0.458 K_L \left(g \cos \theta \rho_L (\rho_L - \rho_V) 4L / \mu_L D_i^2 G \right)^{1/3} \quad (\text{F.14})$$

If the condensate thickness is large or the velocity of the vapor is of medium velocity (gravity force still predominates over the vapor shear force) the resulting turbulent film condensation can be predicted by the correlation developed by Kirkbride:^(7,8)

$$h_i = 0.0077 K_L \left(g \sin \theta \rho_L (\rho_L - \rho_V) / \mu_L^2 \right)^{1/3} (\text{Re}_L (1 - X_0))^{0.4} \quad (\text{F.15})$$

When the annular ring of condensate is mainly controlled by the vapor shear force (predominating over the gravity force), the correlation by Boyko and Kruzhilin⁽⁹⁾ was used for the turbulent liquid film heat transfer coefficient:

$$h_i = 0.024 K_L \text{Re}_L^{0.8} \text{Pr}_L^{0.43} / D_i \frac{\sqrt{1 + (\rho_L / \rho_V - 1) X_i} + \sqrt{1 + (\rho_L / \rho_V - 1) X_0}}{2} \quad (\text{F.16})$$

The range of values found by the optimization code for the inside coefficient is from 1000 to 1600 Btu/hr-°F-ft². The Reynolds number based on the liquid varies from 5000 to 15,000 with the entering vapor velocity ranging from 10 to 20 feet per second. The correlation most often used by the code to define the inside coefficient is Equation F.16.

Pressure Drop Correlation - Tower Heat Exchanger

The two-phase pressure drop in the tubes of the heat exchanger is found by the same set of equations as for the pressure drop in the condenser/reboiler.

The only difference is that the Martinelli function (ϕ_L) is provided by a functional relationship of the Lockhart-Martinelli parameter (X) and not as a curve fit of the parameter.

PIPING

Pressure Drop Correlations

The pressure drop correlations in the optimization code are used to calculate the pressure drops for the supply and return piping. The supply piping transports vapor while the return line transports liquid.

The pressure drop in the vapor line is found on an incremental basis where each length of pipe of a particular diameter is divided into ten sections. The pressure drop across each section is calculated; then new vapor properties are found to be used to find the pressure drop in the next section.

The pressure drop in the liquid line is calculated for the whole length of pipe of one specific diameter.

Supply Piping

The pressure drop in the supply piping of the cooling loop is calculated by using the Fanning equation:

$$\Delta P = 4f_v \frac{L}{D_i} \frac{G_v^2}{2\rho_v} \quad (\text{F.17})$$

The pressure drops found by the optimization code vary from approximately 10 to 20 pounds per square inch.

Return Piping

The pressure drop in the return piping is also calculated by using the Fanning equation:

$$\Delta P = 4f_L \frac{L}{D_i} \frac{G_L^2}{2\rho_L} \quad (\text{F.18})$$

The pressure drops for the return piping vary from 2 to 6 pounds per square inch.

Temperature Drop Correlation

Shown in Figure F.4 is a pressure-enthalpy diagram of the vapor dome for ammonia and a typical cycle ammonia passes through when it goes around the cooling loop. The diagram shows five important points of the cycle. Point A to Point B shows what happens to the ammonia in the condenser/reboiler. Point C to Point D shows the condensation of ammonia in the tower.

Point B to Point C is what occurs in the piping from the condenser/reboiler to the dry/wet tower. The process is controlled by the pressure drop in the pipeline. Since the transfer of heat through the pipe walls is negligible and no pumping is done on the vapor the process through the pipe is

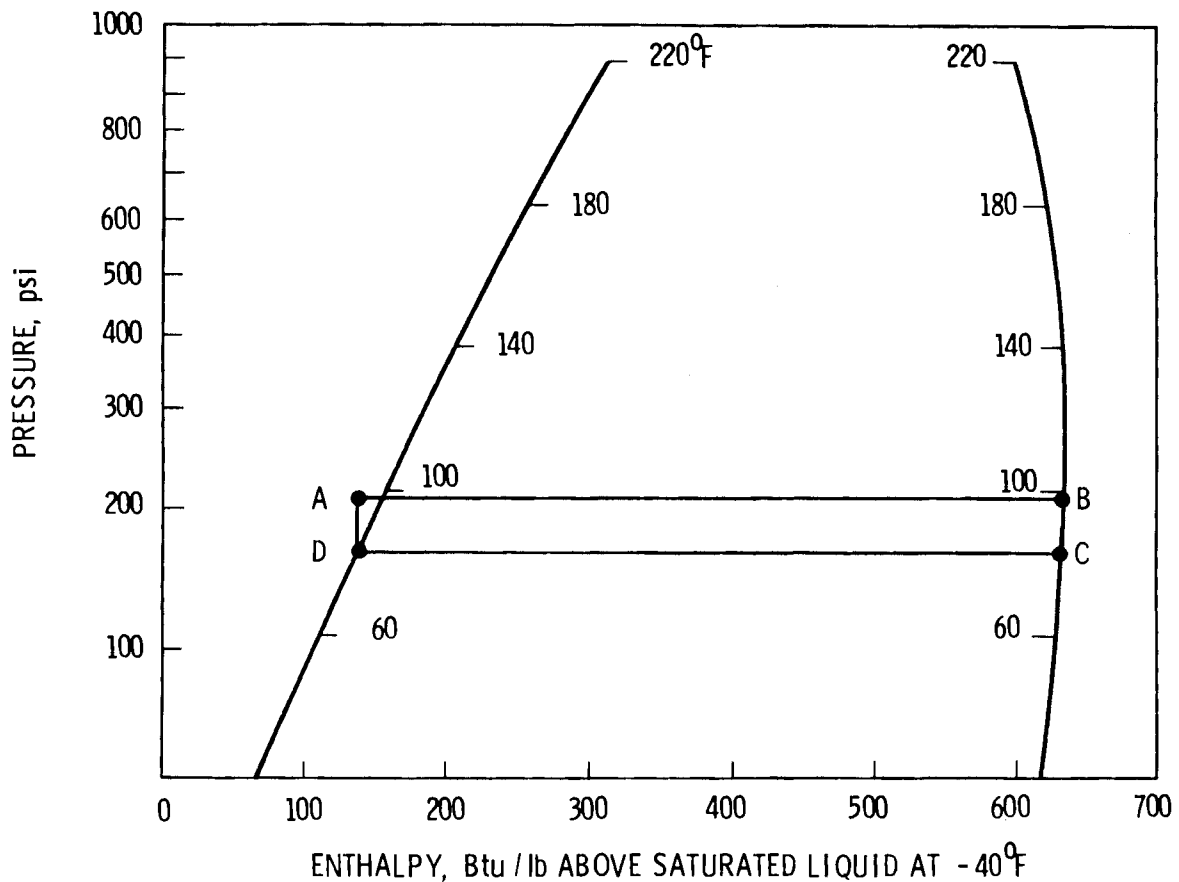


FIGURE F.4. Pressure-Enthalpy Diagram of Ammonia Vapor Dome

isenthalpic. With the flow being isenthalpic and having a pressure drop the ammonia encounters a temperature drop from the beginning to the end of the supply piping.

The pressure and temperature drops are calculated along the main piping and the quadrant supply runs by dividing the pipes into ten sections and calculating the pressure drop for each section. The temperature drop is calculated for each section of pipe by using the new pressure at the end of each section and a curve fit of the saturation line of pressure versus temperature.

$$P = a + bT + cT^2 \quad (F.19)$$

The optimization code typically calculates a temperature drop of the vapor from 3 to 5°F.

NOMENCLATURE

- g - acceleration of gravity (ft/hr^2)
- ρ_L - density of liquid (lbm/ft^3)
- ρ_V - density of vapor (lbm/ft^3)
- K_L - thermal conductivity of liquid ($\text{Btu/hr-}^\circ\text{F-ft}$)
- h_{fg} - heat of vaporization (Btu/lbm)
- D_o - outside diameter of tube (in.)
- D_i - inside diameter of tube (in.)
- μ_L - viscosity of liquid (lbm/ft-hr)
- N - number of tubes in depth
- ΔT_s - temperature difference between saturated steam and tube surface ($^\circ\text{F}$)
- h_i - inside heat transfer coefficient of tube ($\text{Btu/hr-}^\circ\text{F-ft}$)
- h_{fc} - inside heat transfer coefficient of tube due to forced convection ($\text{Btu/hr-}^\circ\text{F-ft}^2$)
- h_B - inside heat transfer coefficient of tube due to boiling ($\text{Btu/hr-}^\circ\text{F-ft}^2$)
- Re_L - liquid Reynolds number
- Pr_L - liquid Prandtl number
- Cp_L - liquid specific heat ($\text{Btu/lbm-}^\circ\text{F}$)
- ΔT_a - temperature difference between saturated ammonia and inside tube surface ($^\circ\text{F}$)
- σ - surface tension of liquid (lb/ft)
- ΔP - pressure drop (lb/ft^2)
- ϕ_L - Martinelli function
- X - Lockhart-Martinelli parameter

f_L - liquid friction factor

f_V - vapor friction factor

L - length of pipe (ft)

G - mass flux through tube ($\text{lbm}/\text{ft}^2\text{-hr}$)

G_L - mass flux of liquid ($\text{lbm}/\text{ft}^2\text{-hr}$)

G_V - mass flux of vapor ($\text{lbm}/\text{ft}^2\text{-hr}$)

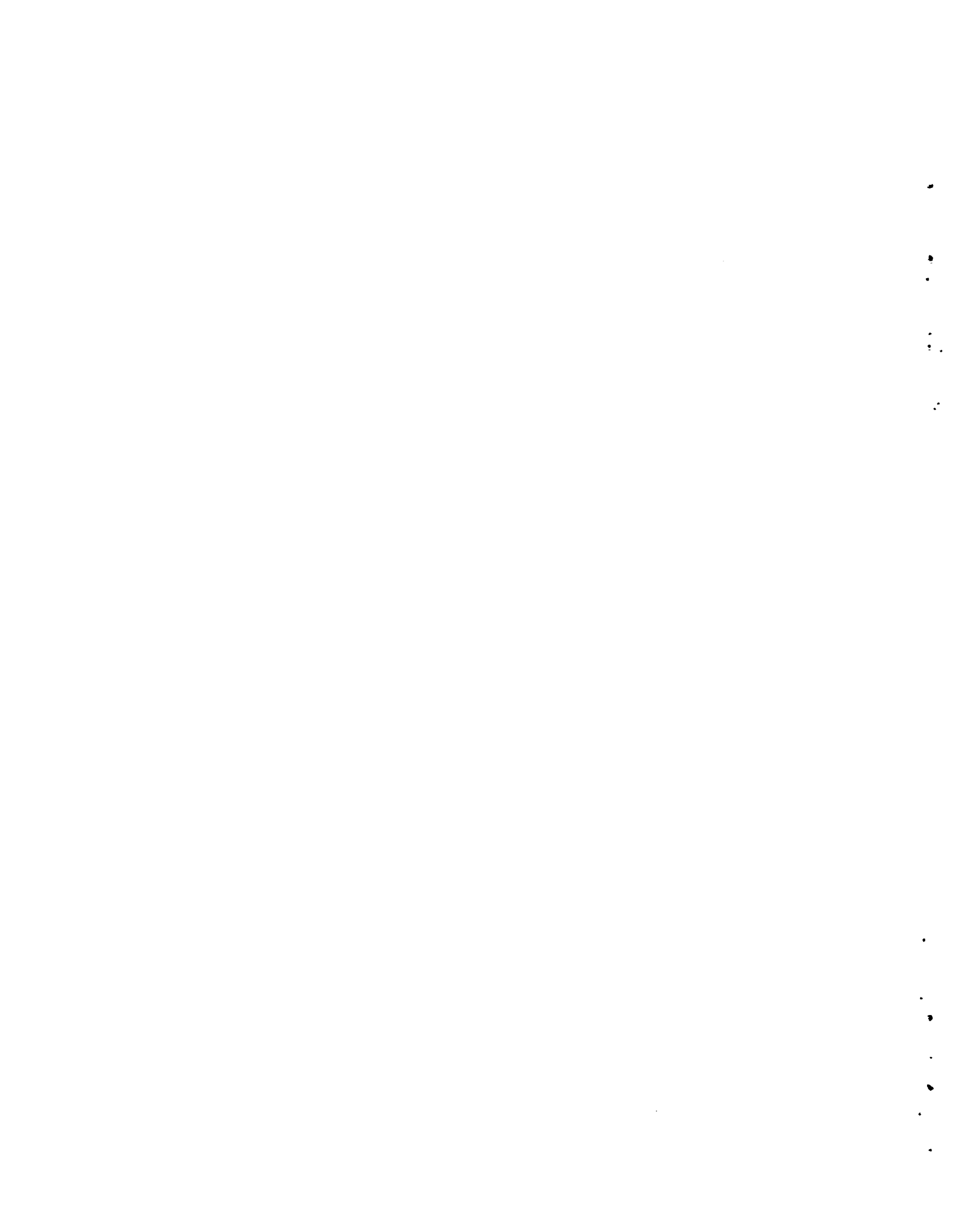
θ - angle of tubes from the horizontal

X_0 - quality of fluid leaving tubes

X_i - quality of fluid entering tubes

APPENDIX F REFERENCES

1. W. Z. Nusselt, Ver. Dent. Ing. 60:541, 569, 1916.
2. F. W. Dittus and L. M. K. Boelter, Univ. Calif., Pubs. Eng. 2:443, 1930.
3. W. M. Rohsenow, "Heat Transfer with Boiling." Modern Developments in Heat Transfer. 85-158, 1963.
4. Heat Rejection by Dry Cooling in Steam Electric Power Stations. LINDE Division, Union Carbide, New York, NY, April 1976.
5. R. W. Lockhart and R. C. Martinelli, "Proposed Correlations for Isothermal Two-Phase, Two-Component Flow in Pipes." Chem. Eng. Prog. 45:39, 1949.
6. J. C. Chato, "Laminar Condensation," ASHRAE Journal 4:52-60, 1962.
7. C. G. Kirkbride, Trans. Am Inst. Chem. Engrs. 30:170-186, 1933-1934.
8. C. G. Kirkbride, Ind. Eng. Chem. 26:425-428, 1934.
9. L. D. Boyko and G. N. Kruzhilin, Int. Jour. Heat and Mass Transfer. 10:361-373, 1967.



APPENDIX G

COST ALGORITHMS FOR THE HÖTERV PLATE
FIN HEAT EXCHANGER BUNDLE

APPENDIX G
COST ALGORITHMS FOR THE HÖTERV PLATE
FIN HEAT EXCHANGER BUNDLE

The cost algorithms contained in this appendix were developed and used in the BNW-II dry/wet code for costing the HÖTERV heat exchanger bundle. The algorithms were developed on the same basis as those reported in Reference 1. The reader is referred to Chapter 3 of this reference for a detailed description of the algorithms given below. The cost algorithms for the HÖTERV bundle were developed for ammonia condensation in steel or aluminum tubes and galvanized steel or aluminum header and section joints. Because the HÖTERV bundle consists of sections combined together to make the full-length bundle, a method was devised to combine these sections without costly welding.

At each interface point between the sections of surface, a section joint is made up at which the tube ends are rolled into the joint. The joints are then bolted together to form a tight seal using a gasket. The bundle and section joint are shown in Figure G.1. As shown, the section joints allow for draining the condensate off at several points along the bundle length.

The HÖTERV bundle normally comprises three to 5 sections, each ~16 feet long. The bolted joints between sections act as intermediate headers for removing condensate NH_3 . The overall bundle supported at each section joint and header.

The various components of the HÖTERV bundle are costed separately. These separate costs are then summed to obtain the final cost of the bundle. The costs of the following components are determined:

1. Heat transfer elements--tubing, fins, bundle stiffeners, and section joints
2. Bundle header
3. Bundle frame

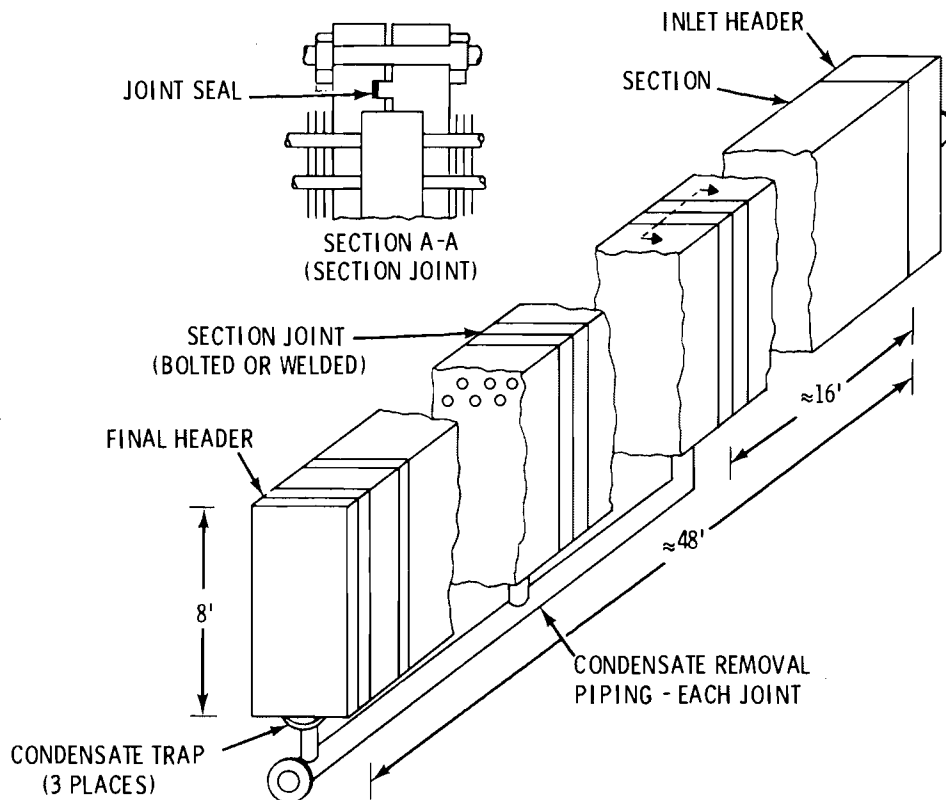


FIGURE G.1. NH₃ - HÖTERV Bundle

4. Delugeate drain plate
5. Bundle assembly.

Because the BNW-II dry/wet code optimizes a heat rejection system using the HÖTERV surface, some parameters used in the following cost algorithms are variables. These variables are not set to a numerical value in the following description. The parameters which are given the numerical values are set internal to the code or read in as basic input data.

HEAT TRANSFER ELEMENTS

1. Tubing Cost

$$C_{\ell} = (C_{\ell m} W_{\ell} + C'_{\ell}) \text{ FM} = \$/\text{ft}$$

Weight of tubing

$$W_{\ell} = 12\pi\rho_{\ell} (D_{\ell} - t_w) t_w$$

t_w = tube wall thickness (in.)

D_{ℓ} = OD of tubing

ρ_{ℓ} = density of tubing material (#/in.³)

For cost factors $C_{\ell m}$ and C'_{ℓ} see Reference 1, Table 3-2.

2. Finning Cost (C_F)

Aluminum plate fins with integral plate spacers

Weight of Fin

$$W_{PF} = 12 [A_p t_s P_F + \pi(D_{\ell} + T_r) T_r] \rho_F = \$/ft$$

A_p = plate fin area/tube = $P_t \cdot P_r$

P_t = tube pitch

P_r = tube row spacing

t_s = fin stock thickness

T_r = fin spacer thickness = 0 (integral spacer)

ρ_F = fin material density = 0.0975 (#/in.³)

P_F = fin pitch

$$\text{Finning Cost } (C_F) = C_{FM} W_{PF} + C'_F = \$/ft$$

Cost Factors

$C_{PM} = \$1.00/\#$ (integral spacers)

$C'_p = \$0.20$ (Reference 1, Table 3-4)

3. Bundle Stiffeners (Aluminum Plate)

$$C_{\hat{s}p} = C_p \left(P_t \frac{H_d}{R} - A_t \right) t_{sp} \rho_s + C_{sh} = \$/\text{tube/spacer}$$

C_p = cost factor = \$0.95/#

P_t = tube pitch

H_d = header depth (Reference 1, Figure 3-14)

R = no. tube rows

A_t = tube cross section (material)

t_{sp} = plate thickness = 0.125 in.

ρ_s = material density = 0.0975 #/in.³

C_{sh} = hole cost ~ \$0.05/hole

Total stiffener cost (C_s) = $C_{sp} \left(\frac{L_B}{S_s}\right) N_B N_S = \$/\text{bundle}$

L_B = bundle length

S_s = spacer separation

N_B = number of tubes/bundle

N_S = number of sections/bundle

4. Section Joint

Joint comprised of tube sheet plates - (2 plates each joint)

C_{SJ} (joint cost) = plate costs + tube hole costs + bolted
or welded joint costs

$$C_{SJ} = \left\{ 2 \left[C_p \left(P_t \frac{H_d}{R} - A_t \right) t_{sp} \rho_s + C'_{sh} \right] N_B + C_F \left(\frac{H_d}{12} + W_b \right) \right\} N_{SJ} = \$/\text{joint}$$

C_p = cost of Al joint - \$1.20/#

= cost for galvanized steel joint = \$0.65

P_t = tube pitch

H_d = header depth

R = tube rows

t_{sp} = plate thickness = 1-1/2 in. for Al

= 1 in. for steel

ρ_s = plate material density = 0.204 for steel

= 0.0978 for aluminum

C'_{sh} = tube hold cost = \$0.50

C_F = bolted joint cost = \$8.00/ft

N_B = number of tubes in bundle

N_{SJ} = number of section joints in bundle

BUNDLE HEADER COSTS (C_H)

Use header algorithms (Reference 1, p. 24-26) with:

$t_w = 1$ in. for steel header thickness

$t_w = 1\text{-}1/2$ in. for aluminum header thickness

$A = 4 N_p$ for the bolted header

$B = 1$ for the hole factor

$C_f =$ bolted header joint cost = \$8/ft (high pressure system)

BUNDLE FRAME

Use algorithms for vertical bundle in Reference 1, p. 28:

$$C_{VF} = C_{st} L_B (77 + 2 W_B) = \$/\text{bundle}$$

*Use 77 #/ft to cover side channels and cross bracing
(assume structure support at each section end ~16 feet
apart)

$C_{st} =$ material cost = \$0.53/# for galvanized steel

$L_B =$ bundle length

$W_B =$ bundle width

ALUMINUM DRAIN PLATE COSTS

The position of the aluminum drain plate is shown in Figure G.2.

$$C_{DP} = C_p \rho W_p t_p (12 L_B) \$/\text{bundle}$$

$C_p =$ \$0.95/# for Al plate

$\rho = 0.0975$ #/in.³

$W_p =$ plate width

$L_B =$ length of bundle

$t_p =$ plate thickness = 1/4 in.

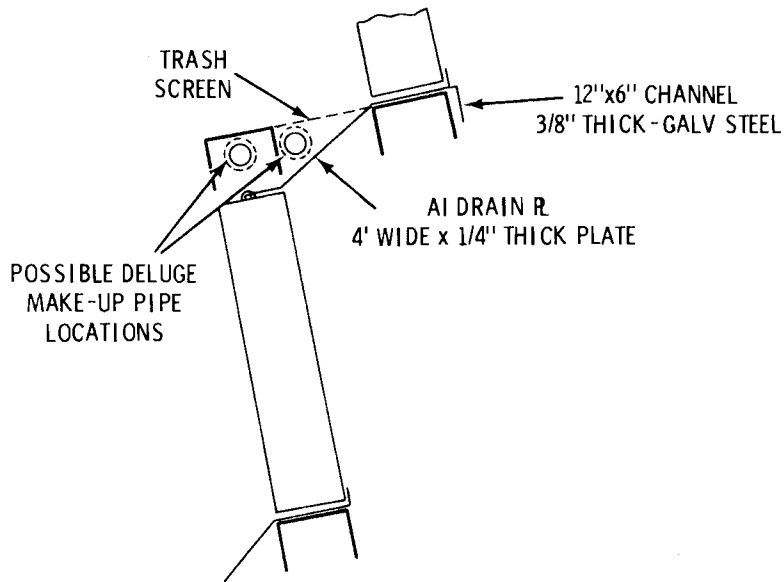


FIGURE G.2. Deluge Transfer and Make-up System

BUNDLE ASSEMBLY

Section junction and header assembly

$$C_A = (C_{rj} + C_{wj}) N_B N_{SE}$$

C_{AS} = cost/bundle (\$)

C_{rj} = rolled joint cost ~ \$1.00/section (two tube ends)

C_{wj} = tube to tube sheet weld ~ \$1.50/section (two tube ends)

N_B = number tubes/bundle

N_{SE} = number of sections

TOTAL BUNDLE COSTS

(FOB Manufacturer's Plant)

$$C_{TB} = [C_S + C_H + C_{SJ} + C_{VF} + C_{DP} + C_A]$$

C_S = bundle tube, surface and spacer costs

$$= C_\lambda + C_F + C_S$$

C_H = header cost

C_{SJ} = section joint cost
 C_{VF} = bundle frame costs
 C_{DP} = bundle drain plate costs
 C_A = bundle assembly costs

REFERENCE

1. P. A. Ard, Costs and Cost Algorithms for Dry Cooling Tower Systems. BNWL-2123, Battelle, Pacific Northwest Laboratories, Richland, WA 99352, September 1976.

APPENDIX H

OPTIMIZATION TECHNIQUE

APPENDIX H OPTIMIZATION TECHNIQUE

As mentioned in Section 3.0, an optimization technique developed by Andeen and Glicksman⁽¹⁾ was used to determine the values of the five internally independent variables which give minimum incremental cost. Only minor changes were made to the subroutines incorporating the MIT optimization technique; these changes, described in Section 5.1, are related to system constraints, not to the optimization procedure. The basic optimization technique was not changed. However, major changes were made in the computational logic, cost algorithms, etc.

Approval was obtained from Dr. Glicksman to publish that portion of Reference 1 dealing with the optimization routine used in the BNW-II code. The prose and flow charts of the subroutines are reproduced in this appendix.

Subroutine SERCH was modified for BNW-II. As indicated in the attached write up all five variables are single optimized using a hill climbing technique. However, the process is repeated four times. If the result of the fifth optimization is within 1% of the fourth, then the optimization is complete. Otherwise, successive optimizations are developed until the improvement in cost is less than 1%.

VERBATIM DESCRIPTION OF MIT OPTIMIZATION TECHNIQUE

With a given heat exchanger surface, a given design temperature, cost data, and power generation, the heat transfer and cost equations may be reduced to five variables which can be varied independently and which must be optimized:

T_1	steam cycle output temperature ($^{\circ}$ F) at the low pressure turbine
RANGE	change in temperature ($^{\circ}$ F) of the water while passing through the cooler

CWARA	ratio of the heat capacity of water to that of air, where heat capacity of a fluid is the product of its specific heat and its mass flow rate
AFRON	the air side frontal area (ft^2) of the heat exchanger
WLRAT	ratio of width to length of AFRON, length being the tube length

Thus the cost of adding the dry cooling tower to the power plant is a function of these five variables. The problem, or the optimization process, is to minimize this cost for given values of $TD^{(a)}$ and, by comparison, to choose the TD with the least cost.

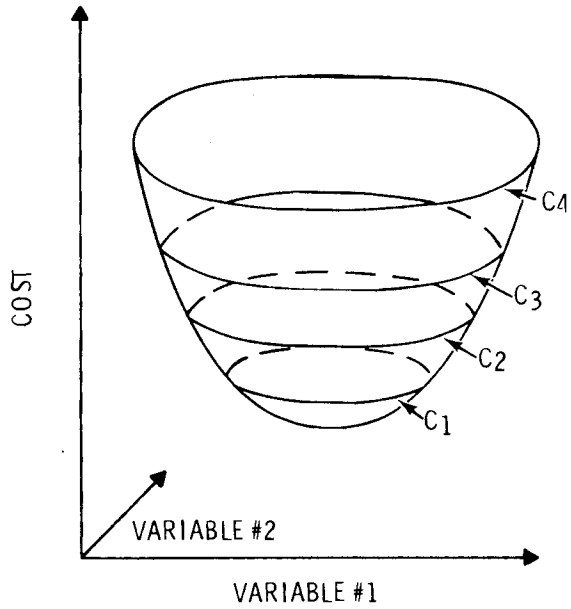
In order to explain the minimizing procedure used, let us consider a simplified case. Assume cost is a function of only two independent variables. Hence, cost may be pictured as a surface in three-dimensional space. Figure IV-1A shows this surface in a three-dimensional sketch. Figure IV-1B shows the same figure, with lines of constant cost projected on the plane defined by variables 1 and 2, the horizontal plane of Figure IV-1A.

For any given starting point, the minimum may be approached by: (1) holding variable 1 fixed (e.g. staying in plane A of Figure IV-2A and finding the minimum costs, point 2 on plane A); (2) holding variable 2 fixed, staying in plane B, and finding a second minimum, point 3, plane B; and (3) continuing the process indefinitely, thus "spiraling in" on the absolute minimum. Figure IV-2B illustrates this same process in a two-dimensional projection of Figure IV-2A.

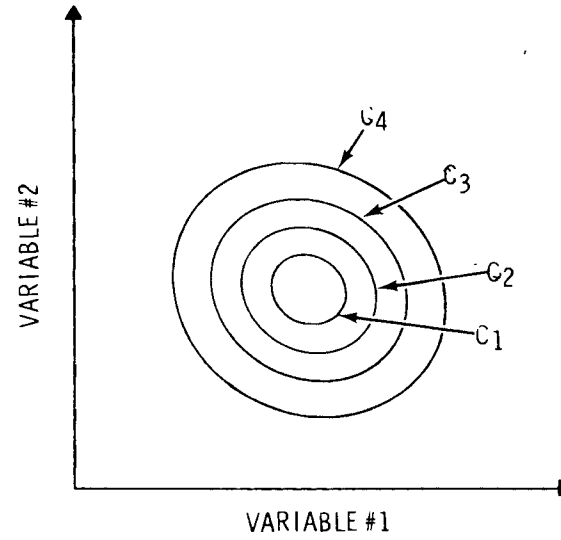
However, if the surface is not as well-behaved as that drawn in Figure IV-2, but has multiple minimal points as in Figure IV-3 the search procedure may end by "minimizing" in a relative minimum trough. To avoid such relative minima, two approaches have been taken: (1) the cost is evaluated at multiple points and the lowest cost point is used as the starting point for the minimizing procedure. This is a sort of "shotgun"

(a) PNL NOTE: TD is design temperature

C's - LINES OF CONSTANT COST - $C_1 < C_2 < C_3 < C_4$

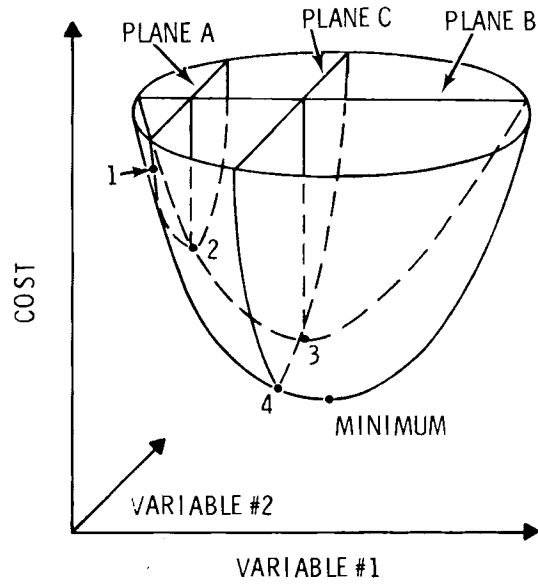


Three-Dimensional
Visualization
Figure IV-1A

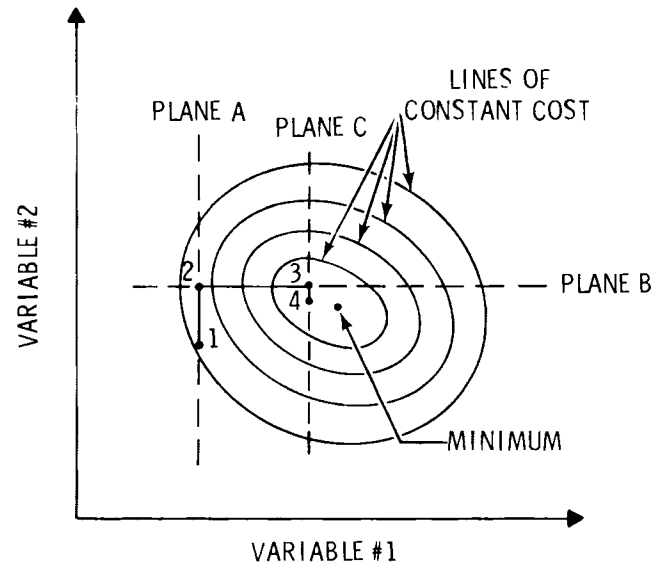


Two-Dimensional
Visualization with
Constant Cost Loci
Figure IV-1B

FIGURE IV-1. Cost as a Function of Two Variables

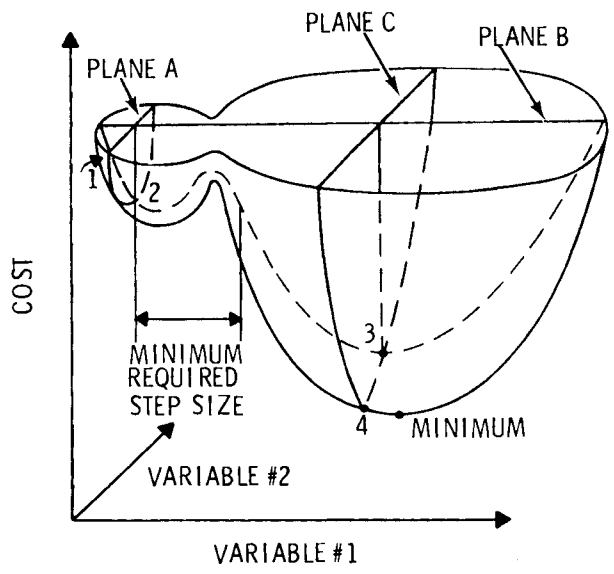


Three-Dimensional
Visualization
Figure IV-2A

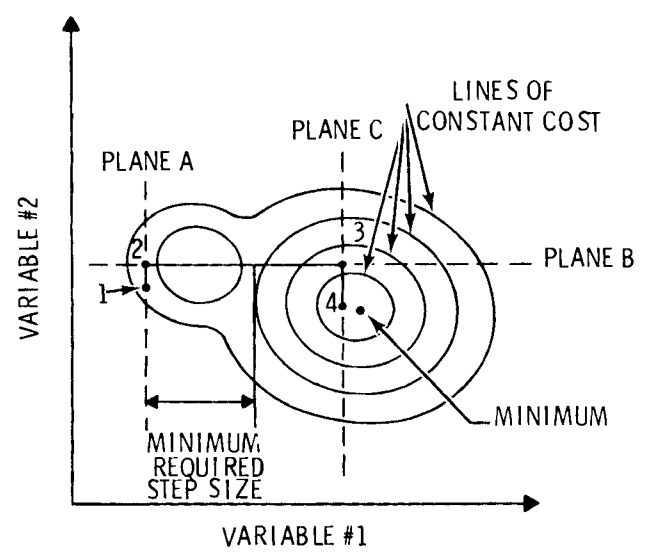


Two-Dimensional
Visualization
Figure IV-2B

FIGURE IV-2. Minimization Technique on Simple Surface



Three-Dimensional
Visualization
Figure IV-3A



Two-Dimensional
Visualization
Figure IV-3B

FIGURE IV-3. Minimization Technique on Simple Surface

H.5

approach, sampling many points chosen to represent a cross-section of reasonable values. A minimum of 687 initial points are checked. (2) the cost is evaluated at discrete, incremental step changes in the variable's magnitude. Both positive and negative step changes are searched for points of minimum cost. If lower cost is not determined by the initial step size, the step size is diminished and the process is checked again. Hence the step size decreases as the minimum is approached.

The use of the shotgun approach affords a starting point somewhere in the proximity of the minimum, while the second approach allows the search procedure to step over, or out of, non-minimum troughs.

Imposed restrictions must also be considered. For example, flow abnormalities through the heat exchanger may be experienced as a result of external conditions such as wind. An air stream flowing over a surface of heat exchanger creates locations of both high and low external pressures. A location of increased external pressure will experience an enhancement of air flow through the exchanger, while a point of decreased external pressure will be "starved" of flow. Hence, depending on the shape of the heat exchanger, improperly directed wind could nullify or greatly hinder local air flows through the exchanger. As flow abnormalities tend to reduce the effectiveness of the heat exchanger, it is desirable to reduce flow abnormalities.

Initially the air velocities (VAIR) through the exchanger were maintained above a specified minimum. It was hypothesized that a high VAIR would minimize the effects of the ambient air velocity. However, specifying a minimum VAIR penalizes heat exchanger configurations having an inherently high air side friction. Specifying a minimum VAIR is the same as specifying a very high air side pressure drop for configurations with high friction factors. This in turn requires a much larger fan power to create this air side pressure drop. A more logical requirement is a minimum air side pressure drop, DELPA, through the heat exchanger. Since the driving force for the air flow is the pressure differential, as long as the

maintained pressure differential is greater than an external differential caused by wind, flows through the exchanger will not be greatly affected. Note that this allows the "high friction" configurations to adopt lower values of VAIR, so long as DELPA is above a minimum, thereby saving on fan power.

To approximate the pressure differential caused by wind, consider the case of potential non-viscous flow around a cylinder. This would be analogous to wind blowing around a chimney or a heat exchanger of cylindrical configuration. Pressures caused by a wind of 20 mph would range from a pressure increase of 1.02 lbf/ft^2 at the stagnation point to a decrease of 3.06 lbf/ft^2 at a point 90° from the wind direction. In the present optimization runs, the minimum air side pressure drop ($\text{DELPA}_{\text{min}}$) was specified as 4.0 lbf/ft^2 . Since flow rate is directly proportional to the square root of the pressure differential, a heat exchanger designed for a 4 psf minimum pressure drop and being subjected to 20 mph winds would experience approximately a 10% increase of flow at the point facing the wind (stagnation point) and approximately a 50% reduction in flow at a point 90° from the direction of the wind. Computer runs made without pressure drop restrictions optimize at air pressure drops of about 1 psf. Such a design in a 20 mph wind would experience a 40% increase in flow at the stagnation point, and a reversal of flow at a point 90° to the wind direction. There would also be a point of no flow somewhere between these two extremes. This definitely indicates a need for the pressure drop restriction. Flow irregularities may be further minimized by specifying a higher minimum pressure drop, an input variable to the optimization program.^(a)

Pictorially, restrictions on the air velocity or tube length pass a plane or surface through the three-dimensional cost surface, eliminating from consideration certain areas of the cost surface. As illustrated in Figure IV-4, the eliminated points may well include the absolute minimum, making some other point (point B) the desired minimum.

(a) PNL close minimum pressure drop values well below the economically optimum values (in effect, no pressure drop constraint was applied).

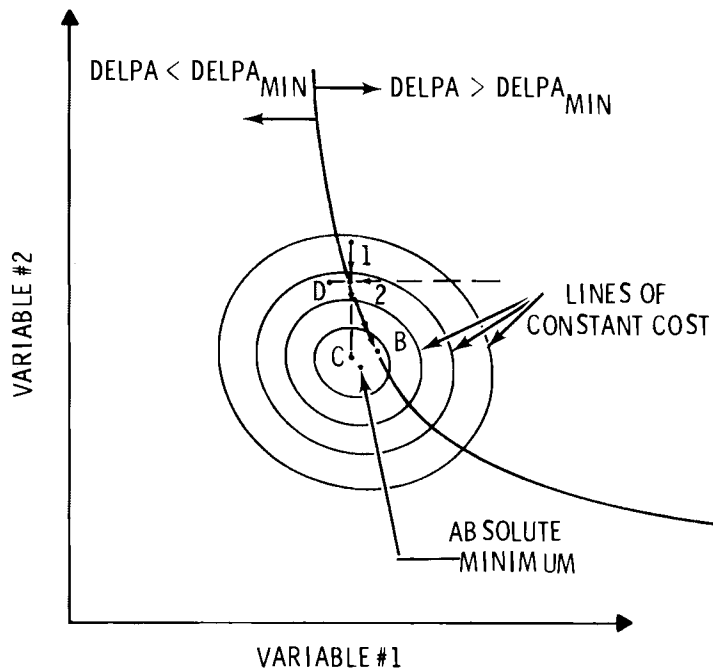


FIGURE IV-4. Minimization with Imposed Restrictions

Simple restrictions on the value of the variables may lead to incorrect answers if only the minimization procedure of Figure IV-2 is used. For example, in Figure IV-4, suppose the search started at point 1 with variable #1 being fixed. Attempting to reach planar minimum C, variable #2 is stopped at point 2 by the restriction on DELPA. Now holding variable #2 constant, variable #1, attempting to reach planar minimum D, cannot pass point 2 either. The search procedure could not proceed further, and would evaluate point 2 as the minimum. To arrive at B, both variables are allowed to change simultaneously, thus proceeding down line 2B towards B. In the five-variable case,

$$\text{DELPA} = f(T_1, \text{RANGE}, \text{CWARA}, \text{AFRON}, \text{WLRAT})$$

So long as this function, or DELPA is maintained constant, we are at liberty to modify the variables which compose the function. Thus, if RANGE

and AFRON are variables #1 and #2 respectively in Figure IV-4 an increase in range accompanied by a decrease in AFRON will move down line 2B towards B, while keeping DELPA fixed.

Since one can also expect to encounter sub-minimal troughs while moving along line 2B, a step size procedure similar to that in Figure IV-2 is used. Again, the step size diminishes as the minimum is approached.

In order both to widen the initial search range and to more accurately determine a starting point, the shotgun method has been changed in the following manner: The original one-step shotgun has been replaced with a multi-step shotgun. Initially, a starting point is prescribed by specifying values for the five variables, and a sequence of 432 points in the vicinity of the starting point are checked. The point of lowest cost with a DELPA greater than $DELPA_{min}$ is taken, and becomes the initializing point for the next procedure. Holding four of the five variables constant, the cost is evaluated, taking extreme values of the fifth variable both above and below the values searched by the initial shotgun. This is sequentially done for each variable. If the minimum of one of these "extended" valued costs is at least 1% less than the minimum cost as calculated in the initial shotgun, this point becomes the prescribed point, and a new initial shotgun is performed about this point. If no new minimum is found by checking the extremes, the minimum cost point determined by the initial shotgun becomes the initial point for a second, "finer", shotgun check. This second shotgun search is "finer" in that the points checked are closer to the "initializing point" than in the "coarse" shotgun. This is the so-called "double shotgun" method.

This double shotgun method is pictured in Figure IV-5 for a two-variable case. Point 1 is the initial prescribed starting point. The first shotgun search investigates those points designated as circles, and yields point 2 as the minimum cost point. Extreme values, the diamonds, are then checked for lower cost points. Finding none in this case, a "finer" shotgun pattern is searched about point 2, yielding 3 as a lower cost point. Point 3 then becomes the starting point for the search procedure as described in Figure IV-2.

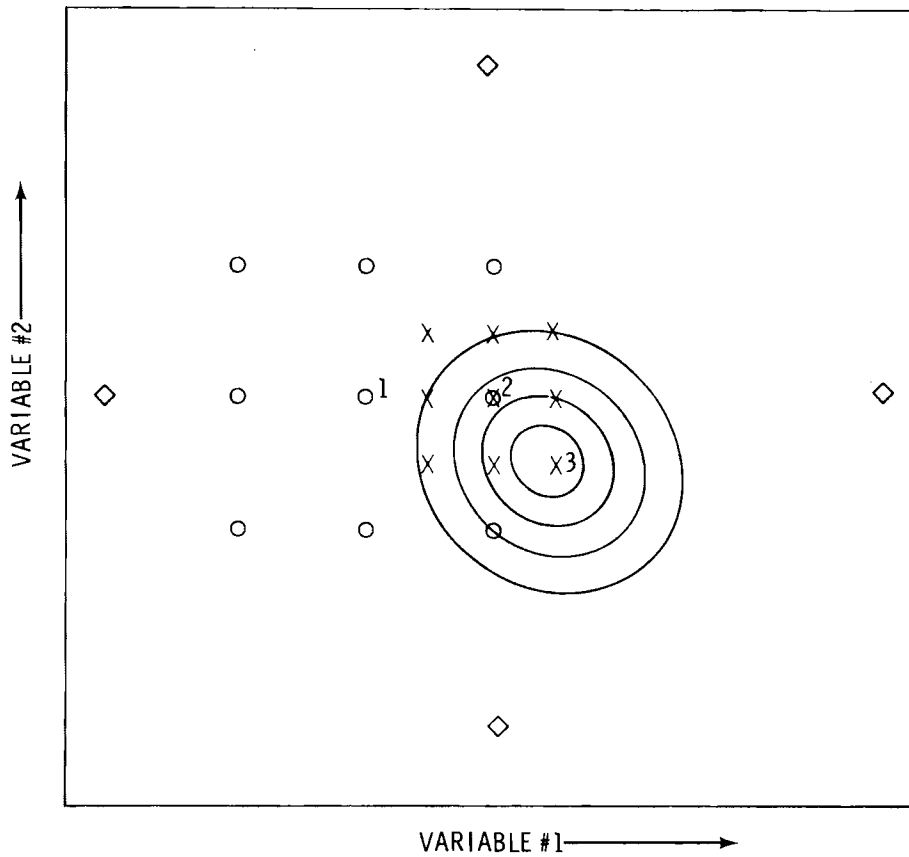


FIGURE IV-5. Double Shotgun Initializing Method

Expanding the process from two variables to five is like working in six-dimensional space rather than three-dimensional: pictorially clumsy, but not conceptually difficult. It merely entails sequentially holding all variables but one constant, while finding the planar minima, and repeating the process a given number of times. If an imposed restriction is encountered, the variable is allowed to change simultaneously with, in turn, each of the other variables.

MIT SUBROUTINES

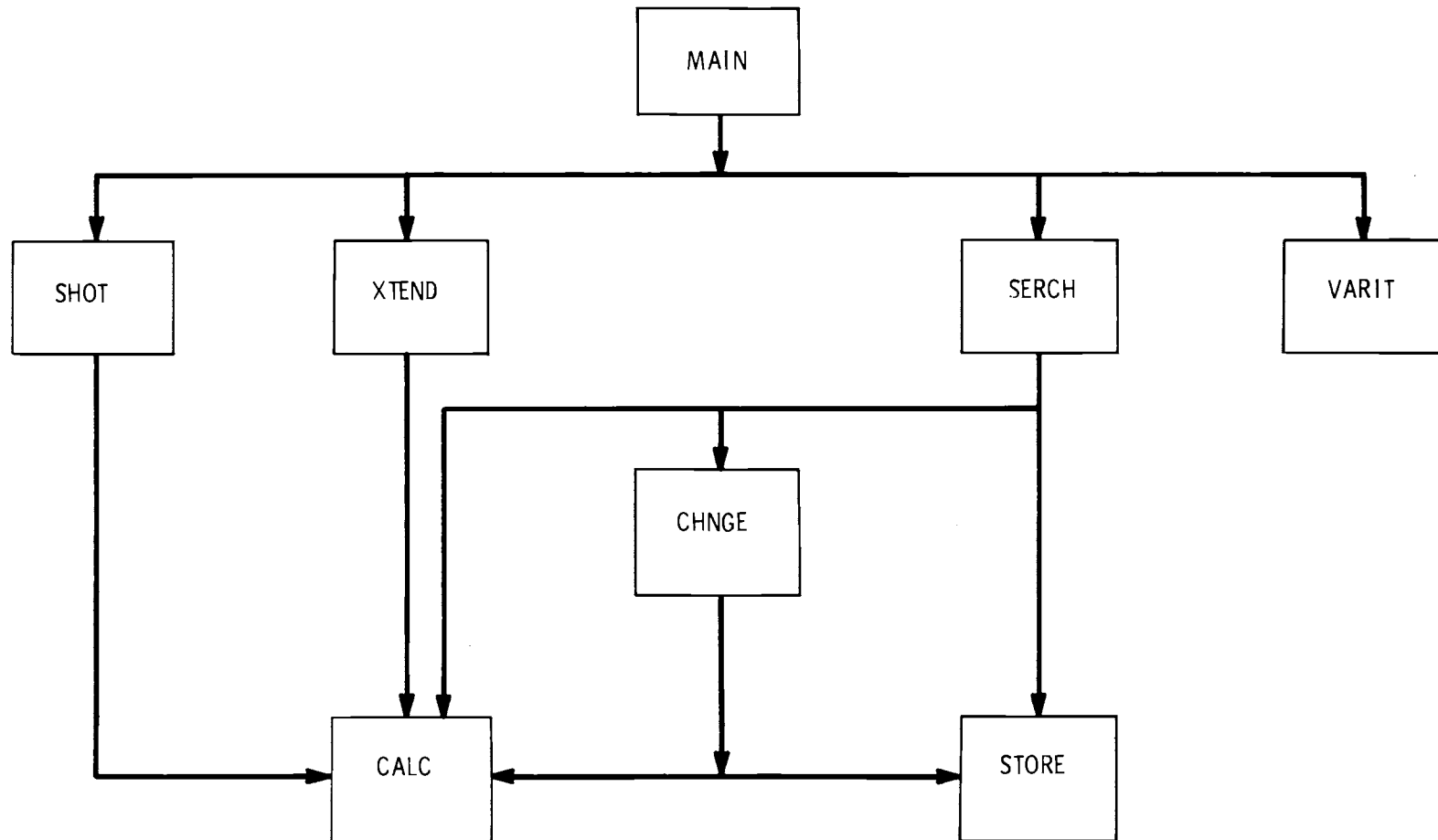
FUNCTION OF SUBROUTINES

SHOT	Tests multiple points. Performs "shotgun" search.
EXTEND	Tests extreme values of minimal cost point, as determined from "coarse" shotgun.
SERCH	Seeks minimum by means of one variable search method.
CHNGE	Seeks minimum when pressure drop restriction encountered by two variable search method.
VARIT	Evaluates system performance and cost, considering average annual temperature fluctuations.
CALC	Calculates cost for a given set of five variables.
STORE	Stores variable and calculated values of minimum cost.

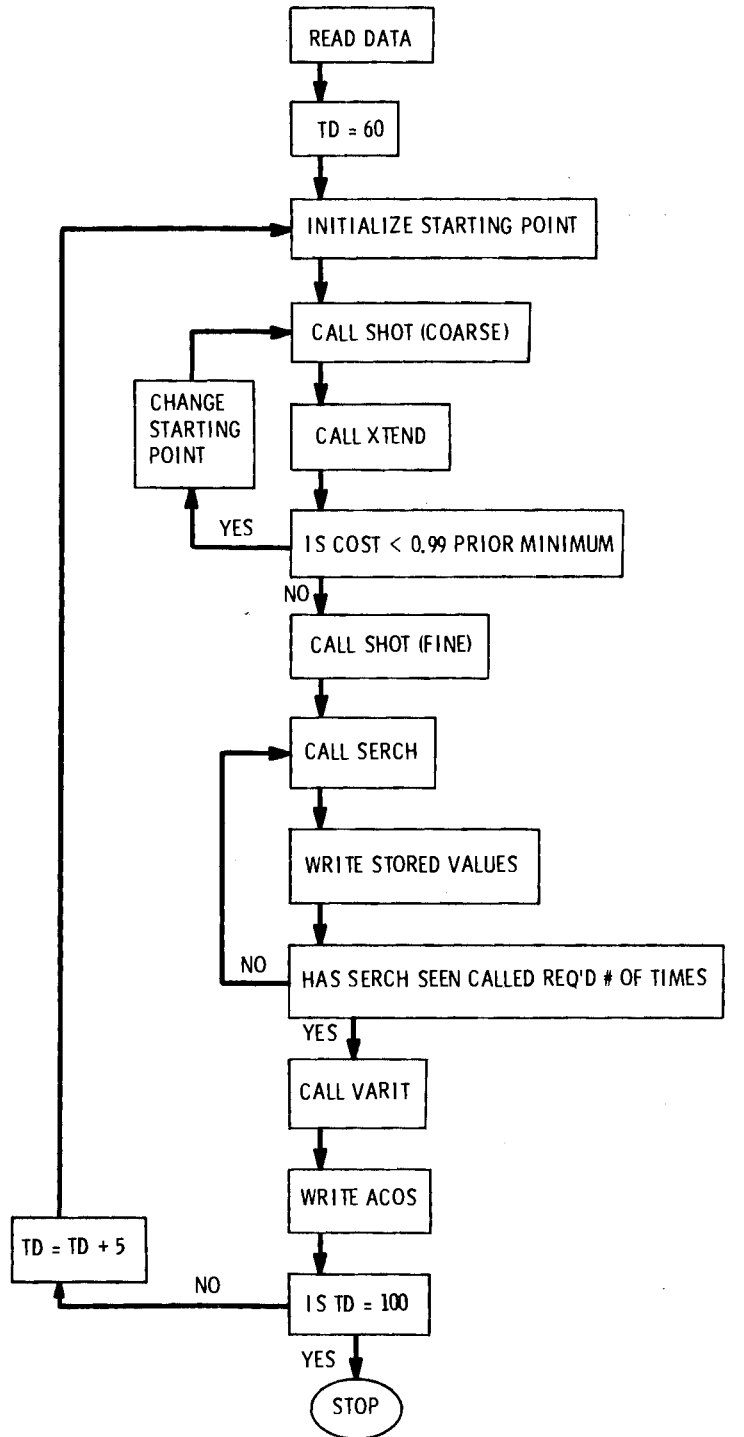
REFERENCE

1. B.R. Andeen and L. R. Glicksman, Dry Cooling Towers for Cooling Plants. Technical Report 73047-1, Engineering Project Laboratory, Department of Mechanical Engineering, Massachusetts Institute of Technology, Cambridge, MA, February 1972.

FLOW DIAGRAM OF SUBROUTINE CALLING

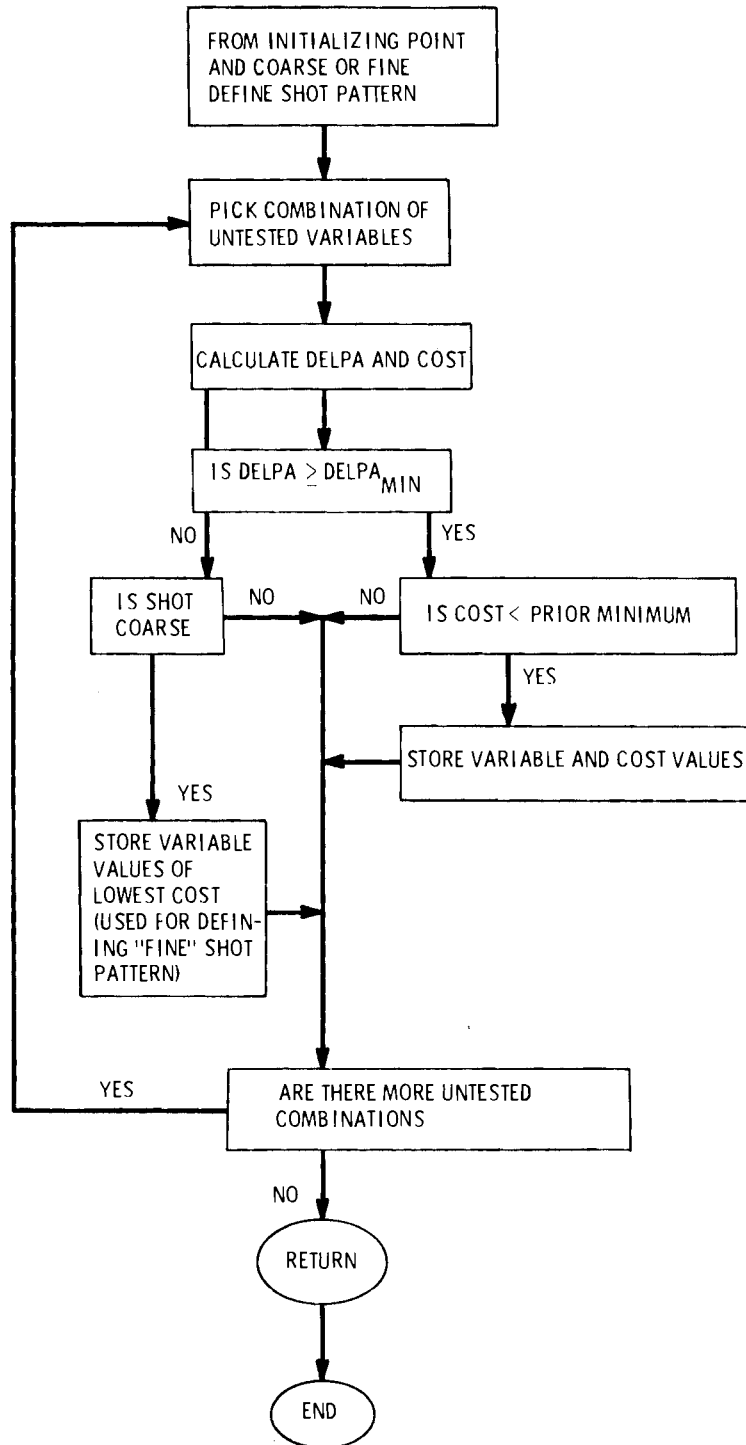


MAIN PROGRAM

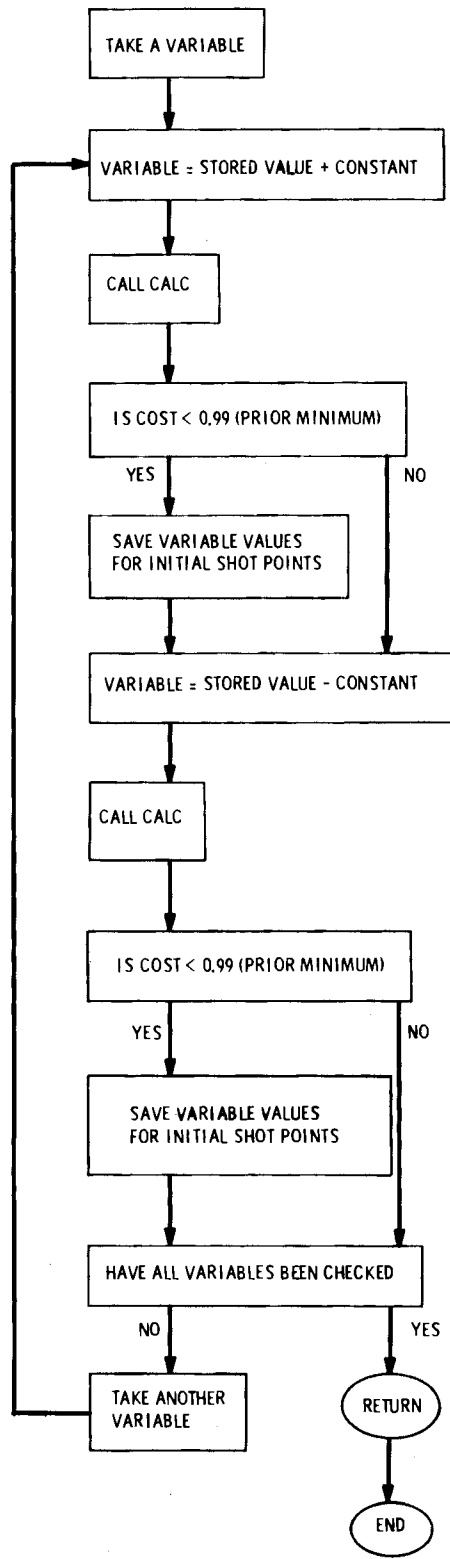


TD = DESIGN TEMPERATURE

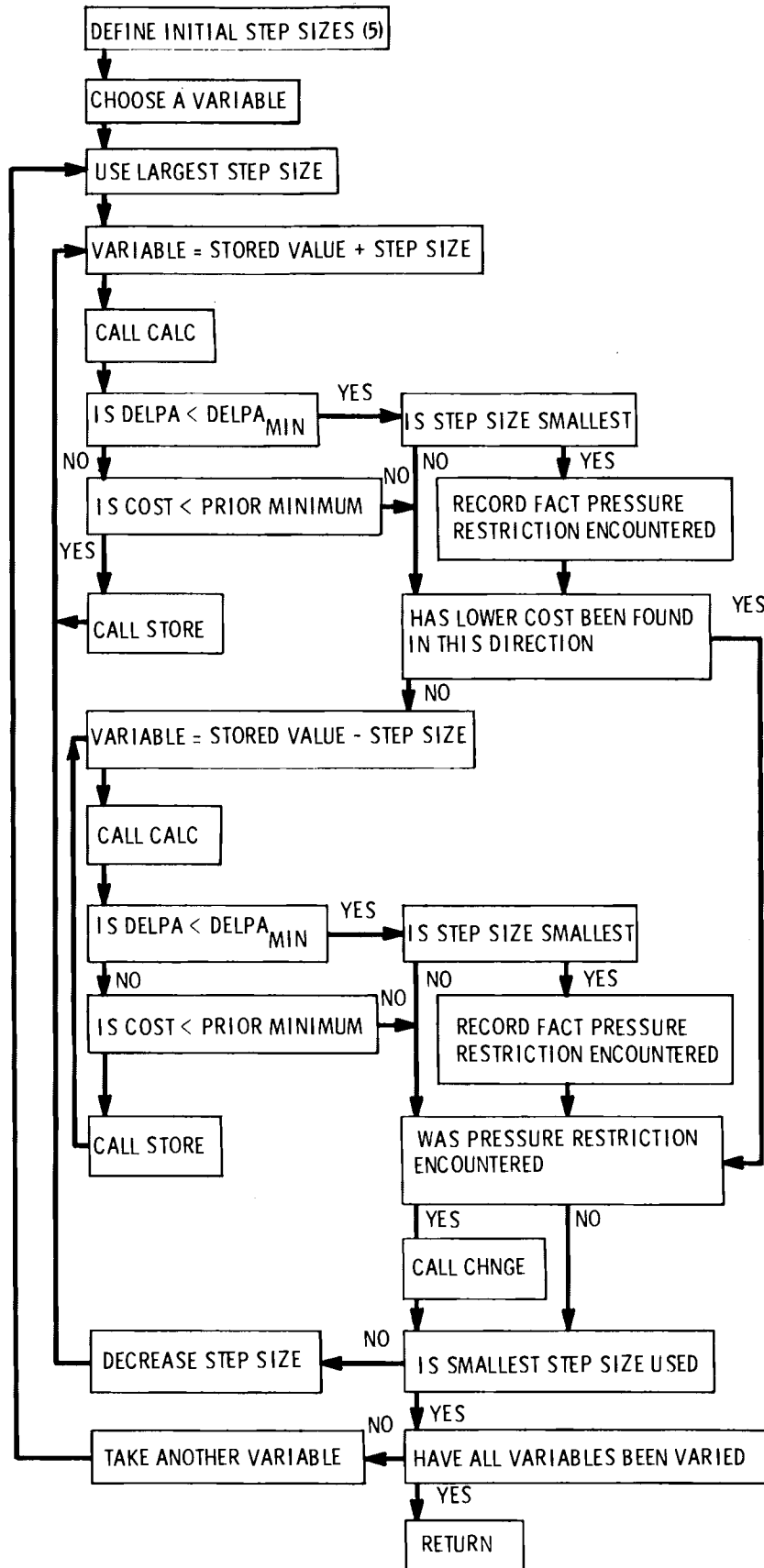
SHOT



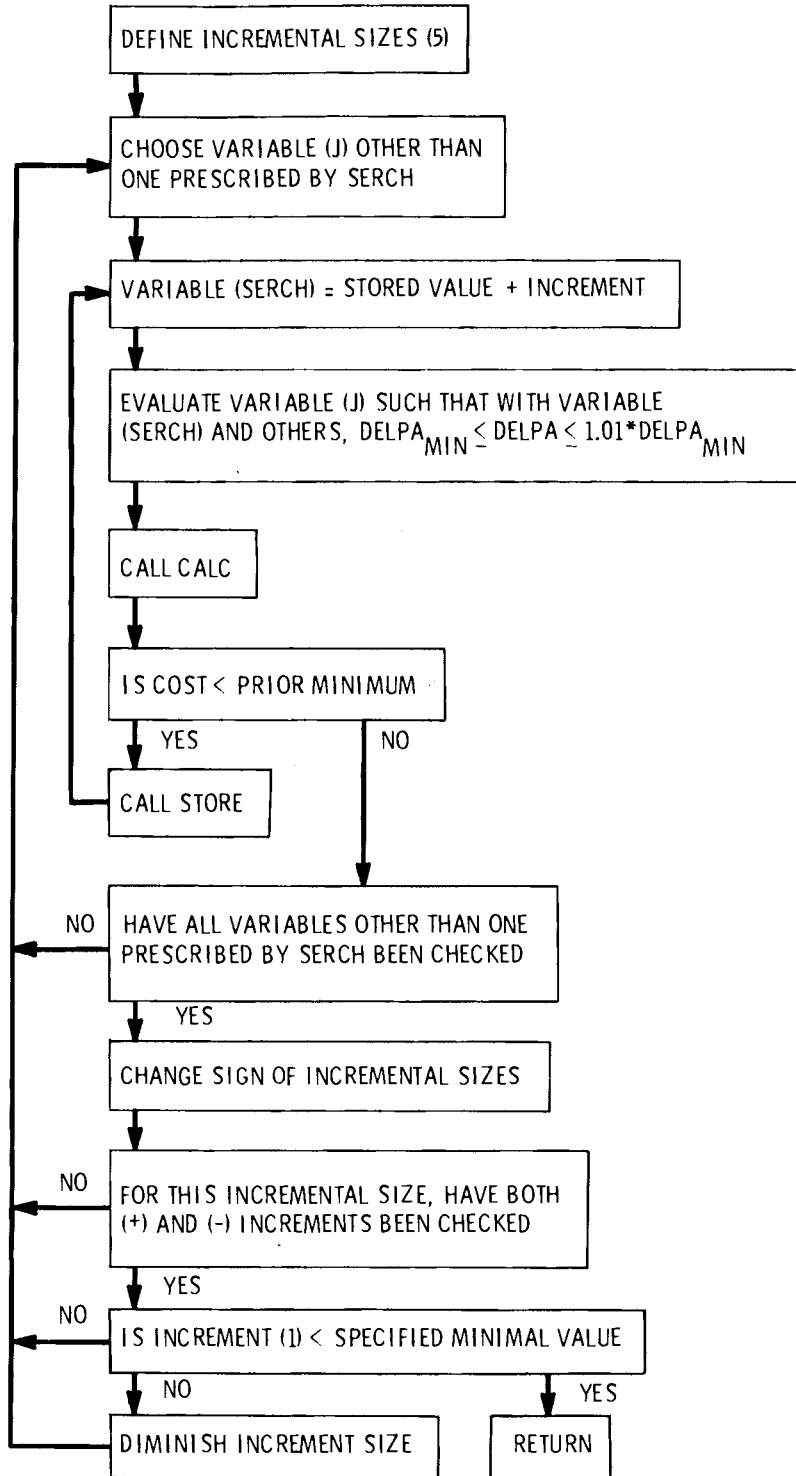
XTEND



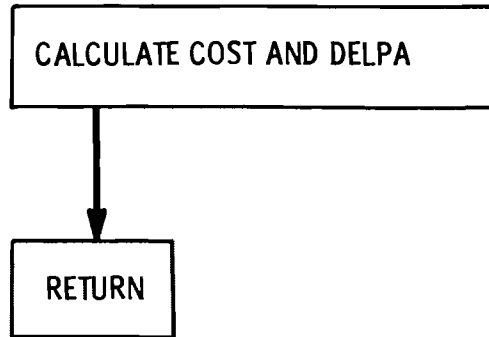
SERCH



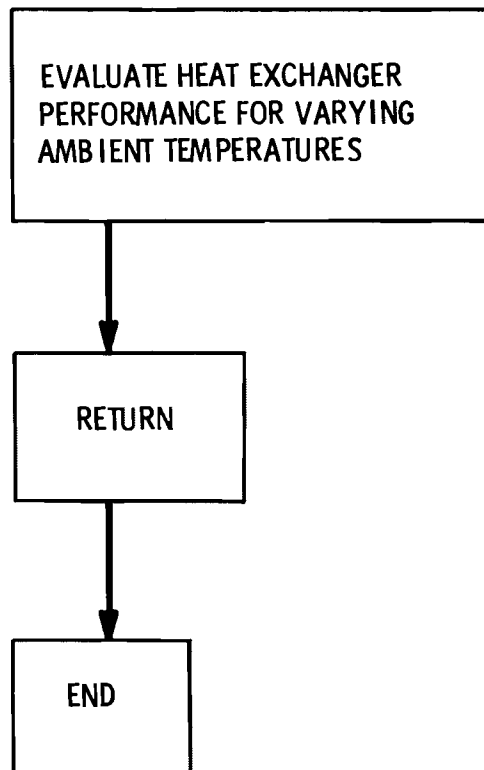
CHNGE



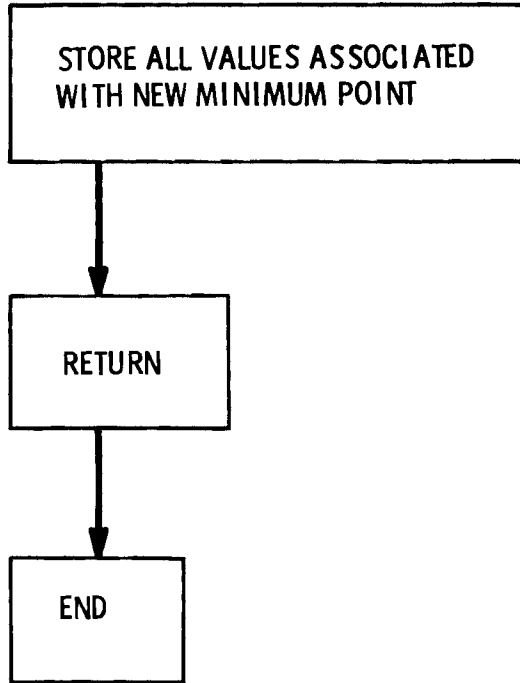
CALC



VARIT



STORE



4
3
2
1

·
·
)
·
·
·

DISTRIBUTION

<u>No. of Copies</u>		<u>No. of Copies</u>
	<u>OFFSITE</u>	
	U.S. Department of Energy A. A. Churm Chicago Patent Group 9800 South Cass Avenue Argonne, IL 60439	U.S. Department of Energy N. Gerstein Chief, Special Projects Branch Division of Advanced Systems and Materials Washington, DC 20545
	U.S. Department of Energy Office of Assistant General Counsel for Patents Washington, DC 20545	U.S. Department of Energy W. E. Mott Director, Energy Control Technology Division of Biomedical and Environmental Research Washington, DC 20545
27	DOE Technical Information Center	U.S. Department of Energy G. A. Newby Assistant Director, Office of Technical Development Division of Advanced Systems and Materials Washington, DC 20545
10	U.S. Department of Energy I. Helms Advanced Concepts Evaluation Branch - G-434 Division of Advanced Systems and Materials Washington, DC 20545	Allied Chemical Company B. R. Dickey 550 2nd Street Idaho Falls, ID 83401
	U.S. Department of Energy W. F. Savage Chief, Advanced Concepts Evaluation Branch Division of Advanced Systems and Materials Washington, DC 20545	Allis-Chalmers Power Systems, Inc. J. S. Joyce 1135 South 70th Street West Allis, WI 53214
	U.S. Department of Energy D. C. Bauer Director, Division of Advanced Systems and Materials Washington, DC 20545	Aluminum Company of America E. T. Wanderer Alcoa Technical Center Alcoa Center, PA 15069
	U.S. Department of Energy R. B. Morrow Special Projects Branch Division of Advanced Systems and Materials Washington, DC 20545	American Electric Power H. J. Janzon 2 Broadway New York, NY 10004
		American Electric Power Service Corporation C. Swenson 2 Broadway New York, NY 10004

No. of
Copies

No. of
Copies

Aqua-Chem
R. M. Ahlgren
P.O. Box 421
Milwaukee, WI 53201

R. W. Beck and Associates
J. P. Rossie
400 Prudential Plaza
Denver, CO 80202

Arizona Public Service Co.
W. E. Campbell
P.O. Box 21666
Phoenix, AZ 85036

Betz Environmental Engineers
J. Soost
9317 J, Highway 99
Vancouver, WA 98665

Arizona Public Service Co.
T. Woods
2121 W. Cheryl Drive
Phoenix, AZ 85021

Black, Crow and Eidsness, Inc.
C. G. Thompson
807 South McDonough
Montgomery, AL 35104

Babcock & Wilcox
M. W. Peterson
Fossil Power Division
20 South Van Buren
Barberton, OH 44203

Black Hills Power and Light
Company
B. Westre
P.O. Box 1400
Rapid City, SD 57701

Baltimore Aircoil Co., Inc.
E. Schinner
P.O. Box 7322
Baltimore, MD 21227

Boeing Aerospace Division
D. Gilbert (M.S. 2R00)
P.O. Box 3999
Seattle, WA 98124

Baltimore Gas & Electric Co.
G. C. Creel
Gas & Electric Building
Baltimore, MD 21203

Bonneville Power Administration
E. H. Hall
1002 N.E. Holladay Street
Box 3621
Portland, OR 97208

Battelle-Geneva
J. P. Budliger
7 Route De Drizi
1227 Geneva, SWITZERLAND

Burns and Roe, Inc.
700 Kinder Kamack Rd.
Oradel, NY 07649

Bechtel Corporation
P. Leung
P.O. Box 60860
Terminal Annex
Los Angeles, CA 90060

California Energy Commission
C. Webb
1111 Howe Avenue
Sacramento, CA 95825

Bechtel Corporation
G. R. Reti
P.O. Box 3965
San Francisco, CA 94119

California State Energy
Resources Conservation
and Development Commission
L. E. Stamets
1111 Howe Avenue
Sacramento, CA 95825

No. of
Copies

Carolina Power & Light Co.
J. Sell
336 Fayetteville Street
Raleigh, NC 27602

Catalytic Construction Corp.
J. Morse
P.O. Box 11402
Charlotte, NC 28029

Ceramic Cooling Tower Co.
P. A. Frohwerk
P.O. Box 425
Fort Worth, TX 76101

Columbus and Southern Ohio
Electric Co.
L. W. Meridith
General Manager, Generation
Department
215 North Front Street
Columbus, OH 43215

Combustion Engineering
H. H. Osborn
Air Preheater Company
Wellsville, NY 14895

Commonwealth Edison
R. H. Holyoak
One First Plaza
P.O. Box 767
Chicago, IL 60690

Consolidated Edison Co.
of New York, Inc.
W. A. Messner
4 Irving Place
New York, NY 10003

Consolidated Edison Co.
of New York, Inc.
C. L. Newman
4 Irving Place
New York, NY 10003

No. of
Copies

Cornell University
F. K. Moore
Ithaca, NY 14850

Curtiss-Wright Corporation
R. J. Haberski
One Passaic Street
Wood Ridge, NJ 07075

Dames & Moore
L. Craton
Suite 1000
1100 Glendon Avenue
Los Angeles, CA 90024

Dames & Moore
P. Gottlieb
Suite 1000
1100 Glendon Avenue
Los Angeles, CA 90024

Delmarva Power & Light
F. Cook
800 King Street
Wilmington, DE 19801

Dow Chemical Company
E. Wagener
2800 Mitchell Drive
Walnut Creek, CA 94598

Duke Power Company
S. K. Blackley
P.O. Box 2178
Charlotte, NC 28201

Duquesne Light Co.
J. Latshaw
435 6th Avenue
Pittsburgh, PA 15219

Dynatech Company
E. Guyer
99 Erie Street
Cambridge, MA 02139

No. of
Copies

No. of
Copies

Ecodyne
J. Slotnik
607 First Street, S.W.
Massillon, OH 44646

Ecodyne Cooling Products Co.
J. K. Swindt
P.O. Box 1267
Santa Rosa, CA 95403

Ecodyne Cooling Products
K. D. Whitehead
P.O. Box 1267
Santa Rosa, CA 95403

Electric Power Research
Institute
J. Maulbetsch
3412 Hillview Avenue
P.O. Box 10412
Palo Alto, CA 94304

Empire State Electric Energy
Research Corp.
L. Geller
1271 Avenue of the Americas
New York, NY 10020

Environmental Protection
Agency
T. G. Brna (MD-61)
IERL/RTP
Research Triangle Park, NC 27711

Environmental Protection
Agency
A. Galley (WH-552)
401 M. Street SW
Washington, DC 20460

Environmental Protection Agency
M. Maxwell (MD-61)
IERL/RTP
Research Triangle Park, NC 27711

Environmental Protection Agency
F. H. Rainwater
Pacific Northwest Water
Laboratory
200 S.W. 35th Street
Corvallis, OR 97330

Environmental Protection Agency
F. A. Roberts
200 S.W. 35th Street
Corvallis, OR 97330

Environmental Sciences and
Services
W. G. Hoydysch
150 East 73rd Street
New York, NY 10021

Environmental Systems Corporation
K. Wilber
P.O. Box 2525
Knoxville, TN 37901

ERG Incorporated
G. M. Benson
Lowell 57th Street
Oakland, CA 94608

Exxon Research Center
J. G. Stevens
Bldg. 1, Rm. 2048
P.O. Box 8
Linden, NJ 07036

Federal Power Commission
E. Sligh
825 N. Capitol Street
Washington, DC 20426

Florida Power & Light Co.
C. Henderson
9250 W. Flagler Street
Miami, FL 33174

No. of
Copies

No. of
Copies

Foster Wheeler Energy Co.
E. L. Damon
110 S. Orange Avenue
Livingston, NJ 07039

Hudson Products
M. W. Larinoff
6855 Horwin Drive
Houston, TX 77036

Franklin Institute
A. M. Rubin
Twentieth & Parkway
Philadelphia, PA 19103

Hudson Products
E. C. Smith
6855 Horwin Drive
P.O. Box 36100
Houston, TX 77036

GEA Airexchangers, Inc.
B. Davis
P.O. Box 1377
Thomasville, GA 31792

H2M Corporation
H. D. Freudenthal
500 Broad Hollow Road
Melville, NY 11746

General Atomic Company
A. C. Eulberg
P.O. Box 81608
San Diego, CA 92138

Ingersoll-Rand
W. R. Scott, Jr.
Phillipsburg, NJ 08865

General Electric Co.
E. H. Miller
Large Steam Turbine Division
300 Nott Street
Schenectady, NY 12301

Italimpianti-Societa
Italiana Impianti p.a.
C. Rocco
Piazza, Piccapietra 9
18121 Genoe, ITALY

General Motors Corp.
R. K. Shah
Harrison Radiator Division
Lockport, NY 14094

Los Angeles Department of
Water and Power
J. L. Mulloy
111 N. Hope Street
Los Angeles, CA 90012

Georgia Power Co.
T. E. Byerley
P.O. Box 4545
Atlanta, GA 30302

Louisiana Power & Light Co.
D. L. Aswell
142 Delaronde Street
New Orleans, LA 70174

Gilbert Associates, Inc.
J. F. Sebald
525 Lancaster Avenue
Reading, PA 19603

The Charles T. Main Co.
E. S. Miliaras
Southeast Tower
Prudential Center
Boston, MA 02199

Heat Transfer Research Inc.
J. E. Taborek
1000 S. Fremont Avenue
Alhambra, CA 91802

Marley
C. A. Baird
12 S. 12th Street
Philadelphia, PA 19107

No. of
Copies

No. of
Copies

Marley
J. D. Holmberg
5800 Fox Ridge Drive
Mission, KS 66202

Minnesota Power Cooperative, Inc.
L. A. Hillier
Box 1318
Grand Forks, ND 58201

Marley
R. Landon
5800 Fox Ridge Drive
Mission, KS 66202

Montana Power Co.
R. Hofacher
40 E. Broadway
Butte, MT 59701

Martin Marietta Laboratories
L. Bongers
1450 South Rolling Road
Baltimore, MD 21227

Niagara Blower
W. Kals
405 Lexington Avenue
New York, NY 10017

Massachusetts Institute of
Technology
L. R. Glicksman
77 Massachusetts Avenue
Cambridge, MA 02139

Northeast Utilities
R. H. Meyer
P.O. Box 270
Hartford, CT 06101

Massachusetts Institute of
Technology
M. W. Golay
77 Massachusetts Avenue
Cambridge, MA 02139

Northern States Power Co.
R. Stansfield
414 Nicollet Mall
Minneapolis, MN 55401

Massachusetts Institute of
Technology
R. Harleman
Department of Civil Engineering
77 Massachusetts Avenue
Cambridge, MA 02139

N.U.S. Corporation
S. Lefton
2 Palo Alto Square (Suite 624)
Palo Alto, CA 94304

McDonnell Douglas
Astronautics Co.
W. H. P. Drummond
5301 Balsa Avenue
Huntington Beach, CA 92647

Oak Ridge National Laboratory
J. W. Michel
OTEC Heat Exchange Project
Activity
Box Y
Oak Ridge, TN 37830

McDonnell Douglas
Astronautics Co.
S. O'Hare
5301 Balsa Avenue
Huntington Beach, CA 92647

Orange & Rockland Utilities, Inc.
R. H. Metzger
Environmental Services Manager
75 West Route 59
Spring Valley, NJ 10977

No. of
Copies

Oregon State University
L. P. Davis
Department of Mechanical
Engineering
Corvallis, OR 97330

Oregon State University
C. E. Wicks
Department of Chemical
Engineering
Corvallis, OR 97330

Oregon State University
J. G. Knudson
Engineering Experiment
Station
Corvallis, OR 97330

Pacific Gas & Electric
A. A. Arie
77 Beale Street
San Francisco, CA 94106

Pacific Gas & Electric
F. F. Mautz
77 Beale Street
San Francisco, CA 94106

Pacific Power & Light Co.
W. C. Bruaer
Public Service Bldg.
Portland, OR 97204

Pennsylvania Power & Light
W. Dussinger
2 North Ninth Street
Allentown, PA 18101

Pennsylvania Power & Light
D. G. Pfeiffer
2 North Ninth Street
Allentown, PA 18101

PFR Engineering Systems, Inc.
T. Rozenmann, President
Suite 832
4676 Admiralty Way
Marina del Rey, CA 90291

No. of
Copies

Philadelphia Electric Co.
J. Allen
2301 Market Street
Philadelphia, PA 19101

Philadelphia Electric Co.
S. J. Kowalski
2301 Market Street, NZ-1
Philadelphia, PA 19101

Philadelphia Electric Co.
J. B. Machel
2301 Market Street, NZ-1
Philadelphia, PA 19101

Philadelphia Electric Co.
D. Marano
2301 Market Street, NZ-1
Philadelphia, PA 19101

Prof. Ing. Carlo Roma
Piazza delle Muse 8
Rome, ITALY

Pickard Low & Garrick
L. Rust
1200 18th St. NW
Suite 612
Washington, DC 20036

Power Generation Cooling
Systems
G. L. Henderson
4714-52nd Street S.
Seattle, Wa 98118

Public Service of Colorado
R. F. Walker
5900 E. 39th Avenue
Denver, CO 80207

Public Service Company
of Indiana
S. W. Shields
V. P. Engineering
100 E. Main Street
Plainfield, IN 46168

No. of
Copies

Public Service Company
of New Mexico
C. D. Bedford
P.O. Box 2267
Albuquerque, NM 87103

Public Service Company
of New Mexico
J. D. Maddox
Corporate Planning Dept.
Albuquerque, NM 87103

Quirk, Lawler and Mattusky,
Eng.
J. Lawler
505 5th Avenue
New York, NY 10017

Radian Corporation
F. B. Mesich
P.O. Box 9948
Austin, TX 78766

Research Cottrell
G. E. Collins
Hamon Cooling Tower Division
Box 750
Bound Brook, NJ 08805

Research Cottrell
R. H. Hannon
Hamon Cooling Tower Division
Box 750
Bound Brook, NJ 08805

Resources Conservation Company
H. Herrigel
P.O. Box 936
Renton, WA 98055

Resources for the Future
D. Abbey
1755 Massachusetts Avenue NW
Washington, DC 20036

No. of
Copies

Reynolds Aluminum Co.
R. Lindberg
Reynolds Metallurgical
Research Laboratory
Richmond, VA 23261

Richmond Field Station
H. H. Sephton
47th and Hoffman Blvd.
Richmond, CA 94804

San Diego Gas & Electric
R. G. Lacy
101 Ash Street
San Diego, CA 92107

Seattle City Light
T. R. Miller
Principal Mechanical Engineer
1015 Third Avenue
Seattle, WA 98104

Seattle City Light
R. L. Skone
1015 Third Avenue
Seattle, WA 98104

Southern California Edison
R. S. Currie
2244 Walnut Grove Avenue
Rosemead, CA 91770

Southern California Edison
W. C. Martin
2244 Walnut Grove Avenue
Rosemead, CA 91770

Southern California Edison
F. A. McCracken
2244 Walnut Grove Avenue
Rosemead, CA 91770

Southern Services, Inc.
C. H. Goodman
P.O. Box 2625
Birmingham, AL 35202

No. of
Copies

P. Sporn
Consultant Engineer
74 Trinity Pl., Suite 511
New York, NY 10006

Stanford University
A. L. London
Department of Mechanical
Engineering
Stanford, CA 94305

Stearns-Rogers, Inc.
J. Y. Parce
Box 5888
Denver, CO 80217

Stone & Webster Engineering
Corp.

D. H. Guild
225 Franklin Street
Boston, MA 02107

Tampa Electric Co.
H. I. Wilson
P.O. Box 111
Tampa, FL 33601

Tennessee Valley Authority
H. B. Flora, III
1320 Commerce Union Bank Bldg.
Chattanooga, TN 37401

Texas Electric Service Co.
W. Keel
115 W. Seventh Street
Fort Worth, TX 76102

Tucson Gas & Electric
A. A. Ward
220 W. 6th Street
Tucson, AZ 85701

Union Carbide Corp.
J. A. Bartz
Linde Division
61 East Park Drive
Tonawanda, NY 14150

No. of
Copies

Union Carbide Corp.
G. J. Kidd
ORGDP - K-25
P.O. Box P, Mail Stop 197
Oak Ridge, TN 37803

Union Carbide Corp.
F. Notaro
Linde Division
61 East Park Drive
Tonawanda, NY 14150

United Engineers &
Constructors
G. A. Engleson
30 S. 17th Street
Philadelphia, PA 19103

United Engineers &
Constructors, Inc.
M. Hu
30 S. 17th Street
Philadelphia, PA 19103

University of Bremen
K. Simhan
Bremen, WEST GERMANY

University of Iowa
J. F. Kennedy
Hydraulic Research Institute
Iowa City, IA 52240

University of Kentucky
T. E. Eaton
Mechanical Engineering
Department
Lexington, KY 40506

U.S. Congress
G. Haimes
214 Massachusetts Avenue NE
Washington, DC 20510

No. of
Copies

No. of
Copies

U.S. Fish and Wildlife
Service
B. L. Foder
Information Transfer
Specialist
National Power Plant Team
1451 Green Road
Ann Arbor, MI 48105

United States Steel Corp.
T. L. Myron
Research Laboratory
Monroeville, PA 15146

Utah Power & Light
M. W. Russon
1407 W. N. Temple
Salt Lake City, UT 84103

Vermont Yankee Nuclear Power
E. Gaines, Jr.
77 Grove Street
Rutland, VT 05701

Virginia Electric & Power Co.
S. Ragone
700 E. Franklin Street
Richmond, VA 23261

Washington Public Power
Supply System
J. Chasse
P.O. Box 968
300 George Washington Way
Richland, WA 99352

Washington State University
R. W. Crain, Jr.
Department of Mechanical
Engineering
Pullman, WA 99164

Washington Water Power Co.
D. L. Olson
E. 1411 Mission Avenue
Spokane, WA 99202

Water Purification Associates
H. Gold
238 Main Street
Cambridge, MA 02142

Western States Water Council
J. A. Barnett
Executive Director
220 South 2nd East
Suite 200
Salt Lake City, UT 84111

Westinghouse Electric Corp.
G. E. Jablonka
Power Generation Systems
Engineering
700 Braddock Avenue, Room 9L51
East Pittsburgh, PA 15112

Westinghouse Electric Corp.
K. Kesavan
Advanced Reactor Division
P.O. Box 158
Madison, PA 15663

Westinghouse Electric Corp.
G. J. Silvestri
Steam Turbines Division - G108
Lester Branch
Box 9175
Philadelphia, PA 19113

Westinghouse Electric Corp.
K. A. Oleson
Steam Turbines Division - G108
Lester Branch
Box 9175
Philadelphia, PA 19113

L. E. Wilkinson
Consultant
6582 Ganon Street, S.E.
Salem, OR 97301

No. of
Copies

No. of
Copies

William M. Rice University
W. G. Characklis
Environmental Science and
Engineering
Houston, TX 77001

Pacific Northwest Laboratory (contd)

ONSITE

DOE Richland Operations Office
Energy Programs Division

H. E. Ransom

Westinghouse Hanford Company
Hanford Engineering Develop-
ment Laboratory

J. Fletcher

Pacific Northwest Laboratory

R. T. Allemann
J. A. Bamberger
Daniel J. Braun
David J. Braun
J. W. Currie
D. E. Deonigi
R. L. Dillon
D. W. Dragnich
R. L. Drake
D. W. Faletti
J. W. Finnigan
T. J. Foley
B. C. Fryer
J. D. Goodenough
J. J. Hauth
A. J. Haverfield
C. H. Henager
A. B. Johnson
W. S. Kelly
R. S. Kemper
C. J. Knoll
W. V. Loscutoff
R. P. Marshall
D. E. Olesen

Y. Onishi
H. L. Parry
L. T. Pederson
H. C. Riches
J. R. Sheff
G. C. Smith
J. S. Stoakes
A. M. Sutey
R. D. Tokarz
D. S. Trent
M. Vagins
R. A. Walter
R. L. Watts
R. D. Widrig
L. E. Wiles
C. E. Willingham
F. R. Zaloudek
File - B. M. Johnson (30)
Technical Information (5)
Publishing Coordination (2)

